Modeling and Simulation in Science, Engineering and Technology

Antonio Romano
Roberto Cavaliere

Geometric Optics

Theory and Design of Astronomical Optical Systems Using *Mathematica*®

Second Edition

EXTRAS ONLINE

Birkhäuser

Birkhäuser

Modeling and Simulation in Science, Engineering and Technology

Series editor

Nicola Bellomo
Department of Mathematics
Faculty of Sciences
King Abdulaziz University
Jeddah, Saudi Arabia

Tayfun E. Tezduyar
Department of Mechanical Engineering
Rice University
Houston, TX USA

Editorial Advisory Board

K. Aoki
Kyoto University
Kyoto, Japan

K.J. Bathe
Department of Mechanical Engineering
Massachusetts Institute of Technology
Cambridge, MA, USA

Y. Bazilevs
Department of Structural Engineering
University of California, San Diego
La Jolla, CA, USA

M. Chaplain
Division of Mathematics
University of Dundee
Dundee, Scotland, UK

P. Degond
Department of Mathematics
Imperial College London
London, UK

A. Deutsch
Center for Information Services
and High-Performance Computing
Technische Universität Dresden
Dresden, Germany

M.A. Herrero
Departamento de Matematica Aplicada
Universidad Complutense de Madrid
Madrid, Spain

P. Koumoutsakos
Computational Science & Engineering
Laboratory
ETH Zürich
Zürich, Switzerland

H.G. Othmer
Department of Mathematics
University of Minnesota
Minneapolis, MN, USA

K.R. Rajagopal
Department of Mechanical Engineering
Texas A&M University
College Station, TX, USA

K. Takizawa
Department of Modern Mechanical
Engineering
Waseda University
Tokyo, Japan

Y. Tao
Dong Hua University
Shanghai
China

More information about this series at http://www.springer.com/series/4960

Antonio Romano · Roberto Cavaliere

Geometric Optics

Theory and Design of Astronomical Optical Systems Using *Mathematica*®

Second Edition

Birkhäuser

Antonio Romano
Dipartimento di Matematica e Applicazioni
"R. Caccioppoli"
Università degli Studi di Napoli Federico II
Naples
Italy

Roberto Cavaliere
Mercato San Severino
Italy

Additional material to this book can be downloaded from http://extras.springer.com.

ISSN 2164-3679 ISSN 2164-3725 (electronic)
Modeling and Simulation in Science, Engineering and Technology
ISBN 978-3-319-43731-6 ISBN 978-3-319-43732-3 (eBook)
DOI 10.1007/978-3-319-43732-3

Library of Congress Control Number: 2016949093

Mathematics Subject Classification (2010): 7802, 8501, 4901

1st edition: © Birkhäuser Boston 2010
2nd edition: © Springer International Publishing Switzerland 2016
This work is subject to copyright. All rights are reserved by the Publisher, whether the whole or part of the material is concerned, specifically the rights of translation, reprinting, reuse of illustrations, recitation, broadcasting, reproduction on microfilms or in any other physical way, and transmission or information storage and retrieval, electronic adaptation, computer software, or by similar or dissimilar methodology now known or hereafter developed.
The use of general descriptive names, registered names, trademarks, service marks, etc. in this publication does not imply, even in the absence of a specific statement, that such names are exempt from the relevant protective laws and regulations and therefore free for general use.
The publisher, the authors and the editors are safe to assume that the advice and information in this book are believed to be true and accurate at the date of publication. Neither the publisher nor the authors or the editors give a warranty, express or implied, with respect to the material contained herein or for any errors or omissions that may have been made.

Printed on acid-free paper

This book is published under the trade name Birkhäuser
The registered company is Springer International Publishing AG
The registered company address is: Gewerbestrasse 11, 6330 Cham, Switzerland
(www.birkhauser-science.com)

Preface

A very wide selection of excellent books are available to the reader interested in geometric optics. Roughly speaking, these texts can be divided into three main classes.

In the first class (see, for instance, [1–14]), we find books that present the theoretical aspects of the subject, usually starting from the Lagrangian and Hamiltonian formulations of geometric optics. These texts analyze the relations between geometric optics, mechanics, partial differential equations, and the wave theory of optics. The second class comprises books that focus on the applications of this theory to optical instruments. In these books some essential formulae, which are reported without proofs, are used to propose exact or approximate solutions to real-world problems (an excellent example of this class is represented by [26]). The third class contains books that approach the subject in a manner that is intermediate between the first two classes (see, for instance, [15–21]).

The aim of this book, which could be placed in the third class, is *to provide the reader with the mathematical background needed to design many optical combinations that are used in astronomical telescopes and cameras*.[1] The results presented here were obtained by using a different approach to third-order aberration theory as well as the extensive use of the software package ***Mathematica***®.

The third-order approach to third-order aberration theory adopted in this book is based on Fermat's principle and on the use of particular optical paths (not rays) termed *stigmatic paths*. This approach makes it easy to derive the third-order aberration formulae. In this way, the reader is able to understand and handle the formulae required to design optical combinations without resorting to the much more complex Lagrangian and Hamiltonian formalisms and Seidel's relations. On the other hand, the Lagrangian and Hamiltonian formalisms have unquestionable theoretical utility considering their important applications in optics, mechanics, and the theory of partial differential equations. For this reason the Lagrangian and Hamiltonian optics are widely discussed in Chapters 10–12.

[1] A professional textbook in astronomical optics is [22].

The use of *Mathematica*® to design optical combinations is shown to be very convenient. In fact, although the aberration formulae are obtained in an elementary way, their application in the design process necessitates a lot of calculations. Using *Mathematica*® it is possible to implement programs that allow us to realize the third-order optics of all the astronomical combinations described in this book. Although experience has shown that a design based on third-order optics is not always acceptable, this approach can be used as a starting point of any optimization method available in professional softwares, like ***Oslo*** and ***Atmos***, the simplest versions of which can be freely downloaded from the Internet. However, we must bear in mind that the optimization methods will only give correct results if the data used in the approximate design are very similar to those determined in final project. These methods must be handled with great care, since they will very often lead to a new design that is worse than the original one. The reason is that the function to be minimized contains many minima which are very close to each other and do not correspond to an effective improvement in the optical combination. For this reasons the author, with the help of A. Limongiello, developed the software ***Optisoft***, working under *Microsoft Windows*, which allows the *final* forms of all the optical combinations considered in this book to be obtained.

In the first chapter, the essential aspects of an optical system $\mathbb{S}$ with an axis of rotational symmetry are introduced. Moreover, we analyze all the data supplied by optical software in order to *check* whether a given optical system $\mathbb{S}$ is acceptable or not. In Chapter 2 Gaussian optics is developed from Fermat's principle. In this chapter the Gaussian characteristics of $\mathbb{S}$ are described: conjugate planes, magnification, focal and nodal points, principal planes and optical invariants. The matrix form of the Gaussian approximation is presented in detail. All of the Gaussian data for an optical system can be derived using the notebook ***TotalAberrations***.[2] Finally, the approach via Fermat's principle is compared with a more traditional presentation of Gaussian optics.

In Chapter 3 a new approach to the third-order monochromatic aberrations that is based on both Fermat's principle and *stigmatic paths* is described. Here it is shown that these optical paths can be used in Fermat's principle instead of the real rays, with the advantage that the stigmatic paths are completely known, since they are determined by Gaussian optics. A new section contains the evaluation of third-order aberrations in the exit pupil. The third-order aberrations for any optical system can be obtained in mathematical form using the notebook ***TotalAberrations***. It should be noted that the symbolic formulae are so dense for optical systems containing many elements with finite thicknesses that they are not practical to apply.

Chapter 4 contains a brief introduction to fifth-order aberrations and their classification. It is also shown that third-order aberrations contribute to fifth-order aberrations. Finally, a proposal is presented to evaluate the fifth-order aberrations starting from the third-order ones in the image plane and exit pupil.

[2]A programm written with ***Mathematica***® can be implemented as notebook or package.

Chapter 5 contains an analysis of the Newtonian and Cassegrain telescopes based on conic mirrors. In Chapters 6 and 7, we study photographic cameras containing lenses and mirrors (Schimdt, Wright, Houghton, Maksutov) as well as the corresponding catadioptric Cassegrain telescopes. Finally, the third-order design of achromatic doublets or apochromatic doublets and triplets is discussed in Chapter 8. Some other interesting optical devices, including the Klevtsov combination, the Baker–Schmidt flat-field camera, the Buchroeder camera, the Baker–Nunn camera, and the Petzval objective optical combinations with sub-corrector are studied in Chapter 9.

Finally, the Lagrangian and Hamiltonian formulations of geometric optics and Seidel's third-order aberration theory are treated in Chapters 10–12. Optics in anisotropic media is sketched in Chapter 13.

Each optical combination analyzed in the book is accompanied by a notebook that automates its third-order design. All these notebooks work in version 10.x, 11 of *Mathematica*® and may be downloaded from the publisher's website at: http://extras.springer.com. These notebooks represent an integral part of the book for many reasons. First, they contain many calculations that appear in the book and many worked exercises. Moreover, many other exercises can be carried out by the reader him- or herself. Finally, carefully studying the programs contained in the notebooks could provide a good way for readers to learn how to program with *Mathematica*®.

We conclude by noting that amateurs with sufficient knowledge of mathematics may find it interesting to learn how to derive the formulae listed in many manuals from the general laws of geometric optics. On the other hand, amateurs who are not interested in learning the mathematical background of optics can use the notebooks contained in the book to rapidly obtain the third-order designs of many cameras and telescopes used in astronomy.

Naples, Italy — Antonio Romano
Mercato San Severino, Italy — Roberto Cavaliere

Contents

1 Fermat's Principle and General Considerations Regarding Centered Optical Systems 1
1.1 An Introduction to Fermat's Principle 1
1.2 Forming an Image 5
1.3 Axial Chromatic Aberrations 9
1.4 Monochromatic Aberrations 10
1.5 Surfaces of Revolution 12
1.6 Ray Tracing in Axially Symmetric Systems 16
1.7 Exercises 19

2 Gaussian Optics 23
2.1 Gaussian Approximation for a Single Surface 23
2.2 Compound Systems 27
2.3 Useful Decompositions of Matrix $\mathbb{T}$ 29
2.4 Principal Planes and Focal Lengths 32
2.5 Stops and Pupils 34
2.6 Some Gaussian Optical Invariants 36
2.7 Gaussian Analysis of Compound Systems 38
2.8 A Graphical Method 42
2.9 Thick and Thin Lenses 43
2.10 A Different Approach to Gaussian Optics 45
2.11 Exercises 48

3 Fermat's Principle and Third-Order Aberrations 53
3.1 Introduction 53
3.2 The Aberration Function 54
3.3 A New Aberration Function 58
3.4 The Aberration Function Φ for a Single Surface 62
3.5 The Total Aberration Function for a Compound System 67
3.6 Analysis of Third-Order Aberrations 72

3.7 Petzval's Theorem 76
3.8 Aberration Formulae 78
3.9 Combined Effect of Third-Order Aberrations 79
3.10 Primary or Axial Chromatic Aberrations 80
3.11 Third-Order Aberrations in the Exit Pupil 83
3.12 Plate with Parallel Plane Faces 88

4 About Higher Order Aberrations 91
4.1 Aplanatism and Sine Condition 91
4.2 Aplanatic Refractive Surfaces 95
4.3 Introduction to Fifth-Order Aberrations 96
4.4 Meaning of the Terms of (4.33), (4.34) 100
4.5 The Light Diffraction and the Airy Disk 102

5 Newtonian and Cassegrain Telescopes 107
5.1 The Newtonian Telescope 107
5.2 Location and Dimension of Flat Mirror 110
5.3 Newtonian Telescope with Spherical Primary Mirror 112
5.4 Cassegrain Telescopes 113
5.5 Spherical Aberration and Coma in Cassegrain Telescopes 115
5.6 Concluding Remarks 116
5.7 Examples 117

6 Cameras for Astronomy 119
6.1 Introduction 119
6.2 Aberrations for a Single Mirror 120
6.3 Schmidt's Camera 121
6.4 Examples of Schimdt's Camera 125
6.5 Wright's Camera 127
6.6 Houghton's Camera 129
6.7 Examples 138
6.8 Maksutov Camera 139
6.9 Examples 143

7 Compound Cassegrain Telescopes 145
7.1 Introduction to Cassegrain Telescopes 145
7.2 Schmidt–Cassegrain Telescopes 147
7.3 Examples 148
7.4 Houghton–Cassegrain Telescopes 151
7.5 Examples 154
7.6 Maksutov–Cassegrain Telescopes 157
7.7 Examples 159
7.8 Final Remarks 161

8 Doublets and Triplets 163
8.1 Achromatic Doublets 163
8.2 Elimination of Spherical Aberration and Coma 165

8.3 Examples . . . 167
8.4 Triplets . . . 170
8.5 Examples . . . 171

9 Other Optical Combinations . . . 175
9.1 Schmidt–Cassegrain Telescope with Spherical Surfaces . . . 175
9.2 The Flat-field Baker–Schmidt Camera . . . 177
9.3 Cassegrain Telescope with the Corrector at the Prime Focus . . . 180
9.4 The Klevtsov Telescope . . . 182
9.5 A First Analysis of the Meniscus . . . 183
9.6 Analysis of Mangin Mirror . . . 184
9.7 Buchroeder's Camera . . . 185
9.8 The Baker–Nunn Camera . . . 187
9.9 Houghton–Cassegrain Telescope with Sub-Aperture Corrector . . . 190
9.10 Petzval's Objective . . . 193

10 Fermat's Principle and Wave Fronts . . . 197
10.1 Fermat's Principle . . . 197
10.2 The Boundary Value Problem . . . 206
10.3 Maupertuis' Principle . . . 208
10.4 Fermat's Principle and the Formation of Mirages . . . 210
10.5 Rotational Symmetry and Lagrange's invariant . . . 212
10.6 Wave Fronts and Fermat's Principle . . . 215
10.7 Huygens' Principle . . . 219

11 Hamiltonian Optics . . . 221
11.1 Hamilton's Equations in Geometric Optics . . . 221
11.2 Hamilton's Principal Functions . . . 223
11.3 Symmetries and Characteristic Functions . . . 227
11.4 Lagrange's Optical Invariant for Axially Symmetric Systems . . . 229
11.5 Hamiltonian Equations and Primary Aberrations . . . 230
11.6 Equations of Primary Aberrations . . . 234
11.7 The Case of Spherical Surfaces . . . 238
11.8 Recalls of Symplectic Mechanics . . . 239
11.9 Symplectic Optics . . . 244

12 Principal Functions and Primary Aberrations . . . 247
12.1 Introduction to Third-Order Aberrations . . . 247
12.2 Third-Order Aberrations via Angular Function . . . 248
12.3 Reduced Coordinates . . . 251
12.4 Schwarzschild's eikonal . . . 253
12.5 Addition Theorem for Third-Order Aberrations . . . 256
12.6 Fourth-Order Expansion of Angular Function . . . 258
12.7 Aberrations of Axially Symmetric Systems . . . 261

13 Introduction to Optics in Anisotropic Media 265
13.1 Maxwell's Equations in Anisotropic Media 265
13.2 Refractive Index in Anisotropic Media 267
13.3 Fermat's Principle in Anisotropic Media 270

Appendix A: First-Order PDE 273

Appendix B: Symplectic Vector Spaces 281

References 285

Index 287

Chapter 1
Fermat's Principle and General Considerations Regarding Centered Optical Systems

1.1 An Introduction to Fermat's Principle

Faraday and Lentz discovered that a varying magnetic field produces an electric field. Subsequently, Maxwell hypothesized that the inverse process was possible, i.e., that a varying electric field will produce a magnetic field, and he postulated a set of equations relating to electromagnetism in his famous *Treatise of Electricity and Magnetism*. Ever since then, electric and magnetic phenomena have been regarded as two interconnected aspects of the electromagnetic field, which, in turn, is propagated by electromagnetic waves. Moreover, Maxwell showed that light waves are a particular type of electromagnetic waves so that the field of optics merged with electromagnetism. This suggests that one could study the propagation of light waves across an optical system using Maxwell's equations along with suitable boundary conditions, depending on the nature of the media involved. However, although theoretically possible, such an approach is not practical since it introduces insurmountable technical difficulties. For example, the simple analysis of light propagation across an obstacle (i.e., of diffraction of light) is so complex that it is necessary to apply the approximate procedure expressed by Huygens–Kirchhoff's principle.

Consequently, we must follow an approach that is frequently used in Physics—we must resort to using a simpler model to describe such phenomena. ***Geometric optics***, which amounts to a drastic simplification of light propagation, is applicable when the dimensions of the bodies across which light propagates are large compared with the wavelength of the light.

Let us consider the propagation of a monochromatic light wave in an isotropic medium Σ that has a refractive index $N(\mathbf{x})$ which depends on the point $\mathbf{x}$. If we suppose that the wavelength of the light is small compared with the dimensions of both the interposed obstacles ("stops") and the regions traversed, the propagation of the light can be described by either the ***wave fronts*** (***Huygens principle***) or by ***rays***, which are the curves normal to wave fronts (***Fermat's principle***).

© Springer International Publishing Switzerland 2016

A. Romano and R. Cavaliere, *Geometric Optics*,
Modeling and Simulation in Science, Engineering and Technology,
DOI 10.1007/978-3-319-43732-3_1

From now on, we will postulate Fermat's principle without criticism and apply it to derive the Gaussian optics and the third-order aberration theory in an elementary way. The results of the first two chapters will be used to analyze and to design many astronomical optical systems. Finally, the theoretical aspects of geometric optics will be developed in Chapters 10–13 of this book.

The ***optical path length*** $OPL(\gamma)$ along *any curve* γ is defined by the following formula

$$OPL(\gamma) = \int_{\gamma} N(\mathbf{x})ds. \tag{1.1}$$

If the curve γ is a light ray, v denotes the speed of light in medium Σ, and c is the speed of light in a vacuum, then we have

$$Nds = \frac{c}{v}ds = cdt,$$

so that the optical path length along a *ray* is proportional to the time taken for the light to propagate along γ.

The starting point of geometric optics is ***Fermat's principle*** whose original formulation is as follows:

The optical path length of a light ray passing from point $\mathbf{x}_a$ ***to point*** $\mathbf{x}_b$ ***is the length of the shortest optical path between the same points***.

Let $Ox_1x_2x_3$ be a Cartesian frame of reference and is denoted by $\mathbf{x}(t)$, $t \in [a, b]$ the parametric equation of a curve γ passing from the point $\mathbf{x}_a$ to $\mathbf{x}_b$, i.e., such that

$$\mathbf{x}(a) = \mathbf{x}_a, \quad \mathbf{x}(b) = \mathbf{x}_b.$$

Then, in view of (1.1), the optical path length of γ from $\mathbf{x}_a$ to $\mathbf{x}_b$ can be written as follows:

$$OPL(\gamma) = \int_a^b N(\mathbf{x})\sqrt{|\dot{\mathbf{x}}|^2}dt, \tag{1.2}$$

where $|\dot{\mathbf{x}}|^2 = \dot{x}_1^2 + \dot{x}_2^2 + \dot{x}_3^2$. Formula (1.2) is a map between a suitable set A of functions $\mathbf{x}(t)$ and the set of real numbers $\Re$, that is, it defines a functional and Fermat's principle is a variational principle.

We must now answer the following fundamental questions:

- Does this principle determine the ray γ between two given points $\mathbf{x}_a$ and $\mathbf{x}_b$ when the refractive index $N(\mathbf{x})$ is assigned?
- Is the ray uniquely determined?
- How do we take into account the discontinuities of the refractive index $N(\mathbf{x})$ along the path of the ray?

Fermat's principle of the minimum optical path was one of the first example of a variational principle in Physics. Since it was formulated, the number of these

principles has grown substantially in both Physics and Mathematics, leading to problems that do not (for the most part) currently have explicit exact solutions.

Briefly, a variational principle characterizes the unknown of a problem (for instance, the ray between two points $\mathbf{x}_a$ and $\mathbf{x}_b$), by requiring that it minimizes a suitable integral expression (for instance, the optical path length). This kind of principle leads to a mathematical problem that is quite different from the initial value problem that Cauchy stated for ordinary differential equations. In the latter, we search for a function, which satisfies suitable initial data and, *for any value of the independent variable*, a differential equation (i.e., a relation among the function itself and its derivatives). However, it is not appropriate here to dive deeply into the subject of variational principles, presenting their abstract and general formulations. The aim here is simply to remind the reader that many problems expressed in terms of differential equations could, equivalently, be formulated by resorting to a variational principle. Initially the fact that Nature seems to verify this "minimum principle" suggested to some that it had a divine origin, and so they attributed a metaphysical meaning to variational principles.

We answer all the above questions in Chapter 10. In particular, it will be shown that a ray is characterized by the condition that the optical path length is *stationary* along it, this does not necessarily imply a minimum. However, for now, the contents of the first nine chapters are based on the following remarks, which derive from Fermat's principle.

1. ***In regions with a constant refractive index, rays are straight lines***.
   In fact, in these regions, the optical path length $OPL(\gamma)$ of a curve γ between two points $\mathbf{x}_1$ and $\mathbf{x}_2$ is proportional to the geometric length of γ. Consequently, the minimum value of $OPL(\gamma)$ corresponds to the length of the shortest curve between $\mathbf{x}_1$ and $\mathbf{x}_2$, which is a straight line.
2. ***Let S be a surface separating two homogeneous media M and M' with refractive indices N and N', respectively. If $\mathbf{x}$ is the point at which a ray meets S, $\mathbf{t}$, $\mathbf{t}'$ denote the tangent unit vectors to the ray at $\mathbf{x}$ in the first and in the second media, respectively, and $\mathbf{n}$ is the internal unit normal to S at $\mathbf{x}$, then the vectors $\mathbf{t}$, $\mathbf{t}'$, and $\mathbf{n}$ verify the equation*** (see Exercise 1):

$$N'\mathbf{t}' - N\mathbf{t} = \lambda\mathbf{n}, \tag{1.3}$$

   where λ is a scalar quantity. In particular, the vectors $\mathbf{t}$, $\mathbf{t}'$, and $\mathbf{n}$ are coplanar. Moreover, after denoting the incident and refractive angles, (i.e., the angles that $\mathbf{t}$ and $\mathbf{t}'$ form with $\mathbf{n}$, see Figure 1.1), by i and i', respectively, and evaluating the vector and the scalar product of (1.3) with $\mathbf{n}$, the following relations are obtained:

$$\sin i' = \frac{N}{N'} \sin i, \tag{1.4}$$

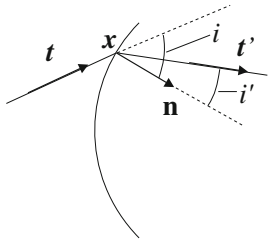

Fig. 1.1 The refraction law

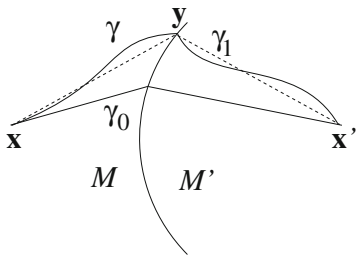

Fig. 1.2 Curve and broken paths

$$\lambda = N'\sqrt{1 - \frac{N^2}{N'^2}\sin^2 i} - N\cos i. \tag{1.5}$$

Relations (1.3)–(1.5), which express the ***refraction law***, will be considered again in Chapter 11.

3. ***Let S be a surface separating two homogeneous media M and M' with refractive indices N and N', respectively, (see Figure 1.2) and γ_0 the unique ray between the points $\mathbf{x} \in M$ and $\mathbf{x}' \in M'$. The above two remarks and Fermat's principle imply that γ_0 is a broken line whose optical path length is smaller than or equal to the optical path length of any curve γ with the same end points, i.e.***

$$OPL(\gamma_0) \leq OPL(\gamma). \tag{1.6}$$

Then, γ_0 is a ray if and only if (1.6) is satisfied for any broken line γ_1 between the same points $\mathbf{x}$ and $\mathbf{x}'$.
In fact, if (1.6) is verified by any curve γ it is verified by any broken line γ_1. To the contrary, suppose that

$$OPL(\gamma_0) \leq OPL(\gamma_1),$$

for any broken line γ_1. Then, let γ be any curve between $\mathbf{x}$ and $\mathbf{x}'$ and denote by $\mathbf{y}$ the intersection point of γ with S. Then, the broken line $\gamma_1 = \mathbf{xyx}'$ verifies the condition

$$OPL(\gamma_0) \leq OPL(\gamma_1) \leq< OPL(\gamma).$$

4. ***Let S be a surface separating two regions C_1 and C_2 with constant refractive indices N_1 and N_2, respectively. We denote the family of all broken lines starting from a point $\mathbf{x}_1 \in C_1$ and ending at the point $\mathbf{x}_2 \in C_2$*** by Γ. ***If the optical path length $OPL(\gamma)$, with $\gamma \in \Gamma$, is independent of γ, then all the broken lines of Γ are rays.*** In fact, since $OPL(\gamma)$ has the same value on any $\gamma \in \Gamma$, it is stationary along any path.
   Under these conditions, the initial and final points of the rays belonging to Γ are said to be ***stigmatic*** with respect to S.
5. ***Let $I(\mathbf{x})$ be a spatial region containing the point $\mathbf{x}$. Suppose that for any point $\mathbf{x}' \in I(\mathbf{x})$ one and only one ray γ exists between $\mathbf{x}$ and $\mathbf{x}'$. Then, denoting the unit tangent vector to γ by $\mathbf{t}$, the optical path length along γ***

$$V(\mathbf{x}, \mathbf{x}') = \int_{\mathbf{x}}^{\mathbf{x}'} N\mathbf{t} \cdot d\mathbf{x}, \tag{1.7}$$

   is a function of $\mathbf{x}$ and $\mathbf{x}'$. Moreover, the following relations hold:

$$\nabla_{\mathbf{x}} V(\mathbf{x}, \mathbf{x}') = -N(\mathbf{x})\mathbf{t}(\mathbf{x}), \quad \nabla_{\mathbf{x}'} V(\mathbf{x}, \mathbf{x}') = N(\mathbf{x}')\mathbf{t}(\mathbf{x}'), \tag{1.8}$$

   Formulae (1.8), which derive from the well-known Leibnitz's rule, will be proven in Chapter 11.

Remark 1.1 We note that the ***reflection law***, according to which the incident angle i and the reflection angle i' satisfy the condition $i' = -i$, can be obtained by the refraction law (1.4) by putting into it $N = -N' = 1$.

In Chapters 2-9 we show many applications of the above consequences of Fermat's principle.

1.2 Forming an Image

Throughout this book, we consider centered optical systems $\mathbb{S}$ consisting of surfaces with a common axis a of revolution that separate homogeneous optical media with different (but constant for each medium) refractive indices. The axis a is called the ***optical axis*** of $\mathbb{S}$. We also suppose that the object that $\mathbb{S}$ must image is contained in a plane π, which is orthogonal to a and is called the ***object plane***.

All the considerations discussed in the following sections of this chapter refer to a ***given*** optical system $\mathbb{S}$ with the above characteristics.

To analyze the behavior of the rays originating from a point of the object and crossing the optical system $\mathbb{S}$, we can use the refraction and reflection laws. This procedure, which is called ***ray tracing***, will be analyzed in detail in Section 1.6. It is evident that it requires that the mathematical quantities that define a ray are assigned. Now, if we introduce Cartesian axes Oxy in the object plane π, then a ray γ coming

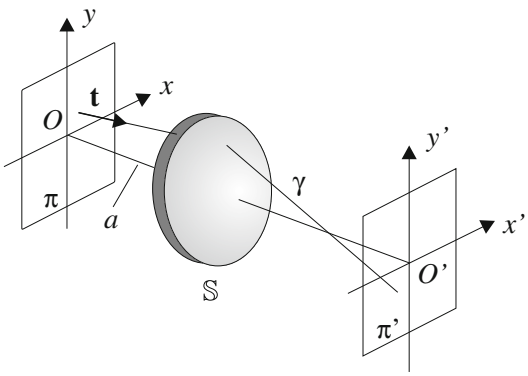

Fig. 1.3 A ray γ from the object plane to the image plane

from (x, y) is determined by providing the unit vector $\mathbf{t}$ along γ, i.e., two director cosines α and β of γ (see Figure 1.3). It should be noted that the quantities $x, y, \mathbf{t}$, although natural, are not the most convenient variables to use. In fact, it is evident that some rays coming from $(x, y) \in \pi$ do not reaches the optical system $\mathbb{S}$, due to either the finite dimensions of the optical components or the presence of a stop along the optical path.

Let us consider the set of the rays arising from the point $O \in a$. In Figure 1.4 the rim of the first surface of the optical path limits the cone C of rays from O. It is then natural to identify a ray γ by providing the coordinates (x, y) of the point of the object in π and the coordinates (x_e, y_e) of the point of intersection of γ with the tangent plane π_e at the vertex of the first surface of $\mathbb{S}$. In Figure 1.5, the cone C is determined by a stop in the plane π_e, and we can again identify (x_e, y_e) with the coordinates of the intersection point of a ray with π_e. However, in Figure 1.6 the stop is located after the optical system. In this case, owing to Fermat's principle, a ray

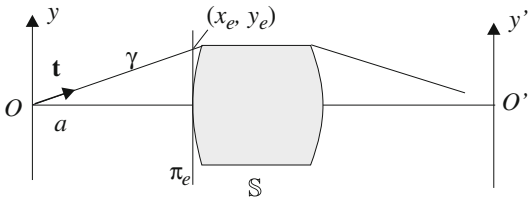

Fig. 1.4 Stop on the first surface

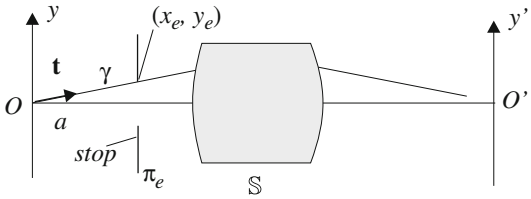

Fig. 1.5 Stop before the first surface

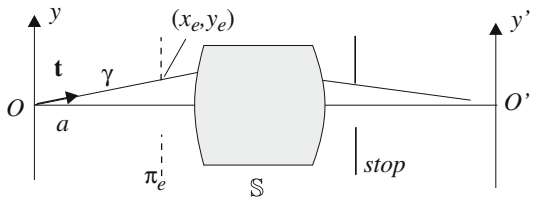

Fig. 1.6 Stop behind the last surface

from O is still determined by providing the coordinates of its point of intersection with the plane of the stop, but we cannot explicitly write the equation of the ray by providing these coordinates. In this case, we must choose a suitable plane π_e, in front of the object plane π, and determine the coordinates (x_e, y_e) of the point of intersection of γ with π_e of any ray which *succeeds in crossing* $\mathbb{S}$. In Chapter 2 we discuss the criterion for defining a suitable reference plane π_e. This analysis, which lead us to the definitions of ***entrance pupil*** and ***exit pupil*** in particular, shows that the reference plane is just given by π_e in the cases of Figures 1.4, 1.5, whereas it gives the correct position of the plane π_e in the case of Figure 1.6. In conclusion, from now on, a ray will be identified by the variables x, y, x_e, y_e.

Let π' be another plane orthogonal to the optical axis a. Two points $\mathbf{x} \in \pi$ and $\mathbf{x}' \in \pi'$ are said to be ***stigmatic for*** $\mathbb{S}$ if all of the rays from $\mathbf{x}$ reach the point $\mathbf{x}'$ after crossing the system $\mathbb{S}$. The system $\mathbb{S}$ is said to be an ***ideal system*** or an ***aberration-free system*** for the pair of the object plane π and the plane π' if the following conditions are satisfied:

1. There is a plane π' such that points $\mathbf{x} \in \pi$ exhibit a one-to-one correspondence with points in π', independent on wavelength of the light. In other words, each point $\mathbf{x}' \in \pi'$ corresponds to one and only one point $\mathbf{x} \in \pi$.
2. The above correspondence preserves the form of the object.

In this case, the plane π' is the ***image plane*** and π and π' are said to be ***conjugate planes***.

Consider two Cartesian frames $Oxyz$ and $Ox'y'z'$ that have their origins O, O' in π, π', respectively, and that have the axes Oz, Oz' coinciding with the optical axis a of $\mathbb{S}$. The coordinate plane Oyz is called the ***meridional*** or ***tangential plane*** whereas Oxz is said to be the ***sagittal plane***. Due to the refraction law, the rays which are present in the plane Oyz before meeting $\mathbb{S}$ remain in this plane after crossing $\mathbb{S}$. They are called ***meridional*** or ***tangential rays*** whereas the rays that lie in the plane Oxz are said to be ***sagittal rays*** (see Figures 1.7 and 1.8). All the other rays are called ***skew rays***.

The region containing the object, which by convention is always supposed positioned on left-hand side of $\mathbb{S}$, is the ***object space*** whereas the region containing the image formed by $\mathbb{S}$ is the ***image space***.

If π_e is the above mentioned auxiliary plane in the object space, then any ray r coming from the point (x, y) in the object plane π is completely determined by providing the Cartesian coordinates (x_e, y_e) or the polar coordinates (r, φ) of the

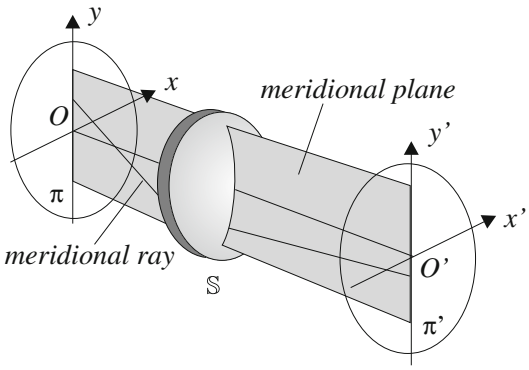

Fig. 1.7 Meridional rays

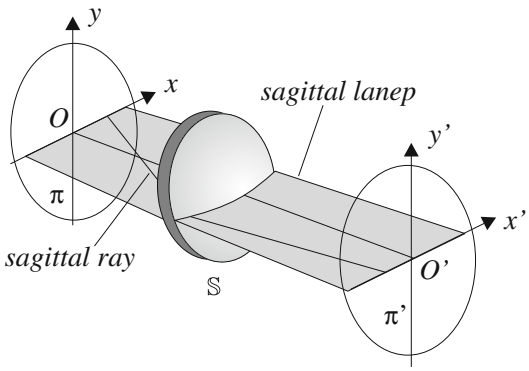

Fig. 1.8 Sagittal rays

point at which r intersects with π_e. Let (x', y') be the point of the image plane π' reached by r. Using these notations, we can say that the system $\mathbb{S}$ is ideal if

$$\begin{aligned} x' &= Mx, \\ y' &= My, \end{aligned} \tag{1.9}$$

where M, which is called the ***magnification*** of $\mathbb{S}$ with respect to the pair of conjugate planes π and π', is independent of (x, y), (x_e, y_e), and the wavelength of light λ (i.e., of the object point, the ray, and the wavelength).

In other words, an optical system is ideal if the the following properties hold:

- The image of the object is planar and does not exhibits distortion;
- Any point of the object and its corresponding point on the image are stigmatic.
- The above properties are independent of the wavelength of light λ.

In the following chapter it is shown that, *for a given wavelength λ and object plane π*, any centered optical system is almost ideal; in other words, there is a unique image plane π'—termed the ***Gaussian image plane***—for which the first two of the above properties are true, at least for points on the object and image belonging to

two small neighborhoods of π and π', around the optical axis (***Gaussian or paraxial approximation***). However, in this case, both the position of the ideal image plane π' and the magnification depend on λ.

Remark 1.2 The above definition of an ideal system, which is based on geometric optics, is too restrictive since it does not take into account the wave character of light. In fact, as we shall see in Chapter 3, due to the wave nature of light propagation, the light rays from an object point $\mathbf{x} \in \pi$ do not converge at the same image point $\mathbf{x}' \in \pi'$. They are actually spread in a complex way over a small circle, which is called ***Airy's disk***. Consequently, the optical system will be ***perfect*** if the geometric spot produced by the rays from $\mathbf{x} \in \pi$ is contained in the Airy disk. When this happens, the optical system is said to be ***diffraction limited***. Finally, if the optical combination is designed for photographic aims, the lowest limit of the geometric spot is represented by the grain of the film or the size of pixels of the ccd.

1.3 Axial Chromatic Aberrations

Let us suppose that the paraxial approximation can be applied to the optical system we are considering.

In this approximation, the dependence of the image plane π' on the wavelength λ results in ***axial chromatic aberration***. If the image plane π'_b corresponding to blue light is closer to the optical system $\mathbb{S}$ than the image plane π'_r corresponding to red light, then the axial chromatic aberration is said to be ***undercorrected***; in the opposite case it is ***overcorrected***. Denoting the distances of π'_b and π'_r from the last surface of $\mathbb{S}$ by z'_b and z'_r, respectively, the difference

$$\mathrm{PAC} = z'_b - z'_r, \tag{1.10}$$

is called ***primary axial color***, abbreviated to PAC.

The optical system $\mathbb{S}$ is said to be ***achromatic*** if $\pi'_b \equiv \pi'_r$. Since the refractive index depends on the wavelength, generally speaking the image planes for different colors do not coincide. This circumstance causes the ***secondary spectrum***. An optical system is said to be ***apochromatic*** when the image planes corresponding to three colors (for instance, blue, red, and green) coincide.

Another important paraxial chromatic aberration is the ***primary lateral color***. This is related to the dependence of the magnification $M(\lambda)$ on the wavelength λ. Consequently, the size of the blue image is not equal to the size of the red image. This aberration is defined by the difference:

$$PLC = (M(\lambda_b) - M(\lambda_r))y, \tag{1.11}$$

where λ_b, λ_r are the wavelengths of blue and red light, respectively, and y is the height of the object on the optical axis.

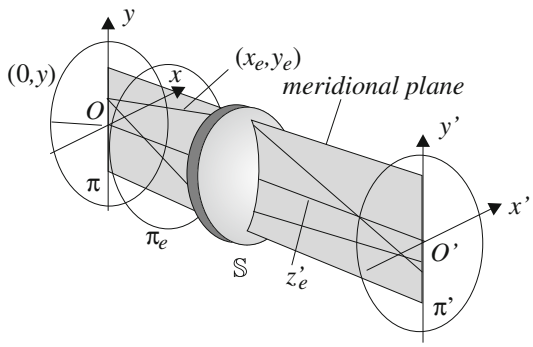

Fig. 1.9 Meridional rays, object plane, entrance pupil, and image plane

Other chromatic defects derive from the dependence of the monochromatic aberrations on the wavelength. These aberrations will be discussed in the next section.

1.4 Monochromatic Aberrations

In this section we suppose that:

- *the wavelength of the light is fixed*
- *the paraxial approximation is not verified*
- *the plane π' is the Gaussian image plane corresponding to the fixed wavelength.*

In order to define a ray from the object point (x, y), we can give the cosines of the angles that it forms with the axes. Equivalently, if we introduce an auxiliary plane π_e,[1] the ray is defined by the coordinates (x, y) of the object point from which it originated as well as by the Cartesian coordinates (x_e, y_e) or the polar coordinates (r_e, φ_e) of the point at which it intersects π_e (see Figure 1.9). In general, the coordinates (x', y') of the point at which a ray from (x, y) meets the image plane π' depend on both the object point and the ray, that is

$$x' = f_x(x, y, x_e, y_e) = g_x(x, y, r_e, \varphi_e),$$
$$y' = f_y(x, y, x_e, y_e) = g_y(x, y, r_e, \varphi_e).$$

The functions,

$$\epsilon_x = x' - Mx, \tag{1.12}$$
$$\epsilon_y = y' - My, \tag{1.13}$$

[1] In what follows, π_e will correspond to the Gaussian entrance pupil of the optical system.

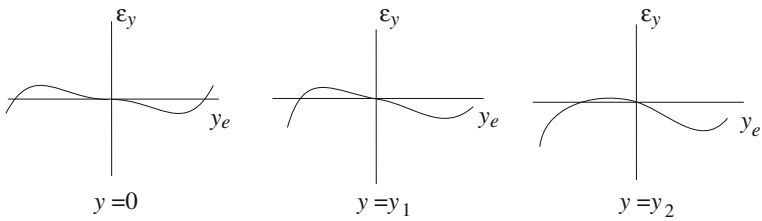

Fig. 1.10 Ray-intercept curves

which describe the departure of the optical system from the ideal behavior, are called ***monochromatic aberration functions***.

It is very important to know these functions in order to control or eliminate the aberrations in an optical system. However, only the first terms of Taylor's expansion of functions (1.12) and (1.13) are known.[2] If the third-order powers of the independent variables are taken into account, Von Seidel–Schwarzschild's third-order aberration theory is obtained, whereas Buchdal's aberration theory also includes the fifth-order powers. The third-order aberrations will be discussed in the next chapters, together with many applications. We also discuss the fifth-order aberrations just to show how difficult is their formulation.

Another way to analyze a *given* optical system is through ***ray tracing***. This method is easy to perform using today's powerful computers. Essentially, it involves computing the ***exact*** trajectories of rays through a ***given*** optical system $\mathbb{S}$ using the refraction law at any surface of $\mathbb{S}$. In this way, the point (x', y') at which any ray meets the image plane π' can be determined (see Section 1.6). Using this procedure it is possible to obtain very accurate representations of the aberrations. For instance, consider an object point $(0, y)$. If only meridional rays are analyzed, starting from $(0, y)$, then $\epsilon_x = 0$ and the aberration function ϵ_y depends only on the variables y and y_e (see Figure 1.10):

$$\epsilon_y = f_y(y, y_e) - My. \tag{1.14}$$

This equation, for a fixed y, defines a curve of the plane y_e, ϵ_y, called ***ray-intercept curve***, which supplies the displacement along $O'y'$ with respect to the ideal image $(0, My)$ of the all meridional rays starting from the object point $(0, y)$. For an ideal system, it reduces to a straight line that passes through the origin with a zero slope. This curve is usually traced for meridional rays starting from an object point on the optical axis and for two other points $(0, y_1)$, $(0, y_2)$, where y_2 corresponds to the greatest ordinate of the object and y_1 to a fraction of y_2, usually $0.7y_2$.

If we consider a set of rays coming from $(0, y)$ and intercepting the plane π_e along the $Ox-$axis, then the functions (1.12) reduce to:

$$\epsilon_x = f_x(y, x_e). \tag{1.15}$$

[2] In the next sections we prove that only odd powers of the variables x, y, x_e, y_e appear into Taylor's expansion of (1.12) and (1.13).

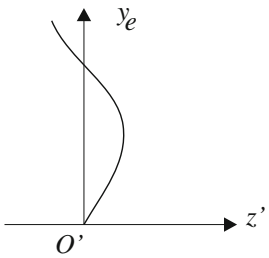

Fig. 1.11 Longitudinal spherical aberration curve

Again, for a fixed y, relation (1.15) defines a curve in the plane x_e, ϵ_x, which, due to symmetry of the optical system, is symmetric with respect to the ϵ_x−axis. Then, it is sufficient to represent it only in the region $x_e > 0$.

Also important is the ***longitudinal spherical aberration curve***. Consider the rays that come from the object point (0, 0) on the optical axis and lying in the meridional plane Oyz. Each of these rays, which cross π_e at $(0, y_e)$, meets the optical axis at a distance z' from the last surface of the system $\mathbb{S}$, which depends only on y_e. The longitudinal spherical aberration curve is just the locus of all points (z', y_e) (see Figure 1.11).

It is important to remark that all these curves can be plotted for different colors.

Finally, if we choose a certain number of rays and some wavelengths, then, the set of the points at which these rays intersect the image plane provides a useful representation of the aberrations of a given system; this is called a ***spot diagram***. Many examples of spot diagrams will be shown in the next chapters.

1.5 Surfaces of Revolution

In this section the basic aspects of the surfaces of revolution will be reviewed, since such surfaces are the type most frequently used in optical systems. A ***surface of revolution*** S is obtained by rotating a curve γ about an axis z which is called the symmetry axis of S. The intersection of S with any plane π containing z is a curve, and the equation of this curve always takes the same form $z = z(\rho)$, where ρ is the distance from z of any point on γ (see Figure 1.12). Due to the symmetry of S, the curve γ is an even function of ρ:

$$z(\rho) = z(-\rho). \tag{1.16}$$

We now suppose that S is obtained by rotating a ***conic*** γ about the axis z. There are many ways to define such a curve. First, a conic is obtained by intersecting a cone with a plane. It can also be defined as the locus of the points P such that the ratio e of their distances from a straight line a and a point $F \notin a$ is constant. The straight line a, the point $F \equiv (0, c)$, and the constant e are called ***directrix***,

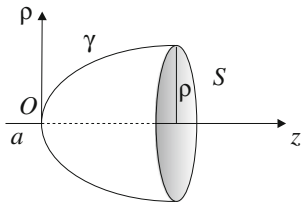

Fig. 1.12 Surface of revolution

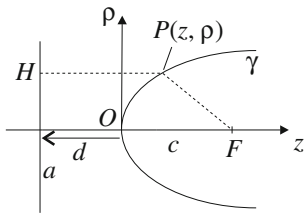

Fig. 1.13 A possible definition of a conic

focus, and ***eccentricity*** of γ, respectively. If P is any point of γ, then it results (see Figure 1.13):

$$\frac{PF}{PH} = \frac{\sqrt{(z-c)^2+\rho^2}}{|\, z-d \,|} = e > 0. \tag{1.17}$$

In particular, when $P \equiv O$, we have

$$e = \frac{c}{|d|} > 0 \Rightarrow d = -\frac{c}{e}. \tag{1.18}$$

Equation (1.17) can also be written in the form

$$z^2(1-e^2) - 2(c - d\,e)z + c^2 - d^2e^2 + \rho^2 = 0,$$

and taking into account (1.18), it can be reduced to the condition

$$(1-e^2)z^2 - 2c(1+e)z + \rho^2 = 0.$$

In turn, using the relation

$$c(1+e) = 2f, \tag{1.19}$$

this becomes

$$(1-e^2)z^2 - 4fz + \rho^2 = 0. \tag{1.20}$$

It is more convenient to introduce the ***conic parameter***

$$K = -e^2 < 0,$$

which allows us to write (1.20) as follows

$$(1+K)z^2 - 4fz + \rho^2 = 0. \tag{1.21}$$

In particular, when $K = -1$, we have the equation of a ***parabola***

$$z = \frac{\rho^2}{4f}. \tag{1.22}$$

In the other cases, we have the equivalent explicit form

$$z = \frac{2f \mp \sqrt{4f^2 - \rho^2(1+K)}}{1+K}. \tag{1.23}$$

Through analysis it can be shown that the radius of curvature R of a curve $z = z(\rho)$ at the origin is expressed by the following relation

$$\frac{1}{R} = \frac{|z^{(2)}(0)|}{(1+z'(0))^{3/2}}, \tag{1.24}$$

which, when applied to (1.23) yields

$$\frac{1}{R} = \frac{1}{2f} \Leftrightarrow f = \frac{R}{2}. \tag{1.25}$$

Finally, in terms of the radius of curvature R at the vertex, (1.22) and (1.23) assume the form

$$\begin{aligned} z &= \frac{\rho^2}{2R}, \\ z &= \frac{R \mp \sqrt{R^2 - \rho^2(1+K)}}{1+K}. \end{aligned} \tag{1.26}$$

Table 1.1 describes the classification scheme for quadric surfaces of revolution S:

It is worthwhile to note that we obtain the sag z of the points of the quadric S that are close to the origin if we adopt the sign—in (1.26) and the points of S far from

Table 1.1 Classification of conics

Parameter K	Eccentricity	Surface
$K = 0$	$e = 0$	sphere
$-1 < K < 0$	$0 < e < 1$	ellipsoid
$K = -1$	$e = 1$	paraboloid
$K < -1$	$e > 1$	hyperboloid

the origin if we choose the sign $+$. From now on we choose the sign—since we are interested in the points of S close to the origin. In literature this equation is often written in the form

$$z = \frac{c\rho^2}{1 + \sqrt{1 - (1 + K)c^2\rho^2}} \tag{1.27}$$

that can be obtained from (1.26) multiplying the numerator and the denominator of (1.26) by $R + \sqrt{R^2 - (1 + K)\rho^2}$ and introducing the curvature $c = 1/R$ of S at its vertex. Note that (1.27) includes the paraboloid ($K = -1$). Finally, the equation of any aspheric surface of revolution is written as follows

$$z = \frac{c\rho^2}{1 + \sqrt{1 - (1 + K)c^2\rho^2}} + a_4\rho^4 + a_6\rho^6 + \cdots \tag{1.28}$$

In the following, we frequently use the approximate form of a quadric surface of revolution, which is derived by Taylor's expansion of Equation (1.26) when the sign minus is chosen

$$z = \frac{\rho^2}{2R} + \frac{(1 + K)\rho^4}{8R^3} + \frac{(1 + K)^2\rho^6}{16R^5} + \cdots . \tag{1.29}$$

Finally, an arbitrary aspheric surface of revolution is obtained by arbitrarily assigning the constants c_4, c_6. In conclusion, the most general Taylor expansion is

$$z(\rho) = \frac{\rho^2}{2R} + \left(\frac{1 + K}{8R^3} + a_4\right)\rho^4 + \left(\frac{(1 + K)^2}{16R^5} + a_6\right)\rho^6 + \cdots . \tag{1.30}$$

We conclude with the following remarks:

- Up to second order, all the surfaces of revolution differ only for the curvature radius at the vertex;
- The paraboloid is exactly represented by the first term of the expansion (1.30).

In some cases, it is more convenient to represent any surface of revolution by the equation

$$z = \frac{1}{2R}\rho^2 + \overline{a}_4\rho^4 + \overline{a}_6\rho^6 \cdots , \tag{1.31}$$

where

$$\overline{a}_4 = \frac{1 + K}{8R^3} + a_4, \ \overline{a}_6 = \frac{(1 + K)^2}{16R^5} + a_6. \tag{1.32}$$

1.6 Ray Tracing in Axially Symmetric Systems

All of the graphical representations of the aberrations described in Section 1.4 are based on following the path of a ray across the whole optical system $\mathbb{S}$.

The optical system $\mathbb{S}$ is assumed to contain n surfaces of revolution S_i, $i = 1, \ldots, n$. We denote by N_i and N_{i+1} the refractive indices of the media before and after S_i, respectively. Finally, t_i represents the distance between S_i and S_{i+1} along the optical axis, i.e., the distance between their vertices. A ***single*** Cartesian coordinate system O_1xyz is introduced that has its origin O_1 at the vertex of S_1 and the O_1z-axis along the optical axis (see Figure 1.14). We denote with z the distance of the object plane from S_1, provided that it is situated at a finite distance from S_1. Finally, w_e is the distances of the reference plane π_e (see Section 1.2)[3] from S_1 and z' denotes the distance of the image plane from the last surface S_n of $\mathbb{S}$. *The sign of the all above quantities is evaluated using the rules of analytical geometry.*

Based on the results of the previous section, the equation $z = f_i(x, y)$ of any surface S_i is

$$
\begin{aligned}
z &= \sum_{j=1}^{i-1} t_j, \quad \text{if } S_i \text{ is planar,} \\
z &= \sum_{j=1}^{i-1} t_j + \frac{x^2 + y^2}{2R_i}, \quad \text{if } K_i = -1 \text{ (paraboloid),} \\
z &= \sum_{j=1}^{i-1} t_j + \frac{R_i \mp \sqrt{R_i^2 - (1 + K_i)(x^2 + y^2)}}{1 + K_i}, \quad \text{if } K_i \neq -1, \\
z &= \sum_{j=1}^{i-1} t_j + \overline{a}_{4,i}(x^2 + y^2) + \overline{a}_{6,i}(x^2 + y^2)^2, \\
&\quad \text{if } S_i \text{ is any aspheric surface.}
\end{aligned}
\tag{1.33}
$$

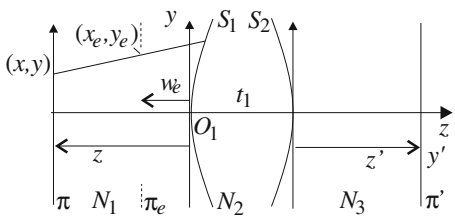

Fig. 1.14 Adopted notations

[3] As we have already said in Section 1.2, this plane will be identified with the plane π_e of entrance pupil of the system (see Section 2.4).

In the third equation, we choose the minus sign when $R_i > 0$ and the plus sign in the opposite case.

In order to follow the path of a ray Γ across $\mathbb{S}$, we must first determine its equations before it intersects with the first surface S_i of $\mathbb{S}$. If the object is situated at a finite distance from the first surface of the optical system $\mathbb{S}$, the object point (x, y) can be identified together with the point of the reference plane π_e intercepted by the ray. Based on these quantities, we evaluate the director cosines α_1, β_1, and γ_1 of Γ, oriented according to the direction of propagation of the light:

$$\begin{aligned}
\alpha_1 &= \frac{x_e - x}{\sqrt{(x_e - x)^2 + (y_e - y)^2 + (w_e - z)^2}}, \\
\beta_1 &= \frac{y_e - y}{\sqrt{(x_e - x)^2 + (y_e - y)^2 + (w_e - z)^2}}, \\
\gamma_1 &= \frac{w_e - z}{\sqrt{(x_e - x)^2 + (y_e - y)^2 + (w_e - z)^2}}.
\end{aligned} \tag{1.34}$$

If the object is at infinity, Γ is assigned by the director cosines α_1, β_1, and γ_1 and the coordinates (x_e, y_e).

In both cases, the parametric equations of the ray Γ write:

$$\begin{aligned}
\xi_1 &= x_e + \alpha_1 s, \\
\eta_1 &= y_e + \beta_1 s, \\
\zeta_1 &= w_e + \gamma_1 s,
\end{aligned} \tag{1.35}$$

where (ξ_1, η_1, ζ_1) are the coordinates of the moving point on Γ and s is a parameter that coincides with the distance between (x_e, y_e, w_e) and (ξ_1, η_1, ζ_1). Recall that the director cosines are not independent since they satisfy the condition $\alpha_1^2 + \beta_1^2 + \gamma_1^2 = 1$.

Now, in order to determine the intersection point $P_1 \equiv (x_1, y_1, z_1)$ between Γ and S_1, the following equation must be solved

$$w_e + \gamma_1 s = f_1(x_e + \alpha_1 s, y_e + \beta_1 s), \tag{1.36}$$

which supplies the value of s corresponding to P_1. This equation is not linear, so that we must apply Newton's method to solve it. However, this method requires that we know an approximated value of the solution. To this end, it is sufficient to consider the point of intersection P_1^* of the ray with the tangent plane π_1^* to S_1 at its vertex. The value s_1^* of the parameter corresponding to P_1^* is obtained by putting $\zeta_1 = 0$ into the third equation (1.35) and solving the resulting equation with respect to s:

$$s_1^* = -\frac{w_e}{\gamma}. \tag{1.37}$$

Starting from this value of the parameter, it is possible to determine the solution s_1 of (1.36) by Newton's method. Then, the coordinates of P_1 result the following:

$$\begin{aligned} x_1 &= x_e + \alpha_1 s_1, \\ y_1 &= y_e + \beta_1 s_1, \\ z_1 &= w_e + \gamma_1 s_1, \end{aligned} \tag{1.38}$$

To follow the ray Γ across $\mathbb{S}$, it is sufficient to prove that—assuming the equations of Γ before the surface S_i of $\mathbb{S}$ are known together with the point $P_i \equiv (x_i, y_i, z_i) \in S_i$ at which it intersects S_i—it is possible to find the parametric equations of the ray Γ arriving at $P_{i+1} \equiv (x_{i+1}, y_{i+1}, z_{i+1}) \in S_{i+1}$.

First, the refraction law at P_i must be applied. To this end, we consider the components of the unit normal to S_i at P_i, oriented in the direction of propagation of the light:

$$\begin{aligned} n_{i,x} &= -\mu_i \frac{\partial f_i}{\partial x}, \\ n_{i,y} &= -\mu_i \frac{\partial f_i}{\partial y}, \\ n_{i,z} &= \mu_i, \end{aligned} \tag{1.39}$$

where

$$\mu_i = \frac{1}{\sqrt{1 + \left(\frac{\partial f_i}{\partial x}\right)^2 + \left(\frac{\partial f_i}{\partial y}\right)^2}}. \tag{1.40}$$

The following quantities can now be determined at P_i (see (1.3) and (1.4)):

$$\begin{aligned} &\cos i_i = n_{i,x}\alpha_i + n_{i,y}\beta_i + n_{i,z}\gamma_1, \quad \sin i_i = \sqrt{1 - \cos^2 i_i}, \\ &\lambda_i = N_{i+1}\sqrt{1 - \frac{N_i^2}{N_{i+1}^2}\sin^2 i_i} - N_i \cos i_i, \end{aligned} \tag{1.41}$$

and the director cosines of the refracted ray become

$$\begin{aligned} \alpha_{i+1} &= \frac{1}{N_{i+1}}\left(N_i\alpha_i + \lambda_i n_{i,x}\right), \\ \beta_{i+1} &= \frac{1}{N_{i+1}}\left(N_i\beta_1 + \lambda_i n_{i,y}\right), \\ \gamma_{i+1} &= \frac{1}{N_{i+1}}\left(N_i\gamma_i + \lambda_i n_{i,z}\right). \end{aligned} \tag{1.42}$$

Consequently, the parametric equations of the refracted ray are:

$$\begin{aligned} \xi_{i+1} &= x_i + \alpha_{i+1} s, \\ \eta_{i+1} &= y_i + \beta_{i+1} s, \\ \zeta_{i+1} &= z_i + \alpha_{i+1} s. \end{aligned} \tag{1.43}$$

This ray meets the tangent plane π^*_{i+1} to S_{i+1} at its vertex when the parameter s has the value:

$$s^* = \frac{1}{\alpha_{i+1}} (\sum_{j=1}^{i} t_j - z_i). \tag{1.44}$$

The procedure which we have described can be iterated starting from these last equations.

1.7 Exercises

1. Show that Fermat's principle implies the refraction law.
   Let $\mathbf{x}_0$ and $\mathbf{x}_1$ be two arbitrary points in two media with constant refractive indices N and N', respectively. Moreover, let S denote a regular surface that separates these two media. According to Fermat's principle, any ray from $\mathbf{x}_0$ to $\mathbf{x}_1$ follows a rectilinear path γ_0 from $\mathbf{x}_0$ to a point $\mathbf{x} \in S$, and another rectilinear path γ_1 from $\mathbf{x}$ to $\mathbf{x}_1$. Moreover, the point $\mathbf{x}$ must be determined under the condition that the optical path length OPL along $\gamma_0 \cup \gamma_1$ is stationary with respect to all of the broken lines with the same end points. Consequently, if $F(\mathbf{x}) = 0$ denotes the equation of S and

$$G(\mathbf{x}) = N \sqrt{\sum_{i=1}^{3} (x_i - x_{0i})^2} + N' \sqrt{\sum_{i=1}^{3} (x_{1i} - x_i)^2} \tag{1.45}$$

   is the optical path length, we must minimize the function

$$G + \lambda F,$$

   where λ is a suitable Lagrangian multiplier. Consequently, we have the necessary condition

$$\nabla G + \lambda \nabla F = \mathbf{0}$$

   which can also be written as follows

$$\nabla G - \lambda \mathbf{n} |\nabla F| \equiv \nabla G + \mu \mathbf{n} = \mathbf{0}, \tag{1.46}$$

where $\mathbf{n}$ is the internal normal to S and μ is another Lagrangian multiplier. Since this relation implies

$$\mu = -\nabla G \cdot \mathbf{n}, \tag{1.47}$$

the condition (1.46) can also be written in the form

$$\nabla G - (\nabla G \cdot \mathbf{n})\mathbf{n} = \mathbf{0}, \tag{1.48}$$

and the following relation is obtained

$$\nabla G \times \mathbf{n} = \mathbf{0}. \tag{1.49}$$

On the other hand, from (1.45) we can easily derive the relation

$$\nabla G = N\mathbf{t} - N'\mathbf{t}', \tag{1.50}$$

being $\mathbf{t}$ and $\mathbf{t}'$ the unit vectors along γ_0 and γ_1, respectively. Results (1.50) and (1.49) can be put in the form

$$\begin{aligned} N\mathbf{t} - N'\mathbf{t}' &= -\mu\mathbf{n}, \\ N\mathbf{t} \times \mathbf{n} &= N'\mathbf{t}' \times \mathbf{n}. \end{aligned} \tag{1.51}$$

The first of these relations shows that γ_0, γ_1 and $\mathbf{n}$ are contained in the same plane, whereas the second one implies the refraction law.

2. Verify that the foci of an ellipsoidal mirror are stigmatic points.
   Consider a reflecting surface S that is an ellipsoid of revolution about the axis a. Let A, A' be its foci. If P is the point at which the ray from $\mathbf{x}$ meets the mirror, then, according to the definition of ellipsoid of revolution around a, it results (see Figure 1.15)

$$AP + PA' = \text{const.} \tag{1.52}$$

   The optical path length of any such a path between A and A' is thus independent of P and A, A'. Consequently, these paths are rays (see Section 1.1) and A, A' are stigmatic points.
3. Let S be a mirror whose surface is a paraboloid of revolution. Verify that all of the rays parallel to the axis of revolution a of S intercept a at the focus A of S

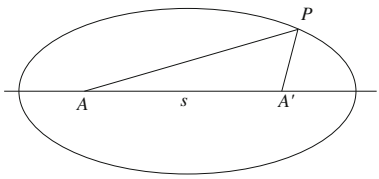

Fig. 1.15 Reflecting ellipsoid

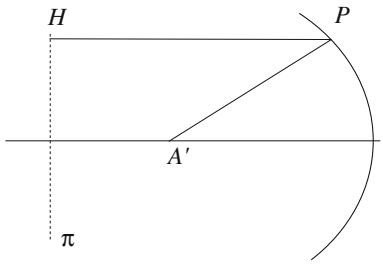

Fig. 1.16 Reflecting paraboloid

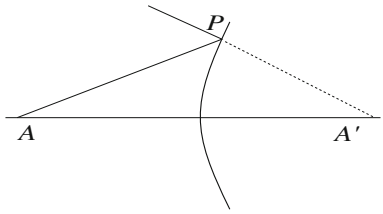

Fig. 1.17 Reflecting hyperboloid

(see Figure 1.16).
It is sufficient to consider an orthogonal plane π to a and to denote with H the point at which a ray meets π. If the definition of a paraboloid of revolution around a is taken into account

$$HP + PA' = \text{const.}, \tag{1.53}$$

we can conclude that, along any ray parallel to a, the optical path length from H to the focus a is constant.

4. Verify that the foci of an hyperbolic mirror are stigmatic points.
   The reflecting surface is a hyperboloid of revolution and A, A' are its foci (see Figure 1.17). Therefore,

$$AP - PA' = \text{const.} \tag{1.54}$$

   and the foci are stigmatic points.
5. Let S be a refractive surface of revolution separating two media with refractive indices N, N', and let a be the axis of S. Verify that two points A, A' of a, which are both located at a finite distance from S, are stigmatic if

$$N\ AP + N'\ PA' = \text{const.} \tag{1.55}$$

   The corresponding revolution refractive surface S is said to be an ovoid.

Chapter 2
Gaussian Optics

2.1 Gaussian Approximation for a Single Surface

In this chapter, we present the Gaussian analysis of an optical system $\mathbb{S}$. In particular, we introduce all of the optical characteristics of $\mathbb{S}$ (pupils, focal points, nodal points, principal planes, etc.). All these data can be obtained using the notebook ***TotalAberrations***.

Among the many potential ways of presenting this topic, we use Fermat's principle in order to introduce an approach that will be extended to third-order aberration theory.[1]

Let $\mathbb{S}$ be a single surface S with a symmetry of revolution about an axis a. N and N' denote the (constant) refractive indices of the media before and after S. Finally, let $Oxyz$ be a Cartesian frame of reference with $Oz \equiv a$ and the origin O located at the vertex of S (see Figure 2.1).

Note that Oyz is the meridional plane whereas Oxz is the sagittal plane (see Section 1.2).

Suppose that the object lies in a plane and denote by P a point of π. Finally, let π' be a plane in the image space. Due to the symmetry of S, it is always possible to choose P to be on the axis Oy, so it will have coordinates $(0, y, z)$. Consider the bundle Γ of polygonal lines γ that, starting from $(0, y, z)$, intersect S at the point (X, Y, Z) and the plane π' at $(0, My, z')$ (see Figure 2.2). In particular, the ray γ_0, which originates at $(0, y, z)$ and intersects S at its vertex, and the plane π' at $(0, My, z')$, belongs to Γ. We wish to know the conditions under which Γ is formed from *rays* or, equivalently, the points $(0, y, z)$ and $(0, My, z')$ are stigmatic (see Section 1.1).

Due to Fermat's principle and the remark 3 in Section 1.1, this happens if and only if the optical paths along the polygonal lines of Γ have the same value or, equivalently, if the following optical path difference vanishes:

[1] Another elementary way of introducing the paraxial optics is shown in Section 2.10 of this chapter.

© Springer International Publishing Switzerland 2016

A. Romano and R. Cavaliere, *Geometric Optics*,
Modeling and Simulation in Science, Engineering and Technology,
DOI 10.1007/978-3-319-43732-3_2

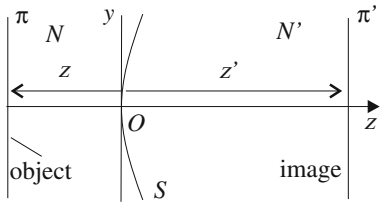

Fig. 2.1 Notations for a single surface

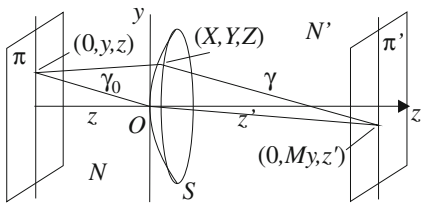

Fig. 2.2 γ and γ_0 rays

$$\begin{aligned}\Phi \equiv\ & N\sqrt{X^2+(Y-y)^2+(Z-z)^2}\\ &+N'\sqrt{X^2+(My-Y)^2+(z'-Z)^2}\\ &-N\sqrt{y^2+z^2}-N'\sqrt{M^2y^2+z'^2}=0\end{aligned} \tag{2.1}$$

for any choice of $(X, Y, Z) \in S$. It is very simple to verify that the quantities

$$\xi = y^2, \quad \eta = X^2+Y^2, \quad \zeta = yY, \tag{2.2}$$

are rotational invariants, i.e., they are invariant under an arbitrary rotation of the plane Oxy about the Oz-axis.[2] Introducing (2.2) into (2.1) we obtain

$$\begin{aligned}\Phi \equiv\ & N\sqrt{z^2+\eta-2\zeta+\xi-2zZ+Z^2}\\ &+N'\sqrt{z'^2+\eta-2M\zeta+M^2\xi-2z'Z+Z^2}\\ &-N\sqrt{z^2+\xi}-N'\sqrt{z'^2+M^2\xi}=0.\end{aligned} \tag{2.3}$$

This condition is analyzed here using the ***Gaussian or paraxial approximation*** which is defined as follows:

the optical path difference Φ ***among all the optical paths*** $\gamma \in \Gamma$ ***and*** γ_0 ***is constant to within second-order terms in the variables*** ξ, η ***and*** ζ ***or, equivalently, to within fourth-order terms in the variables*** y, X, Y.

In other words, we are supposing that the angles, that all of the rays that intersect with the surface S form with the optical axis a, as well as the distances of the object points from a, comply with the following condition: that the coordinates y, X, Y of

[2] In fact, ξ, η are the lengths of the vectors $\mathbf{u} = (0, y)$ and $\mathbf{v} = (X, Y)$ belonging to the plane Oxy and $\zeta = \mathbf{u} \cdot \mathbf{v}$.

all the points at which the rays intersect with the base-planes π, π' and the surface S are so small that, to a first approximation, it is possible to neglect the fourth-order powers of y, X, and Y in the optical paths.

In order to determine the consequences of (2.3), we start by noting that, due to the symmetry of revolution of S, the equation $Z = F(X, Y)$ of S necessarily takes the form

$$Z = F(X^2 + Y^2).$$

Consequently, in the Gaussian approximation, it can be written as follows (see Section 1.5):

$$Z = \frac{1}{2R}(X^2 + Y^2) = \frac{1}{2R}\eta, \tag{2.4}$$

where R denotes the curvature radius of S at its vertex O.

In view of Taylor's expansion

$$\sqrt{a^2 + x} = \pm a \pm \frac{x}{2a} + O(2), \tag{2.5}$$

where we take the sign + when $a > 0$ and the sign minus in the opposite case, from (2.3) we obtain

$$\Phi = \frac{1}{2}\left(\frac{N}{R} - \frac{N}{z} - \frac{N'}{R} + \frac{N'}{z'}\right)\eta + \left(\frac{N}{z} - M\frac{N'}{z'}\right)\zeta + O(2) = 0. \tag{2.6}$$

It is evident that the first-order terms vanish for any value of ξ, η, and ζ, if and only if

$$Q \equiv \frac{N}{R} - \frac{N}{z} = \frac{N'}{R} - \frac{N'}{z'}, \tag{2.7}$$

$$M \equiv \frac{y'}{y} = \frac{Nz'}{N'z}. \tag{2.8}$$

The following conclusions can be derived from the above equations:

1. The image of an object point along the axis Oy is located along the axis $O'y'$, for any (X, Y). Consequently, in this approximation, we only need to consider rays in this plane in order to obtain the image of a given object.
2. Relation (2.7) supplies the position of the image plane π' with respect to the surface S when S and the position of the object plane π are given. The quantity Q is called ***Abbe's invariant***. The planes π and π' are said to be ***conjugate*** when z and z' satisfy (2.7).
3. The ***magnification factor*** (2.8) is independent of y, meaning that the image is proportionally reduced if $|M| < 1$ and enlarged if $|M| > 1$. When $M < 0$, the image is inverted with respect to the object.

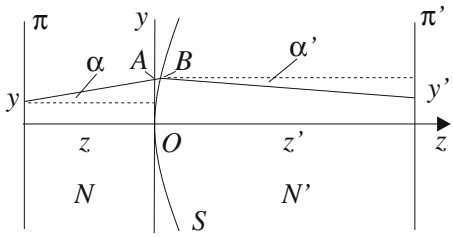

Fig. 2.3 Principal and marginal rays

We conclude this section by showing that, using the above results, it is possible to deduce the correspondence that exists between the angles α and α', which are the angles that a ray originating from an object point on y forms with the optical axis, before and after the refraction, respectively. The angles are supposed to be positive if the oriented optical axis coincides with the oriented ray after a counterclockwise rotation, negative in the opposite case[3].

In the Gaussian approximation, the points A and B in Figure 2.3 coincide and we have the relation

$$y - z\alpha = y' - z'\alpha', \tag{2.9}$$

which, in view of (2.8), can also be written as follows

$$\alpha' = \frac{1}{N'}\left(\frac{N}{z} - \frac{N'}{z'}\right) y + \frac{z}{z'}\alpha. \tag{2.10}$$

Taking into account (2.7), we finally obtain

$$\alpha' = -\frac{P}{N'} y + \frac{z}{z'}\alpha, \tag{2.11}$$

where

$$P = \frac{N' - N}{R}, \tag{2.12}$$

is the ***power*** of the surface S.

Equations (2.8) and (2.11) lead to the following system

$$y' = \frac{Nz'}{N'z} y,$$
$$\alpha' = -\frac{P}{N'} y + \frac{z}{z'}\alpha,$$

that, in view of (2.8), becomes

[3]Note that in the Figure 2.3, $z < 0$, $\alpha > 0$, $z' > 0$, $\alpha' < 0$.

$$\begin{aligned} y' &= My, \\ \alpha' &= -\frac{P}{N'}y + \frac{N}{N'}\frac{1}{M}\alpha. \end{aligned} \tag{2.13}$$

Remark 2.1 If θ and θ' denote the angles that the ray starting from (y, z) and reaching the vertex O of S forms with the optical axis before and after the refraction, the following relations hold:

$$y = \theta z, \quad y' = \theta' z',$$

and the equations (2.13) can equivalently be written as follows

$$\begin{aligned} y' &= Mz\theta, \\ \alpha' &= -\frac{P}{N'}z\theta + \frac{N}{N'}\frac{1}{M}\alpha. \end{aligned} \tag{2.14}$$

When the object is at infinity, (2.13) become meaningless and they can be replaced by (2.14). The corresponding value f' of z' is called the ***posterior focal length*** of the surface. From (2.7) we can derive

$$f' = \frac{N'}{P}, \tag{2.15}$$

and $(2.14)_1$ gives

$$y' = \frac{N}{P}\theta. \tag{2.16}$$

In particular, if S is a mirror, $N = -N' = 1$, $P = -2/R$, and we have

$$f' = \frac{R}{2}, \quad y' = -\frac{R}{2}\theta. \tag{2.17}$$

2.2 Compound Systems

Let $\mathbb{S}$ be an optical system containing n surfaces of revolution $S_1 \dots S_n$ with the same optical axis a. The distance and the refractive index between the surface S_i and the next surface S_{i+1} will be denoted by t_i and N_i', respectively. Finally, z_1 and z_n' represent the distances of the object plane π from S_1 and the distance of the image plane π' from S_n (see Figure 2.4).

By applying (2.7) and (2.13) to each surface S_i, we get

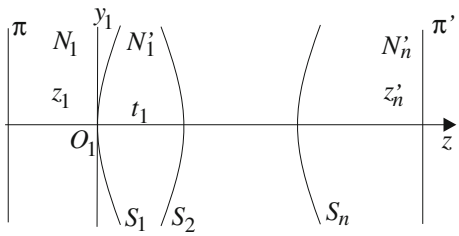

Fig. 2.4 Notations for a compound system

$$\frac{N_i}{R_i} - \frac{N_i}{z_i} = \frac{N'_i}{R_i} - \frac{N'_i}{z'_i}, \tag{2.18}$$

$$y'_i = M_i y_i, \tag{2.19}$$

$$\alpha'_i = -\frac{P_i}{N'_i} y_i + \frac{N_i}{N'_i}\frac{1}{M_i}\alpha_i, \tag{2.20}$$

and using the evident equations

$$y_{i+1} = y'_i, \tag{2.21}$$

$$z_{i+1} = z'_i - t_i, \tag{2.22}$$

$$\alpha_{i+1} = \alpha'_i, \tag{2.23}$$

$$N_{i+1} = N'_i, \tag{2.24}$$

it is possible to evaluate the path of any ray through the whole system $\mathbb{S}$.

Although the above formulae allow us to determine the image plane and the size of the image of any object in the Gaussian approximation, it is interesting to rewrite them in a form which gives prominence to some fundamental properties of a compound system $\mathbb{S}$. First, we write relations (2.19), (2.20) in the matrix form

$$\begin{pmatrix} y'_i \\ \alpha'_i \end{pmatrix} = \mathbb{T}_i \begin{pmatrix} y_i \\ \alpha_i \end{pmatrix}, \tag{2.25}$$

where

$$\mathbb{T}_i = \begin{pmatrix} M_i & 0 \\ -\dfrac{P_i}{N'_i} & \dfrac{N_i}{N'_i}\dfrac{1}{M_i} \end{pmatrix} = \begin{pmatrix} \dfrac{N_i z'_i}{N'_i z_i} & 0 \\ -\dfrac{P_i}{N'_i} & \dfrac{z_i}{z'_i} \end{pmatrix}. \tag{2.26}$$

In (2.26) we have taken into account (2.8). In conclusion, the linear map between the object plane π_1 and the image plane π'_n is obtained composing the n linear mappings (2.25)

$$\begin{pmatrix} y'_n \\ \alpha'_n \end{pmatrix} = \mathbb{T} \begin{pmatrix} y_1 \\ \alpha_1 \end{pmatrix}, \tag{2.27}$$

where the matrix $\mathbb{T}$

$$\mathbb{T} = \mathbb{T}_n \cdots \mathbb{T}_1 \tag{2.28}$$

has the following form

$$\mathbb{T} = \begin{pmatrix} M & 0 \\ A & \dfrac{N_1}{N_n'}\dfrac{1}{M} \end{pmatrix}. \tag{2.29}$$

Further,

$$M = M_1 \cdots M_n$$

is the total magnification factor of $\mathbb{S}$ and A is a convenient combination of the powers of the single surfaces S_i. For the sake of simplicity, we limit ourselves to prove (2.29) when $n = 2$. In this case, remembering the condition $N_1' = N_2$, we have that

$$\mathbb{T} = \begin{pmatrix} M_2 & 0 \\ -\dfrac{P_2}{N_2'} & \dfrac{N_2}{N_2'}\dfrac{1}{M_2} \end{pmatrix} \begin{pmatrix} M_1 & 0 \\ -\dfrac{P_1}{N_2} & \dfrac{N_1}{N_2}\dfrac{1}{M_1} \end{pmatrix}.$$

The product of the matrices on the left-hand side of the above equality gives

$$\mathbb{T} = \begin{pmatrix} M_1 M_2 & 0 \\ -\dfrac{1}{N_2'}\left(\dfrac{P_1}{M_2} + M_1 P_2\right) & \dfrac{N_1}{N_2'}\dfrac{1}{M_1 M_2} \end{pmatrix}$$

and (2.29) is proven.

Finally, the linear transformation (2.27) assume the final form

$$\begin{aligned} y_n' &= M y_1, \\ \alpha_n' &= A y_1 + \frac{N_1}{N_n'}\frac{1}{M}\alpha_1. \end{aligned} \tag{2.30}$$

2.3 Useful Decompositions of Matrix $\mathbb{T}$

In this section, we propose two important decompositions of the matrix $\mathbb{T}$. To this end, we first decompose the matrix $\mathbb{T}_i$ into the product of three matrices. In the Exercise 1 of this chapter the following identity is proven:

$$\mathbb{T}_i = \mathbb{D}_i^l \mathbb{R}_i \mathbb{D}_i^r, \tag{2.31}$$

where

$$\mathbb{D}_i^l = \begin{pmatrix} 1 & z_i' \\ 0 & 1 \end{pmatrix}, \qquad \mathbb{D}_i^r = \begin{pmatrix} 1 & -z_i \\ 0 & 1 \end{pmatrix}, \tag{2.32}$$

and

$$\mathbb{R}_i = \begin{pmatrix} 1 & 0 \\ -\dfrac{P_i}{N_i'} & \dfrac{N_i}{N_i'} \end{pmatrix}. \tag{2.33}$$

It is evident that the matrix $\mathbb{D}_i^r$ represents the linear transformation

$$y_i^* = y_i - z_i\alpha_i, \quad \alpha_i^* = \alpha_i, \tag{2.34}$$

determined by the rectilinear rays between the object plane π_i of S_i and the tangent plane π_i^* to S_i at its vertex. A similar meaning must be attributed to the matrix $\mathbb{D}_i^l$ which refers to the corresponding transformation between π_i^* and the image plane π_i' of S_i. In other words, in the decomposition (2.31), the linear transformation between π_i and π_i' is regarded as the combination of the following linear transformations:

1. $$y_i^* = y_i - z_i\alpha_i,$$
   $$\alpha_i^* = \alpha_i,$$
   between π_i and π_i^*,
2. $$y_i^{*\prime} = y_i^*,$$
   $$\alpha_i^* = -\frac{P_i}{N_i'}y_i^* + \frac{N_i}{N_i'}\alpha_i^*,$$
   between π_i^* and π_i^* itself, which takes into account the refraction that occurs at the surface S_i, and
3. $$y_i' = y_i^{*\prime} - z_i'\alpha_i^{*\prime},$$
   $$\alpha_i' = \alpha_i^{*\prime},$$
   between π_i^* and π_i'.

The above considerations allow us to conclude that the total transformation between π_1 and π_n' generated by the whole system $\mathbb{S}$ is described by the linear transformation

$$\begin{pmatrix} y_n' \\ \alpha_n' \end{pmatrix} = \begin{pmatrix} 1 & z_n' \\ 0 & 1 \end{pmatrix} \mathbb{M} \begin{pmatrix} 1 & -z_1 \\ 0 & 1 \end{pmatrix} \begin{pmatrix} y_1 \\ \alpha_1 \end{pmatrix}, \tag{2.35}$$

where

$$\mathbb{M} = \mathbb{R}_n \mathbb{D}_n^r \mathbb{D}_{n-1}^l \cdots \mathbb{D}_2^r \mathbb{D}_1^l \mathbb{R}_1. \tag{2.36}$$

The expression of $\mathbb{M}$ can be simplified by noting that, using (2.22) and (2.32), we have

$$\mathbb{D}_i \equiv \mathbb{D}_{i+1}^r \mathbb{D}_i^l = \begin{pmatrix} 1 & t_i \\ 0 & 1 \end{pmatrix}. \tag{2.37}$$

This matrix describes the linear transformation between the tangent planes π_i^* and π_{i+1}^* at the vertices of the surfaces S_i and S_{i+1}. In view of this result, we write the matrix $\mathbb{M}$ in the form

$$\mathbb{M} = \mathbb{R}_n \mathbb{D}_{n-1} \cdots \mathbb{D}_1 \mathbb{R}_1 = \begin{pmatrix} M_{11} & M_{12} \\ M_{21} & M_{22} \end{pmatrix}, \tag{2.38}$$

so that $\mathbb{M}$ is the composition of the all transformations (refractions at π_i^* and translations from π_i^* to π_{i+1}^*) inside the system $\mathbb{S}$ and, consequently, $\mathbb{M}$ ***depends only on the characteristics of*** $\mathbb{S}$. From (2.33), (2.37), and (2.38) it follows that

$$\det \mathbb{M} = \frac{N_1}{N_n'}. \tag{2.39}$$

We conclude this section writing (2.35) in another useful form. Consider the matrices

$$\mathbb{D}_1^r = \begin{pmatrix} 1 & -z_1 \\ 0 & 1 \end{pmatrix}, \quad \mathbb{D}_n^l = \begin{pmatrix} 1 & z_n' \\ 0 & 1 \end{pmatrix}. \tag{2.40}$$

The first matrix corresponds to the translation from the object plane π_1 to the first surface S_1 of the optical system $\mathbb{S}$. The second matrix corresponds to the translation from the last surface S_n of $\mathbb{S}$ to the image plane π_n'. Consider a plane $\overline{\pi}_1$ at a distance $\overline{z}_1$ from the first surface S_1 of S and a plane $\overline{\pi}_n$ at a distance $\overline{z}_n$ from the last surface S_n of $\mathbb{S}$ (see Figure 2.5). Translation $\mathbb{D}_1^r$ can be obtained as the composition of the translation from π_1 to $\overline{\pi}_1$ and the translation from $\overline{\pi}_1$ to π_1^*, which is tangent to S_1 at its vertex, that is

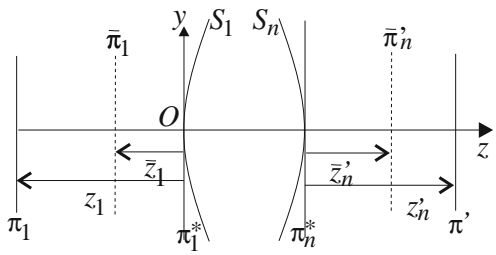

Fig. 2.5 A change of reference planes

$$\mathbb{D}_1^r = \begin{pmatrix} 1 & -\overline{z}_1 \\ 0 & 1 \end{pmatrix} \begin{pmatrix} 1 & -z_1 + \overline{z}_1 \\ 0 & 1 \end{pmatrix} \equiv \overline{\mathbb{D}}_1 \mathbb{L}_1. \tag{2.41}$$

Similarly, we can write

$$\mathbb{D}_n^l = \begin{pmatrix} 1 & -z_n' + \overline{z}_n \\ 0 & 1 \end{pmatrix} \begin{pmatrix} 1 & -\overline{z}_n \\ 0 & 1 \end{pmatrix} \equiv \mathbb{L}_n \overline{\mathbb{D}}_n. \tag{2.42}$$

Introducing (2.41) and (2.42) in (2.35), we finally get

$$\begin{pmatrix} \overline{y}_n' \\ \alpha_n' \end{pmatrix} = \begin{pmatrix} 1 & \overline{z}_n' \\ 0 & 1 \end{pmatrix} \mathbb{M} \begin{pmatrix} 1 & -\overline{z}_1 \\ 0 & 1 \end{pmatrix} \begin{pmatrix} \overline{y}_1 \\ \alpha_1 \end{pmatrix}, \tag{2.43}$$

for any pair of planes $\overline{\pi}_1$ *and* $\overline{\pi}_n'$.

2.4 Principal Planes and Focal Lengths

In this section and the next, the matrix formulation of the linear transformation between the object and image planes is shown to be very useful for defining some global properties of the optical system $\mathbb{S}$.

First, omitting the overline, the matrix equation (2.43) explicitly gives

$$\begin{aligned} y_n' &= (M_{11} + M_{21} z_n') y_1 \\ &\quad + (-M_{11} z_1 + M_{12} - M_{21} z_1 z_n' + M_{22} z_n') \alpha_1, \end{aligned} \tag{2.44}$$

$$\alpha_n' = M_{21} y_1 + (M_{22} - M_{21} z_1) \alpha_1. \tag{2.45}$$

The plane π_1 (whose distance from S_1 is z_1) and the plane π_n' (whose distance from S_n is z_n') are conjugate if y_n' is independent of α_1; in other words, if the following condition of stigmatism is valid

$$M_{12} - M_{11} z_1 - M_{21} z_1 z_n' + M_{22} z_n' = 0. \tag{2.46}$$

When the optical system $\mathbb{S}$ (i.e., the matrix $\mathbb{M}$) and the distance z_1 are given, it supplies the value of z_n' corresponding to the conjugate plane π_n'

$$z_n' = -\frac{M_{11} z_1 - M_{12}}{M_{21} z_1 - M_{22}}. \tag{2.47}$$

Moreover, the quantity

$$M = M_{11} + M_{21} z'_n = \frac{1}{M_{22} - M_{21} z_1}, \tag{2.48}$$

gives the total magnification of $\mathbb{S}$ with respect to the conjugate planes π and π'_n. For the last equality, we used (2.39) and (2.47).

In particular, from (2.47) we have

$$\lim_{z_1 \to \infty} z'_n = -\frac{M_{11}}{M_{21}} \equiv f'_b, \tag{2.49}$$

and the quantity f_b is called ***back focal*** of $\mathbb{S}$. The ***frontal focal*** f_f can be defined in a similar way.

Two conjugate planes π_p and π'_p are called ***anterior principal plane*** and ***posterior principal plane***, if the magnification related to them is equal to 1

$$M_{11} + M_{21} z'_n = 1. \tag{2.50}$$

From the conditions (2.47), (2.50), and (2.39), we obtain the following expressions for the distances z_p and z'_p of π_p and π'_p from the surfaces S_1 and S_n, respectively:

$$z_p = \frac{1}{M_{21}} \left(M_{22} - \frac{N_1}{N'_n} \right), \quad z'_p = \frac{1 - M_{11}}{M_{21}}, \tag{2.51}$$

Further, (2.44) and (2.45) become

$$y'_p = y_p, \tag{2.52}$$

$$\alpha'_p = M_{21} y_p + \frac{N_1}{N'_n} \alpha_p. \tag{2.53}$$

Moreover, the quantities (see (2.51) and (2.49))

$$f = f_f - z_p, \quad f' = f'_b - z'_p = -\frac{1}{M_{21}}, \tag{2.54}$$

are the ***anterior focal length*** and the ***posterior focal length***.

Finally, the ***nodal points*** are two *conjugate* points on the optical axis a ($y = 0$) such that any ray which intercepts one of them forming an angle α with a, intercepts the other one, forming the same angle with a. From (2.44) and (2.45), the values z_{nd} and z'_{nd}, which define these two points, are given by the system

$$z'_{nd} = -\frac{M_{11} z_{nd} - M_{12}}{M_{21} z_{nd} - M_{22}}, \quad M_{22} - M_{21} z_{nd} = 1. \tag{2.55}$$

Relations (2.52) and (2.53) show that the nodal points coincide with the intersections of the principal planes with a, if $N_1 = N_n'$.

An optical system $\mathbb{S}$ is said to be ***telescopic*** or ***afocal*** if $M_{21} = 0$, i.e., if $f' = \infty$.

2.5 Stops and Pupils

Predicting the Gaussian position and the size of the image produced by an optical system $\mathbb{S}$ is not the only important task of the paraxial analysis. It is equally important to establish the brightness of the image and the size of the field of view. These characteristics of the image are strongly conditioned by the presence of obstacles in the optical system as well as by the existence of lens rims, which control both the angular and spatial extension of the light beams.

Consider an object point P located on the optical axis of the system $\mathbb{S}$ and the collection c of all the rays emitted from P that pass through $\mathbb{S}$. The **aperture stop** AS is the stop that effectively controls the angular extension of c and consequently determines the amount of light arriving at the image. Figures 2.6, 2.7 and 2.8 show different positions of the aperture stop.

Let K^a be the part of the optical system $\mathbb{S}$ that is situated before the aperture stop; in other words, the part through which the light passes before meeting the aperture stop.

The image EnP of AS formed by K^a is called the **entrance pupil** of $\mathbb{S}$. Similarly, let K^b denote the part of $\mathbb{S}$ that light passes through after AS. The image ExP of AS formed by K^b is called the **exit pupil** (see Figures 2.7–2.9 and the exercises at the end of the chapter). A ray from an off-axis object P^* through the center of the entrance pupil is called a **principal ray**. Since AS, EnP and ExP are conjugate,

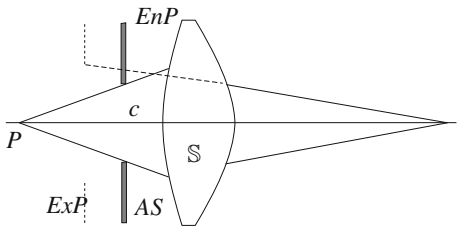

Fig. 2.6 Stop before the system

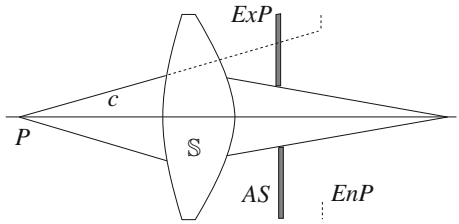

Fig. 2.7 Stop after the system

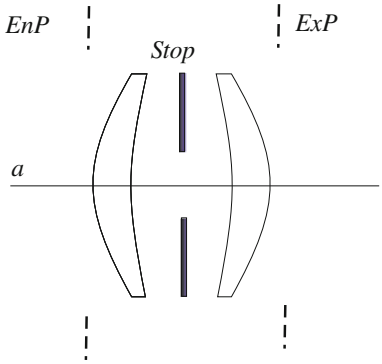

Fig. 2.8 Stop inside the system

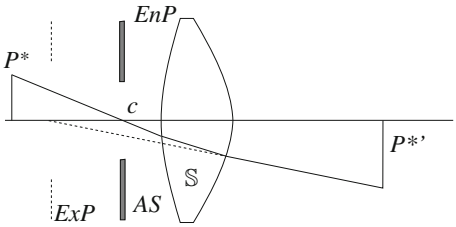

Fig. 2.9 Principal ray

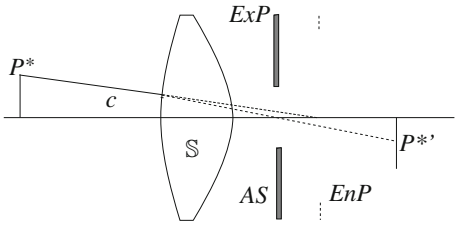

Fig. 2.10 Principal ray

the principal ray will intercept the optical axis at the centers of the pupils and at the aperture stop.

Figures 2.9 and 2.10 show the path of the principal ray for the same cases depicted in Figures 2.6 and 2.7. The presence of the aperture stop usually determines a different distribution of light on the image surface. This phenomenon is called the **vignetting**. Because of it, the intensity of the light decreases from the axis to the periphery of the image. Figure 2.11 shows why the vignetting occurs.

As the off-axis object point P^* is shifted away from the optical axis, the angular extension of the beam c' limited by the aperture stop reduces; moreover, this reduced amount of light is distributed over the same surface S which is not orthogonal to the axis of c'.

Upon increasing the distance of P^* from the axis still further, some of the beam c' is intercepted by the rim of the lens in the optical system, and so the light arriving at the image is further reduced.

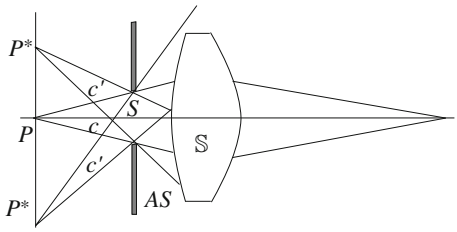

Fig. 2.11 Vignetting

2.6 Some Gaussian Optical Invariants

At the end of Section 2.2 we proved that the transformation between *any* pair of conjugate planes π_1 and π'_n assumes the form

$$y'_n = My_1, \quad \alpha'_n = Ay_1 + \frac{N_1}{N'_n}\frac{1}{M}\alpha_1. \tag{2.56}$$

When these relations refer to the conjugate principal planes, $M = 1$. Moreover, the ray intersecting the anterior principal plane at $y_1 = 0$ has a corresponding ray that crosses the posterior principal plane on the optical axis ($y'_n = 0$) and forms an angle with it of (see (2.56))

$$\alpha'_n = \frac{N_1}{N'_n}\alpha_1.$$

We find again that *if* $N_1 = N'_n$, *then the intersection points of the principal planes with a are also nodal points*.

Some important Gaussian invariants will now be derived. Let π, π' an arbitrary pair of object and image planes of the optical system $\mathbb{S}$ or of an arbitrary part S_p of $\mathbb{S}$. By π_e and π'_e we denote, respectively, the entrance and exit pupils of the considered part of $\mathbb{S}$. Due to (2.56), the marginal ray originating from O ($y = 0$, see Figure 2.12) and forming the angle α with the optical axis Oz will be transformed into the ray intersecting the optical axis at O' ($y' = 0$) and forming the angle α' with Oz, that in view of (2.56) is given by

$$\alpha' = \frac{N}{N'M}\alpha, \tag{2.57}$$

where M is the magnification relative to the conjugate planes π, π' and N, N' are the refractive indices before and after S_p, respectively. We now denote by y the starting point of the principal ray γ_p that intercepts the entrance pupil π_e at the point A and forms the angle α_p with Oz. This ray is transformed into the ray crossing the exit pupil π'_e at A' and the image plane π' at y'. Since it is

$$y' = My, \tag{2.58}$$

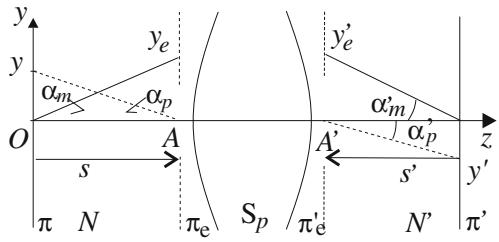

Fig. 2.12 Optical invariants

we obtain from (2.57) the ***Helmholtz-Lagrange invariant***

$$\mathfrak{H} \equiv N' y' \alpha'_m = N y \alpha_m, \tag{2.59}$$

which, with the notations of Figure 2.12, can also be written

$$\frac{N'_n y'_n y'_e}{s'} = \frac{N y y_e}{s}, \tag{2.60}$$

since in our approximation it is $\alpha = y_e/s$, $\alpha' = y'_e/s'$.

We can derive important consequences from (2.59), (2.60).

- First, exchange the role of the pairs of conjugate planes π, π' and π_e, π'_e. In other words, π_e, π'_e become the object and image planes whereas π, π' are the entrance and exit pupils. Consequently, the marginal ray Oy_e now becomes the principal ray and the principal ray yA is now the marginal ray. Equation (2.59) in this new interpretation gives

$$N' y'_e \alpha'_p = N y_e \alpha_p, \tag{2.61}$$

  where α_p denotes the angle that the principal ray forms with the optical axis and α'_p the corresponding angle in the exit pupil.
- Further, in view of (2.60) and (2.61), we obtain another optical invariant that is still named Lagrange invariant

$$\Gamma \equiv N'(y' \alpha'_m - y'_e \alpha'_p) = N(y \alpha_m - y_e \alpha_p), \tag{2.62}$$

- If the conjugate planes π_e and π'_e coincide, respectively, with the entrance and the exit pupils *of the whole system* $\mathbb{S}$, we have $y'_e = M_e y_e$, $y = y_1$, and $y' = y'_n$. From (2.60), we then derive

$$\frac{y'_n}{s'_n} = \frac{N_1}{N'_n} \frac{1}{M_e} \frac{y_1}{s_1}, \tag{2.63}$$

  where M_e is the magnification related to the pair π_e and π'_e. Since $y = -s\alpha_p$, $y' = -s'\alpha'_p$, the previous relation assumes the form

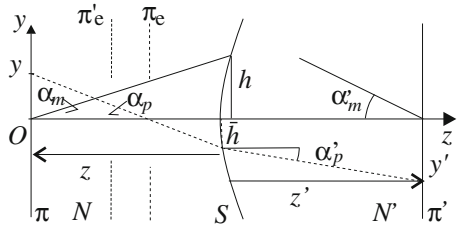

Fig. 2.13 Optical invariants

$$\alpha'_p = \frac{N}{N'}\frac{1}{M_e}\alpha_p. \tag{2.64}$$

- Moreover, if π_e and π'_e coincide, respectively, with the anterior and posterior principal planes π_p and π'_p *of the whole system* $\mathbb{S}$, the magnification related to this pair of planes is equal to unity, and (2.63) implies that

$$\frac{s}{y} = \frac{N}{N'}\frac{s'}{y'}. \tag{2.65}$$

If the object goes to infinity ($s, y \to \infty$) s' coincides with the posterior focal length f' of $\mathbb{S}$. Therefore, since $\alpha_p = -y/s$, from the previous relation we have

$$f' = -\frac{N'}{N}\frac{y'}{\alpha_p}. \tag{2.66}$$

- Finally, we apply the Lagrange invariant to a single dioptric S of $\mathbb{S}$ and use the notations of Figure 2.13. Due to the conventions about the sign of the optical quantities that we have introduced in Section 2.1, we have that y, α_m, h_m, z' are positive whereas z, h_p, y', α_p and α'_p are negative. Therefore, we obtain

$$y = \alpha_p z + \overline{h}, \quad y' = \alpha'_p z' + \overline{h}. \tag{2.67}$$

In view of (2.67), the Lagrange invariant (2.59) becomes

$$\mathfrak{H} \equiv N(h\alpha_p - \alpha_m\overline{h}) = N'(h\alpha'_p - \alpha'_m\overline{h}). \tag{2.68}$$

2.7 Gaussian Analysis of Compound Systems

It has already been emphasized that the transformation (2.44)–(2.45) can be used to determine the image formed by an axially symmetric optical system $\mathbb{S}$, provided that y_1, α_1 are first-order quantities. In other words, the results of the above transformation

are acceptable only for points next to the optical axis a and for rays which form small angles with a. However, the paraxial approximation is very important since the paraxial behavior of an optical system usually represents its ideal behavior. For this reason, defects or aberrations of $\mathbb{S}$ are defined as deviations from the paraxial response.

In this section, a complete Gaussian description of an optical system $\mathbb{S}$ is generated in detail using all of the considerations discussed in the above sections. The subject is presented in a way that facilitate its implementation in a programming language.

- First, the matrices (2.32) and (2.33)

$$\mathbb{R}_i = \begin{pmatrix} 1 & 0 \\ -\dfrac{P_i}{N_i'} & \dfrac{N_i}{N_i'} \end{pmatrix}, \tag{2.69}$$

$$\mathbb{D}_i = \begin{pmatrix} 1 & t_i \\ 0 & 1 \end{pmatrix}, \tag{2.70}$$

  have to be written for each surface of the system. They describe, respectively, the refraction at the surface S_i and the behavior of meridional rays in the space between S_i and S_{i+1}.
- Consequently, the matrices

$$\mathbb{B}_i = \begin{cases} \mathbb{D}_i \mathbb{R}_i, & i = 1, \ldots, n-1, \\ \mathbb{R}_n, & i = n, \end{cases} \tag{2.71}$$

  fully describe the behavior of meridional rays from S_i to S_{i+1}.
- Then, the three matrices

$$\mathbb{M} = \mathbb{B}_n \cdots \mathbb{B}_1, \tag{2.72}$$

$$\mathbb{M}^{(en)} = \mathbb{R}_k \mathbb{B}_{k-1} \cdots \mathbb{B}_1, \quad \mathbb{M}^{(ex)} = \mathbb{B}_n \cdots \mathbb{B}_{k+1}, \tag{2.73}$$

  must be evaluated. In (2.73) the index $k, 0 \leq k \leq n$, relates to last surface S_k before the stop. The matrix $\mathbb{M}$ describes the behavior of meridional rays throughout the whole system, whereas $\mathbb{M}^{(en)}$ and $\mathbb{M}^{(ex)}$ represent the action on these rays at the surfaces before and after the stop, respectively. It is worth noting that

$$\begin{aligned} \mathbb{M}^{(en)} &= \mathbb{I}, \qquad \text{if } k = 0, \\ \mathbb{M}^{(ex)} &= \mathbb{I}, \qquad \text{if } k = n. \end{aligned} \tag{2.74}$$

- The distances z_p and z_p' of the principal planes, respectively from the surface S_1 and S_n, are given by the relations (see (2.47) and (2.50))

$$z_p = \frac{M_{22} - 1}{M_{21}}, \quad z'_p = \frac{1 - M_{11}}{M_{21}}. \tag{2.75}$$

- Let t_s be the distance of the stop from the surface S_k. Since the entrance pupil π_e is the image of the stop formed by the surfaces which precede it, we evaluate the distance w_e of the entrance pupil from the surface S_1 using the formula of conjugate points (2.47)

$$w_e = \frac{M_{22}^{(en)} t_s + M_{12}^{(en)}}{M_{21}^{(en)} t_s + M_{11}^{(en)}}. \tag{2.76}$$

  If $k = 0$ (the whole system $\mathbb{S}$ follows the stop), note that, due to (2.66), $\mathbb{M}^{(en)}$ is the identity matrix and the above formula gives $w_e = t_s$. Moreover, if the stop is situated after the system $\mathbb{S}$, then $\mathbb{M}^{(en)} = \mathbb{M}$.
- Similarly, the distance t_{ex} of the stop from the surface S_{k+1} is given by

$$t_{ex} = \begin{cases} -t_s & \text{if } \ k = 0, \\ -(t_k - t_s) & \text{if } \ 0 < k. \end{cases}$$

  Then, the distance w'_e of the exit pupil from the last surface S_n results

$$w'_e = -\frac{M_{11}^{(ex)} t_{ex} - M_{12}^{(ex)}}{M_{21}^{(ex)} t_{ex} - M_{22}^{(ex)}}. \tag{2.77}$$

- If r_s denotes the radius of the aperture stop, the radii r_{en} and r_{ex} of the entrance and exit pupils are given by

$$r_{en} = \frac{r_s}{M_{11}^{(en)} + M_{21}^{(en)} t_s},$$
$$r_{ex} = r_s (M_{11}^{(ex)} + M_{21}^{(ex)} w'),$$

- The distance z'_n of the image from the last surface S_n of the whole system $\mathbb{S}$ is given by the usual formula of conjugate points

$$z'_n = -\frac{M_{11} z_1 - M_{12}}{M_{21} z_1 - M_{22}}, \tag{2.78}$$

  where z_1 denotes the distance of the object from S_1. In particular, when $z_1 \to \infty$, we obtain the back focal length f'_b

$$f'_b = -\frac{M_{11}}{M_{21}}, \tag{2.79}$$

  so that the posterior focal length f' is given by (see (2.54))

Fig. 2.14 View angle

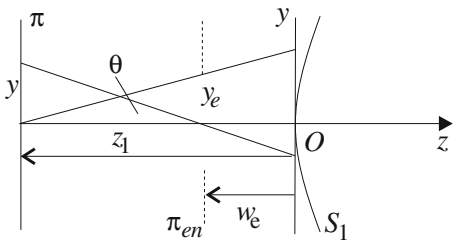

$$f' = f'_b - z'_{np}. \tag{2.80}$$

- Finally, we need to evaluate the heights of the marginal ray and the principal ray on each surface S_i as well as the angles they form with the optical axis. In the Figure 2.14 are represented the marginal and principal rays. It is easy to verify that the point at which these rays intercept the entrance pupil π_e as well as the angles that they form with the optical axis are given by the relations

$$\text{marginal ray} = \left(y_e, -\frac{y_e}{z_1 - w_e}\right), \tag{2.81}$$

$$\text{principal ray} = \left(0, \frac{y}{z_1 - w_e}\right). \tag{2.82}$$

In particular, if the object is situated at infinity, (2.81), (2.82) become

$$\text{marginal ray} = (y_e, 0)\,, \quad \text{principal ray} = (0, \theta)\,. \tag{2.83}$$

Consequently, the characteristics of these rays across the system are obtained by the relations

$$\begin{pmatrix} y'_i \\ \alpha'_i \end{pmatrix} = \mathbb{B}_i \cdots \mathbb{B}_1 \begin{pmatrix} 1 & -w_e \\ 0 & 1 \end{pmatrix} \begin{pmatrix} y \\ \alpha \end{pmatrix}, \tag{2.84}$$

where $i = 1, \ldots, n-1$ and the matrix

$$\begin{pmatrix} 1 & -w_e \\ 0 & 1 \end{pmatrix}, \tag{2.85}$$

describes the correspondence between the entrance pupil π_e and the tangent plane π_1^* at the vertex of S_1. In this formula (y, α) is one of the rays (2.81), (2.82) (or (2.83) if the object is at infinity). Finally, the equation

$$\begin{pmatrix} y'_n \\ \alpha'_n \end{pmatrix} = \begin{pmatrix} 1 & z'_n \\ 0 & 1 \end{pmatrix} \mathbb{M} \begin{pmatrix} 1 & -w_e \\ 0 & 1 \end{pmatrix} \begin{pmatrix} y \\ \alpha \end{pmatrix}, \tag{2.86}$$

where z'_n is the distance of the image plane from the last surface S_n, supplies the characteristic of the marginal and principal rays that cross the image plane.

The notebook ***TotalAberrations*** supplies all the Gaussian characteristic of a compound optical system.

2.8 A Graphical Method

When the characteristic points of $\mathbb{S}$ have been determined, it is possible to obtain graphically the image of an object with the simple procedure presented in this section. For the sake of simplicity, in the sequel we refer to the most common case $N_1 = N'_n$, in which the nodal and principal points coincide.

- Let y_1 be an object point and γ_0 be a ray parallel to a, in other words, a ray for which $\alpha_1 = 0$. Denote the point at which γ_0 (or its extension) meets the first principal plane π_p by y_p (see Figure 2.15)
  In the correspondence between the conjugate principal planes π_p and π'_p, the magnification is equal to 1. Consequently, at the exit of the whole optical system, the ray γ_0, or its extension, will meet the posterior principal plane π'_p at a point $y'_p = y_p$.
- The transformation (2.45) between the object plane and the posterior focal one π'_f, when the condition (2.38) is taken into account, is described by the following matrix:
  $$\begin{pmatrix} 1 & -\dfrac{M_{11}}{M_{21}} \\ 0 & 1 \end{pmatrix} \begin{pmatrix} M_{11} & M_{12} \\ M_{21} & M_{22} \end{pmatrix} \begin{pmatrix} 1 & -z_1 \\ 0 & 1 \end{pmatrix},$$
  which reduces to the form
  $$\begin{pmatrix} 0 & A \\ M_{21} & B \end{pmatrix},$$
  where A and B have suitable expressions. Consequently, the correspondence between the object plane and the focal one becomes

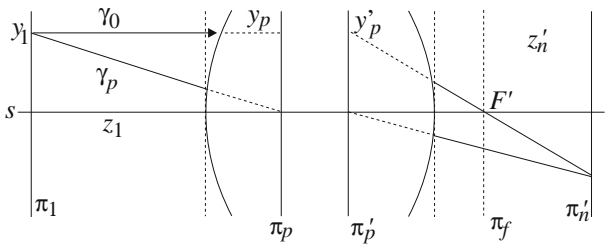

Fig. 2.15 Graphical construction of the image

$$y'_f = A\alpha_1,$$
$$\alpha'_f = M_{21}y_1 + B\alpha_1.$$

In particular, these relations imply that any ray that starts from the object point y_1 and is parallel to the optical axis a ($\alpha_1 = 0$), meets to the focal plane on a.

- The ray γ_p, directed towards the anterior principal point (or node), has a corresponding parallel ray that intersects with the posterior principal point (or node).

Using these properties, the paraxial image can be obtained in the way illustrated in the Figure 2.15.

When the refractive indices N and N' are different, it is sufficient to refer the last conclusion to the nodal points.

2.9 Thick and Thin Lenses

In this section, we consider an optical system $\mathbb{S}$ of a single lens in the air ($N = 1$). Let P_1 and P_2 be the powers, respectively, of the first surface S_1 and the second surface S_2 of $\mathbb{S}$. If t denotes the thickness of the lens and N its refractive index, then the effect of $\mathbb{S}$ on the rays of light is described by the matrix (see Section 2.3)

$$\mathbb{M} = \mathbb{R}_2\mathbb{D}_1\mathbb{R}_1, \tag{2.87}$$

where

$$\mathbb{R}_1 = \begin{pmatrix} 1 & 0 \\ -\dfrac{P_1}{N} & \dfrac{1}{N} \end{pmatrix}, \quad \mathbb{D}_1 = \begin{pmatrix} 1 & t \\ 0 & 1 \end{pmatrix}, \tag{2.88}$$

$$\mathbb{R}_2 = \begin{pmatrix} 1 & 0 \\ -P_2 & N \end{pmatrix}. \tag{2.89}$$

Therefore, $\mathbb{M}$ is the matrix

$$\mathbb{M} = \begin{pmatrix} 1 - \dfrac{P_1}{N}t & \dfrac{t}{N} \\ -P_1 - P_2 + \dfrac{P_1P_2t}{N} & 1 - \dfrac{P_2t}{N} \end{pmatrix}. \tag{2.90}$$

Formulae (2.75) and (2.90) give us the distance z_p of the first principal point from the vertex of S_1 and the distance z'_p of the second principal point from the vertex of S_2:

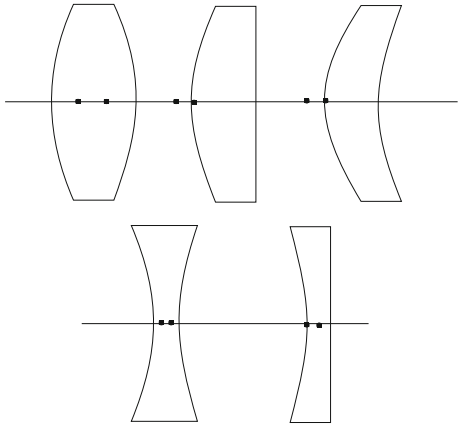

Fig. 2.16 Positions of principal points in thick lenses

$$z_p = \frac{P_2 t}{N(P_1 + P_2) - P_1 P_2 t}, \quad z'_p = -\frac{P_1 t}{N(P_1 + P_2) - P_1 P_2 t}. \tag{2.91}$$

Remembering (2.12), we have

$$P_1 = \frac{N-1}{R_1}, \quad P_2 = -\frac{N-1}{R_2}. \tag{2.92}$$

In view of (2.91) and (2.92), we easily verify that the principal points H_1 and H_2 of different kinds of thick lenses is positioned as it is shown by the black dots in Figure 2.16. Finally, the posterior and anterior focal lengths are equal since $N_1 = N'_2 = 1$. Due to (2.54), the focal length is given by

$$\frac{1}{f} = P_1 + P_2 - \frac{1}{N} P_1 P_2 t. \tag{2.93}$$

When the thickness t can be neglected in the above formulae, we say that S is a ***thin lens***. In this condition, (2.91), (2.93) reduce to

$$z_p = z'_p = 0, \tag{2.94}$$

and

$$\frac{1}{f} = P_1 + P_2 = (N-1)\left(\frac{1}{R_1} - \frac{1}{R_2}\right), \tag{2.95}$$

respectively.

2.10 A Different Approach to Gaussian Optics

In Section 2.1 we derived Gaussian optics starting from a single dioptric S and requiring that all of the stigmatic paths between the object point $(0, y, z)$ and the image point $(0, My, z')$ were rays up to fourth-order terms in the variables y, X, Y, where X and Y are the coordinates of the intersection point of a ray with S. In other words, we derived Gaussian optics by requiring that Fermat's principle were satisfied by all of the broken lines between $(0, y, z)$ and $(0, My, z')$ up to fourth-order terms in the variables y, X, Y. In this section, we present a more traditional approach to Gaussian optics (see, for instance, [5, 13]). According to the conventions we adopted in Section 2.1 about the sign of angles and distances, the quantities of Figure 2.17 have the following signs:

$$\begin{aligned} &\alpha > 0,\ \beta < 0,\ \alpha' < 0,\\ &z < 0,\ z' > 0,\ R > 0,\\ &\theta < 0,\ \theta' < 0,\ h > 0. \end{aligned}$$

From Figure 2.17 and elementary results of Euclidean geometry, we easily obtain

$$i = |\alpha| + |\beta| = \alpha - \beta, \tag{2.96}$$

$$r = |\beta| - |\alpha'| = -\beta + \alpha'. \tag{2.97}$$

In the paraxial approximation, the refraction law is

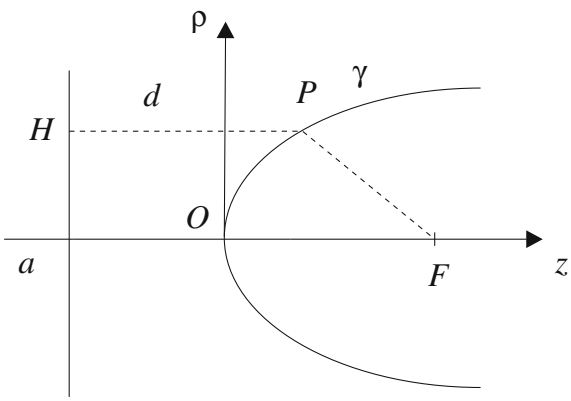

Fig. 2.17 Gaussian approximation

$$Ni = N'r, \tag{2.98}$$

where N and N' are the refractive indices of the media before and after the surface S, respectively. Moreover, denoting by R the radius of S and $c = 1/R$ its curvature, we have

$$\alpha = -\frac{h}{z}, \quad \beta = -\frac{h}{R} = -hc, \quad \alpha' = -\frac{h}{z'}. \tag{2.99}$$

Introducing (2.97) and (2.99) into (2.98), we verify that the refraction law is equivalent to the Abbe invariant

$$\frac{N}{R} - \frac{N}{z} = \frac{N'}{R} - \frac{N'}{z'}. \tag{2.100}$$

Finally, applying the refraction law to the ray γ' that intersects S at the optical axis, we deduce the condition

$$N\theta = N'\theta', \tag{2.101}$$

which can also be written in the form

$$\frac{y'}{y} = \frac{z'N}{zN'}. \tag{2.102}$$

Formula (2.100) of Abbe invariant is often written in terms of curvature c of S, the angles α and α' that the marginal ray r forms with the optical axis and the height h with respect to the optical axis of the intersection point of r with the surface S of dioptric. In view of (2.96), (2.97), we easily verify that (2.100) can also be written as follows:

$$N'\alpha' = N\alpha - (N' - N)ch. \tag{2.103}$$

Further, (2.96) and (2.97) allow us to give the refraction law (2.98) the form

$$a \equiv N(ch + \alpha) = N'(ch + \alpha'), \tag{2.104}$$

where a is said to be the ***refraction invariant***.

We note that applying (2.100) and (2.102) to any dioptric S_i of an optical system $\mathbb{S}$ we localize the image formed by S by resorting to the object and image distances z_i and z_i' and evaluate its dimension by the object and image heights y_i and y_i'.

In contrast, (2.103) localizes the position of the image by the angles α_i and α_i' that the marginal ray r_i forms with the optical axis before and after the refraction on S_i, whereas the dimension of the image is given by (2.101) that contains the angles θ_i, θ_i' that the ray r' forms with the optical axis. It is worthwhile to formulate the Lagrange invariant (2.68) in terms of the new variables we are adopting. It is simple to verify that in view of (2.104) we can write H as follows:

$$H = \overline{a}_i h_i - a_i \overline{h}_i, \tag{2.105}$$

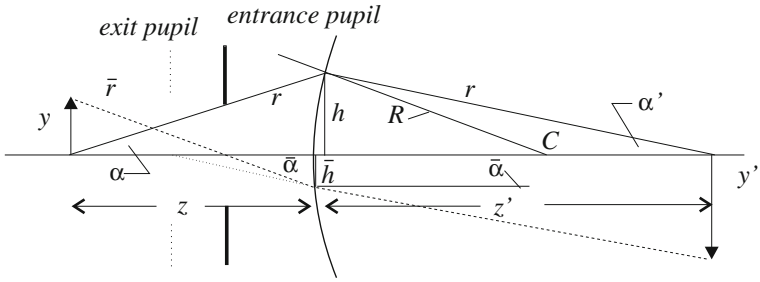

Fig. 2.18 Marginal and principal rays

where

$$\overline{a}_i = N_i(c_i\overline{h}_i + \overline{\alpha}_i) = N'(c_i\overline{h}_i + \overline{\alpha}'_i) \tag{2.106}$$

is the refraction invariant relative to the principal ray (see Figure 2.18).

It is evident that we can obtain the localization of the image and its size by applying (2.103) and (2.101) to any dioptric S_i of $\mathbb{S}$. If t_i is the distance of the dioptrics S'_i from the dioptric S_i, we have

$$h'_i = h_i + \alpha_i t_i, \quad h_{i+1} = h'_i. \tag{2.107}$$

Therefore, the matrix equation that describes the transfer from S_i to S_{i+1} is

$$\begin{pmatrix} h'_i \\ \alpha'_i \end{pmatrix} = \begin{pmatrix} 1 & t_i \\ 0 & 1 \end{pmatrix} \begin{pmatrix} h_i \\ \alpha_i \end{pmatrix}. \tag{2.108}$$

Further, the matrix equation that gives the refraction across S_{i+1} is

$$\begin{pmatrix} h'_i \\ \alpha'_i \end{pmatrix} = \begin{pmatrix} 1 & 0 \\ -c_i(1-\mu_i) & \mu_i \end{pmatrix} \begin{pmatrix} h'_i \\ \alpha_i \end{pmatrix}, \tag{2.109}$$

where $\mu = N_i/N'_i$. Finally, by combining (2.108) and (2.109) we obtain the matrix equation that represents a refraction followed by a transfer

$$\begin{pmatrix} h'_i \\ \alpha'_i \end{pmatrix} = \begin{pmatrix} 1 & t_i \\ 0 & 1 \end{pmatrix} \begin{pmatrix} 1 & 0 \\ -c_i(1-\mu_i) & \mu_i \end{pmatrix} \begin{pmatrix} h_i \\ \alpha_i \end{pmatrix}. \tag{2.110}$$

2.11 Exercises

1. Verify that

$$\begin{pmatrix} \dfrac{N_i z_i'}{N_i' z_i} & 0 \\ -\dfrac{P_i}{N_i'} & \dfrac{z_i}{z_i'} \end{pmatrix} = \begin{pmatrix} 1 & z_i' \\ 0 & 1 \end{pmatrix} \begin{pmatrix} 1 & 0 \\ -\dfrac{P_i}{N_i'} & \dfrac{N_i}{N_i'} \end{pmatrix} \begin{pmatrix} 1 & -z_i \\ 0 & 1 \end{pmatrix}. \tag{2.111}$$

The matrix composition on the right-hand side yields

$$\begin{pmatrix} 1 - \dfrac{z_i' P_i}{N_i'} & -z_i \left(1 - \dfrac{z_i' P_i}{N_i'}\right) + \dfrac{z_i' N_i}{N_i'} \\ -\dfrac{P_i}{N_i'} & \dfrac{z_i P_i}{N_i'} + \dfrac{N_i}{N_i'} \end{pmatrix}. \tag{2.112}$$

On the other hand, from (2.7), it is easy to derive

$$\frac{N_i'}{z_i'} - \frac{N_i}{z_i} = P_i,$$

in other words,

$$1 - \frac{P_i z_i'}{N_i'} = \frac{N_i z_i'}{N_i' z_i}.$$

It is now straightforward to show that the matrix (2.112) is equal to the left-hand side of (2.111).

2. Evaluate the Gaussian characteristics of a single spherical mirror S having a curvature radius $R = -1000$ and the aperture stop that lyes in the plane of the center of curvature.
The power of the mirror is

$$P = \frac{1}{500} = 0.002$$

and the refractive matrix is

$$\mathbb{R} = \begin{pmatrix} 1 & 0 \\ 0.002 & -1 \end{pmatrix}$$

whereas the matrices $\mathbb{M}^{en}$ and $\mathbb{M}^{ex}$ (see Section 1.7) are

$$\mathbb{M}^{en} = \begin{pmatrix} 1 & 0 \\ 0 & 1 \end{pmatrix}, \quad \mathbb{M}^{ex} = \begin{pmatrix} 1 & 0 \\ 0.002 & -1 \end{pmatrix},$$

and the entrance and exit pupils are situated in the curvature center. Finally, the matrix M relative for the whole system is

$$\mathbb{M} = \begin{pmatrix} 1 & 0 \\ 0.002 & -1 \end{pmatrix}.$$

Consequently, the distances of the principal planes from S (see (2.36) and (2.44)) are

$$z_{1p} = z_{2p} = 0,$$

and the focal length is (see (2.45))

$$f = -500.$$

3. Evaluate the Gaussian characteristics of a single plane-convex lens for which the anterior curvature radius is 50, the posterior one is infinite, the thickness is equal to 8 and the refractive index in green light is 1.518722. The aperture stop is -6 far from the lens.
The powers of the two surfaces are respectively,

$$P_1 = 0.0103744, \quad P_2 = 0,$$

Consequently, the refractive matrices are

$$\mathbb{R}_1 = \begin{pmatrix} 1 & 0 \\ -0.0068 & 0.6584 \end{pmatrix}, \quad \mathbb{R}_2 = \begin{pmatrix} 1 & 0 \\ 0 & 1.518722 \end{pmatrix},$$

whereas the translation matrix $\mathbb{D}$ is

$$\mathbb{D} = \begin{pmatrix} 1 & 8 \\ 0 & 1 \end{pmatrix}.$$

Moreover, the matrices $\mathbb{M}^{en}$, $\mathbb{M}^{ex}$ and $\mathbb{M}$ result

$$\mathbb{M}^{en} = \begin{pmatrix} 1 & 0 \\ 0 & 1 \end{pmatrix}, \quad \mathbb{M}^{ex} = \begin{pmatrix} 0.9453 & 5.2675 \\ -0.0103 & 1 \end{pmatrix},$$

$$\mathbb{M} = \begin{pmatrix} 0.9453 & 5.2675 \\ -0.0103 & 1 \end{pmatrix}.$$

From the previous matrices, we derive

$$z_{1p} = 0, \quad z_{2p} = -5.267,$$

$$f = 96.39.$$

Evaluate the distance of the image z_2' when $z_1 = -200$.

4. Evaluate the Gaussian characteristics of the following optical system: the radii are $50, \infty, \infty, -50$; the distances are $8, 12, 8$; the refractive indices are $1, 1.518722, 1, 1.58722$; the aperture stop is situated between the second and third surface and its distance from the second surface is 6.
We have

$$P_1 = 0.0104, \quad P_2 = P_3 = 0, \quad P_4 = 0.0104;$$

$$\mathbb{R}_1 = \begin{pmatrix} 1 & 0 \\ -0.0068 & 0.6584 \end{pmatrix}, \quad \mathbb{R}_2 = \begin{pmatrix} 1 & 0 \\ 0 & 1.5187 \end{pmatrix},$$

$$\mathbb{R}_3 = \begin{pmatrix} 1 & 0 \\ 0 & 0.6584 \end{pmatrix}, \quad \mathbb{R}_4 = \begin{pmatrix} 1 & 0 \\ -0.0103 & 1.5187 \end{pmatrix},$$

$$\mathbb{D}_1 = \mathbb{D}_3 \begin{pmatrix} 1 & 8 \\ 0 & 1 \end{pmatrix}, \quad \mathbb{D}_2 = \begin{pmatrix} 1 & 12 \\ 0 & 1 \end{pmatrix}.$$

Consequently,

$$\mathbb{M}^{en} = \begin{pmatrix} 0.945 & 5.267 \\ -0.0103 & 1 \end{pmatrix}, \quad \mathbb{M}^{ex} = \begin{pmatrix} 1 & 5.267 \\ -0.0103 & 0.9453 \end{pmatrix},$$

$$\mathbb{M} = \begin{pmatrix} 0.762 & 22.53 \\ -0.018 & 0.766 \end{pmatrix};$$

$f = 54.57$ and the distances w_e of the entrance pupil from the first surface and w_e' of the exit pupil from the last surface are

$$w_e = 12.76, \quad w_e' = 0.727.$$

5. Let $\mathbb{S}$ the system in Figure 2.19. The radii of the eight surfaces (from left to right) are

$$15.9, 30.2, 18.5, 12, -12, -18.5, -30.2, -15.9.$$

The thicknesses and refractive indices of lenses are

$$4, 0.5, 1, 15.2, 1, 0.5, 4;$$

$$1, 1.609937, 1, 1.624082, 1, 1.624082, 1, 1.609937, 1,$$

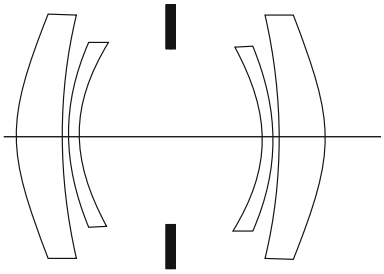

Fig. 2.19 Projector of unit magnification

respectively. Finally the stop is 7.6 far from the fourth surface. Evaluate all the Gaussian characteristics of $\mathbb{S}$. In particular prove that, when the distance of the object plane from the first surface is 212.2, the magnification of S is -1.

6. Using (2.48), (2.54), and (2.51), prove that (2.44) and (2.45) can also be written as follows:

$$y'_n = M y_1, \tag{2.113}$$

$$\alpha'_n = -\frac{1}{f'} y_1 + \frac{1}{M} \alpha_1. \tag{2.114}$$

Chapter 3
Fermat's Principle and Third-Order Aberrations

3.1 Introduction

Starting from Fermat's principle, Hamilton introduced ***characteristic functions*** for analyzing the behavior of the rays in a general optical system (see [23]). Subsequently, Seidel [24] and Schwarzschild [25] defined a new characteristic function, termed ***Schwarzschild's eikonal***. This is related to the Hamiltonian angle characteristic, but it depends on suitable nondimensional variables. Using this function, authors succeeded in developing a complete analysis, with evident geometrical meaning, of the third-order monochromatic aberrations of a compound optical system with a symmetry of revolution about the optical axis. Another approach to the optical aberration theory is based on the ***aberration function*** Φ_1, the determination of which again requires the knowledge of Schwarzschild's eikonal (see, for instance, [7, 14]). All of these concepts will be discussed in Chapters 11, 12, which are devoted to Hamiltonian optics.[1]

Whichever approach we choose to employ in order to obtain third-order aberration formulae, we must first understand the whole Hamiltonian formalism. In this chapter, a different approach is presented that is based only on Fermat's principle. It represents the natural generalization of the procedure we followed in order to introduce the Gaussian optics. To be more specific, we introduce the classical aberration function Φ_1 via Fermat's principle and we show that knowledge of it allows us to determine aberrations in the optical system. Then, we define ***auxiliary optical paths***, each of which behaves in the optical system in a manner that is known "a priori." Next, we introduce a new function Φ, which denotes the optical path length along these auxiliary paths. Finally, we prove that this function, which is easy to evaluate, is still an aberration function; in other words, it can be used to derive the third-order monochromatic aberrations instead of Φ_1.

[1] For other, more recent, approaches to the aberrations, see [27]–[30]

© Springer International Publishing Switzerland 2016

A. Romano and R. Cavaliere, *Geometric Optics*,
Modeling and Simulation in Science, Engineering and Technology,
DOI 10.1007/978-3-319-43732-3_3

The notebook ***TotalAberrations*** supplies the third-order aberrations of all of the optical systems we consider in this book. For more complex systems containing many optical elements with finite thicknesses, ***Mathematica*** may not be able to handle the symbolic calculations necessary to find the final third-order aberration coefficients. Even if it succeeds in this task, the expressions of these coefficients may be to complex to be useful.

3.2 The Aberration Function

Let $\mathbb{S}$ be an optical system with a symmetry of revolution about an optical axis a. We use the same notations we adopted in Chapter 2. In particular, z'_n denotes the distance of the image plane π'_n from the last surface S_n of $\mathbb{S}$, z_1 is the distance of the object plane π_1 from the first surface S_1 of $\mathbb{S}$, N'_n is the refractive index of the medium between S_n and S_{n+1}, and π_e, π'_e are the planes of the entrance and exit pupil of $\mathbb{S}$, respectively. Let $P_1 \equiv (0, y_1, z_1)$ be an object point and let $P_g \equiv (0, My_1, z'_n)$ be its Gaussian image, where M is the magnification of $\mathbb{S}$. Finally, we denote the point at which a ray γ originating from P_1 strikes the image plane π'_n by $P'_n \equiv (x'_n, y'_n, z'_n)$ (see Figure 3.1).

Let us consider the sphere Σ_g, which has its center at P_g and has a radius R_g equal to the distance between P_g and the center O'_e of the exit pupil. If w'_e is the distance of O'_e from the vertex of S_n, and we put

$$z_* = z'_n - w'_e, \tag{3.1}$$

then the radius of Σ_g is

$$R_g^2 = z_*^2 + M^2 y_1^2, \tag{3.2}$$

and, in a reference frame that has its origin at O'_e, the equation of Σ_g assumes the form

$$f(X_g, Y_g, Z_g) \equiv X_g^2 + (Y_g - My_1)^2 + (Z_g - z_*)^2 - R_g^2 = 0, \tag{3.3}$$

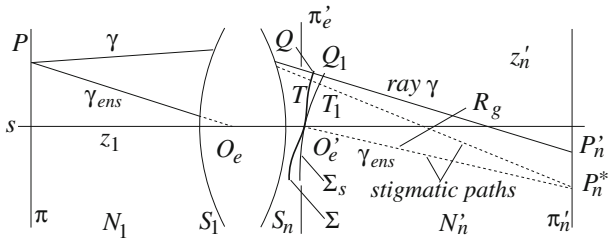

Fig. 3.1 Wave front Σ and Gaussian reference sphere Σ_g

where (X_g, Y_g, Z_g) are the coordinates of the moving point of Σ_g.

Let γ_{ex} be the ray from P_1 that crosses the exit pupil at $O'_e(0, 0, w'_e)$. In view of (1.7), we denote the optical path length along γ_{ex} from P_1 to O'_e by $V(y_1, z_1, w'_e)$. We now choose a point $Q(X, Y, Z)$ on any ray γ originating from P_1 such that the optical path length $V(y_1, z_1, X, Y, Z)$ from P_1 to Q along the ray γ verifies the condition

$$V(y_1, z_1, X, Y, Z) = V(y_1, z_1, w'_e). \tag{3.4}$$

This equation defines a surface Σ (containing the point O'_e) that is the locus of the points $Q \in \gamma$ such that the optical path length along any ray γ from P_1 to Q has the value $V(y_1, z_1, w'_e)$. Moreover, in view of (1.8), the ray γ is orthogonal to Σ at Q, since

$$\frac{\partial V}{\partial X}(y_1, z_1, X, Y, Z) = N'_n \alpha_x, \tag{3.5}$$

$$\frac{\partial V}{\partial Y}(y_1, z_1, X, Y, Z) = N'_n \alpha_y, \tag{3.6}$$

$$\frac{\partial V}{\partial Z}(y_1, z_1, X, Y, Z) = N'_n \alpha_z, \tag{3.7}$$

where α_x, α_y, and α_z are the director cosines of γ with respect to the coordinate axes.

Finally, if $Q_g(X_g, Y_g, Z_g)$ is the point of intersection of γ with the sphere Σ_g, then the function

$$\begin{aligned} \Phi_1 &= V(y_1, z_1, X_g, Y_g, Z_g) - V(y_1, z_1, X, Y, Z) \\ &= V(y_1, z_1, X_g, Y_g, Z_g) - V(y_1, z_1, w'_e) \end{aligned} \tag{3.8}$$

is said to be the ***aberration function*** [7]. Comparing (3.4) and (3.8) we have that, if $\Phi_1 = 0$, then the two surfaces Σ and Σ_g coincide and all of the rays—which for (3.5)–(3.7) are orthogonal to Σ—arrive at the same point P_g so that there is no aberration.

Denote by Γ the set of all of the rays originating from P_1. Since the optical path length up to Σ is the same for all of the rays belonging to Γ, in (3.8) γ can be substituted by another arbitrary but fixed ray of Γ. We choose the ray γ_{en}, which starts from P_1 and intercepts the center O_e of the entrance pupil. Since this ray is completely determined by these two points, the corresponding optical path length is only a function of y_1 and the distance w_e of the entrance pupil from the first surface S_1 of $\mathbb{S}$. These remarks imply that the function Φ_1 can also be written as follows

$$\Phi_1 = V(y_1, z_1, X_g, Y_g, Z_g) - V(y_1, z_1, w_e), \tag{3.9}$$

where $V(y_1, z_1, w_e)$ is the optical path length along γ_{en} up to Σ. Since Q_g is a point of the Gaussian sphere Σ_g, its coordinates verify equation (3.3); consequently, by Dini's theorem on implicit functions, we derive the result

$$\begin{aligned}\frac{\partial \Phi_1}{\partial X_g} &= \frac{\partial V}{\partial X_g} + \frac{\partial V}{\partial Z_g}\frac{\partial Z_g}{\partial X_g} \\ &= \frac{\partial V}{\partial X_g} - \frac{\partial V}{\partial Z_g}\frac{\dfrac{\partial f}{\partial X_g}}{\dfrac{\partial f}{\partial Z_g}} \\ &= \frac{\partial V}{\partial X_g} - \frac{\partial V}{\partial Z_g}\frac{X_g}{Z_g - z_*} \\ &= N_n'\alpha_x - N_n'\alpha_z\frac{X_g}{Z_g - z_*}. \end{aligned} \tag{3.10}$$

On the other hand, in the frame of reference with its origin at O_e', we also have

$$\begin{aligned}\alpha_x &= \frac{x_n' - X_g}{R'}, \\ \alpha_y &= \frac{y_n' - Y_g}{R'}, \\ \alpha_z &= \frac{z_* - Z_g}{R'}, \end{aligned} \tag{3.11}$$

where R' is the distance between the points Q_g and P_n' (see Figure 3.1). Finally, collecting the results (3.5)–(3.7), and (3.10), (3.11) together, we have

$$\begin{aligned}\frac{\partial \Phi_1}{\partial X_g} &= N_n'\frac{x_n'}{R'} \\ \frac{\partial \Phi_1}{\partial Y_g} &= N_n'\frac{y_n' - My_1}{R'}. \end{aligned}$$

If we term $(\epsilon_x, \epsilon_y) = (x_n', y_n' - My_1)$ the ***aberration vector***, the above relations can then also be written as follows

$$\epsilon_x = \frac{R'}{N_n'}\frac{\partial \Phi_1}{\partial X_g}, \tag{3.12}$$

$$\epsilon_y = \frac{R'}{N_n'}\frac{\partial \Phi_1}{\partial Y_g}. \tag{3.13}$$

Remark 3.1 Due to the symmetry of revolution of $\mathbb{S}$ about the optical axis a, the aberration function $\Phi_1(y_1, X_g, Y_g)$ depends on the rotational invariants

$$\xi = y_1^2, \quad \eta_g = y_1 Y_g, \quad \zeta_g = X_g^2 + Y_g^2. \tag{3.14}$$

Consequently, the power expansion of Φ_1 in terms of these variables has the form

$$\Phi_1 = \Phi_1^{(1)} + \Phi_1^{(2)} + \Phi_1^{(3)} + \cdots + O_{inv}(n+1), \tag{3.15}$$

where $\Phi_1^{(n)}$ is a homogeneous polynomial in the variables ξ, η_g, and ζ_g and $O_{inv}(n+1)$ denotes quantities of at least order $n+1$ in these invariants. Equivalently, the expansion contains only even powers of y_1, X_g, and Y_g. When we wish to refer the order of the neglected terms in (3.15) to these variables instead, then we write $O(2(n+1))$ rather than $O_{inv}(n+1)$.

Remark 3.2 If the object and image planes are chosen according to Gaussian optics, the first term $\Phi_1^{(1)}$ of the expansion (3.15) vanishes since it corresponds to the Gaussian approximation in which there is no aberration (see Section 2.1). This implies that ϵ_x and ϵ_y depend on at least third-order powers of y_1, X_g, and Y_g.

Remark 3.3 These relations, although exact, do not allow us to determine the aberrations of the system even when the aberration function is given as a function of y_1, X_g and Y_g, since the quantity R' depends on the ray in an unknown way. To make them useful, we can expand R' in terms of known quantities so that we can use (3.12), (3.13) to determine approximately the aberrations when Φ_1 is given.

In order to express R' into (3.12), (3.13) in terms of known quantities, we first note that, in view of (3.2), (3.3), we have

$$\begin{aligned} R'^2 &= (x_n' - X_g)^2 + (y_n' - Y_g)^2 + (z_* - Z_g)^2 \\ &= x_n'^2 - 2x_n'X_g + y_n'^2 - 2y_n'Y_g + X_g^2 + Y_g^2 + (z_* - Z_g)^2 \\ &= x_n'^2 - 2x_n'X_g + y_n'^2 - 2y_n'Y_g + z_*^2 + 2My_1Y_g. \end{aligned}$$

Taking into account the definitions $\epsilon_x = x_n'$, $\epsilon_y = y_n' - My_1$, and the last remark, we derive

$$\begin{aligned} R'^2 &= z_*^2 + M^2y_1^2 + (\epsilon_x^2 + \epsilon_y^2) + 2My_1\epsilon_y - 2(\epsilon_x X_g + \epsilon_y Y_g) \\ &= z_*^2 + M^2y_1^2 + O(4). \end{aligned}$$

Finally, we have the approximate relation

$$R' = z_* + \frac{M^2y_1^2}{2z_*} + O(4), \tag{3.16}$$

which allows us to write (3.12) and (3.13) in the form

$$\epsilon_x = \frac{1}{N_n'}\left(z_* + \frac{M^2}{2z_*}y_1^2\right)\frac{\partial\Phi_1}{\partial X_g} + O(7), \tag{3.17}$$

$$\epsilon_y = \frac{1}{N_n'}\left(z_* + \frac{M^2}{2z_*}y_1^2\right)\frac{\partial\Phi_1}{\partial Y_g} + O(7). \tag{3.18}$$

The third-order quantities

$$\epsilon_x^{(3)} = \frac{z_*}{N_n'} \frac{\partial \Phi_1^{(2)}}{\partial X_g}, \tag{3.19}$$

$$\epsilon_y^{(3)} = \frac{z_*}{N_n'} \frac{\partial \Phi_1^{(2)}}{\partial Y_g}, \tag{3.20}$$

in the variables y_1, X_g, Y_g are called the ***primary aberrations*** or the ***third-order aberrations***.

3.3 A New Aberration Function

Although formulae (3.17), (3.18) supply the aberrations of an optical system $\mathbb{S}$ to within seventh-order terms in the variables y_1, X_g, Y_g, they can only be used if we are able to determine

- the function $\Phi_1(y_1, X_g, Y_g)$;
- the relations between the coordinates (X_g, Y_g) of the point $Q_g \in \Sigma_g$ and the coordinates of the entering ray γ, which are given by y_1 and the coordinates (x_e, y_e) of the point at which γ intersects the entrance pupil.

Answering these questions is a very difficult task, even for the third-order aberrations, since we do not know the behavior of the rays. These problems will be discussed in the Hamiltonian framework in Chapter 10. In this section, we define a new function $\Phi(y_1, x_e, y_e)$ which measures the optical path length on particular *known* paths that are not rays. Moreover, we prove that this new function $\Phi(y_1, x_e, y_e)$ can be used to evaluate the third-order aberrations instead of Φ_1 [31].

First, we define these particular paths. Let $\mathbb{S}$ be an optical system with a symmetry of revolution about an axis a. If $P_1 \equiv (0, y_1, z_1)$ is an object point and $P_g \equiv (0, My_1, z_n')$ is its Gaussian image, then the ***stigmatic path*** from P_1 to P_g associated with the ray γ is the broken line γ_s obtained with the following procedure. The path coincides with γ from P_1 up to the point A_1, where γ intersects the first surface S_1 of $\mathbb{S}$; then, denoting the magnification relative to the planes z_1 and z_1' by M_1, we consider the line from A_1 up to the Gaussian image $P_1' \equiv (0, M_1 y_1, z_1')$ formed by S_1 and the point A_2, where this line intersects the second surface S_2 of $\mathbb{S}$. Proceeding in this way, we obtain a broken line $P_1 A_1 A_2 \cdots P_g$ that reaches the final point P_g (see Figure 3.2).

In conclusion, a unique stigmatic path γ_s can be associated with any ray γ; moreover, the behavior of γ_s is completely determined by the Gaussian optics. In what follows, we denote the stigmatic path associated with the principal ray γ_{en} that enters the entrance pupil of $\mathbb{S}$ by γ_{ens} (see Figure 3.3).

In order to introduce the new aberration function Φ, we denote with $Q_s \equiv (X_s, Y_s, Z_s)$ the point on the Gaussian sphere Σ_g at which the stigmatic ray γ_s

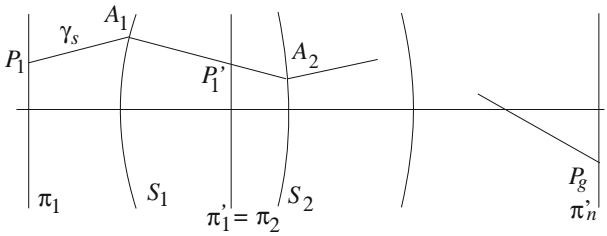

Fig. 3.2 Stigmatic path

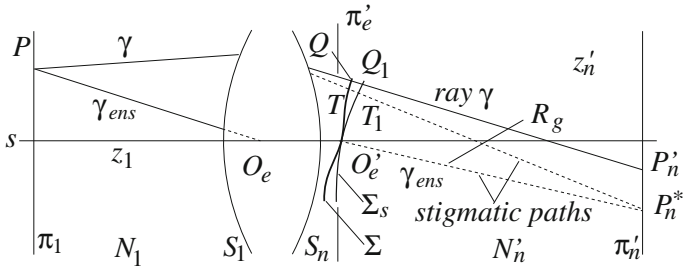

Fig. 3.3 New aberration function

meets Σ_g (see Figure 3.4). Since the coordinates (X_s, Y_s, Z_s) of Q_s have to verify the equation (3.3) of Σ_g, we have $Z_s = Z_s(X_s, Y_s)$. Then, we consider the function

$$\Phi(y_1, X_s, Y_s) = L_s - L_{ens}, \tag{3.21}$$

where L_s is the optical path length from the object point $(0, y_1, z_1)$ to Q_s along the stigmatic ray γ_s and L_{ens} is the optical path length along the stigmatic path γ_{ens} from P to O_e'. By adding the radius R_g to both L_s and L_{ens}, we obtain the optical lengths Δ_s and Δ_{ens} from P to P_g along the stigmatic paths γ_s and γ_{ens}, respectively

$$\Phi(y_1, X_s, Y_s) = \Delta_s - \Delta_{ens}, \tag{3.22}$$

Remark 3.4 In the absence of aberrations, the quantities Φ and Φ_1 vanish. In fact, if $\Phi_1 = 0$, the surfaces Σ and Σ_s coincide so that all of the rays orthogonal to Σ arrive at the Gaussian image P_n^* and vice versa. Analogously, if $\Phi = 0$, the optical lengths of all stigmatic paths are equal so that, according to Fermat's principle, they are rays that arrive at P_g.

More generally, the following result holds.

Theorem 3.1 *The functions Φ and Φ_1 verify the relations*

$$\frac{\partial \Phi}{\partial X_g} = \frac{\partial \Phi_1}{\partial X_g} + O(5), \tag{3.23}$$

$$\frac{\partial \Phi}{\partial Y_g} = \frac{\partial \Phi_1}{\partial Y_g} + O(5), \tag{3.24}$$

where $O(5)$ denotes a fifth-order quantity in the variables y_1, X_g, Y_g.

Proof Let γ be a ray originating from the object point $P_1 \equiv (0, y_1, z_1)$ and arriving at the point $Q_g \equiv (X_g, Y_g, Z_g)$ on the Gaussian sphere Σ_g. We denote the stigmatic path relative to γ by γ_s and the point at which γ_s intersects Σ_g by $Q_s \equiv (X_s, Y_s, Z_s)$ (see Figure 3.4).

With the notations of Section 3.2, we have

$$\begin{aligned} L_s - V\left(y_1, X_g, Y_g, Z_g\left(X_g, Y_g\right)\right) \\ = \left(\frac{\partial V}{\partial X_g}\right)_{Q_g} (X_s - X_g) + \left(\frac{\partial V}{\partial Y_g}\right)_{Q_g} (Y_s - Y_g) \\ + \left(\frac{\partial V}{\partial Z_g}\right)_{Q_g} (Z_s - Z_g) + O\,(2)\,, \end{aligned} \tag{3.25}$$

where $O\,(2)$ is a second-order quantity with respect to the differences $X_s - X_g$, $Y_s - Y_g$, and $Z_s - Z_g$.

If the same procedure is applied to the pair γ_{ens} and γ_{en}, then we obtain

$$L_{ens} - V\,(y_1) = \psi\,(y_1)\,. \tag{3.26}$$

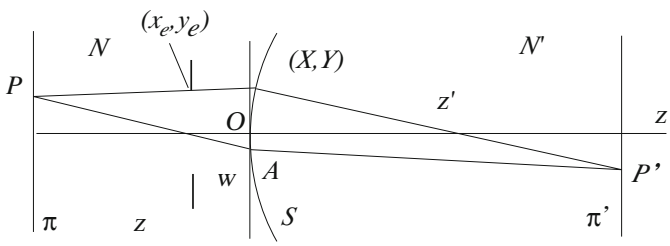

Fig. 3.4 Coordinates in the entrance pupil

Finally, we have

$$\begin{aligned}(L_s - L_{ens}) - \left(V\left(y_1, X_g, Y_g, Z_g\left(X_g, Y_g\right)\right) - V\left(y_1\right)\right) \\ = \left(\frac{\partial V}{\partial X_g}\right)_{Q_g}\left(X_s - X_g\right) + \left(\frac{\partial V}{\partial Y_g}\right)_{Q_g}\left(Y_s - Y_g\right) \\ + \left(\frac{\partial V}{\partial Z_g}\right)_{Q_g}\left(Z_s - Z_g\right) - \psi\left(y_1\right) + O\left(2\right).\end{aligned}$$

Because of (3.8) and (3.21), this relation becomes

$$\begin{aligned}\Phi - \Phi_1 = \left(\frac{\partial V}{\partial X_g}\right)_{Q_g}\left(X_s - X_g\right) + \left(\frac{\partial V}{\partial Y_g}\right)_{Q_g}\left(Y_s - Y_g\right) \\ + \left(\frac{\partial V}{\partial Z_g}\right)_{Q_g}\left(Z_s - Z_g\right) - \psi\left(y_1\right) + O\left(2\right).\end{aligned} \tag{3.27}$$

Moreover, from (3.10) and (3.11) we derive

$$\frac{\partial V}{\partial X_g} = \frac{\partial \Phi_1}{\partial X_g} - \frac{\partial V}{\partial Z_g}\frac{\partial Z_g}{\partial X_g}, \tag{3.28}$$

$$\frac{\partial V}{\partial Y_g} = \frac{\partial \Phi_1}{\partial Y_g} - \frac{\partial V}{\partial Z_g}\frac{\partial Z_g}{\partial Y_g}, \tag{3.29}$$

$$\frac{\partial V}{\partial Z_g} = N_n' \alpha_z. \tag{3.30}$$

Since (X_s, Y_s, Z_s) and $\left(X_g, Y_g, Z_g\right)$ belong to Σ_g, we get

$$Z_s - Z_g = \left(\frac{\partial Z_g}{\partial X_g}\right)_{Q_g}\left(X_s - X_g\right) + \left(\frac{\partial Z_g}{\partial Y_g}\right)_{Q_g}\left(Y_s - Y_g\right) + O_1\left(2\right),$$

where $O_1\left(2\right)$ is a second-order quantity with respect to the differences $X_s - X_g, Y_s - Y_g$. Taking into account the above result, (3.27) assumes the form

$$\begin{aligned}\Phi - \Phi_1 = \left(\frac{\partial \Phi_1}{\partial X_g}\right)_{Q_g}\left(X_s - X_g\right) + \left(\frac{\partial \Phi_1}{\partial Y_g}\right)_{Q_g}\left(Y_s - Y_g\right) \\ - \psi\left(y_1\right) + O_2\left(2\right),\end{aligned} \tag{3.31}$$

where $O_2\left(2\right) = N_n' \alpha_z O_1\left(2\right) + O(2)$.

Since $X_s = X_g$ and $Y_s = Y_g$ in the Gaussian approximation, we have

$$X_s = X_g + O(3), \;\; Y_s = Y_g + O(3) \tag{3.32}$$

so that (recalling that Φ_1 is a fourth-order function in the variables y_1, X_g, Y_g) we can write

$$\Phi - \Phi_1 = -\psi(y_1) + O(6),$$

where $O(6)$ denotes a sixth-order function of the variables X_g and Y_g, and we have proved the theorem. □

To conclude this section we note that the coordinates x'_e, y'_e in the exit pupil coincide with X_g, Y_g in the Gaussian approximation. Therefore, we have

$$X_g = M_e x_e + O(3), \quad Y_g = M_e x_e + O(3), \tag{3.33}$$

where M_e is the magnification related to the pupils, and the formulae (3.19) and (3.20), in view of (3.23), (3.24), can also be written as follows

$$\epsilon_x^{(3)} = \frac{z_*}{M_e N'_n} \frac{\partial \Phi^{(2)}}{\partial x_e}, \tag{3.34}$$

$$\epsilon_y^{(3)} = \frac{z_*}{M_e N'_n} \frac{\partial \Phi^{(2)}}{\partial y_e}. \tag{3.35}$$

In the following two sections, the aberration function Φ will be evaluated for a compound optical system as a fourth-order function of the coordinates y_1, x_e, y_e so that the third-order aberrations can be obtained from (3.34) and (3.35).

3.4 The Aberration Function Φ for a Single Surface

In this section we consider an optical system $\mathbb{S}$ containing a single surface S. To simplify the notations, we make $y_1 = y$, $z_1 = z$, $y'_1 = y'$, $z'_1 = z'$. The equation $Z = Z(X, Y)$ of S, up to fourth-order terms in the variables X, Y, is given by (see Section 1.5)

$$Z = \frac{1}{2R}\eta + \overline{a}_4 \eta^2 + O(3), \tag{3.36}$$

where $\eta = X^2 + Y^2$. In particular, if S is obtained by rotating a conic with a conic constant K about a or is an arbitrary aspheric surface of revolution, we have (see Section 1.5)

$$\overline{a}_4 = \frac{1+K}{8R^3}, \quad \overline{a}_4 = \frac{1}{8R^3} + c_4, \tag{3.37}$$

respectively.

The following expansion

$$\sqrt{a^2 + x + y^2} = a + \frac{x}{2a} - \frac{x^2}{8a^3} + \frac{y^2}{2a} + O(3) \tag{3.38}$$

allows us to prove the next theorem

Theorem 3.2 *Up to fourth-order terms in the coordinates* (y, X, Y) *the function* $\Phi(y, X, Y)$ *is given by the expression*

$$\Phi = C_1\eta^2 + \frac{1}{z}C_2\eta\zeta + \frac{1}{z^2}C_3\eta\xi + \frac{1}{z^2}(C_4 - C_3)\zeta^2 + \frac{1}{z^3}C_5\xi\zeta + C_6\xi^2 + O(3), \tag{3.39}$$

where $\xi = y_1^2$, $\eta = X^2 + Y^2$, $\zeta = y_1 Y$, *and*

$$C_1 \equiv -\frac{N^2}{8}\left(\frac{1}{N'z'} - \frac{1}{Nz}\right)\left(\frac{1}{z} - \frac{1}{R}\right)^2 + \frac{N' - N}{8R^3} - (N' - N)\overline{a}_4, \tag{3.40}$$

$$C_2 \equiv \frac{N^2}{2}\left(\frac{1}{N'z'} - \frac{1}{Nz}\right)\left(\frac{1}{z} - \frac{1}{R}\right), \tag{3.41}$$

$$C_3 \equiv \frac{N}{4}\left(\frac{N'^2 - N^2}{N'^2}\right)\left(\frac{1}{z} - \frac{1}{R}\right), \tag{3.42}$$

$$C_4 \equiv C_3 - \frac{N^2}{2}\left(\frac{1}{N'z'} - \frac{1}{Nz}\right), \tag{3.43}$$

$$C_5 \equiv -\frac{N}{2z^3}\frac{N'^2 - N^2}{N'^2}. \tag{3.44}$$

$$C_6 \equiv \frac{1}{8}\left(M^4\frac{N'}{z'^3} - \frac{N}{z^3}\right). \tag{3.45}$$

Proof Let γ be an arbitrary *ray* that starts from $(y, 0, z)$ and intersects S at the point (X, Y, Z). The stigmatic ray γ_s associated with γ coincides with γ from $(y, 0, z)$ to (X, Y, Z). After this point, it coincides with the straight line going from (X, Y, Z) to $(My, 0, z')$. In view of Theorem 3.1, it is sufficient to evaluate the optical path length along γ_s up to the point (X_g, Y_g, Z_g) at which γ_s intersects the Gaussian sphere of radius R_g and center at $(My, 0, z')$. However, if we evaluate the optical path length along γ_s up to the point $(My, 0, z')$, we add the *same* quantity $R_g N'$ to any stigmatic ray γ_s. For a single surface S the optical path difference (3.21) between the points $(y, 0, z)$ and $(My, 0, z')$ along the stigmatic path γ_s

$$\Phi = N\sqrt{X^2 + (Y - y)^2 + (Z - z)^2} + N'\sqrt{X^2 + (Y - My)^2 + (Z - z')^2} - N\sqrt{\xi + z^2} - N'\sqrt{M^2\xi + z'^2} \tag{3.46}$$

when the variables ξ, η, and ζ are used, assumes the form

$$\Phi = N\sqrt{z^2+\eta-2\zeta+\xi-\frac{z}{R}\eta+\left(\frac{1}{4R^2}-2a_4z\right)\eta^2}$$
$$+\,N'\sqrt{z'^2+\eta-2M\zeta+M^2\xi-\frac{z'}{R}\eta+\left(\frac{1}{4R^2}-2\overline{a}_4z'\right)\eta^2}$$
$$-\,N\sqrt{\xi+z^2}-N'\sqrt{M^2\xi+z'^2}. \tag{3.47}$$

We identify the first-order quantity x appearing in (3.38) with the term $\eta-2\zeta+\xi-\frac{z}{R}\eta$ of (3.47), the second-order quantity x^2 with the terms $(1/4R^2-2a_4z)\eta^2$ and we choose the values of z' and M in such a way as to eliminate the first-order terms of the expansion of Φ (see (2.7), (2.8)). In this way we have

$$\Phi = N\left(\frac{1}{8z^3}\left(\eta-2\zeta+\xi-\frac{z}{R}\eta\right)^2-\frac{1}{2z}\left(\frac{1}{4R^2}-2\overline{a}_4z\right)\eta^2\right)$$
$$+\,N'\left(-\frac{1}{8z'^3}\left(\eta-2M\zeta+M^2\xi-\frac{z'}{R}\eta\right)^2+\frac{1}{2z'}\left(\frac{1}{4R^2}-2\overline{a}_4z'\right)\eta^2\right)$$
$$-\,\frac{N}{8z^3}\xi^2+M^4\frac{N'}{8z'^3}\xi^2. \tag{3.48}$$

Expanding the above expression, we obtain a quadratic with η^2, $\eta\zeta$, $\eta\xi$, ζ^2, and $\xi\zeta$. The coefficient C_1 of η^2 is C_1 of η^2 is

$$C_1 = \frac{N}{8z}\left(\frac{1}{z^2}-\frac{2}{Rz}\right)+\frac{N'}{8z'}\left(-\frac{1}{z'^2}+\frac{2}{Rz'}\right)-(N'-N)\overline{a}_4$$
$$=\frac{N}{8z}\left[\left(\frac{1}{z}-\frac{1}{R}\right)^2-\frac{1}{R^2}\right]+\frac{N'}{8z'}\left[-\left(\frac{1}{z'}-\frac{1}{R}\right)^2+\frac{1}{R^2}\right]-(N'-N)\overline{a}_4$$
$$=-\frac{N^2}{8}\left(\frac{1}{N'z'}-\frac{1}{Nz}\right)\left(\frac{1}{z}-\frac{1}{R}\right)^2+\frac{N'-N}{8R^3}-(N'-N)\overline{a}_4, \tag{3.49}$$

provided that (2.8) is taken into account. Similarly, the coefficient C_2/z of $\eta\zeta$ is

$$\frac{C_2}{z} = -\frac{1}{2z^2}\left(\frac{N}{z}-\frac{N}{R}\right)+\frac{M}{2z'^2}\left(\frac{N'}{z'}-\frac{N'}{R}\right)$$
$$=\frac{N^2}{2z}\left(\frac{Mz}{Nz'^2}-\frac{1}{Nz}\right)\left(\frac{1}{z}-\frac{1}{R}\right)$$
$$=\frac{N^2}{2z}\left(\frac{1}{N'z'}-\frac{1}{Nz}\right)\left(\frac{1}{z}-\frac{1}{R}\right), \tag{3.50}$$

where (2.7) and (2.8) have been used. Moreover, the coefficient C_3/z^2 of $\eta\xi$ takes the form

$$\begin{aligned}\frac{C_3}{z^2} &= \frac{1}{4z^2}\left(\frac{N}{z}-\frac{N}{R}\right)-\frac{M^2}{4z'^2}\left(\frac{N'}{z'}-\frac{N'}{R}\right)\\ &= \frac{1}{4}\left(\frac{1}{z^2}-\frac{M^2}{z'^2}\right)\left(\frac{N}{z}-\frac{N}{R}\right)\\ &= \frac{N}{4z^2}\left(\frac{N'^2-N^2}{N'^2}\right)\left(\frac{1}{z}-\frac{1}{R}\right),\end{aligned} \tag{3.51}$$

whereas the coefficient $(C_4 - C_3)/z^2$ of ζ^2 becomes

$$\frac{1}{z^2}(C_4 - C_3) = \frac{N}{2z^3} - \frac{M^2 N'}{2z'^3} = -\frac{N^2}{2z^2}\left(\frac{1}{N'z'} - \frac{1}{Nz}\right). \tag{3.52}$$

Finally, the coefficient C_5/z^3 of $\xi\zeta$ is

$$\frac{C_5}{z^3} = -\frac{N}{2z^3} + \frac{M^3 N'}{2z'^3} = -\frac{N}{2z^3}\frac{N'^2 - N^2}{N'^2}. \tag{3.53}$$

and the coefficient C_6 of ξ^2 is

$$C_6 \equiv \frac{1}{8}\left(M^4\frac{N'}{z'^3} - \frac{N}{z^3}\right).$$

In conclusion, the optical path difference Φ (assuming that the first-order part has been eliminated through appropriate selection of Gaussian conjugate planes and magnification) becomes

$$\begin{aligned}\Phi = {} & C_1\eta^2 + \frac{1}{z}C_2\eta\zeta + \frac{1}{z^2}C_3\eta\xi + \frac{1}{z^2}(C_4 - C_3)\zeta^2 + \frac{1}{z^3}C_5\xi\zeta\\ & + C_6\xi^2 + O(3),\end{aligned} \tag{3.54}$$

and the theorem is proved. □

Now we must substitute the variables (X, Y) with the coordinates (x_e, y_e) of the intersecting point on the stigmatic path that intersects with the plane π_e of the entrance pupil (see Figure 3.5).

To this end, we consider the straight line

$$\begin{aligned}X_c &= Xt,\\ Y_c &= y + (Y - y)t,\\ Z_c &= z + (Z - z)t,\end{aligned} \tag{3.55}$$

between the points $(0, y, z) \in \pi$ and $(X, Y, Z) \in S_i$, where $Z = Z(X, Y)$ is the equation (3.36) of S.

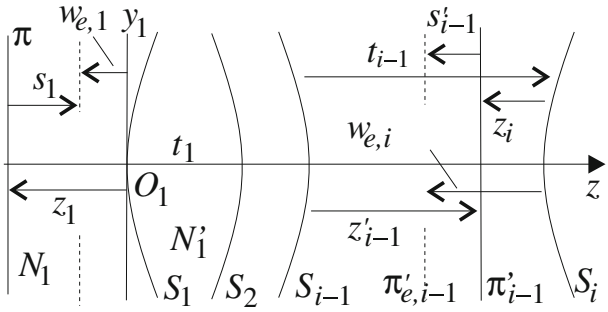

Fig. 3.5 Notations for a compound system

Denoting the distance of π_e from the vertex O of S by w, this straight line meets the plane π_e when

$$t = \frac{w - z}{Z - z} = \frac{z - w}{z}\left(1 + \frac{\eta}{2Rz_i}\right) + O(4). \tag{3.56}$$

Upon substituting this value of the parameter into (3.55), the following functions are derived:

$$\begin{aligned} x_e &= \frac{z - w}{z} X + O(3), \\ y_e &= \frac{w}{z} y + \frac{z - w}{z} Y + O(3), \end{aligned} \tag{3.57}$$

Inverting these functions, we obtain

$$\begin{aligned} X &= c x_e + O(3), \\ Y &= c y_e - d y + O(3), \end{aligned} \tag{3.58}$$

with

$$c = \frac{z}{z - w}, \quad d = \frac{w}{z - w}. \tag{3.59}$$

In view of (3.58), the relation (3.54) then becomes

$$\Phi = C_1^* \eta^2 + \frac{c}{z} C_2^* \eta\zeta + \frac{c^2}{z^2} C_3^* \eta\xi + \frac{c^2}{z^2}(C_4^* - C_3^*)\zeta^2 + \frac{c^3}{z^3} C_5^* \xi\zeta + O(6), \tag{3.60}$$

where the invariants ξ, η and ζ are now related to the variables y, x_e and y_e. Moreover,

$$C_1^* = c^4 C_1, \tag{3.61}$$
$$C_2^* = c^2(C_2 - 4zdC_1), \tag{3.62}$$
$$C_3^* = C_3 - zdC_2 + 2z^2d^2C_1, \tag{3.63}$$
$$C_4^* = C_4 - 3zdC_2 + 6z^2d^2C_1, \tag{3.64}$$
$$C_5^* = \frac{1}{c^2}(C_5 - 2zdC_4 + 3z^2d^2C_2 - 4z^3d^3C_1). \tag{3.65}$$

In (3.60) we omitted the term $C_6\xi^2$ since, in view of (3.34) and (3.35), it has no effect on the third-order aberrations. As a function of the variables (y, x_e, y_e), (3.60) becomes

$$\Phi = C_1^*(x_e^2 + y_e^2)^2 + \frac{c}{z}C_2^*(x_e^2 + y_e^2)yy_e + \frac{c^2}{z^2}C_3^*(x_e^2 + y_e^2)y^2 + \frac{c^2}{z^2}(C_4^* - C_3^*)y^2y_e^2 + \frac{c^3}{z^3}C_5^*y^3y_e + O(6). \tag{3.66}$$

The next sections are devoted to calculating the aberration function Φ of a compound system.

3.5 The Total Aberration Function for a Compound System

Let $\mathbb{S}$ be a compound optical system and π_e, π'_e the planes of entrance pupil and exit pupil, respectively. Moreover, we put $\pi_{e,1} = \pi_e$ and denote the conjugate Gaussian plane of π_e with respect to the first surface S_1 of $\mathbb{S}$ by $\pi'_{i,1}$. Similarly, we put $\pi_{e,2} = \pi'_{e,1}$, and denote the conjugate Gaussian plane of $\pi_{e,2}$ with respect to the surface S_2 by $\pi'_{e,2}$, and so on. It is evident that $\pi'_{e,n} = \pi'_e$. Finally, we denote the Gaussian magnification relative to the pair of planes $\pi_{e,i}$ and $\pi'_{e,i}$ by $M_{e,i}$. Relation (3.66), referring to surface S_i, then becomes

$$\Phi_i = C_{i,1}^*\eta_i^2 + \frac{c_i}{z_i}C_{i,2}^*\eta_i\zeta_i + \frac{c_i^2}{z_i^2}C_{i,3}^*\eta_i\xi_i + \frac{c_i^2}{z_i^2}(C_{i,4}^* - C_{i,3}^*)\zeta_i^2 + \frac{c_i^3}{z_i^3}C_{i,5}^*\xi_i\zeta_i + O(6), \tag{3.67}$$

where the coefficients are expressed by (3.61)–(3.65) referring to surface S_i

$$C^*_{i,1} = c_i^4 C_{i,1}, \tag{3.68}$$
$$C^*_{i,2} = c_i^2 (C_{i,2} - 4z_i d_i C_{i,1}), \tag{3.69}$$
$$C^*_{i,3} = C_{i,3} - z_i d_i C_{i,2} + 2z_i^2 d_i^2 C_{i,1}, \tag{3.70}$$
$$C^*_{i,4} = C_{i,4} - 3z_i d_i C_{i,2} + 6z_i^2 d_i^2 C_{i,1}, \tag{3.71}$$
$$C^*_{i,5} = \frac{1}{c_i^2}(C_{i,5} - 2z_i d_i C_{i,4} + 3z_i^2 d_i^2 C_{i,2} - 4z_i^3 d_i^3 C_{i,1}), \tag{3.72}$$

and the invariants ξ_i, η_i and ζ_i refer to the coordinates y_i, $x_{e,i}$ and $y_{e,i}$. Here, y_i denotes the ordinate of the Gaussian image on the plane π_i and $x_{e,i}$, $y_{e,i}$ are the coordinates of the point of intersection of the stigmatic path with the plane $\pi_{e,i}$. Note that the order of the neglected quantities refers to the coordinates y_i, $x_{e,i}$ and $y_{e,i}$, not to the corresponding invariants.

To express the total aberration function in terms of the invariants ξ_1, η_1 and ζ_1, related to the variables y_1, $x_{e,1} = x_e$ and $y_{e,1} = y_e$, we recall that

$$x'_{e,i} = M_{e,i} x_{e,i} + O(3), \tag{3.73}$$
$$y'_{e,i} = M_{e,i} y_{e,i} + O(3), \tag{3.74}$$
$$x_{e,i+1} = x'_{e,i}, \tag{3.75}$$
$$y_{e,i+1} = y'_{e,i}. \tag{3.76}$$

Then, we have

$$\xi_i = y_i^2 = M_{1,i-1}^2 y_1 = M_{1,i-1}^2 \xi_1, \tag{3.77}$$
$$\eta_i = x_{e,i}^2 + y_{e,i}^2 = M_{e,1,i-1}^2 \eta_1 + O(4), \tag{3.78}$$
$$\zeta_i = y_i y_{e,i} = M_{1,i-1} M_{e,1,i-1} \zeta_1 + O(4) \tag{3.79}$$

where $M_{e,1,i}$ is the Gaussian magnification between the planes $\pi_{e,1}$ and $\pi'_{e,i}$. Consequently, the total aberration function Φ becomes

$$\Phi = D_1 \eta_1^2 + \frac{c_1}{z_1} D_2 \eta_1 \zeta_1 + \frac{c_1^2}{z_1^2} D_3 \eta_1 \xi_1 + \frac{c_1^2}{z_1^2}(D_4 - D_3)\zeta_1^2 + \frac{c_1^3}{z_1^3} D_5 \xi_1 \zeta_1 + O(6), \tag{3.80}$$

where

$$D_1 = C^*_{1,1} + \sum_{i=2}^{n} M_{e,1,i-1}^4 C^*_{i,1}, \tag{3.81}$$

$$D_2 = C^*_{1,2} + \sum_{i=2}^{n} \frac{z_1}{z_i} \frac{c_i}{c_1} M_{e,1,i-1}^3 M_{1,i-1} C^*_{i,2}, \tag{3.82}$$

$$D_3 = C^*_{1,3} + \sum_{i=2}^{n} \left(\frac{z_1}{z_i} \frac{c_i}{c_1} \right)^2 M^2_{e,1,i-1} M^2_{1,i-1} C^*_{i,3}, \tag{3.83}$$

$$D_4 = C^*_{1,4} + \sum_{i=2}^{n} \left(\frac{z_1}{z_i} \frac{c_i}{c_1} \right)^2 M^2_{e,1,i-1} M^2_{1,i-1} C^*_{i,4}, \tag{3.84}$$

$$D_5 = C^*_{1,5} + \sum_{i=2}^{n} \left(\frac{z_1}{z_i} \frac{c_i}{c_1} \right)^3 M^2_{e,1,i-1} M^2_{1,i-1} C^*_{i,5}. \tag{3.85}$$

If the object is located at infinity, ($z_1 \to \infty$), we have $y_1 \to \infty$ and the above formulae are meaningless. However, upon introducing the field angle

$$\theta = \frac{y_1}{z_1 - w} + O(3) = \frac{c_1}{z_1} y_1 + O(3), \tag{3.86}$$

and noting that

$$\lim_{z_1 \longrightarrow \infty} z_1 d_1 = w, \quad \lim_{z_1 \longrightarrow \infty} c_1 = 1, \tag{3.87}$$

(3.80) assumes the following other form

$$\begin{aligned} \Phi = {} & D_1 (x_e^2 + y_e^2)^2 + D_2 (x_e^2 + y_e^2) y_e \theta \\ & + (D_3 x_e^2 + D_4 y_e^2) \theta^2 + D_5 y_e \theta^3 + O(6), \end{aligned} \tag{3.88}$$

where the notations $x_{e,1} = x_e$ and $y_{e,1} = y_e$ are again used.

It is possible to put the coefficients (3.81)–(3.85) in a more simple form by proving that

$$\frac{z_1}{z_i} \frac{c_i}{c_1} M_{e,1,i-1} M_{1,i-1} = \frac{N_1}{N_i}. \tag{3.89}$$

In fact, with the help of the Figure 3.6 and (3.59), it is straightforward to verify the following identities

$$\frac{z_1}{z_i} \frac{c_i}{c_1} = \frac{z_1}{z_i} \frac{z_1 - w}{z_1} \frac{z_i}{z_i - w_i} = \frac{z_1 - w}{z_i - w_i} = \frac{-s_1}{z_i - w_i} = \frac{s_1}{s'_{i-1}}, \tag{3.90}$$

since $s'_{i-1} = -(z_i - w_i)$. By resorting to (2.54), we have

$$\frac{z_1}{z_i} \frac{c_i}{c_1} = \frac{N_1}{N'_{i-1}} \frac{1}{M_{1,i-1} M_{e,1,i-1}}, \tag{3.91}$$

and (3.89) is proved, when we recall that $N'_{i-1} = N_i$.

Finally, we arrive at the following simplified expressions for the coefficients D_i:

$$D_1 = C^*_{1,1} + \sum_{i=2}^{n} M^4_{e,1,i-1} C^*_{i,1}, \tag{3.92}$$

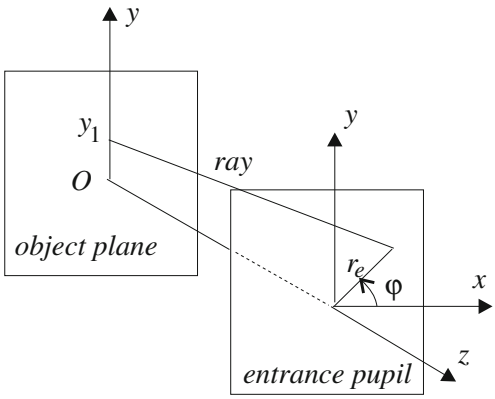

Fig. 3.6 Polar coordinates in the entrance pupil

$$D_2 = C^*_{1,2} + N_1 \sum_{i=2}^{n} \frac{1}{N_i} M^2_{e,1,i-1} C^*_{i,2}, \tag{3.93}$$

$$D_3 = C^*_{1,3} + N_1^2 \sum_{i=2}^{n} \frac{1}{N_i^2} C^*_{i,3}, \tag{3.94}$$

$$D_4 = C^*_{1,4} + N_1^2 \sum_{i=2}^{n} \frac{1}{N_i^2} C^*_{i,4}, \tag{3.95}$$

$$D_5 = C^*_{1,5} + N_1^3 \sum_{i=2}^{n} \frac{1}{N_i^3 M^2_{e,1,i-1}} C^*_{i,5}. \tag{3.96}$$

To evaluate the aberrations in the compound system, we insert (3.88) into (3.34), (3.35) to obtain

$$\epsilon_x^{(3)} = \frac{z'_n - w'_n}{N'_n M_{e,1,n}} \left(4D_1(x_e^2 + y_e^2)x_e + 2D_2 x_e y_e \theta + 2D_3 x_e \theta^2\right), \tag{3.97}$$

$$\epsilon_y^{(3)} = \frac{z'_n - w'_n}{N'_n M_{e,1,n}} \left(4D_1(x_e^2 + y_e^2)y_e + D_2(x_e^2 + 3y_e^2)\theta + 2D_4 y_e \theta^2 + D_5 \theta^3\right), \tag{3.98}$$

where the coefficients $D_1, \ldots D_5$ are given by (3.92)–(3.96).

For the analysis presented in the next section, it is more convenient to write the above formulae by introducing polar coordinates (r_e, φ) for the entrance pupil (see Figure 3.7).

In these coordinate system, we have

$$x_e = r_e \cos\varphi, \quad y_e = r_e \sin\varphi. \tag{3.99}$$

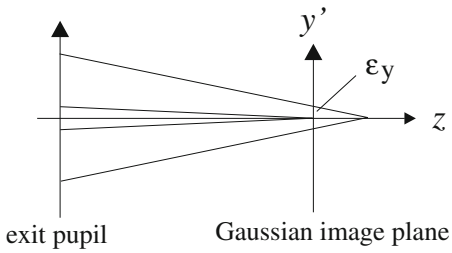

Fig. 3.7 Transverse Overcorrected spherical aberration for $\mathbb{D}_1 > 0$

Moreover, noting that

$$\cos^2\varphi + 3\sin^2\varphi = 3 - 2\cos^2\varphi \tag{3.100}$$

and taking into account the trigonometric identities

$$\cos 2\varphi = \cos^2\varphi - \sin^2\varphi = 2\cos^2\varphi - 1, \tag{3.101}$$

we obtain

$$\cos^2\varphi + 3\sin^2\varphi = 2 - \cos 2\varphi. \tag{3.102}$$

It is now easy to change (3.97), (3.98) into the following forms

$$\epsilon_x^{(3)} = \mathbb{D}_1 r_e^3 \cos\varphi + \mathbb{D}_2 r_e^2\theta \sin 2\varphi + \mathbb{D}_3 r_e\theta^2 \cos\varphi, \tag{3.103}$$

$$\begin{aligned}\epsilon_y^{(3)} &= \mathbb{D}_1 r_e^3 \sin\varphi + \mathbb{D}_2 r_e^2\theta\,(2 - \cos 2\varphi)\\ &\quad + \mathbb{D}_4 r_e\theta^2 \sin\varphi + \mathbb{D}_5\theta^3,\end{aligned} \tag{3.104}$$

where

$$\mathbb{D}_1 = 4\frac{z_n' - w_n'}{N_n' M_{e,1,n}} D_1, \tag{3.105}$$

$$\mathbb{D}_2 = \frac{z_n' - w_n'}{N_n' M_{e,1,n}} D_2, \tag{3.106}$$

$$\mathbb{D}_3 = 2\frac{z_n' - w_n'}{N_n' M_{e,1,n}} D_3, \tag{3.107}$$

$$\mathbb{D}_4 = 2\frac{z_n' - w_n'}{N_n' M_{e,1,n}} D_4, \tag{3.108}$$

$$\mathbb{D}_5 = \frac{z_n' - w_n'}{N_n' M_{e,1,n}} D_5. \tag{3.109}$$

3.6 Analysis of Third-Order Aberrations

In this section, the meaning of each term that appears in (3.65) as well as their combined effect on the final image are analyzed.

1. Spherical Aberration We consider rays originating from the axial object point. For all these rays $\theta = 0$ and (3.103), (3.104) supply the conditions

$$\epsilon_x^{(3)} = \mathbb{D}_1 r_e^3 \cos\varphi, \tag{3.110}$$

$$\epsilon_y^{(3)} = \mathbb{D}_1 r_e^3 \sin\varphi, \tag{3.111}$$

which, in turn, imply that

$$|\epsilon| = \sqrt{\epsilon_x^2 + \epsilon_y^2} = |\mathbb{D}_1| r_e^3. \tag{3.112}$$

Equation (3.112) shows that all of the rays that originate from the axial object point and cross the entrance pupil along a circumference of radius r_e centered on the optical axis, instead of striking the *same* axial image point, spread along a circumference centered on the Gaussian image $(0, 0)$ and with radius $\mathbb{D}_1 r_e^3$ (see Figure 3.8). The spherical aberration is *symmetric* around the optical axis. Moreover, let γ be a ray that intersects the entrance pupil at the point $(\pi/2, r_e)$. Then $\epsilon_x = 0$, $\epsilon_y = \mathbb{D}_1 r_e^3$; thus, if $\mathbb{D}_1 > 0$, $\epsilon_y > 0$ and γ meets the optical axis after the Gaussian plane (see Figure (3.8). The opposite situation happens if $\mathbb{D}_1 < 0$ (see Figure 3.9)). In the first case, the transversal spherical aberration is said to be overcorrected whereas in the second case it is said to be undercorrected.

We note that all of the rays that arise from the object point on the axis and intercepting the entrance pupil along a circumference of radius r_e meet the optical axis at a same point. It can also be proved that the distance of this point from the Gaussian object plane is equal to

$$l(r_e) = \frac{\mathbb{D}_1}{z_n' - w_n'} r_e^2. \tag{3.113}$$

1. Coma In order to understand the contribution of the terms

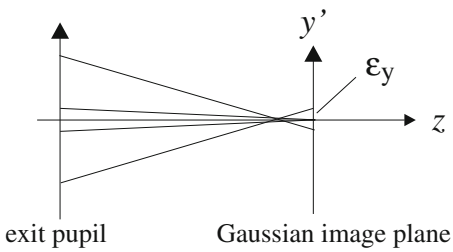

Fig. 3.8 Transverse undercorrected spherical aberration for $\mathbb{D}_1 < 0$

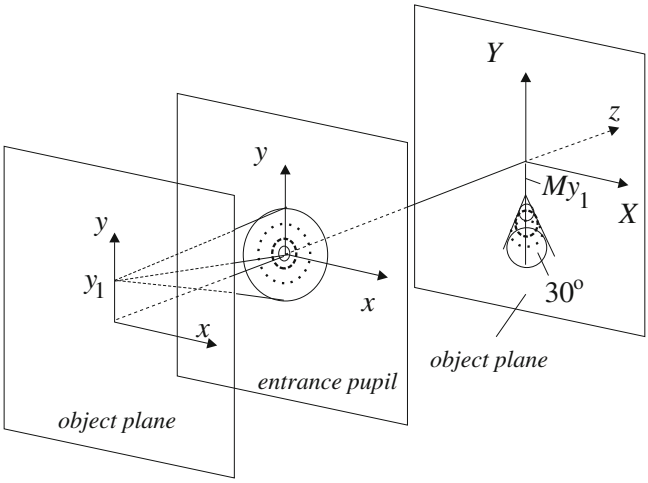

Fig. 3.9 Coma

$$\epsilon_x^{(3)} = \mathbb{D}_2 r_e^2 \theta \sin 2\varphi, \tag{3.114}$$
$$\epsilon_y^{(3)} = \mathbb{D}_2 r_e^2 \theta \left(2 - \cos 2\varphi\right), \tag{3.115}$$

to the aberrations, the set Γ of rays from $(0, \theta)$, for which r_e is constant is considered. These rays intersect with the image plane in the points with coordinates $(\epsilon_x^{(3)}, y_n' + \epsilon_y^{(3)})$. Since (3.12) and (3.13) imply the equation

$$(\epsilon_x^{(3)})^2 + (\epsilon_y^{(3)} - y_n' - \mathbb{D}_2 r_e^2 \theta)^2 = (\mathbb{D}_2 r_e^2 \theta)^2,$$

the rays of Γ intersect with the image plane in a circle of radius

$$R = \mathbb{D}_2 r_e^2 \theta, \tag{3.116}$$

that is centered at the point

$$(0, My + 2R)\,. \tag{3.117}$$

The resulting image of a point of the object plane is given by the superposition of these circles upon varying r_e. If (X, Y) denotes a moving point of the object plane, the envelope of this one-parameter family Δ of circles can be obtained by eliminating the parameter R between the two equations

$$f(X, Y, R) = X^2 + (Y - 2R)^2 - R^2 = 0, \tag{3.118}$$
$$f_{,R}(X, Y, R) = -4(Y - 2R) - 2R = 0, \tag{3.119}$$

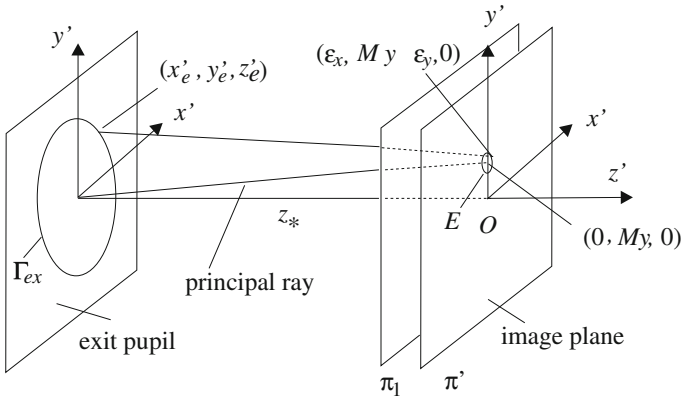

Fig. 3.10 Astigmatism and field curvature

where (3.118) describes the family Δ and (3.119) is the derivative of the first equation with respect to the parameter R. A straightforward calculation leads to the following equation for the envelope

$$X^2 - \frac{1}{3}Y^2 = 0, \tag{3.120}$$

which is therefore represented by two straight lines at an angle of 30° with the axis Oy.

This aberration, which is not symmetric, is called ***coma*** (see Figure 3.9).

1. Astigmatism and Curvature of Field We now analyze the terms

$$\epsilon_x^{(3)} = \mathbb{D}_3 r_e \theta^2 \cos\varphi, \tag{3.121}$$
$$\epsilon_y^{(3)} = \mathbb{D}_4 r_e \theta^2 \sin\varphi, \tag{3.122}$$

for given θ and r_e upon varying φ. Let y be the abscissa of the object point corresponding to the view angle θ. We denote the set of all the rays coming from y and crossing the exit pupil π'_e at a distance r'_e from the optical axis by Γ_{ex}. The rays of Γ_{ex} intercept an ellipse E with axes $\mathbb{D}_3 r_e \theta^2$, $\mathbb{D}_4 r_e \theta^2$ that is centered at $(0, My)$ on the Gaussian image plane π'. Here M is the magnification of the optical system (see Figure 3.10).

To analyze this aberration we consider the curve of intersection of Γ_{ex} with another plane π_1 at a distance z_1 from π'. If (x'_1, y'_1) and (x', y') denote the coordinates in π_1 and π', respectively, then we suppose that z_1 is of the order of y'^2.

The parametric equations of a ray from the point $(x'_e, y'_e) \in \Gamma_{ex}$ to the point $(\epsilon_x, My + \epsilon_y) \in \pi'$, when the origin of the axes is taken to be O, are

$$X = \epsilon_x + (x'_e - \epsilon_x)t, \tag{3.123}$$
$$Y = My + \epsilon_y + (y'_e - My - \epsilon_y)t, \tag{3.124}$$
$$Z = -z_* t. \tag{3.125}$$

The value of the parameter t when the ray intercepts the plane π_1 is

$$t = -\frac{z_1}{z_*}, \tag{3.126}$$

so that the coordinates of the intersection point in the plane π_1 are

$$x_1 = \epsilon_x - x_e' \frac{z_1}{z_*}, \tag{3.127}$$

$$y_1 = My + \epsilon_y - (y_e' - My)\frac{z_1}{z_*}. \tag{3.128}$$

In writing the above equations we have taken into account the condition $z_1 \simeq M^2 y^2$ and noted that ϵ_x, ϵ_y are third-order quantities.

In view of (3.123), (3.124), the relations (3.127), (3.128) can also be written as follows

$$x_1 = \left(\mathbb{D}_3\theta^2 - M_{e,1,n}\frac{z_1}{z_*}\right) r_e \cos\varphi, \tag{3.129}$$

$$y_1 = My\left(1 + \frac{z_1}{z_*}\right) + \left(\mathbb{D}_4\theta^2 - M_{e,1,n}\frac{z_1}{z_*}\right) r_e \sin\varphi. \tag{3.130}$$

where $M_{e,1,n}$ is the magnification between the pupils.

Then, we conclude that the intersection of Γ_{ex} with the plane π_1 is again an ellipse with different axes and a different center. For a given θ, the axis along x' of this ellipse becomes zero when

$$z_1 = \frac{z_*}{M_{e,1,n}}\mathbb{D}_3\,\theta^2, \text{ (meridional or tangential focus)}, \tag{3.131}$$

whereas the axis along y' vanishes when

$$z_2 = \frac{z_*}{M_{e,1,n}}\mathbb{D}_4\,\theta^2, \text{ (primary or sagittal focus)}. \tag{3.132}$$

It is possible to change the above two relations into a form that allows us to recognize the geometrical meaning of the quantities $\mathbb{D}_3$ and $\mathbb{D}_4$. Recalling (2.64) and noting that $y' = \theta' z_*$, (3.131) and (3.132) then assume the forms:

$$z_1 = \frac{z_* M_{e,1,n} N_n'^2}{N_1^2}\mathbb{D}_3\theta'^2 = \frac{N_n'}{N_1^2}\frac{M_{e,1,n}}{z_*}\mathbb{D}_3 y'^2, \tag{3.133}$$

$$z_2 = \frac{z_* M_{e,1,n} N_n'^2}{N_1^2}\mathbb{D}_4\theta'^2 = \frac{N_n'}{N_1^2}\frac{M_{e,1,n}}{z_*}\mathbb{D}_4 y'^2. \tag{3.134}$$

In conclusion, upon varying y', the loci of sagittal and tangential foci define two curves that, when rotated about the optical axis, define two spheres Σ_1 and Σ_2, called **sagittal and tangential or meridional focal surfaces**, respectively. The curvature radii of these surfaces are given by (see (3.107), (3.108))

$$\frac{1}{2R_s} = \frac{N'_n}{N_1^2}\frac{M_{e,1,n}}{z_*}\mathbb{D}_3 = 2\frac{1}{N_1^2}D_3, \tag{3.135}$$

$$\frac{1}{2R_t} = \frac{N'_n}{N_1^2}\frac{M_{e,1,n}}{z_*}\mathbb{D}_4 = 2\frac{1}{N_1^2}D_4. \tag{3.136}$$

The distance between Σ_1 and Σ_2

$$z_2 - z_1 = \frac{N'_n}{N_1^2}\frac{M_{e,1,n}}{z_*}(\mathbb{D}_4 - \mathbb{D}_3)y'^2, \tag{3.137}$$

is a measure of the ***astigmatism*** of the optical system.

1. Distortion Using the last terms of (3.103), (3.104)

$$\epsilon_x^{(3)} = 0, \tag{3.138}$$

$$\epsilon_y^{(3)} = \mathbb{D}_5\theta^3. \tag{3.139}$$

we obtain

$$x' = 0, \tag{3.140}$$

$$y' = My + \mathbb{D}_5\theta^3 = M\left(y + \frac{\mathbb{D}_5}{M}\theta^2\right). \tag{3.141}$$

Consequently, we conclude that the image point moves away from the axis if $\mathbb{D}_5/M > 0$ and towards the axis in the opposite case. These two cases are known as ***pin-cushion and barrel distortion***, respectively.

3.7 Petzval's Theorem

We are now in the position to prove a very important theorem attributed to the Hungarian mathematician Petzval.

We will first prove the following relation:

$$D_4 - 3D_3 = -N_1^2\sum_{i=1}^{n}\frac{1}{2R_i}\left(\frac{1}{N'_i} - \frac{1}{N_i}\right). \tag{3.142}$$

This relation is very interesting since it shows that, although D_4 and D_3 depend separately on the positions of the stop and the object, the difference $D_4 - 3D_3$ *depends only on the characteristics of the optical system*.

In order to prove (3.142), we start by noting that from (3.44), (3.47), (3.63), (3.64) it follows that

$$\begin{aligned} C^*_{i,4} - 3C^*_{i,3} =& C_{i,4} - 3C_{i,3} \\ =& -\frac{N_i^2}{2}\left(\frac{1}{N'_i z'_i} - \frac{1}{N_i z_i}\right) \\ & -\frac{N_i}{2}\left(1 - \frac{N_i^2}{N_i'^2}\right)\left(\frac{1}{z_i} - \frac{1}{R_i}\right) \end{aligned} \tag{3.143}$$

so that

$$C^*_{i,4} - 3C^*_{i,3} = -\frac{N_i^2}{2}\left(\frac{1}{N'_i z'_i} - \frac{1}{N_i z_i} + \left(\frac{1}{N_i'^2} - \frac{1}{N_i^2}\right)\left(\frac{N_i}{R_i} - \frac{N_i}{z_i}\right)\right).$$

Recalling Abbe's equation (2.7), here written in the equivalent form

$$\frac{1}{N'_i z'_i} = \frac{1}{N'_i R_i} - \frac{N_i}{N_i'^2 R_i} + \frac{N_i}{N_i'^2 z_i}, \tag{3.144}$$

the above condition becomes

$$C^*_{i,4} - 3C^*_{i,3} = -\frac{N_i^2}{2R_i}\left(\frac{1}{N'_i} - \frac{1}{N'_i}\right). \tag{3.145}$$

On the other hand, in view of (3.94), (3.95), it is also

$$D_4 - 3D_3 = \left[C^*_{i,4} - 3C^*_{i,3} + \sum_{i=2}^{n} \frac{N_1^2}{N_i^2}(C^*_{i,4} - 3C^*_{i,3})\right], \tag{3.146}$$

and (3.142) is proved.

Finally, (3.142), (3.135), (3.136) imply that

$$\frac{1}{R_t} - \frac{3}{R_s} = 4\frac{1}{N_1^2}(D_4 - 3D_3). \tag{3.147}$$

Therefore, in view (3.142), the following relation is obtained

$$\frac{3}{R_s} - \frac{1}{R_t} = \frac{2}{R_p}, \tag{3.148}$$

where the quantity

$$\frac{1}{R_p} = \sum_{i=1}^{n} \frac{1}{R_i}\left(\frac{1}{N_i'} - \frac{1}{N_i}\right) \tag{3.149}$$

is called ***Petzval's curvature*** whereas the equation (3.148) expresses the contents of ***Petzval's theorem***.

In particular, (3.147) implies that, in the absence of astigmatism, i.e., when $D_4 = D_3$), or, equivalently, when $1/R_s = 1/R_t$, the two focal surfaces Σ_1 and Σ_2 coincide with the Petzval's surface of radius R_p. In this case, a necessary condition to have no field curvature is given by

$$\frac{1}{R_p} = 0, \tag{3.150}$$

which is independent of the positions of the object and stop.

In conclusion, all the above considerations, lead us to define the following expression

$$\frac{z_n' - w_n'}{N_n' M_{e,n}}(D_4 - 3D_3)\theta^2 r_e = -\frac{1}{2}\frac{z_n' - w_n'}{N_n'^2 M_{e,n}}\frac{N_1^2}{R_p}, \tag{3.151}$$

as the ***curvature of field***.

3.8 Aberration Formulae

In this section all the fundamental third-order aberration formulae are collected for the reader's convenience.

Spherical Aberration

$$\text{Transversal Spherical Aberration} = 4\frac{z_n' - w_n'}{N_n' M_{e,n}} D_1 r_e^3, \tag{3.152}$$

$$D_1 = C_{1,1}^* + \sum_{i=2}^{n} M_{e,i}^4 C_{i,1}^*,$$

where r_e is the radius of entrance pupil.

Sagittal Coma

$$\text{Sag. Coma} = -\frac{z_n' - w_n'}{N_n' M_{e,n}} D_2 \theta r_e^2, \tag{3.153}$$

$$D_2 = C_{1,2}^* + N_1 \sum_{i=2}^{n} \frac{1}{N_i} M_{e,i-1}^2 C_{i,2}^*,$$

Astigmatism

$$\text{Astigmatism} = \frac{z'_n - w'_n}{N'_n M_{e,n}}(D_4 - D_3)\theta^2 r_e, \tag{3.154}$$

$$D_3 = C^*_{1,3} + N_1^2 \sum_{i=2}^{n} \frac{1}{N_i^2} C^*_{i,3},$$

$$D_4 = C^*_{1,4} + N_1^2 \sum_{i=2}^{n} \frac{1}{N_i^2} C^*_{i,4}.$$

Curvature of Field

$$\begin{aligned}\text{Curvature of Field} &= \frac{z'_n - w'_n}{N'_n M_{e,n}}(D_4 - 3D_3)\theta^2 r_e \\ &= -\frac{1}{2}\frac{z'_n - w'_n}{N'^2_n M_{e,n}}\frac{N_1^2}{R_p}\theta^2 r_e,\end{aligned} \tag{3.155}$$

$$\frac{1}{R_p} = N'_n \sum_{i=1}^{n} \frac{1}{R_i}\left(\frac{1}{N'_i} - \frac{1}{N_i}\right) \tag{3.156}$$

Distortion

$$\text{Distorsion} = \frac{z'_n - w'_n}{N'_n M_{e,n}} D_5 \theta^3, \tag{3.157}$$

$$D_5 = C^*_{1,5} + N_1^3 \sum_{i=2}^{n} \frac{1}{N_i^3 M_{e,i}^2} C^*_{i,5}.$$

3.9 Combined Effect of Third-Order Aberrations

In this section the combined effect of all third-order aberrations will be considered. To this end, we write formulae (3.103)–(3.104) as follows

$$\begin{aligned}\epsilon_x^{(3)} &= (\mathbb{D}_1 r_e^3 + \mathbb{D}_3 r_e \theta^2)\cos\varphi + \mathbb{D}_2 r_e^2 \theta \sin 2\varphi, \\ \epsilon_y &= 2\mathbb{D}_2 r_e^2 \theta + \mathbb{D}_5 \theta^3 + (\mathbb{D}_1 r_e^3 + \mathbb{D}_4 r_e \theta^2)\sin\varphi - \mathbb{D}_2 r_e^2 \theta \cos 2\varphi.\end{aligned}$$

and suppose r_e and y to be constant. These equations can be regarded as the parametric equations of a curve in the Gaussian image plane π' with respect to the parameter φ. This curve can be constructed in the following way. We consider the ellipse E which has its center at the point

$$\left(0, 2\mathbb{D}_2 r_e^2 \theta + \mathbb{D}_5 \theta^3\right) \tag{3.158}$$

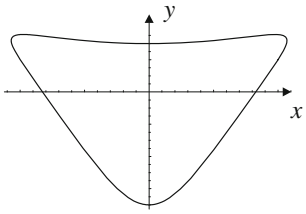

Fig. 3.11 A possible form of the curve Γ

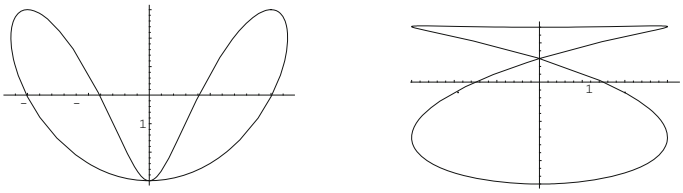

Fig. 3.12 Possible forms of the curve Γ

and axes

$$\mathbb{D}_1 r_e^3 + \mathbb{D}_3 r_e \theta^2, \quad \mathbb{D}_1 r_e^3 + \mathbb{D}_4 r_e \theta^2. \tag{3.159}$$

Then any point of this ellipse is regarded as the center of a circle of radius $\mathbb{D}_2 r_e^2 \theta$. Finally, the resulting curve Γ has the behavior of Figure 3.11.

It is clear that the form of Γ is strongly influenced by the characteristics of its components curves. For instance, in Figure 3.12 two examples of Γ are given when the ellipse degenerates into a straight line.

3.10 Primary or Axial Chromatic Aberrations

In the previous two chapters, the refractive indices were considered as characteristic constants of the media from which the lenses are made. However, it is well known that all substances exhibit a wavelength-dependent refractive indices. This means that all of the results obtained so far only apply to a *fixed* wavelength. For this reason, the aberrations studied in the above sections are called monochromatic third-order aberrations.

A manufacturer of optical glasses will list the refractive indices at various standard wavelength for each type of glass in its catalog (see Table 3.1).

The Abbe numbers

$$V_d = \frac{N_d - 1}{N_F - N_C}, \quad V_e = \frac{N_e - 1}{N_{F'} - N_{C'}}, \tag{3.160}$$

Table 3.1 Wavelengths of different colors

Line	Wavelength (mm)	Element	Color
h	404.66	Hg	violet
g	435.83	Hg	violet
F′	479.99	Cd	blue
F	486.13	H	blue
e	546.07	Hg	green
d	586.56	He	yellow
C′	643.85	Cd	red
C	656.27	H	red
r	706.52	He	deep red

where N_λ denotes the refractive index of the wavelength λ, are a measure of the dispersion power of the glass under consideration.

The refractive index at the d−line for real optical glasses vary from 1.44 to 1.96, whereas the Abbe numbers vary from 20 to 90. We note that a smaller Abbe's number implies a higher dispersion power of the glass.

We begin our analysis of chromatic aberrations by studying the variations in the Gaussian characteristics of an optical system. More precisely, we evaluate *the change in the Gaussian position of the image and the Gaussian magnification on varying the wavelength of the light*. The former is the ***axial chromatic aberration*** whereas the latter is the ***chromatic magnification or lateral color aberration*** (see also Section 1.4). In what follows, the notation Δa is introduced in order to denote the first-order variation in the quantity a, corresponding to a change in the refractive index ΔN.

For the first aberration, we begin by writing Abbe's invariant (2.7) in the equivalent form

$$\frac{N_i'}{z_i'} - \frac{N_i}{z_i} = \frac{N_i' - N_i}{R_i}, \tag{3.161}$$

Supposing the refractive indices and the quantities z_i and z_i' are functions of the wavelength, we differentiate this relation to derive the equation

$$-N_i'\frac{\Delta z_i'}{z_i'^2} + N_i\frac{\Delta z_i}{z_i^2} + \frac{\Delta N_i'}{z_i'} - \frac{\Delta N_i}{z_i} = \frac{\Delta N_i' - \Delta N_i}{R_i}, \tag{3.162}$$

which can be placed in the form

$$N_i'\frac{\Delta z_i'}{z_i'^2} - N_i\frac{\Delta z_i}{z_i^2} = \\ -\frac{\Delta N_i'}{N_i'}\left(\frac{N_i'}{R_i} - \frac{N_i'}{z_i'}\right) + \frac{\Delta N_i}{N_i}\left(\frac{N_i}{R_i} - \frac{N_i}{z_i}\right), \tag{3.163}$$

in other words,

$$N_i' \frac{\Delta z_i'}{z_i'^2} - N_i \frac{\Delta z_i}{z_i^2} = -\left(\frac{\Delta N_i'}{N_i'} - \frac{\Delta N_i}{N_i}\right) Q_i, \tag{3.164}$$

where Q_i is the Abbe invariant of the surface S_i. We must now take into account the recursive relations

$$z_{i+1} = z_i' - t_i, \quad \Delta z_{i+1} = \Delta z_i', \quad N_{i+1} = N_i', \tag{3.165}$$

as well as the condition

$$\Delta z_1 = 0, \tag{3.166}$$

due to the fact that the object position is given.

With these results in mind, adding the equations (3.164) obtained by allowing the index i to vary from 1 to n finally yields

$$\begin{aligned} \Delta z_n' = & \\ & \frac{z_n'^2}{N_n'} \left[\sum_{i=1}^{n-1} N_{i+1} \Delta z_{i+1} \left(\frac{1}{(z_i' + t_i)^2} - \frac{1}{z_i'^2} \right) \right. \\ & \left. - \sum_{i=1}^{n} \left(\frac{\Delta N_i'}{N_i'} - \frac{\Delta N_i}{N_i} \right) Q_i \right], \end{aligned} \tag{3.167}$$

which expresses the changes in the image position as a function of refractive indices and the characteristics of the optical system. In conclusion, the optical system will be free of axial chromatic aberration, if $\Delta z_n' = 0$, that is if

$$\begin{aligned} & \sum_{i=1}^{n-1} N_{i+1} \Delta z_{i+1} \left(\frac{1}{(z_i' + t_i)^2} - \frac{1}{z_i'^2} \right) \\ & - \sum_{i=1}^{n} \left(\frac{\Delta N_i'}{N_i'} - \frac{\Delta N_i}{N_i} \right) Q_i = 0. \end{aligned} \tag{3.168}$$

In particular, when all of the thicknesses in (3.168) can be neglected, the above formula reduces to the following one:

$$\Delta z_n' = -\frac{z_n'^2}{N_n'} \sum_{i=1}^{n} \left(\frac{\Delta N_i'}{N_i'} - \frac{\Delta N_i}{N_i} \right) Q_i. \tag{3.169}$$

It now remains to evaluate the change in the magnification M due to the wavelength-dependent nature of refractive indices. Since $y_{i+1} = y_i'$, we have that

$$M = \frac{y'_n}{y_1} = \frac{y'_n}{y_n}\frac{y'_{n-1}}{y_{n-1}} \cdots \frac{y'_1}{y_1}. \tag{3.170}$$

In view of (2.8), this relation becomes:

$$M = \frac{N_1}{N'_n}\frac{z'_1}{z_1}\frac{z'_2}{z_2} \cdots \frac{z'_n}{z_n}. \tag{3.171}$$

If f is any function, then the following formula holds

$$\Delta\,(\log f) = \frac{\Delta f}{f}. \tag{3.172}$$

On the other hand, if $f = f_1 \cdots f_n$, then we have

$$\Delta(\log f) = \Delta(\log f_1 + \cdots \log f_n) = \frac{\Delta f_1}{f_1} + \cdots \frac{\Delta f_n}{f_n}, \tag{3.173}$$

so that

$$\frac{\Delta f}{f} = \frac{\Delta f_1}{f_1} + \cdots \frac{\Delta f_n}{f_n}. \tag{3.174}$$

By applying this relation to (3.171), we obtain the equation

$$\frac{\Delta M}{M} = \frac{\Delta N_1}{N_1} + N'_n \Delta\left(\frac{1}{N'_n}\right) + \sum_{i=1}^{n} \frac{\Delta z'_i}{z'_i} + \sum_{i=1}^{n} z_i \Delta\left(\frac{1}{z_i}\right), \tag{3.175}$$

which can also be written

$$\frac{\Delta M}{M} = \frac{\Delta N_1}{N_1} - \frac{\Delta N'_n}{N'_n} + \sum_{i=1}^{n}\left(\frac{\Delta z'_i}{z'_i} - \frac{\Delta z_i}{z_i}\right). \tag{3.176}$$

This formula supplies the chromatic variation of magnification, since the changes Δz_i can be evaluated by (3.164) and (3.165).

3.11 Third-Order Aberrations in the Exit Pupil

In some cases, it is important to know the third-order aberrations in the exit pupil for a compound optical system. The best way of evaluating the third-order aberrations in the exit pupil consists in considering the entrance pupil as object plane and the object plane as entrance pupil. Consequently, the image plane becomes the exit pupil and the exit pupil becomes the image plane. In other words, rather than considering the imaging of the object on the image plane through the entrance and exit pupils,

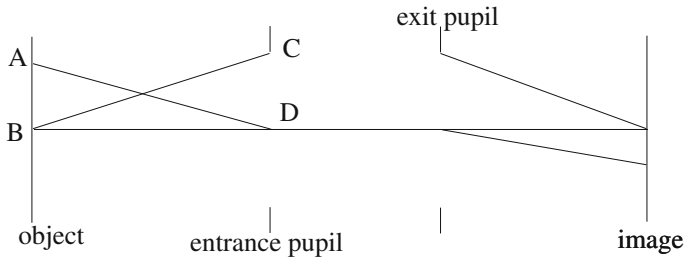

Fig. 3.13 Pupils as object and image planes

we consider the imaging of the entrance pupil onto the exit pupil trough the object and image planes that now replace the entrance and exit pupils, respectively. In this exchange, the marginal ray of the usual imaging becomes the chief ray of the pupil imaging and the chief ray of the ordinary imaging becomes the marginal ray in the pupil imaging. In Figure 3.13 the rays BC and AD are the marginal ray and principal ray, respectively, when we consider the ordinary imaging between the object and image planes. In contrast, DA is the marginal ray and CB the principal ray if we assume the planes of the pupils as object and image planes. So all of the formulae of Sections 3.4 and 3.5 can be used to calculate the pupil aberrations, provided that the quantities x_e and y_e, that refer to the marginal ray, are replaced by the corresponding quantities x_1, y_1. Finally, z_i must be replaced by w_i and viceversa. In this way, we obtain

$$c_i^{(e)} = \frac{w_i}{w_i - z_i}, \quad d_i^{(e)} = \frac{z_i}{w_i - z_i}, \tag{3.177}$$

$$C_{1,i}^{(e)} = -\frac{N_i^2}{8}\left(\frac{1}{N_{i+1}w_i'} - \frac{1}{N_i w_i}\right)\left(\frac{1}{w_i} - \frac{1}{R_i}\right)^2 + \frac{N_{i+1} - N_i}{8R_i^3} - (N_{i+1} - N_i)\overline{a}_{4,i}, \tag{3.178}$$

$$C_{2,i}^{(e)} = \frac{N_i^2}{2}\left(\frac{1}{N_{i+1}w_i'} - \frac{1}{N_i w_i}\right)\left(\frac{1}{w_i} - \frac{1}{R_i}\right), \tag{3.179}$$

$$C_{3,i}^{(e)} = \frac{N_i}{4}\left(\frac{N_{i+1}^2 - N_i^2}{N_{i+1}^2}\right)\left(\frac{1}{w_i} - \frac{1}{R_i}\right), \tag{3.180}$$

$$C_{4,i}^{(e)} = C_{3,i} - \frac{N_i^2}{2}\left(\frac{1}{N_{i+1}w_i'} - \frac{1}{N_i w_i}\right), \tag{3.181}$$

$$C_{5,i}^{(e)} = -\frac{N_i}{2w_i^3}\frac{N_{i+1}^2 - N_i^2}{N_{i+1}^2}. \tag{3.182}$$

$$C_{1,i}^{*(e)} = c_i^{(e)4} C_{1,i}^{(e)}, \tag{3.183}$$

$$C_{2,i}^{*(e)} = c_i^{(e)2}(C_{2,i}^{(e)} - 4w_i d_i^{(e)} C_{1,i}^{(e)}), \tag{3.184}$$

$$C_{3,i}^{*(e)} = C_{3,i}^{(e)} - w_i d_i^{(e)} C_{2,i}^{(e)} + 2w_i^2 d_i^{(e)2} C_{1,i}^{(e)}, \tag{3.185}$$

$$C_{4,i}^{*(e)} = C_{4,i}^{(e)} - 3w_i d_i^{(e)} C_{2,i}^{(e)} + 6w_i^2 d_i^{(e)2} C_{1,i}^{(e)}, \tag{3.186}$$

$$C_{5,i}^{*(e)} = \frac{1}{c_i^{(e)2}}(C_{5,i}^{(e)} - 2w_i d_i^{(e)} C_{4,i}^{(e)} \tag{3.187}$$

$$+3w_i^2 d_i^{(e)2} C_{2,i}^{(e)} - 4w_i^3 d_i^{(e)3} C_{1,i}^{(e)}), \tag{3.188}$$

$$D_1^{(e)} = C_{1,1}^{*(e)} + \sum_{i=2}^{n} M_{1,i-1}^4 C_{1,i}^{*(e)}, \tag{3.189}$$

$$D_2^{(e)} = C_{2,1}^{*(e)} + N_1 \sum_{i=2}^{n} \frac{1}{N_i} M_{1,i-1}^2 C_{2,i}^{*(e)}, \tag{3.190}$$

$$D_3^{(e)} = C_{3,1}^{*(e)} + N_1^2 \sum_{i=2}^{n} \frac{1}{N_i^2} C_{3,i}^{*(e)}, \tag{3.191}$$

$$D_4^{(e)} = C_{4,1}^{*(e)} + N_1^2 \sum_{i=2}^{n} \frac{1}{N_i^2} C_{4,i}^{*(e)}, \tag{3.192}$$

$$D_5^{(e)} = C_{5,1}^{*(e)} + N_1^3 \sum_{i=2}^{n} \frac{1}{N_i^3 M_{1,i-1}^2} C_{5,i}^{*(e)}. \tag{3.193}$$

Introducing polar coordinates (r_1, φ) on the*object plane* and denoting by r_1 is the distance of a point of the object from the optical axis, instead of (3.152)–(3.156), we obtain

Spherical Aberration

$$\text{Transversal Spherical Aberration} = 4\frac{w_n' - z_n'}{N_n' M_n} D_1^{(e)} r_1^3, \tag{3.194}$$

$$D_1^{(e)} = C_{1,1}^{*(e)} + \sum_{i=2}^{n} M_i^4 C_{i,1}^{*(e)},$$

Sagittal Coma

$$\text{Sag. Coma} = -\frac{w_n' - z_n'}{N_n' M_n} D_2^{(e)} \Theta r_1^2, \tag{3.195}$$

$$D_2^{(e)} = C_{1,2}^{*(e)} + N_1 \sum_{i=2}^{n} \frac{1}{N_i} M_{i-1}^2 C_{i,2}^{*(e)}, \tag{3.196}$$

Astigmatism

$$\text{Astigmatism} = \frac{w_n' - z_n'}{N_n' M_n} (D_4^{(e)} - D_3^{(e)}) \Theta^2 r_1, \tag{3.197}$$

$$D_3^{(e)} = C_{1,3}^{*(e)} + N_1^2 \sum_{i=2}^{n} \frac{1}{N_i^2} C_{i,3}^{*(e)},$$

$$D_4^{(e)} = C_{1,4}^{*(e)} + N_1^2 \sum_{i=2}^{n} \frac{1}{N_i^2} C_{i,4}^{*(e)}. \tag{3.198}$$

Curvature of Field

$$\begin{aligned}\text{Curvature of Field} &= \frac{w_n' - z_n'}{N_n' M_n} (D_4^{(e)} - 3D_3^{(e)}) \Theta^2 r_1 \\ &= -\frac{1}{2} \frac{w_n' - z_n'}{N_n'^2 M_n} \frac{N_1^2}{R_p} \theta^2 r_e,\end{aligned} \tag{3.199}$$

$$\frac{1}{R_p} = N_n' \sum_{i=1}^{n} \frac{1}{R_i} \left(\frac{1}{N_i'} - \frac{1}{N_i} \right) \tag{3.200}$$

Distortion

$$\text{Distortion} = \frac{w_n' - z_n'}{N_n' M_n} D_5^{(e)} \Theta^3, \tag{3.201}$$

$$D_5^{e)} = C_{1,5}^{*(e)} + N_1^3 \sum_{i=2}^{n} \frac{1}{N_i^3 M_i^2} C_{i,5}^{*(e)}.$$

where

$$\Theta = \frac{y_e}{w_1 - z_1}. \tag{3.202}$$

The notebook ***TotalAberrations*** evaluates the third-order aberrations in both the image plane.

In Chapter 4 it will be necessary to use the explicit form of the aberration vector $\boldsymbol{\epsilon}_{(e)}^{(3)} \equiv (\epsilon_{x,e}^{(3)}, \epsilon_{y,e}^{(3)})$. This vector cannot be obtained applying the above procedure to

(3.103) and (3.104), that define the aberration vector in the ordinary imaging. We remind how $\epsilon_x^{(3)}$ and $\epsilon_y^{(3)}$ were obtained in Section 3.5. First, (3.80) gave the total aberration function $\Phi(\xi_1, \eta_1, \zeta_1)$ in terms of the optical invariants

$$\xi_1 = y_1^2, \ \eta_1 = x_e^2 + y_e^2, \ \zeta_1 = y_1 y_e. \tag{3.203}$$

Then, introducing the view angle θ, formula (3.67) was transformed into (3.88). Finally, (3.34) and (3.35) led us to the aberration vector (3.97), (3.98). We must note that (3.88) and (3.203) are based on the assumption $x_1 = 0$ that, in turn, is a consequence of the symmetry of rotation of the optical system. In contrast, in our case the object plane is the entrance pupil and we must take into account all of the rays entering the entrance pupil. Therefore, instead of (3.203), we have

$$\xi_1 = x_e^2 + y_e^2, \ \eta = x_1^2 + y_1^2, \ \zeta = x_1 x_e + y_1 y_e, \tag{3.204}$$

and the total aberration function becomes

$$\begin{aligned}\Phi = {} & D_1^{(e)}(x_1^2 + y_1^2)^2 + \frac{1}{w_1 - z_1} D_2^{(e)}(x_1^2 + y_1^2)(x_e x_1 + y_e y_1) \\ & + \frac{1}{(w_1 - z_1)^2} D_3^{(e)}(x_1^2 + y_1^2)(x_e^2 + y_e^2) \\ & + \frac{1}{(w_1 - z_1)^2}(D_4^{(e)} - D_3^{(e)})(x_1 x_e + y_1 y_e)^2 \\ & + \frac{1}{(w_1 - z_1)^3} D_5^{(e)}(x_e^2 + y_e^2)(x_e x_1 + y_e y_1).\end{aligned} \tag{3.205}$$

We must now to derive (3.205) with respect to x_1 and y_1, introduce $x_1 = 0$ into the derivatives and to remind (3.35). In this way we obtain the third-order aberration vector in the exit pupil

$$\begin{aligned}\epsilon_{x,e}^{(3)} = {} & \frac{w_n' - z_n'}{N_{n+1} M_{1,n}} \Big(\alpha D_2^{(e)} x_e y_1^2 + \\ & 2\alpha^2 (D_4^{(e)} - D_3^{(e)}) x_e y_e y_1 + \alpha^3 D_5^{(e)} x_e y_1^2) \Big),\end{aligned} \tag{3.206}$$

$$\begin{aligned}\epsilon_{y,e}^{(3)} = {} & \frac{w_n' - z_n'}{N_{n+1} M_{1,n}} \Big(4 D_1^{(e)} y_1^3 + \\ & 3\alpha D_2^{(e)} y_1^2 y_e + 2\alpha^2 (D_3^{(e)} x_1^2 + D_4^{(e)} y_e^2) y_1 + \\ & \alpha^3 D_5^{(e)} (x_e^2 + y_e^2) y_e \Big),\end{aligned} \tag{3.207}$$

where

$$\alpha = \frac{1}{w_1 - z_1}. \tag{3.208}$$

Finally, we define other quantities that will be useful to compare the third-order aberration formulae that we propose in this book with other formulae that can be found in other books (see [5], [13]). First, we introduce the notation

$$s_{i+1} \equiv \Delta\left(\frac{\alpha_i}{N_i}\right) = \frac{\alpha_i'}{N_i'} - \frac{\alpha_i}{N_i}. \tag{3.209}$$

and the following quantities that are usually introduced to formulate the third-order aberrations:

- Spherical aberration:

$$b_i = -\frac{1}{8}a_i^2 h_i s_i. \tag{3.210}$$

- Coma:

$$\sigma_i = -a_i \overline{a}_i h_i s_i. \tag{3.211}$$

- Astigmatism:

$$c_i = -\overline{a}_i^2 h_i s_i. \tag{3.212}$$

- Distortion:

$$e_i = -\left[\overline{a}_i^2 h_i \Delta\left(\frac{\alpha_{i-1}}{N_{i-1}}\right) + h_i^2 C_i \Delta\left(\frac{1}{N_i}\right)\right]\frac{\overline{a}_i}{a_i}. \tag{3.213}$$

If we decide to adopt the variables y_i, z_i, the quantity b_i assumes the form

$$\begin{aligned} b_i &= -\frac{1}{8}N_i^2 h_i^2\left(\frac{1}{R_i} - \frac{1}{Z_i}\right)^2 h_i\left(\frac{\alpha_i'}{N_i'} - \frac{\alpha_i}{N_i}\right) \\ &= -\frac{1}{8}N_i^2\left(\frac{1}{R_i} - \frac{1}{Z_i}\right)^2\left(\frac{1}{N_i' z_i'} - \frac{1}{N_i z_i}\right)h_i^3. \end{aligned} \tag{3.214}$$

This formula is identical to formula (3.40) for the third-order spherical aberration.

3.12 Plate with Parallel Plane Faces

Let K be a plate with parallel plane faces that has a refractive index N, thickness d, and is surrounded by air (see Figure 3.14).

Applying (1.10) to the first surface S_1, we get

$$z_1' = N z_1$$

whereas, we get the following for the second surface S_2

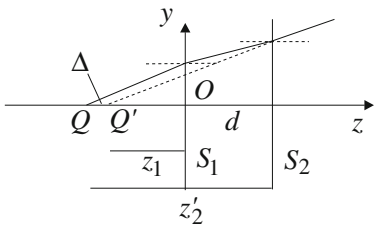

Fig. 3.14 Plan parallel slab

$$z_2' = \frac{z_1' - d}{N} = z_1 - \frac{d}{N}.$$

We can conclude that the Gaussian image of the point Q, regardless of its position, is shifted along the straight line QQ', which is orthogonal to S_1 and S_2, of a quantity

$$\Delta = z_2' + d - z_1 = d\left(1 - \frac{1}{N}\right). \tag{3.215}$$

Note that, since the refractive index N depends on the wavelength λ, the shift given by (3.215) varies with λ, meaning that K introduces an axial chromatism

$$\Delta z' = d\frac{\Delta N}{N^2}.$$

We now wish to evaluate the spherical aberration and coma produced by K under the assumption that the aperture stop of radius r is located on the first face of K. Since the radii of curvature of the two faces of K are equal to infinity, the formulae from Section (3.8) allow us to easily derive the following relations for the spherical aberration, coma and astigmatism, respectively,

$$\text{spherical aberration} = \frac{d(N^2-1)}{N^3 z_1^3} r^3, \tag{3.216}$$

$$\text{coma} = -\frac{d(N^2-1)}{N^3 z_1^3} r^2 y, \tag{3.217}$$

$$\text{astigmatism} = \frac{d(N^2-1)}{N^3 z_1^3} r y^2, \tag{3.218}$$

where y is the height of the object on the axis QQ'.

Note that all the above effects vanish when $z_1 = \infty$ and the rays of light strike the plate orthogonally.

Chapter 4
About Higher Order Aberrations

4.1 Aplanatism and Sine Condition

So far we have considered third-order aberrations. In this chapter, we analyze some topics related to higher order aberrations. We begin with the ***sine condition*** that allows us to control the coma in an optical system that is corrected for the spherical aberration for ***any*** aperture angle. The relation that we are looking for is also called ***Abbe's condition***, since Abbe understood its full meaning and applied it in an extensive way.

Let $\mathbb{S}$ be an optical system having a symmetry of revolution around the optical axis a. The object plane and the Gaussian image plane will be denoted by π and π', respectively, whereas $\mathbf{O}$ and $\mathbf{O}'$ are the intersection points of a with π and π'. Finally, we assume that a stigmatic pair of points in π and π' does not exist, at least in a neighborhood of a. Using the notations of Figure 4.1 and recalling the results of Section 1.1, the optical path length $V(\mathbf{x}, \mathbf{x}')$, along the *unique* ray $\gamma(\mathbf{x}, \mathbf{x}')$ between two points $\mathbf{x} \in \pi$ and $\mathbf{x}' \in \pi'$, allows us to define the tangent vectors to $\gamma(\mathbf{x}, \mathbf{x}')$ at $\mathbf{x}$ and $\mathbf{x}'$ by employing the relations (1.8)

$$\nabla_{\mathbf{x}} V(\mathbf{x}, \mathbf{x}') = -N(\mathbf{x})\mathbf{t}(\mathbf{x}), \quad \nabla_{\mathbf{x}'} V(\mathbf{x}, \mathbf{x}') = N(\mathbf{x}')\mathbf{t}(\mathbf{x}'). \tag{4.1}$$

If $\mathbf{x}$ and $\mathbf{x}'$ are near to the optical axis a, we can expand the function $V(\mathbf{x}, \mathbf{x}')$ to within second-order terms as follows:

$$V(\mathbf{x}, \mathbf{x}') = V(\mathbf{O}, \mathbf{O}') + (\nabla V_{\mathbf{x}})_0 \cdot (\mathbf{x} - \mathbf{O}) + (\nabla V_{\mathbf{x}'})_0 \cdot (\mathbf{x}' - \mathbf{O}'), \tag{4.2}$$

where the notation $(.)_0$ denotes that the gradients are evaluated at the points $\mathbf{O}$ and $\mathbf{O}'$. In view of (4.1), the above expansion can be written as

$$V(\mathbf{x}, \mathbf{x}') = V(\mathbf{O}, \mathbf{O}') - N\mathbf{t}_0 \cdot (\mathbf{x} - \mathbf{O}) + N'\mathbf{t}'_0 \cdot (\mathbf{x}' - \mathbf{O}'). \tag{4.3}$$

© Springer International Publishing Switzerland 2016

A. Romano and R. Cavaliere, *Geometric Optics*,
Modeling and Simulation in Science, Engineering and Technology,
DOI 10.1007/978-3-319-43732-3_4

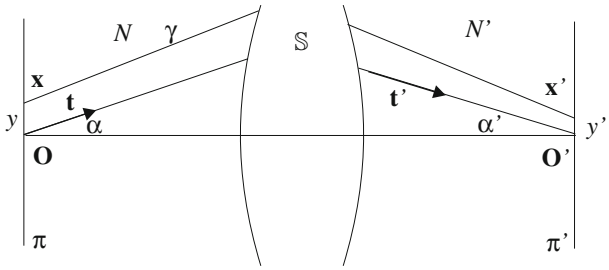

Fig. 4.1 Aplanatism condition

Since $\mathbf{x}$ and $\mathbf{x}'$ belong to the object and image planes respectively and the system exhibits symmetry of revolution around a, the scalar product $\mathbf{t}_O \cdot (\mathbf{x} - \mathbf{O})$ can always be written as $y \cos \beta$, where y is the coordinate of the object point with respect to the optical axis a and β denotes the angle between $\mathbf{t}$ and the axis Oy. Consequently, if α is the angle that $\mathbf{t}$ forms with a, we have $\mathbf{t}_0 \cdot (\mathbf{x} - \mathbf{O}) = y \sin \alpha$. Similar reasoning can also be applied to$\mathbf{t}'_{O'} \cdot (\mathbf{x}' - \mathbf{O}')$. Finally, (4.3) becomes

$$V(\mathbf{x}, \mathbf{x}') = V(\mathbf{O}, \mathbf{O}') - Ny \sin \alpha + N'y' \sin \alpha'. \tag{4.4}$$

In conclusion, let us suppose that

- $\mathbf{x}'$ is the Gaussian image of $\mathbf{x}$ so that $y' = My$, being M the magnification of K
- The sine condition

$$Ny \sin \alpha = N'y' \sin \alpha', \tag{4.5}$$

  is satisfied
- The points $\mathbf{0}$ and $\mathbf{0}'$ on the axis are stigmatic, ($V(\mathbf{0}, \mathbf{0}')$ does not depend on the ray between these two points), i. e., there is no spherical aberration for any α.

In this case, $V(\mathbf{x}, \mathbf{x}')$ does not depend on $\mathbf{x}, \mathbf{x}'$ either, and the system supplies a perfect image of any point $\mathbf{x}$ in a neighborhood of a belonging to π.

As an application of Abbe's condition, let us consider a spherical surface S that separates two media with refractive indices N and $N' < N$, respectively. Now, we prove that, if $N' < N$ and $R < 0$,

- There are two points on the optical axis that are stigmatic
- The sine condition is satisfied for these two points.

Using the notation of Figure 4.2, the condition that the optical path length of all meridional rays between the points $(z, 0)$ and $(z', 0)$ are the same, yields

$$G = N\sqrt{y_s^2 + (z_s - z)^2} - N'\sqrt{y_s^2 + (z_s - z')^2} + Nz - N'z' = 0, \tag{4.6}$$

where R is the radius of the sphere S that is centered at O. The variable y_s can be eliminated by utilizing the sphere equation

Fig. 4.2 Aplanatic meniscus

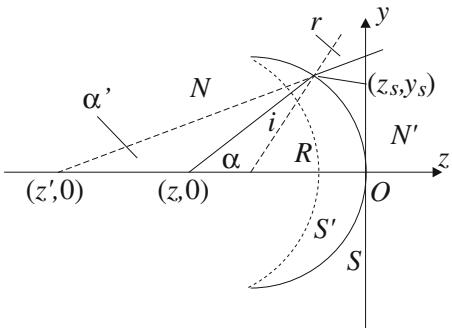

$$y_s^2 = R^2 - (R - z_s)^2, \tag{4.7}$$

so that G reduces to a function of z_s. In other words, (4.6) is equivalent to requiring that

$$G'(z_s) = 0, \quad \forall |z_s| < |R|.$$

On the other hand, this condition can be written as

$$\frac{N(R-z)}{\sqrt{R^2 - (z_s - R)^2 + (z_s - z)^2}} - \frac{N'(R-z')}{\sqrt{R^2 - (z_s - R)^2 + (z_s - z')^2}} = 0,$$

and it is straightforward to verify that the previous condition is satisfied for any compatible value of z_s when

$$N'(z' - R)\sqrt{z^2 + 2Rz_s - 2zz_s} = N(z - R)\sqrt{z'^2 + 2Rz_s - 2z'z_s}.$$

Following simple but tedious calculations, this condition reduces to the following relation:

$$zz_s(R - z)(R - z')(N^2(R - z) - N'^2(R - z')) = 0,$$

which is satisfied for any value of z_s, and for negative values of z and z', when

$$z = R, \quad z' = R, \tag{4.8}$$

$$\frac{R - z}{R - z'} = \frac{N'^2}{N^2}, \tag{4.9}$$

It now remains to impose the sine condition on the solution $(4.9)_2$, since it is not valid in the simple case (4.8).

Applying the sine theorem to the triangles $(R, 0)$, (z_s, y_s), $(z, 0)$ and $(R, 0)$, (z_s, y_s), $(z', 0)$ (see Figure 4.2) yields the relations

$$-\frac{R}{\sin\alpha} = \frac{R-z}{\sin i}, \quad -\frac{R}{\sin\alpha'} = \frac{R-z'}{\sin r},$$

where i and r are the angles of incidence and refraction, respectively. Therefore, taking the refraction law

$$\frac{\sin r}{\sin i} = \frac{N}{N'},$$

into account, we have

$$\frac{\sin\alpha'}{\sin\alpha} = \frac{R-z}{R-z'}\frac{\sin r}{\sin i} = \frac{N}{N'}\frac{R-z}{R-z'}.$$

Finally, from (4.9) and the above relation, we obtain

$$\frac{\sin\alpha'}{\sin\alpha} = \frac{N}{N'}.$$

Consequently, we also have

$$N'y'\sin\alpha' = \frac{N'^2}{N}y'\sin\alpha = \frac{N'^2}{N^2}Ny\sin\alpha.$$

Recalling the magnification formula $y'/y = Nz'/N'z$, we can then derive the condition

$$N'y'\sin\alpha' = \frac{N'}{N}\frac{z'}{z}Ny\sin\alpha,$$

from which we obtain

$$\frac{N'z'}{Nz} = 1. \tag{4.10}$$

In conclusion, we obtain the values of z and z' from (4.9) and (4.10) as follows:

$$z = \frac{N+N'}{N}R, \quad z' = \frac{N'+N}{N'}R. \tag{4.11}$$

In particular, z, z', and R have the same sign.

We note that the object point $(z, 0)$ is located in the medium with refractive index N'. This condition can be achieved in two ways. First, a planar surface orthogonal to the axis Oz at a distance $d < |z + R|$ can be inserted, and the remaining space can then be filled with oil (with a refractive index N'). Alternatively, a second spherical surface S' can be inserted (see Figure 4.2), that is centered at $(z, 0)$. This surface exerts no refractive effects on rays originating from this point.

4.2 Aplanatic Refractive Surfaces

We will now search for a spherical refractive surface which is ***aplanatic***, in other words, it has zero spherical aberration and coma for a fixed pair of conjugate points. This result, which is now obtained by the third-order theory, coincides with the result derived using Abbe's condition in the previous section. Due to (3.32), (3.33), the coefficients C_1 and C_2 vanish if

$$\frac{1}{N'z'} = \frac{1}{Nz},$$

so that

$$z' = \frac{N}{N'}z. \tag{4.12}$$

Substituting this result into (4.9), we obtain

$$R = \frac{N}{N' + N}z.$$

It is worth noting that this values are valid for any aperture stop (see (4.9)). By applying these formulae twice to the system shown in Figure 4.3, where the lenses are made from glass BK7 (N= 1.5168, in green light), we obtain the following data:

$$R_1 = \infty, \quad R_2 = -3.013, \quad d_1 = 5, \quad z_1' = -7.584$$
$$R_3 = -7.584, \quad R_4 = -6.378, \quad d_2 = 3, \quad z_2 = -16.05.$$

Evaluating by OSLO the spherical aberration and coma for an aperture stop of 7 mm. located at the first surface, we have

$$\text{spherical aberration} = 3.1510^{-4}, \quad \text{coma} = -2.510^{-6}.$$

This kind of aplanatic surface is used in oil immersion microscope objectives and microscope condensers.

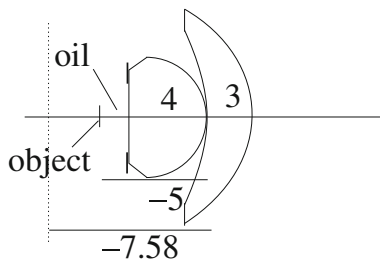

Fig. 4.3 Aplanatic pair of menisci

In contrast, the first surface of dry microscope objectives is centered on the object's axial point, implying that this type of objective has the further advantage of reducing the Petzval curvature of the image. Moreover, due to the presence of the cover glass for the specimen, either the thickness of the first lens or the distance between the first lens and second lens of the objectives can be modified to introduce a residual spherical aberration that compensates the spherical aberration of the cover glass.

4.3 Introduction to Fifth-Order Aberrations

The primary or third-order aberrations analyzed in Chapter 3 represent the basic foundations of aberration theory. In the applications, the formulae of fifth-order aberrations or higher order aberrations are not usually used to design an optical system for the following two reasons. First, the formulae of fifth-order aberrations are so complex that it is very difficult to manage them even by a computer. Further, the elimination of fifth-order aberrations requires a very large number of lenses in the optical system. On the other hand, the main problem in lens design is to prevent or to correct, not only the third-order aberrations, but also the fifth-order or higher order aberrations. A help to solve this problem is represented by the circumstance that, during the optimization of an optical system, the third-order aberrations are much more affected by the variation of characteristics of the optical system than the higher order aberrations. So, if it is not possible to reduce the aberrations of any order to zero, the result of the optimization is a balancing of third-order against higher order aberrations of the same or a similar type.

In Section 3.2 we proved formulae (3.17), (3.18) that define the components of the aberration vector $\boldsymbol{\epsilon}$ up to fifth-order terms in the variables X_g, Y_g, and y_1. Due to the symmetry of the optical system around its optical axis a, we can state that Φ_1 depends on X_g, Y_g, and y_1 through the optical invariants

$$\xi = y_1^2, \quad \eta_g = y_1 Y_g, \quad \zeta_g = X_g^2 + Y_g^2. \tag{4.13}$$

Consequently, we can consider two power expansions of the aberration function Φ_1: the expansion

$$\overline{\Phi}_1(\xi, \eta_g, \zeta_g) = \overline{\Phi}_1^{(2)} + \overline{\Phi}_1^{(3)} + O(4), \tag{4.14}$$

when Φ_1 is intended to be a function $\overline{\Phi}_1(\xi, \eta_g, \zeta_g)$ or the expansion

$$\Phi_1(y_1, X_g, Y_g) = \Phi_1^{(4)} + \Phi_1^{(6)} + O(8), \tag{4.15}$$

when the aberration function is intended to be a function of y_1, X_g, and Y_g. The first-order terms are absent in expansions (4.14) and (4.15) since we choose the object plane and image plane according to Gaussian optics (see Section 3.4). Further, $\overline{\Phi}_1^{(i)}$,

$i = 2, 3$, denotes a homogeneous polynomial of degree i with respect to variables ξ, η_g, ζ_g; similar meaning have $\Phi_1^{(i)}$, $i = 1, 2$.

Introducing expansion (4.15) into (3.17), (3.18) we obtain

$$\epsilon_x = \frac{z_*}{N_{n+1}} \frac{\partial \Phi_1^{(6)}}{\partial X_g} + \frac{1}{N_{n+1}} \left(z_* + \frac{M^2 y_1^2}{2 z_*} \right) \frac{\partial \Phi_1^{(4)}}{\partial X_g} + O(7), \tag{4.16}$$

$$\epsilon_y = \frac{z_*}{N_{n+1}} \frac{\partial \Phi_1^{(6)}}{\partial Y_g} + \frac{1}{N_{n+1}} \left(z_* + \frac{M^2 y_1^2}{2 z_*} \right) \frac{\partial \Phi_1^{(4)}}{\partial Y_g} + O(7). \tag{4.17}$$

where the third-order quantities

$$\epsilon_x^{(3)} = \frac{z_*}{N_{n+1}} \frac{\partial \Phi_1^{(4)}}{\partial X_g}, \tag{4.18}$$

$$\epsilon_y^{(3)} = \frac{z_*}{N_{n+1}} \frac{\partial \Phi_1^{(4)}}{\partial Y_g}, \tag{4.19}$$

denote the *third-order aberrations* that we have already analyzed in Chapter 3. The remaining terms

$$\epsilon_x^{(5)} = \frac{z_*}{N_{n+1}} \frac{\partial \Phi_1^{(6)}}{\partial X_g} + \frac{M^2 y_1^2}{2 z_* N_{n+1}} \frac{\partial \Phi_1^{(4)}}{\partial X_g}, \tag{4.20}$$

$$\epsilon_y^{(5)} = \frac{z_*}{N_{n+1}} \frac{\partial \Phi_1^{(6)}}{\partial Y_g} + \frac{M^2 y_1^2}{2 z_* N_{n+1}} \frac{\partial \Phi_1^{(4)}}{\partial Y_g}, \tag{4.21}$$

describe the *fifth-order aberrations*, when the *variables* y_1, X_g, *and* Y_g *are used*.

These formulae suggest some remarks. The first terms on the right-hand side of (4.4) and (4.5) have the same form than the third-order aberrations except for the substitution of $\Phi_1^{(4)}$ with the sixth-order optical path difference $\Phi_1^{(6)}$. These terms are said to describe the *intrinsic fifth-order aberrations*. The remaining terms, that are due to the presence of third-order aberrations, define the *extrinsic fifth-order aberrations*, when the *variables* y_1, X_g, *and* Y_g *are used*.

In conclusion, the optical path length $\overline{\Phi}_1$ from the object point (z, y_1) to the intersection point (Z_g, X_g, Y_g) of the considered ray with the Gaussian sphere of reference Σ_g, up to third-order terms in the invariants η_g, ζ_g, and ξ can be written as follows:

$$\overline{\Phi}_1 = \overline{\Phi}_1^{(2)} + \overline{\Phi}_1^{(3)}, \tag{4.22}$$

where

$$\overline{\Phi}_1^{(2)} = A_1\eta_g^2 + A_2\eta_g\zeta_g + A_3\eta_g\xi + A_4\zeta_g^2 + A_5\zeta_g\xi \tag{4.23}$$

$$\begin{aligned}\overline{\Phi}_1^{(3)} &= B_1\eta_g^3 + B_2\eta_g^2\zeta_g + B_3\eta_g\zeta_g^2 + B_4\eta_g^2\xi + +B_5\zeta_g\eta_g\xi \\ &\quad + B_6\zeta_g^3 + B_7\zeta_g^2\xi + B_8\eta_g\xi^2 + B_9\zeta_g\xi^2.\end{aligned} \tag{4.24}$$

In (4.22) the term $\overline{\Phi}_1^{(1)}$ does not appear since it vanishes when the object and image planes are chosen according to the Gaussian optics (see Section 2.1). Further, we omitted the terms $A_6\xi^2$ and $B_{10}\xi^3$ in (4.23) and (4.24) since they do not contribute to the aberrations (see (4.4)–(4.21)). Formula (4.24) shows that there are 9 different fifth-order aberrations. In general, the number of terms appearing in the polynomial $\overline{\Phi}_1^{(n)}$ is given by the number of $n-$combinations with repetitions of the three variables η_g, ζ_g, and ξ, that is equal to

$$\binom{3+n-1}{n} - 1 = \binom{n+2}{n} - 1 = \frac{(n+2)!}{2!n!} - 1. \tag{4.25}$$

We need to subtract -1 since the term $B_n\xi^n$ does not contribute to the aberrations. For $n = 2$ (see (4.23)), (4.25) gives 5 primary aberrations whereas for $n = 3$ (see (4.24)) it gives 9 secondary aberrations.

From (4.4)–(4.21), and (4.23), (4.24) we derive the following expression for the components ϵ_x and ϵ_y of the aberration vector $\boldsymbol{\epsilon}$ to within seventh-order terms

$$\begin{aligned}\epsilon_x &= \frac{z_*}{N_n'}\left(4A_1(X_g^2+Y_g^2)X_g + 4A_2X_gY_gy_1 + 2A_3X_gy_1\right) \\ &\quad + \frac{z_*}{N_n'}\left(6B_1(X_g^2+Y_g^2)^2X_g + 4B_2(X_g^2+Y_g^2)X_gY_gy_1\right. \\ &\quad + D_3X_gY_g^2y_1^2 + D_4(X_g^2+Y_g^2)X_gy_1^2 \\ &\quad \left. + D_5X_gY_gy_1^3 + D_6X_gy_1^4\right),\end{aligned} \tag{4.26}$$

$$\begin{aligned}\epsilon_y &= \left(4A_1(X_g^2+Y_g^2)Y_g + A_2(X_g^2+3Y_g^2)y_1 + A_4Y_gy_1^2 + A_5y_1^3\right) \\ &\quad + \frac{z_*}{N_n'}\left(6B_1(X_g^2+Y_g^2)^2Y_g + B_2(X_g^2+5Y_g^2)(X_g^2+Y_g^2)y_1\right. \\ &\quad + D_7(X_g^2+Y_g^2)Y_gy_1^2 + D_8Y_g^3y_1^2 + D_9Y_g^2y_1^3 + D_{10}(X_g^2+Y_g^2)y_1^3 \\ &\quad \left. + D_{11}Y_gy_1^4 + D_{12}y_1^5\right),\end{aligned} \tag{4.27}$$

where the coefficients $D_3, \ldots, D_{12}$ are functions of $B_3, \ldots, B_9$ and $A_1, \ldots, A_5$.

In the application, it is more convenient to adopt the variables (y_1, x_e, y_e), where x_e and y_e are the coordinates of the point at which the ray intersects the entrance pupil. To express (4.23) and (4.24) in terms of these variables, we need to determine

the functions $X_g = X_g(x_e, y_e, y_1)$, $Y_g = Y_g(x_e, y_e, y_1)$. Formulae (4.26), (4.27) show that it is sufficient to determine these functions *up to third-order terms*. In fact, the fifth-order terms of (4.26), (4.27) are not modified by the third-order terms of the functions $X_g = X_g(x_e, y_e, y_1)$, $Y_g = Y_g(x_e, y_e, y_1)$. Differently, the substitution $X_g = X_g(x_e, y_e, y_1)$, $Y_g = Y_g(x_e, y_e, y_1)$ into the third-order terms of (4.26), (4.27) introduces other fifth-order terms to add to the fifth-order terms of (4.26), (4.27). We note that the functions $X_g = X_g(x_e, y_e, y_1)$, $Y_g = Y_g(x_e, y_e, y_1)$ can be written as follows (see Section 3.3):

$$X_g = M_e x_e + f_x(x_e, y_e, y_1) \quad Y_g = M_e y_e + f_y(x_e, y_e, y_1), \tag{4.28}$$

where $f_x(x_e, y_e, y_1)$ and $f_y(x_e, y_e, y_1)$ are third-order functions of the variables y_1, x_e, and y_e. Introduce a Cartesian frame of reference with the origin O at the center of the exit pupil. We can determine these functions considering the ray γ starting from the point $(M_e x_e + \epsilon^{(3)}_{e,x}, M_e y_e + \epsilon^{(3)}_{e,y}, 0)$ in the exit pupil, where $\boldsymbol{\epsilon}^{(3)}$ is the third-order aberration vector in the exit pupil (see Section (3.11)), and crossing the image plane at the point $(\epsilon_x, My_1 + \epsilon_y, z_*)$. Adopting the notations of Chapter 3, the parametric equations of γ are

$$\xi = M_e x_e + \epsilon^{(3)}_{e,x} + (\epsilon_x - M_e x_e - \epsilon^{(3)}_{e,x})t, \tag{4.29}$$

$$\eta = M_e y_e + \epsilon^{(3)}_{e,x} + (My_1 + \epsilon_x - M_e y_e - \epsilon^{(3)}_{e,y})t, \tag{4.30}$$

$$\zeta = z_* t. \tag{4.31}$$

Intersecting this straight line with the surface of the Gaussian sphere of reference (see Section 3.2)

$$Z_g = \frac{X_g^2 + Y_g^2}{2z_*} - \frac{MY_g y_1}{z_*} + O(4), \tag{4.32}$$

we obtain the coordinates of the point (X_g, Y_g, Z_g) as functions of x_e, y_e, and y_1. In particular, we find that f_x and f_y have the same form of $\epsilon^{(3)}_x$ and $\epsilon^{(3)}_y$. Introducing these functions into (4.26), (4.27) and adopting polar coordinates r_e, φ in the entrance pupil

$$x_e = r_e \cos\varphi, \quad y_e = r_e \sin\varphi,$$

we can write the fifth-order terms of (4.26) and (4.27) as follows

$$\begin{aligned}\epsilon^{(5)}_x &= \frac{z_*}{N'_n}\Big(6B_1 r_e^5 \cos\varphi + 2B_2 r_e^4 \sin(2\varphi)\, y_1 + \hat{D}_3 r_e^3 \cos\varphi\, y_1^2 \\ &+ \hat{D}_4 r_e^2 \sin(2\varphi) y_1^3 + \hat{D}_5 r_e \cos\varphi\, y_1^4\Big),\end{aligned} \tag{4.33}$$

$$\begin{aligned}\epsilon^{(5)}_y &= \frac{z_*}{N'_n}\Big(6B_1 r_e^5 \sin\varphi + B_2(3 - 2\cos(2\varphi)) r_e^4\, y_1 + \hat{D}_6 r_e^3 \sin\varphi\, y_1^2 \\ &+ \hat{D}_7(1 - 2\sin^2\varphi) r_e^2 y_1^3 + \hat{D}_8 r_e \sin\varphi\, y_1^4 + \hat{D}_9 y_1^5\Big),\end{aligned} \tag{4.34}$$

where again the coefficients $\hat{D}_3, \ldots, \hat{D}_9$ are functions of $B_3, \ldots, B_9$ and $A_1, \ldots, A_5$.

4.4 Meaning of the Terms of (4.33), (4.34)

In this section we analyze the effect of the different terms of (4.33), (4.34) on imaging. First, we consider rays originating from the axial object point. For all these rays $y_1 = 0$ and (4.33), (4.34) supply the conditions

$$\epsilon_x^{(5)} = \mathbb{D}_1 r_e^5 \cos\varphi, \tag{4.35}$$
$$\epsilon_y^{(5)} = \mathbb{D}_1 r_e^5 \sin\varphi, \tag{4.36}$$

where $\mathbb{D}_1 = 6z_* \hat{D}_1 / N_n'$. These equations imply that

$$|\boldsymbol{\epsilon}^{(5)}| = \sqrt{\epsilon_x^{(5)2} + \epsilon_y^{(5)2}} = |\mathbb{D}_1| r_e^5. \tag{4.37}$$

Equation (4.37) shows that all of the rays that originate from the axial object point and cross the entrance pupil along a circumference of radius r_e centered on the optical axis, instead of striking the *same* axial image point, spread along a circumference centered on the Gaussian image (0, 0) and with radius $\mathbb{D}_1 r_e^5$ (see Figure 4.4). This is the ***fifth-order spherical aberration*** is *symmetric* around the optical axis. Moreover, let γ be a ray that intersects the entrance pupil at the point $(\pi/2, r_e)$. Then $\epsilon_x = 0$, $\epsilon_y = \mathbb{D}_1 r_e^5$; thus, if $\mathbb{D}_1 > 0$, $\epsilon_y > 0$ and γ meets the optical axis after the Gaussian plane (see Figure (4.4). The opposite situation happens if $\mathbb{D}_1 < 0$ (see Figure 4.5). In the first case the transversal spherical aberration is said to be overcorrected whereas in the second case it is said to be undercorrected.

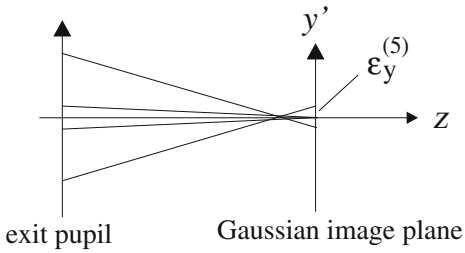

Fig. 4.4 Transverse overcorrected spherical aberration for $\mathbb{D}_1 > 0$

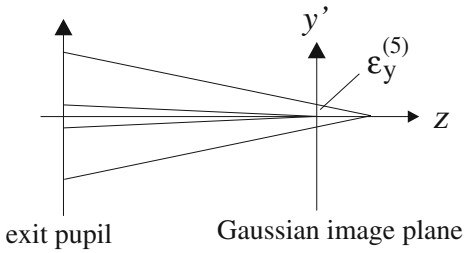

Fig. 4.5 Transverse undercorrected spherical aberration for $\mathbb{D}_1 < 0$

We note that all of the rays that arise from the object point on the axis and intercepting the entrance pupil along a circumference of radius r_e meet the optical axis at a same point.

In order to understand the contribution of the terms

$$\epsilon_x^{(5)} = 2\mathbb{D}_2 r_e^4 y_1 \sin 2\varphi, \tag{4.38}$$
$$\epsilon_y^{(5)} = \mathbb{D}_2 r_e^4 y_1 \left(3 - 2\cos 2\varphi\right), \tag{4.39}$$

where $\mathbb{D}_2 = z_* \hat{D}_2 / N_n'$, to the aberrations we consider the set Γ of rays from $(0, y_1)$, for which r_e is constant. These rays intersect with the image plane in the points with coordinates $(\epsilon_x^{(5)}, My_1 + \epsilon_y^{(5)})$. Since (4.38) and (4.39) imply the equation

$$(\epsilon_x^{(5)})^2 + (\epsilon_y^{(5)} - 3\mathbb{D}_2 r_e^4 y_1)^2 = \mathbb{D}_2^2 r_e^8 y_1^2,$$

the rays of Γ intersect with the image plane in a circle of radius

$$R = \mathbb{D}_2 r_e^4 y_1, \tag{4.40}$$

that is centered at the point

$$(0, My + 3R)\,. \tag{4.41}$$

The resulting image of a point of the object plane is given by the superposition of these circles upon varying r_e. If (X, Y) denotes a moving point of the object plane, the envelope of this one-parameter family Δ of circles can be obtained by eliminating the parameter R between the two equations

$$f(X, Y, R) = X^2 + (Y - 3R)^2 - R^2 = 0, \tag{4.42}$$
$$f_{,R}\,(X, Y, R) = -6(Y - 3R) - 2R = 0, \tag{4.43}$$

where (4.42) describes the family Δ and (4.43) is the derivative of the first equation with respect to the parameter R. A straightforward calculation leads to the following equation for the envelope:

$$X^2 - \frac{1}{8}Y^2 = 0, \tag{4.44}$$

which is therefore represented by two straight lines at an angle of 30° with the axis Oy. This aberration, which is not symmetric, is called ***fifth-order linear coma***.

Now, we analyze the contribution of the terms

$$\epsilon_x^{(5)} = \mathbb{D}_3 r_e^3 y_1^2 \cos\varphi, \tag{4.45}$$
$$\epsilon_y^{(5)} = \mathbb{D}_6 r_e^3 y_1^2 \sin\varphi, \tag{4.46}$$

where $\mathbb{D}_3 = z_* \hat{D}_3/N'_n$, $\mathbb{D}_6 = z_* \hat{D}_6/N'_n$ to the aberrations. Equations (4.45) and (4.46) are the parametric equations of an ellipsis with semi-axes $\mathbb{D}_3 r_e^3 y_1^2$ and $\mathbb{D}_6 r_e^3 y_1^2$ along the axes Ox and Oy, respectively. For this reason the corresponding aberration is called ***elliptic coma***. The remaining terms of (4.33) and (4.34) refer to fifth-order astigmatism and distortion.

4.5 The Light Diffraction and the Airy Disk

All of the results obtained in this chapter have two fundamental limitations:

- Our analysis of aberrations was restricted to the third-order and fifth-order theory;
- the geometric optics we used did not take into account the wave nature of light.

In principle, it would be possible to consider fifth-order aberrations but the corresponding formulae are so heavy to handle that their practical use is very limited. This implies that, after a design in which the third-order aberrations are eliminated, some suitable optimization techniques are applied, to optimize the performance of the optical system. These procedures, which must be used with great attention, often lead to wrong results.

On the other hand, it is not possible to neglect the wave nature of light in designing an optical system, since it is just this nature which determines how much the aberrations have to be corrected. In fact, owing to its wave character, the light propagation across an optical system, beside reflections and refractions, also produces diffraction phenomena which lead to the fundamental result that the image of an object point, however perfect is the optical system, is a very small spot in which the intensity of light is distributed in a very complex way. The analysis of this problem is not easy and it is carried out by suitable approximations which lead us to simplify the difficult calculations. Here, we limit ourselves to comment on the final formulae putting into evidence some their fundamental consequences. First, we suppose that the optical system $\mathbb{S}$ has a symmetry of revolution about the optical axis, is ideal, the object is at infinity, and the light is monochromatic with a wave length λ (Figs. 4.6, 4.7 and 4.8).

In these conditions the light wave-front W is a spherical surface emerging from the exit pupil and centered at the point O determined by the intersection of the Gaussian image plane π' with the optical axis (see Figure 4.6). We also suppose that the exit pupil has a radius a, an obscuration with a radius ϵa, and it is located at a distance R from π'. The amplitude $U(r)$ of the wave in a point $P \in \pi'$ at a distance r from O is a function of r. Moreover, we denote by $I(r) = |U(r)|^2$ the intensity of light at P, and by $PSF(r) = I(r)/I(0)$ the ***point spread function***. It can be proved (see [7]) the following formula due to Airy

$$PSF(r) = \frac{4}{(1-\epsilon^2)v^2}\left[J_1(v) - \epsilon J_1(\epsilon v)\right]^2, \tag{4.47}$$

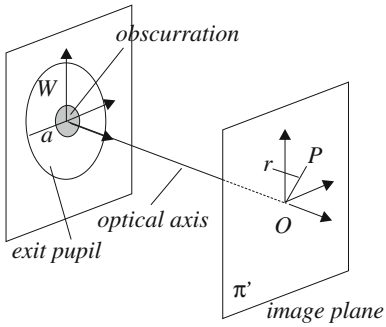

Fig. 4.6 Exit pupil with obscuration

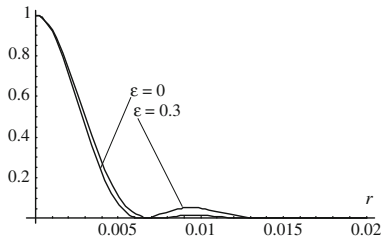

Fig. 4.7 Plot of the function $PSF(r)$

where

$$v = \frac{\pi}{\lambda}\frac{2a}{R}, \tag{4.48}$$

$$J_1(v) = \sum_0^\infty \frac{(-1)^m}{m!\Gamma(m+2)}\left(\frac{v}{2}\right)^{2m+1}, \tag{4.49}$$

is the Bessel function of order 1, and

$$\Gamma(m+2) = \int_0^\infty e^{-x}x^{m+1}\,dx, \tag{4.50}$$

is the Euler Gamma function.

The behavior of the function $PSF(r)$ is shown in Figure 4.7 for $\lambda = 0.5875 \times (10)^{-3}$ mm. and $2a/R = 0.1$.

We can say that the pattern of the diffraction spot is formed by a central disk, the ***Airy's disk***, containing 84 % of the total light coming from a point source. This central disk is surrounded by concentric, alternatively dark and bright rings. In these last ones, the light intensity decreases according to the sequence 7 %, 3 %, and so on. It is apparent that the effect of the central obscuration is to transfer part of the energy from the first maximum to the others.

In view of (4.47), the radii $r_1, r_2, \ldots$ of the different bright rings can be found by solving the equation

$$J_1(v) - \epsilon J_1(\epsilon v) = 0, \tag{4.51}$$

and then using $SF2$. The following table gives the roots $v_1, v_2, \ldots$ of (4.51) for different values of obscuration ϵ.

ϵ	v_1	v_2	v_3
0.00	1.220π	2.233π	4.238π
0.10	1.205π	2.269π	4.182π
0.20	1.167π	2.357π	4.087π
0.33	1.098π	2.424π	4.137π
0.40	1.058π	2.388π	4.300π

In particular, if $R/2a$ is equal to the focal ratio A, then we find that the radius r_a of the first dark ring, i.e., of the ***Airy ring*** is expressed by the formula

$$r_a = 1.22\frac{\lambda}{A}. \tag{4.52}$$

It is also possible to determine the ***encircled energy fraction*** $EE(r)$ which gives the fraction of the total light energy in the image contained in a circle of radius r. It is possible to prove that it is expressed by the function

$$EE(r) = \frac{1}{(1-\epsilon^2)}\left[1 - J_0(v)^2 - J_1(v)^2 + \right. \tag{4.53}$$

$$\epsilon^2\left(1 - J_0(\epsilon v)^2 - J_1(\epsilon v)^2\right) - \tag{4.54}$$

$$\left. 4\epsilon\int_0^v J_1(\epsilon x)\frac{J_1(x)}{x}dx\right], \tag{4.55}$$

where $J_0(v)$ is the Bessel function of order 0. The Figure 4.7 shows a typical plot of this function.

All the above considerations refer to the case of a spherical wave-front centered at the image point O on the optical axis. In the presence of aberrations W is not

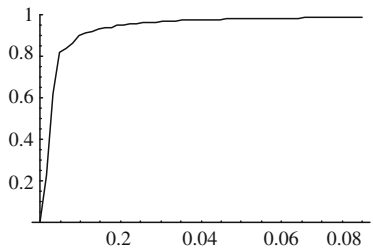

Fig. 4.8 Plot of the function $EE(r)$

spherical and the distribution of light is modified with respect to the ideal case. The reader interested in the more complex formulae describing this new situation can refer to [42, 43].

We conclude with the following fundamental rule: ***an optical system is perfect or diffraction limited if the aberration spot is contained in the Airy disk***.

Chapter 5
Newtonian and Cassegrain Telescopes

5.1 The Newtonian Telescope

The simplest and famous kind of telescope was invented by Newton. It consists of a parabolic primary mirror S_1 and a flat secondary mirror S_2 that is situated in front of the primary and directs the converging cone of light arriving from the primary out of the tube for visual or photographic applications. The aperture stop A coincides with the rim of S_1 (see Figure 5.1).

First, the image of the object, which is located at infinity, lies in the focal plane π'_f of the primary mirror. If $R < 0$ is the curvature radius of S_1, then the focal length $f = R/2 < 0$ is derived from Abbe's invariant (2.7). Since the secondary mirror does not introduce aberrations (if it satisfies the optical tolerances), only the contributions due to S_1 need to be evaluated.[1] To this end, we note that the refractive indices are $N = -N' = 1$, the conic constant K of S_1 is equal to -1, $z = -\infty$ and $z' = R/2$. Moreover, the distances $w = w'$ are equal to zero so that

$$M_e = 1. \tag{5.1}$$

Consequently, from (3.39)–(3.44) and (3.61)–(3.65) the following expressions of total spherical aberration, coma, and astigmatism coefficients are obtained

$$\begin{aligned} C_1 = C_1^* = 0, \quad C_2 = C_2^* = \frac{1}{R^2}, \\ C_3 = C_3^* = 0, \quad C_4 = C_4^* = \frac{1}{R}. \end{aligned} \tag{5.2}$$

These relations show that there is no spherical aberration but there is a coma, which is independent of the stop position. Differently, the astigmatism coefficient results

[1] The aberration coefficients derived in this Chapter can be evaluated by the notebook ***TotalAberrations.***

© Springer International Publishing Switzerland 2016

A. Romano and R. Cavaliere, *Geometric Optics*,
Modeling and Simulation in Science, Engineering and Technology,
DOI 10.1007/978-3-319-43732-3_5

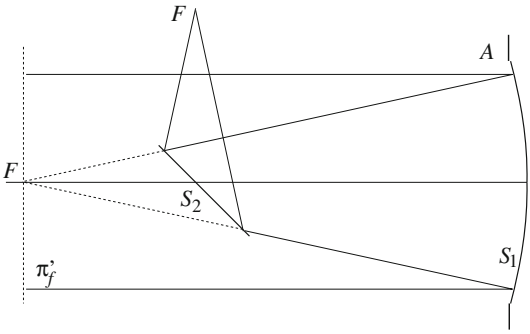

Fig. 5.1 Newtonian telescope

$$D_4 - D_3 = C_4^* - C_3^* = \frac{1}{R}.$$

The above results allow us to write (3.152), (3.195) and (3.197) into the following form[2]

$$\text{sphericalaberration} = 0, \tag{5.3}$$

$$\text{sagittalcoma} = -\frac{d^2\theta}{8R}, \tag{5.4}$$

$$\text{astigmatism} = -\frac{d\theta^2}{2}. \tag{5.5}$$

In (5.20), (5.21) d is the diameter of the mirror S_1 and the field angle θ is expressed in radians. Finally, the height h' of the image on the optical axis is

$$h' = \frac{R}{2}\theta. \tag{5.6}$$

It should be noted that the astigmatism is not an important aberration of this combination. In fact, if we refer back to (5.20) and (5.21), we obtain the ratio a between astigmatism and sagittal coma

$$a = \frac{R\theta}{d}$$

that is small with respect to 1 in standard conditions. For instance, if the primary mirror has a diameter of 200 mm, a curvature radius of -1200 mm and the angle θ is equal to $1^\circ = 0.017$ radians, we get $a = 0.1$. This means that coma is dominant, in other words the limits of this optical combination are determined solely by this aberration.

[2]Compare these results with the results contained in ***TotalAberrations.***

We wish now to analyze the performance of this optical combination in visual and photographic applications. In this section we denote by f the absolute value of the focal length; in other words, $f = |R|/2 > 0$. If d is the diameter of S_1, we define ***aperture*** or ***speed*** of the mirror S_1 the ratio

$$A = \frac{d}{f} \tag{5.7}$$

According to (4.52), the Airy disk has the following diameter

$$d_a = 2.44\frac{\lambda}{A} = 2.44\lambda\frac{f}{d}. \tag{5.8}$$

Consequently, if astigmatism is neglected, then the diameter of the geometrical spot due to coma is twice (5.20) and the optical combination is diffraction limited if

$$\frac{\theta d^2}{8f} \leq 2.44\lambda\frac{f}{d},$$

leading to the following condition for the field angle

$$\theta \simeq 2.44\lambda\frac{8f^2}{d^3}. \tag{5.9}$$

Consequently, the *diameter* $\sigma_v = 2\theta f$ of the useful field in the focal plane results

$$\sigma_v \simeq 2.44\lambda\frac{16f^3}{d^3} = 2.44\lambda\frac{16}{A^3}, \tag{5.10}$$

provided that the instrument is intended for visual use.

In contrast, if it is intended for photographic destination, we obtain

$$\frac{\theta d^2}{8f} \leq d_g, \tag{5.11}$$

where d_g is the photographic grain diameter (for instance 0.025 mm) or the diameter of a single pixel of a CCD. Finally, the useful photographic field is then

$$\sigma_f \leq 16d_g\frac{f^2}{d^2} = 16\frac{d_g}{A^2}. \tag{5.12}$$

The above results are summarized in the following Table 5.1.

For instance, for a parabolic mirror with speed $A = d/f = 1/6$, we have

$$\sigma_f \leq 4.2\,mm, \quad \sigma_f \leq 14.4\,mm$$

Table 5.1 Visual and photographic limits of a parabolic mirror

Focal length	$f = \|R\|/2$
Diameter of useful visual field	$\sigma_v \leq 2.44\lambda 16 f^3/d^3$
Diameter of useful photographic field	$\sigma_f \leq 16 d_g f^2/d^2$

whereas, if $A = d/f = 1/5$, we obtain

$$\sigma_f \leq 2.44\,mm, \quad \sigma_f \leq 10\,mm$$

5.2 Location and Dimension of Flat Mirror

The flat mirror S_2 must intercept all the rays originating from the principal mirror S_1. Consequently, its profile is obtained intersecting the cone C of aperture $\alpha = \arctan d/f$ with the plane π containing the point P in Figure 5.2 and forming an angle of 45° degree with the optical axis a. Therefore, we can state that its profile is an ellipse whose axes depend on the localization of the secondary mirror along the optical axis. The secondary mirror S_2 produces a central obscuration of S_1 that can easily be evaluated. In fact, it is given by the ratio ob between the area σ_P of the transversal section of the cone C at the point P and the area σ of S_2. The radius r_Σ of Σ_P is obtained by the proportion

$$\frac{d}{f} = \frac{r_\Sigma}{a}$$

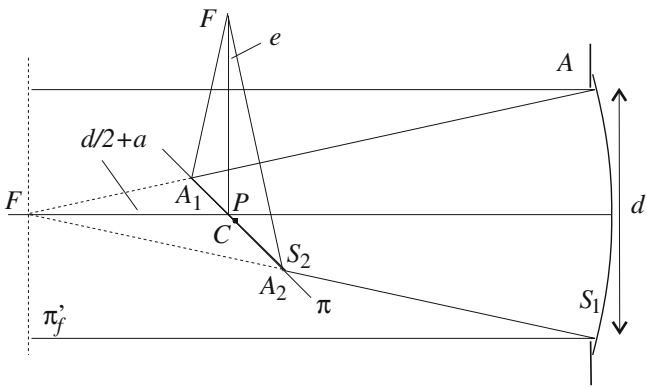

Fig. 5.2 Positioning of flat mirror in a Newtonian telescope

where

$$a = \frac{d}{2} + e. \tag{5.13}$$

Therefore,

$$r_\Sigma = a\frac{d}{f} = aA \tag{5.14}$$

and we have

$$\sigma_P = \pi a^2 A^2, \quad \sigma = \pi\frac{d^2}{4}.$$

Finally, the obscuration factor ob is

$$ob = \frac{\sigma_P}{\sigma} = \frac{4a^2A^2}{d^2} = \frac{4a^2}{f^2}. \tag{5.15}$$

The obstruction factor should be less than 0.33 since its increasing modifies the diffraction pattern (see Section 5.6).

It remains to determine the axes of the elliptic profile of S_2. First, the minor axis is equal to the diameter of the orthogonal section of the cone C; in other words, it is equal to $2r_\Sigma$, where r_Σ is given by (5.14). Determining the major axis is a simple problem of analytical geometry. Introduce Cartesian axes Fxy, with the axis Fx coinciding with the optical axis a. The straight lines containing the pairs of points (F, A_1), (F, A_2), and (A_1, A_2) have equations

$$y = \frac{d}{2f}x = \frac{A}{2}x, \;\; y = -\frac{A}{2}x, \;\; y = -(x - a), \tag{5.16}$$

respectively. We can easily verify that

$$A_1 = \left(\frac{2a}{2+A}, \frac{aA}{A+2}\right), \;\; A_2 = \left(-\frac{2a}{2-A}, -\frac{aA}{A-2}\right).$$

Therefore,

$$\frac{|A_1C|}{r_\Sigma} = \sqrt{2}\frac{A}{A+2}, \;\; \frac{|A_2C|}{r_\Sigma} = \sqrt{2}\frac{A}{2-A}$$

and the major axis of the ellipse is $|A_1C| + |A_2C|$. Finally, it is clear from the above considerations that the center of the plane mirror is vertically downward shifted with respect to the optical axis.

5.3 Newtonian Telescope with Spherical Primary Mirror

In this section we compare the performance of a Newtonian combination, in which the primary mirror is parabolic, with a Newtonian combination in which the primary mirror is spherical. When the two optical combinations have the same performance, we can substitute the parabolic mirror with the less expensive spherical mirror.

In a Newtonian combination with a spherical primary mirror we have again that the refractive indices are $N = -N' = 1$, the conic constant K of S_1 is zero, $z = -\infty$ and $z' = R/2$. Moreover, the distances $w = w'$ are equal to zero so that

$$M_e = 1. \tag{5.17}$$

Consequently, from (3.39)–(3.44) and (3.61)–(3.65) the following expressions of total spherical aberration, coma and astigmatism coefficients are obtained

$$\begin{aligned} C_1 = C_1^* = \frac{1}{4R^3}, \quad C_2 = C_2^* = \frac{1}{R^2}, \\ C_3 = C_3^* = 0, \quad C_4 = C_4^* = \frac{1}{R}. \end{aligned} \tag{5.18}$$

These relations show that there is no spherical aberration but there is a coma, which is independent of the stop position. Differently, the astigmatism coefficient results

$$D_4 - D_3 = C_4^* - C_3^* = \frac{1}{R}.$$

The above results allow us to write (3.152), (3.195) and (3.197) into the following form[3]

$$\text{spherical aberration} = -\frac{d^3}{16R^2}, \tag{5.19}$$

$$\text{sagittal coma} = -\frac{d^2\theta}{8R}, \tag{5.20}$$

$$\text{astigmatism} = -\frac{d\theta^2}{4}. \tag{5.21}$$

In (5.20), (5.21) d is the diameter of the mirror S_1 and the field angle θ is expressed in radians. Finally, the height h' of the image on the optical axis is

$$h' = \frac{R}{2}\theta. \tag{5.22}$$

A comparison with the formulae of Section 5.1 shows that the aberrations of spherical and parabolic mirrors with the same speeds differ for the presence of spherical

[3]Compare these results with the results contained in ***TotalAberrations.***

aberration in spherical mirrors. Consequently, the two combinations have the same performance provided that the aperture of the spherical mirror is such that the spot due to the spherical aberration is contained in the Airy disk. It is possible to prove that this circumstance is verified for speed less than or equal to $f/8$.

We conclude that a Newtonian telescope has a very simple structure but coma limits its efficiency. Further, its length is about equal to its focal length.

5.4 Cassegrain Telescopes

In this section, the family of Cassegrain telescopes is analyzed. All Cassegrain telescopes consist of a concave primary mirror S_1 with a small convex secondary mirror S_2 situated between the primary focus F_1 and S_1. The light that arrives at S_1 is reflected back toward S_2. Then, after another reflection, it arrives at the eyepiece or the film placed behind a hole centered on the vertex of S_1 (see Figure 5.3). The aperture stop is located at the primary mirror.

Usually, the design data are

- The diameter d_1 of S_1
- The focal length $f_1 > 0$ of S_1 or, equivalently, its curvature radius $R = -2f_1$
- The total focal length $f > 0$ of the combination.
- The back distance $e > 0$ from S_1 to the posterior focal point.

We now show that all of the remaining data (i.e., d_2, R_2 and d) are determined by simple geometrical and Gaussian relations. On the other hand, since the imaging process results only from reflections, there is no chromatic aberration. The only way to control the third-order aberrations is to select the aspheric constants K_1 and K_2 of S_1 and S_2 wisely. In particular, this means that the most we can hope to achieve is to eliminate the spherical aberrations and coma.

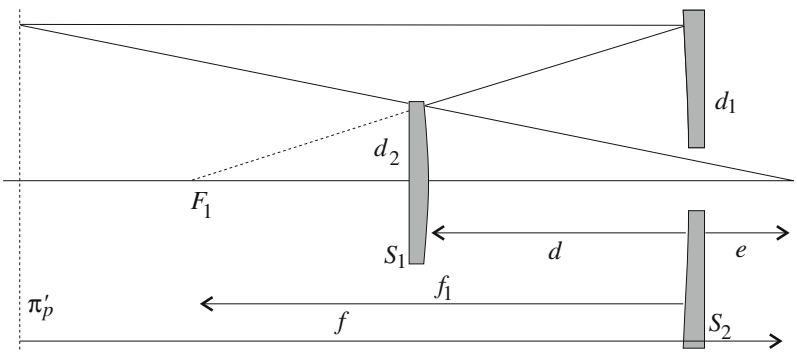

Fig. 5.3 Cassegrain telescope

Starting from the assigned data, the following nondimensional quantities can be evaluated:

$$\alpha = \frac{e}{f_1} > 0, \quad M = \frac{f}{f_1}. \tag{5.23}$$

The problem of determining d_2, R_2 and d is then equivalent to calculating the new nondimensional quantities

$$c = \frac{d_2}{d_1}, \quad \gamma = \frac{R_2}{f_1}, \quad \beta = -\frac{d}{f_1}, \tag{5.24}$$

where

$$c > 0, \quad \gamma < 0, \quad 0 < \beta < 1.$$

First, using Figure 5.3 and the third equation of (5.24), we derive the condition

$$c = \frac{d_2}{d_1} = \frac{f_1 + d}{f_1},$$

in other words

$$c = 1 - \beta. \tag{5.25}$$

From Figure 5.3 and the second equation (5.23), we also have

$$c = \frac{d_2}{d_1} = \frac{-d + e}{f} = \frac{-d + e}{f_1}\frac{f_1}{f} = \frac{\alpha + \beta}{M}.$$

Therefore, taking into account (5.25), we obtain

$$\beta = \frac{M - \alpha}{M + 1}. \tag{5.26}$$

Finally, in order to find γ, we note that

$$z_2 = -f_1 - d, \quad z_2' = -d + e,$$
$$N_2 = -1, \quad N_2' = 1.$$

On the other hand, in view of (5.24), the Abbe invariant

$$\frac{N_2}{z_2} - \frac{N_2}{R_2} = \frac{N_2'}{z_2'} - \frac{N_2'}{R_2},$$

yields

$$\begin{aligned}\frac{2}{\gamma} &= \frac{f_1}{e-d} - \frac{f_1}{f_1+d} \\ &= \frac{f_1}{f}\frac{f}{e-d} - \frac{1}{1-\beta} = \frac{1}{M}\frac{M}{\alpha+\beta} - \frac{1}{1-\beta}.\end{aligned}$$

Therefore, due to (5.26), we have

$$\gamma = \frac{2(1-\beta)(\alpha+\beta)}{1-\alpha-2\beta} = \frac{2M(1+\alpha)}{1-M^2}. \tag{5.27}$$

The Gaussian design is now complete since all of the quantities are expressed in terms of α and M which are, in turn, obtainable from the initial data d_1, f_1 and f.

5.5 Spherical Aberration and Coma in Cassegrain Telescopes

We have already noted that, if no other optical element is introduced into the scheme, the only way to control the aberrations from the Cassegrain combination is to suppose that S_1 and S_2 are quadric surfaces of revolution. Actually, their conic constants K_1 and K_2 constitute two degrees of freedom that can be used to eliminate or reduce some aberrations.

In order to evaluate the aberration coefficients D_i, (see (3.92)–(3.96)), all the quantities that appear in them must be calculated. To avoid having to perform this tedious calculation, the reader can use the notebook ***Cassegrain combination*** instead. This notebook proves that the coefficients of spherical aberration and coma take the following forms, respectively,

$$\begin{aligned}32 f_1^3 D_1 &= B_{1,0} - K_1 + B_{1,2}K_2, \\ 8 f^2 D_2 &= B_{2,0} + B_{2,2}K_2,\end{aligned} \tag{5.28}$$

where

$$\begin{aligned}D_{1,0} &= -\frac{1+M^3+\alpha-M^2(1+\alpha)}{M^3}, \quad B_{1,2} = \frac{(M-1)^3(1+\alpha)}{M^3(1+M)}, \\ B_{2,0} &= \frac{M+M^3+\alpha(1-M^2)}{M^3}, \quad B_{2,2} = \frac{(M-1)^3(M-\alpha)}{M^3(1+M)}.\end{aligned} \tag{5.29}$$

Now, there are many ways to eliminate either spherical aberration or spherical aberration and coma

- The ***Dall-Kirkham*** scheme uses a conic primary and a spherical secondary, i.e., $K_2 = 0$. From the conditions $32 f^3 D_1 = 0$, and $K_2 = 0$, we get

$$K_1 = B_{1,0}. \tag{5.30}$$

- The ***Pressman-Camichel*** configuration uses a spherical primary and a conic secondary. Thus, the conditions $8f^3D_1 = 0$ and $K_1 = 0$ imply

$$K_2 = -\frac{B_{1,0}}{B_{1,2}}. \tag{5.31}$$

- The ***classical Cassegrain*** combination uses a parabolic primary ($K_1 = -1$) and a hyperbolic secondary. From the conditions $D_1 = 0$ and $K_1 = -1$, we derive

$$K_2 = -\frac{(1 + B_{1,0})}{B_{1,2}}. \tag{5.32}$$

- Both Coma and spherical aberration vanish in the ***Ritchey–Cretien*** combination in which both mirrors are conic. From the equations $D_1 = 0$ and $D_2 = 0$, we get

$$K_1 = B_{1,0} - \frac{B_{1,2}B_{2,0}}{B_{2,2}}, \quad K_2 = -\frac{B_{2,0}}{B_{2,2}}. \tag{5.33}$$

An analysis of the aberrations obtained with the different combinations listed above shows that coma is greater in Dall-Kirkham or Pressman-Camichel telescopes than coma in a pure Cassegrain telescope. Moreover, even though if gives excellent performance, the Ritchey–Cretien combination is difficult to realize in practice because it requires two conic mirrors.

The notebook ***Cassegrain combination*** allows the reader to evaluate all the parameters for all of these combinations, as well as the residual third-order aberrations.

5.6 Concluding Remarks

Cassegrain telescopes have the following advantages:

- The total focal of the combination is much longer than the focal length of primary mirror
- The optical system is fully achromatic.

However, they exhibit have some disadvantages too

- Conic surfaces are not easy to make;
- Using the open tube can lead to turbulence phenomena;
- direct light can reach the observer's eye unless an accurate system of baffles is introduced into the tube (see Figure 5.4).

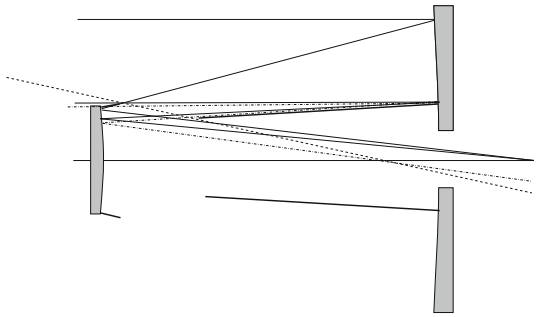

Fig. 5.4 Buffles in a Cassegrain telescope

5.7 Examples

In this section we design a standard Cassegrain telescope and a Ritchey–Cretien telescope by the notebook ***Cassegrain combination*** . Both of the combinations have the following characteristics: the total focal length is 2000 mm, the back distance is 200 mm. and the obstruction factor is 0.30. Moreover, the diameter of the primary conic mirror is 200 mm. and its speed is $F/3$. Finally, we consider a field angle equal to 0.31.

For these input data the notebook ***Cassegrain combination*** gives the following output

$$\begin{aligned} \text{radius of the primary mirror} &= -1200, \\ \text{radius of the secondary mirror} &= -527.473, \\ \text{distance between the two mirrors} &= -415.385, \\ \text{diameter of the secondary mirror} &= 61.54. \qquad (5.34) \\ \text{focal length} &= 2000. \qquad (5.35) \\ \text{height of the image} &= 10.82. \qquad (5.36) \end{aligned}$$

Moreover, for the pure Cassegrain combination, the conic constants K_1 and K_2 of the two mirrors are

$$K_1 = -1, \quad K_2 = -3.449,$$

whereas for the Ritchey–Cretien combination the values of the two constants become

$$K_1 = -1.08, \quad K_2 = -4.207.$$

The spot diagrams, obtained by **Oslo**, corresponding to the above combinations, are shown in the Figures 5.5 and 5.6.

In both figures, the circle is the Airy disk and the spot diagram is drawn on a spherical surface with a radius of curvature of −600 mm. The image is worse on the plane Gaussian surface.

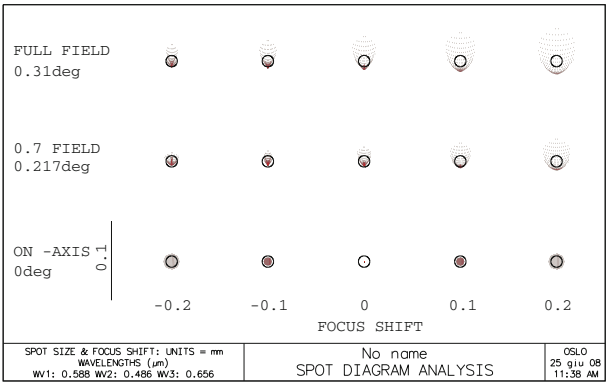

Fig. 5.5 Cassegrain combination

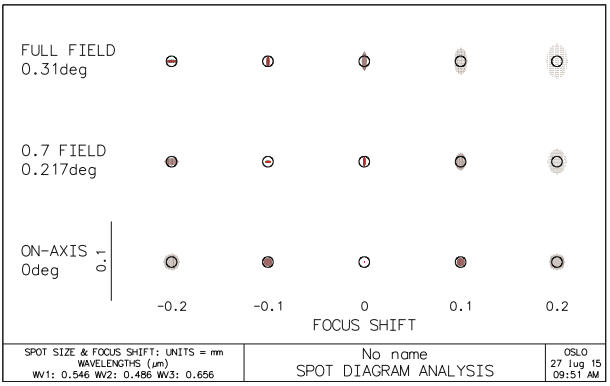

Fig. 5.6 Ritchey–Cretien combination

In conclusion, the Dall-Kirkam and Pressman-Camichel combinations are less expensive since they need only a conic mirror. However, they exhibit relevant coma and astigmatism. The Ritchey–Cretien combination is more expensive since both the mirrors are conic but spherical aberration and coma are eliminated. Field curvature and astigmatism reduce the view field. In the example of Figure 5.6 the view field has a diameter of 20 mm.

Chapter 6
Cameras for Astronomy

6.1 Introduction

This chapter describes the most used cameras for astronomical photography. The main component in these cameras is a concave mirror S that forms the image of objects at infinity on its focal plane. The image formed by such a system usually exhibits aberrations that are too large to be acceptable. In order to improve this situation, we can

- Place an aperture stop A at a suitable distance s in front of S in order to reduce or eliminate some aberrations
- Use a conic mirror S
- Introduce a new optical element at the aperture stop to compensate the aberrations of S.

All the cameras considered here are based on the following principle:

The optical element introduced at the aperture stop is almost afocal and thus compensates for the aberrations from S without modifying its Gaussian behavior. In particular, the image from the whole system is very close to the focal plane of S.

The above considerations indicate that we should study the aberrations of the optical system formed by a conic mirror S with an aperture stop located at a distance s from S in great detail. We denote the absolute value of the focal length and the diameter of S by f and D, respectively.

When an afocal element is introduced at the aperture stop, we only need to add the aberrations coefficients of this element to the corresponding coefficients of S. ***It is evident that all the derived results are only acceptable in the third-order***

© Springer International Publishing Switzerland 2016

A. Romano and R. Cavaliere, *Geometric Optics*,
Modeling and Simulation in Science, Engineering and Technology,
DOI 10.1007/978-3-319-43732-3_6

approximation. In particular, the ***aperture*** or the ***speed*** D/f of the mirror S and the field angle θ must have values that make the third-order theory applicable.

6.2 Aberrations for a Single Mirror

We consider an optical system comprising a single mirror S with a radius of curvature $R = -2f < 0$ and a conic constant K. Moreover, we suppose that an aperture stop A is placed in front of S at a distance $s = \delta f$. In the preceding section it was stated that that all of the cameras considered in this chapter are obtained by inserting a particular afocal optical element into the plane of the aperture stop. To avoid modifying the signs of the quantities that appear in the formulae, it is initially supposed that the aperture stop is the rim of a plate, with planar and parallel faces, where the thickness of the plate can be neglected. Clearly, this optical element has no effect on the aberrations of the primary mirror. All the formulae derived here can be obtained using the notebook ***Schmidt camera***.

Since the object is at infinity and $N = -N' = 1$, we can derive the distance of the image from the mirror from Abbe's invariant (2.8)

$$z' = -f. \tag{6.1}$$

Using (2.7) and (3.59) we also obtain

$$w' = \frac{f\delta}{1-\delta}, \tag{6.2}$$

$$M_e = \frac{1}{1-\delta}, \quad c = 1, \quad d = 0. \tag{6.3}$$

Moreover, the coefficients (3.41)–(3.44) become

$$C_1 = -\frac{K+1}{32f^3}, \tag{6.4}$$

$$C_2 = \frac{1}{4f^2}, \tag{6.5}$$

$$C_3 = 0, \tag{6.6}$$

$$C_4 = -\frac{1}{2f}, \tag{6.7}$$

whereas the relations (3.61)–(3.65) assume the form

$$C_1^* = -\frac{K+1}{32f^3}, \tag{6.8}$$

$$C_2^* = \frac{1}{8f^2}\left(2-(K+1)\delta\right), \tag{6.9}$$

$$C_3^* = \frac{\delta}{16f}\left(4-(K+1)\delta\right), \tag{6.10}$$

$$C_4^* = -\frac{1}{16f}\left(8-12\delta+3(K+1)\delta^2\right), \tag{6.11}$$

$$C_5^* = -\frac{1}{8f}\delta\left(8-6\delta+(K+1)\delta^2\right). \tag{6.12}$$

Since we have just one surface, the coefficients of total spherical aberration and coma, $D_{S,1}$ and $D_{S,2}$, coincide with (6.8), (6.9)

$$32f^3 D_{S,1} = -(K+1), \tag{6.13}$$

$$8f^2 D_{S,2} = 2-(K+1)\delta, \tag{6.14}$$

whereas the total coefficients of astigmatism and field curvature are:

$$8f(D_{S,4}-D_{S,3}) = 8f(C_4^*-C_3^*) = -\left(4-4\delta+(K+1)\delta^2\right), \tag{6.15}$$

$$D_{S,4}-3D_{S,3} = C_4^*-3C_3^* = -\frac{1}{2f}. \tag{6.16}$$

Moreover, the Petzval, sagittal and meridional radii are, respectively, given by the relations

$$R_p = -f, \tag{6.17}$$

$$R_s = -\frac{4f}{\delta(-4+\delta(K+1))}, \tag{6.18}$$

$$R_t = \frac{4f}{8-12\delta+3(K+1)\delta^2}. \tag{6.19}$$

6.3 Schmidt's Camera

Equations (6.8)–(6.12) show that, if the stop is at the mirror S ($\delta = 0$) and S is a sphere ($K = 0$), all of the third-order aberrations are present, except for the distortion. In contrast, if the aperture stop is placed at the curvature center of S ($\delta = 2$) and $K = 0$, then we get

Table 6.1 Focal length, diameter, and speed of a spherical mirror satisfying the photographic criterion

Focal Length	Stop Diameter
400 mm	74.26 (5.4)
500 mm	86.17 (5.8)
600 mm	97.31 (6.1)
700 mm	107.8 (6.5)
800 mm	117.8 (6.8)
900 mm	127.5 (7.1)
1000 mm	136.8 (7.3)
1200 mm	154.5 (7.7)
1500 mm	179.2 (8.4)

$$D_{S,1} = -\frac{1}{32f^3}, \tag{6.20}$$

$$D_{S,2} = 0, \tag{6.21}$$

$$D_{S,4} = D_{S,3}, \tag{6.22}$$

$$D_{S,5} = 0. \tag{6.23}$$

Using $D_{S,4} = D_{S,3}$ we find that the sagittal and tangential curvatures are equal and coincide with Petzval's curvature $2/R$. This conclusion could also be derived by inspecting (6.17)–(6.19).

In other words, when the aperture stop is located at the center of curvature, coma, astigmatism, and distortion vanish, whereas the spherical aberration and field curvature survive. All of these results suggest us that we should use a single spherical mirror with the aperture stop located at its center of curvature, provided that its speed is such that the aberration spot has a size that allows us to use it. More precisely, it is possible to prove that the diameter D of S must satisfy the condition

$$D = 2(4R^2 d_b)^{1/3}, \tag{6.24}$$

where d_b is the diameter of the allowed spot. For photographic applications, $d_b = 0.025$ mm, and the data shown in Table 6.1 is obtained.

In this table, the numbers in parentheses in the second column denote the ratio of the diameter to the focal length $f = |R|/2$ of S (i.e., the speed of S). It is evident that the length $2f$ of the optical combination is convenient only for small diameters of S. positioned at the center of curvature of S with a suitable refractive plate P that has the task of compensating the spherical aberration of S. In this case, the aperture stop will be the rim of P.

The excellent configuration obtained in this case (see Figure 6.1) was invented by the German optician Bernard Schmidt. At the beginning of 1920s he created a very fast optical system that was able to eliminate almost all aberrations. Because

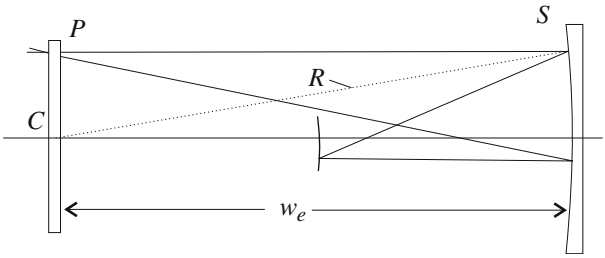

Fig. 6.1 Schmidt camera

of its characteristics and its remarkable optical performance, this configuration is employed when photographing wide star fields.

This configuration essentially consists of two components: a spherical mirror S and a *specially shaped* corrector plate P placed at the center of curvature C of S. This optical design uses the symmetry of the system to eliminate almost all off-axis aberrations, *even those of higher order*, and it entrusts the corrector with the task of eliminating the spherical aberration of the primary mirror. The image is formed on a spherical surface of radius $-f$, onto which a film is posed.

The corrector (the rim of which is the aperture stop) has a much greater focal length than the focal length of S; in other words, the system is almost afocal. This implies that the Gaussian calculations do not need to consider its presence. More precisely, we assume that

- The first surface of P is planar
- Its thickness is very small compared with the radius of curvature of the mirror S
- The profile of the second face is given by the equation (1.30), where the curvature radius R_c at the vertex is much greater than R.

The above hypotheses allow us to conclude that

$$z_1 = z_1' = z_2 = z_2' = \infty,$$
$$w_1 = w_2 = 0,$$
$$M_{e,1} = M_{e,2} = 1.$$
$$C_{1,1}^* = 0, \quad C_{i,2}^* = C_{i,3}^* = C_{i,4}^* = C_{i,5}^* = 0, \quad i = 1, 2,$$
$$C_{2,1}^* = D_{P,1} = a_4(N-1). \tag{6.25}$$

where N is the refractive index of the corrector (see (3.32)). Consequently, all of the coefficients D_i for the whole combination coincide with the coefficients $D_{S,i}$ of the mirror (see (6.9)), except for D_1 which is given by

$$D_1 = D_{P,1} + D_{S,1} = a_4(N-1) - \frac{1}{32f^3}. \tag{6.26}$$

The value of K which allows us to eliminate the spherical aberration is

$$a_4 = \frac{1}{32(N-1)f^3}. \tag{6.27}$$

Because of our hypotheses, the equation of a section of P is (see (1.31))

$$z = \frac{1}{2R_c}y^2 + a_4 y^4, \tag{6.28}$$

where

$$a_4 = \frac{1}{32(N-1)f^3}. \tag{6.29}$$

Up to now, the radius of curvature R_c of the corrector P has not been determined. We can do this by imposing that $z'(\alpha r) = 0$, where r is the radius of P and α is a coefficient belonging to the interval [0, 1]. In this way, we easily derive that

$$R_c = -\frac{8(N-1)f^3}{\alpha^2 r^2}. \tag{6.30}$$

Finally, the radius R_c and the coefficient a_4 in (6.14) are given by

$$R_c = -\frac{8(N-1)f^3}{\alpha^2 r^2}, \quad a_4 = \frac{1}{32(N-1)f^3}. \tag{6.31}$$

Figure 6.2 shows different profiles of P upon varying the value of α. The first corresponds to the value $\alpha = 0$, which, in turn, implies $R_c = \infty$ or $a_2 = 0$. In this case the focal length of the mirror S is not modified by the corrector. The second corresponds to a corrector that has the same thickness at both the edge and the center. The value $\alpha = 0.866$ is preferred since it gives the best chromatic correction.

Note that all of the above formulae are valid given the approximations listed at the beginning of this chapter, and they do not take into account the small contributions of the curvature of the second surface of the corrector and to its thickness to the aberrations. They do however yield good results provided that the main mirror has a speed less than $f/3$.

After focusing mainly on the advantages of this camera in this section, we should also list its advantages. The first of them is its length, which is equal to the radius of curvature of primary mirror. Another is the difficulty involved in generating the correct profile of the corrector, especially if a sixth-order profile is requested in order to control higher order spherical aberration when a high speed principal mirror is employed. Other solutions that overcome these problems—although not without paying a price—are discussed in the following sections of this chapter.

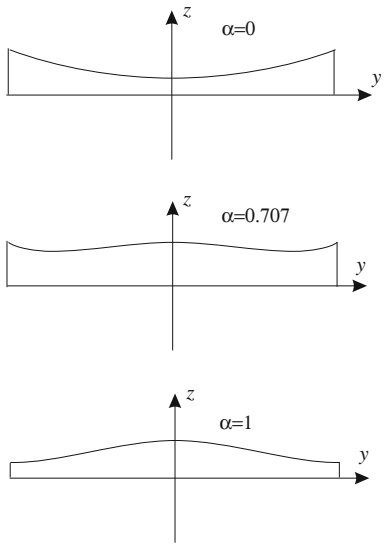

Fig. 6.2 Different profiles for Schmidt corrector

6.4 Examples of Schimdt's Camera

Suppose that $\alpha = 0.8666$, the mirror S has a curvature radius $R = -1600$ mm, the corrector P has a diameter of 200 mm (speed $f/4$) and is made by BK7, whose refractive index for green light is $N = 1.518722$. Using the above formulae or the notebook ***Schmidt camera***, we can derive

$$a_2 = -283296, \quad a_4 = 1.1766\,10^{-10}.$$

Similarly, the corrector associated with a mirror that has a radius of curvature $R = -1200$ (speed $f/3$) has the following characteristics:

$$R_c = -119521, \quad a_4 = 2.789\,10^{-10}.$$

When a camera with a mirror that has a speed $f/2.5$ is considered, we obtain

$$R_c = -69164, \quad a_4 = 4.82\,10^{-10}.$$

We can obtain spot diagrams that can be used to evaluate these cameras using professional software packages like ***OSLO*** or ***ATMOS***. Figures 6.3, 6.4, 6.5 were obtained by ***OSLO***. We can see that a very good correction is achieved on a spherical image surface with radius of curvature $-f$ when the speed is $f/4$ or $f/3$. When the speed is $f/2.5$ the performance of the camera is still acceptable but it is evident that we must resort to more accurate methods if we wish to make faster cameras. More precisely, we must

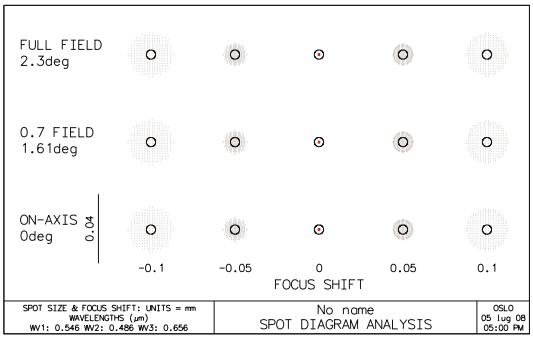

Fig. 6.3 Spot diagram of a Schmidt camera f/4

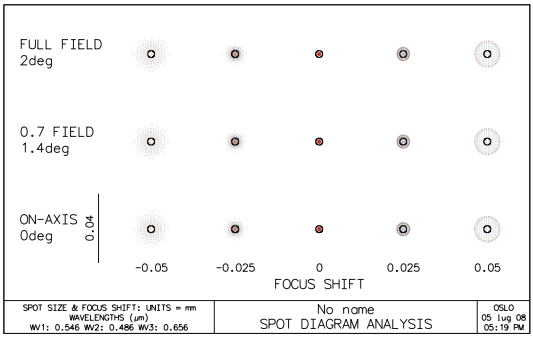

Fig. 6.4 Spot diagram of a Schmidt camera f/3

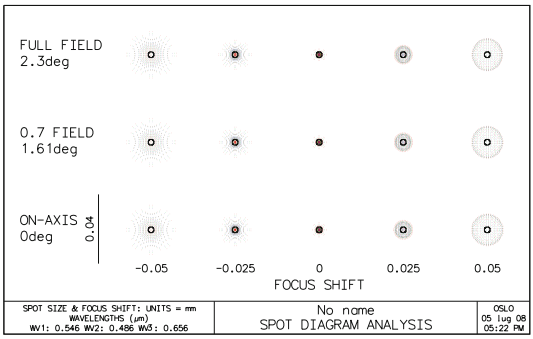

Fig. 6.5 Spot diagram of a Schmidt camera f/2.5

- Take into account the aberrations due to the finite radius and thickness of the second surface of the corrector
- To balance the third-order and fifth-order spherical aberrations; this becomes relevant in a mirror faster than $f/2.5$
- Adopt a corrector whose second face has a sixth-order profile to eliminate (in green light) both the third-order and the fifth-order spherical aberrations. It is evident that this solution is very expansive because of the difficulty of realizing a sixth-order profile

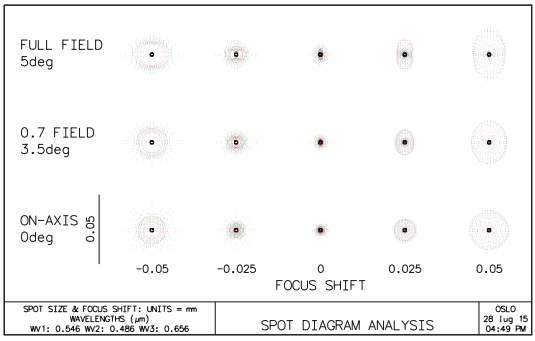

Fig. 6.6 Spot diagram of a Schmidt camera f/1.8

- The spherochromatism introduced by the corrector can be reduced either using less dispersive glass or adopting an achromatic corrector.

Figure 6.6 shows the spot diagram of a Schmidt camera that employs a primary mirror of speed $f/1.8$, diameter 200 mm, and a corrector with a fourth-order profile. It has been designed with the software ***Optisoft*** taking into account the first two items above. The field angle is 5° and the image field has a diameter of 64 mm. The radius of curvature of the image surface is -360 mm. The diameter of the spot at the boundary of the field is about 15 µm. It is important to note that this method is efficient for primary mirrors $f/1.8$ of diameter less than 300 mm. We must resort to a corrector with a sixth-order profile for primary mirrors of diameter greater than 300 mm. We propose another design obtained by ***Optisoft***. Figure 6.7, that is realized by ***Atmos***, shows the spot diagram of a Schmidt camera with a primary mirror $f/1.6$ and diameter 800 mm. The corrector is of glass N-KK56 and has a sixth-order profile. The field angle is 2° and the image field has a diameter of 84 mm. The radius of curvature of the image surface is -1220 mm. The diameter of the spot through the whole field is 20 µm.

6.5 Wright's Camera

In this section we show that we can have a shorter camera provided that we are willing to accept reduce image quality.

We start by noting that any displacement of the corrector from the center of curvature of the primary mirror introduces coma and astigmatism. ***Wright's camera*** contains the same components of a Schmidt camera but the corrector is closer to the mirror, which is now assumed to be *conic*. Consequently, there are only two free parameters in this combination, the coefficient a_4 of the corrector and the conic constant K of the mirror. Therefore, we can hope to control the spherical aberration and coma by choosing these parameters appropriately. A Wright camera is an aplanatic combination; in other words, it is free from spherical aberration and coma.

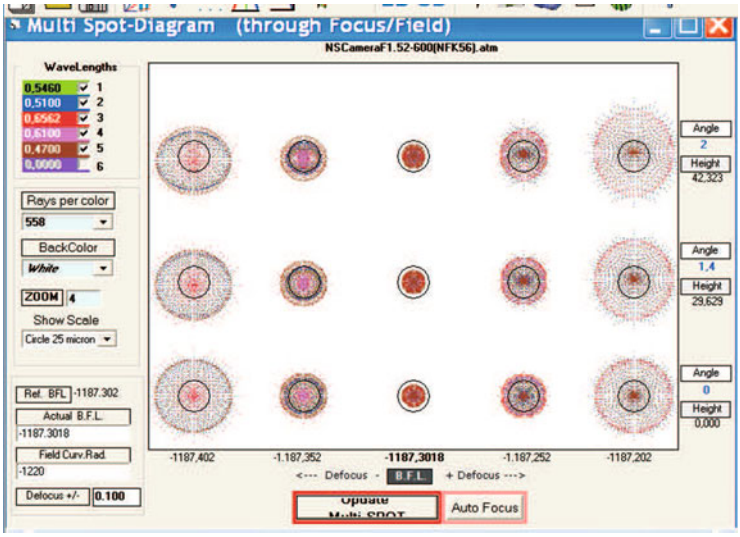

Fig. 6.7 Spot diagram of a Schmidt camera f/1.6

Let us consider a conic mirror S and a Schmidt corrector P that is situated at a distance $\delta f < |R|$ in front of S. If a_4 denotes the aspheric constant of P, N its refractive index, f the focal length of S, and K the conic constant of S, it is straightforward to verify that the spherical aberration, sagittal coma, and astigmatism coefficients of this combination (see (6.6) and the notebook ***Wright camera***) are

$$32 f^3 D_1 = -(K+1) + 32 f^3 a_4 (N-1), \tag{6.32}$$

$$8 f^2 D_2 = 2 - (K+1)\delta, \tag{6.33}$$

$$8 f (D_4 - D_3) = -\left(4 - 4\delta + (K+1)\delta^2\right). \tag{6.34}$$

The expressions (6.32)–(6.34) show that, *for any chosen distance δf between the corrector and the primary mirror, the values of a_4 and K, that allow spherical aberration and coma to be eliminated, satisfy the following system*

$$32 a_4 (N-1) f^3 - K - 1 = 0, \tag{6.35}$$

$$2 - (K+1)\delta = 0. \tag{6.36}$$

The solution of this system is

$$a_4 = \frac{1}{16 f^3 (N-1)\delta}, \quad K = -1 + \frac{2}{\delta}. \tag{6.37}$$

These relations prove that the conic constant K of S and the fourth-order coefficient of the corrector P depend only on the stop position. Finally, the astigmatism coefficient

corresponding to these values reduces to

$$D_4 - D_3 = \frac{\delta - 2}{4f}. \tag{6.38}$$

We note that the astigmatism and the conic constant K tend to zero when δ tends to 2 (the corrector is situated at the curvature center of S). However, for $\delta = 2$, Wright's camera becomes a Schmidt's camera. On the other hand, these quantities increase when the corrector is closer to S. In particular, K assumes very high values when $\delta < 1$; consequently, the mirror becomes more and more difficult to produce. We can therefore conclude that the most convenient values of δ belong to the interval 1.2–1.7. These values allow the tube to be shortened with respect to Schmidt's combination by 40–25 %, respectively.

Moreover, due to the presence of the astigmatism, the surface of the best focus does not coincide with the sphere with the Petzval radius, but rather with a sphere that has a radius that lies between the sagittal and meridional radii.

Some examples of Wright's cameras can be found in the notebook ***Wright camera***. These examples show that this configuration is more difficult to optimize than Schmidt's one. In fact, when the speed increases, a higher order astigmatism appears, which reduces the efficiency of the third-order correction.

6.6 Houghton's Camera

Another way to make an aplanatic camera using ***spherical surfaces*** only is given by ***Houghton's combination*** (see Figure 6.6). This is realized by replacing the aspherical Schmidt corrector with a pair H of spherical lenses, made from the same glass, whose radii of curvature R_i, $i = 1, \ldots, 4$, satisfy the conditions

$$R_1 = -R_3, \quad R_2 = -R_4. \tag{6.39}$$

It is straightforward to show that,*for any wavelength*, an afocal system is obtained *when the thickness of these lenses goes to zero*. In fact, the focal length of two adjacent thin lenses is (see ***Houghton camera***)

$$f = \frac{1}{(c_1 - c_2 + c_3 - c_4)(N - 1)}, \tag{6.40}$$

where $c_i = 1/R_i$, $i = 1, \ldots, 4$ denote the curvatures of the corrector surfaces, that goes to infinity when (6.39) holds.

We therefore reach the following conclusions:

- H does not modify the Gaussian description of the primary mirror S so the aberrations coefficients of the whole combination are obtained by adding the coefficients from (6.6) to the corresponding coefficients for the two lenses;

- No axial chromatic aberration is introduced by the corrector provided that *we can neglect the thickness of the two lenses*.

The expressions of the spherical aberration, coma, and astigmatism coefficients of S are obtained via (6.32)–(6.34) for $a_4 = K = 0$:

$$D_{S,1} = -\frac{1}{32f^3}, \tag{6.41}$$

$$D_{S,2} = \frac{1}{8f^2}(2-\delta), \tag{6.42}$$

$$D_{S,4} - D_{S,3} = -\frac{1}{8f}(2-\delta)^2. \tag{6.43}$$

If we assume that the thickness of the lens comprising Houghton's corrector is zero, application of the notebook ***Hoghton camera*** yields the following aberration coefficients[1]

$$D_{H,1} = (c_1 - c_2)^2(c_1 + c_2)\frac{(N+1)(N-1)^2}{4N}, \tag{6.44}$$

$$D_{H,2} = -(c_1^2 - c_2^2)\frac{(N^2-1)}{2N}, \tag{6.45}$$

$$D_{H,4} - D_{H,3} = 0. \tag{6.46}$$

where N is the refractive index of the lenses and $c_1 = 1/R_1$, $c_2 = 1/R_2$ are their curvatures.

The system is aplanatic if the curvatures verify the following equations (and $D_{S,1}$, $D_{S,2}$ have been assigned):

$$D_{H,1} + D_{S,1} = 0, \quad D_{H,2} + D_{S,2} = 0. \tag{6.47}$$

When the expressions (6.44)–(6.46) are inserted into (6.47), the following sixth-degree system is obtained:

$$(c_1 - c_2)^2(c_1 + c_2)\frac{(N+1)(N-1)^2}{4N} = -D_{S,1}, \tag{6.48}$$

$$(c_1^2 - c_2^2)\frac{(N^2-1)}{2N} = D_{S,2}. \tag{6.49}$$

Solving this yields the curvatures of the two lenses needed to eliminate spherical aberration and coma. It is very important to remark that this system is equivalent to a linear one, so these derived solutions (for the curvatures) are unique. In fact, from (6.49), we have

[1]The analysis of a Houghton camera presented in this section can be found in [32].

$$c_1^2 - c_2^2 = \frac{2ND_{S,2}}{N^2 - 1}, \tag{6.50}$$

and substituting this expression into $(6.48)_1$, gives

$$c_1 - c_2 = -\frac{2D_{S,1}}{(N-1)D_{S,2}}.$$

Using this formula, the following linear system can be derived:

$$c_1 - c_2 = -\frac{2D_{S,1}}{(N-1)D_{S,2}}, \tag{6.51}$$

$$c_1 + c_2 = -\frac{ND_{S,2}}{(N-1)D_{S,1}}, \tag{6.52}$$

which has the unique solution

$$c_1 = -\frac{2(N+1)D_{S,1} + N(N-1)D_{S,2}^3}{2(N^2-1)D_{S,1}D_{S,2}}, \tag{6.53}$$

$$c_2 = \frac{2(N+1)D_{S,1}^2 - N(N-1)D_{S,2}^3}{2(N^2-1)D_{S,1}D_{S,2}}. \tag{6.54}$$

Finally, using (6.6) to express $D_{S,1}$ and $D_{S,2}$ and recalling the relations $R_i = 1/c_i$, we obtain the radii of the doublet

$$\begin{aligned} R_1 &= f\frac{4(N^2-1)(2-\delta)}{(N+1) + N(N-1)(2-\delta)^3}, \\ R_2 &= -f\frac{4(N^2-1)(2-\delta)}{(N+1) - N(N-1)(2-\delta)^3}. \end{aligned} \tag{6.55}$$

Moreover, the astigmatism is absent when (see (6.7))

$$\begin{aligned} &(D_{H,4} + D_{S,4}) - (D_{H,3} + D_{S,3}) = \\ &D_{S,4} - D_{S,3} = -\frac{1}{8f}(2-\delta)^2 = 0, \end{aligned} \tag{6.56}$$

in other words, when the aperture stop A is placed at the curvature center of S ($\delta = 2$). It increases when A is closer to the mirror S. Therefore, the astigmatism of the whole combination coincides with the astigmatism of the primary mirror, since the doublet does not contribute to it, at least when the thickness of the lenses of the doublet is negligible.

We could consider eliminating the astigmatism by positioning the aperture stop at the curvature center of the mirror. However, when $\delta \to 2$, the radii R_1 and R_2 go to zero because of (6.55). Consequently, higher order aberrations appear and it

becomes impossible to produce lenses of the requested diameter. When $\delta > 2$, the radii R_1 and R_2 again increase, changing their sign, but the tube is longer. The Figure 6.7 shows all of these conclusions graphically and suggests that we should choose $\delta \in [0.7, 1.2]$.

When $\delta \simeq 1.2$, the radii R_1 and R_2 are still sufficiently high and the astigmatism is acceptable for a photographic use. Moreover, the tube is shorter than in an equivalent Schmidt Camera.

We now consider the case of a corrector with different radii to reduce the curvature of the lenses, and consequently the higher order aberrations. We show that these radii can be determined requiring that

- The curvature c_4 makes afocal the doublet (see (6.40)), in other words,

$$c_4 = c_1 - c_2 + c_3; \tag{6.57}$$

- The curvatures c_1 and c_2 make aplanatic the whole combination
- c_3 is chosen adopting a convenient criterion;

In the notebook ***Hoghton camera*** , it is proved that relations (6.51), (6.52) are replaced with the following:

$$\begin{aligned}&(c_1 - c_2)(c_2 - c_3)(-\frac{1}{8}(3c_1 - 2c_2 + c_3)(N + 1)-\\&\frac{1}{4N}(2c_1 - c_2 + c_3) - \frac{1}{4}(c_1 - c_2)N^2) = -D_{S,1},\\&-(c_1 - c_2)(c_2 - c_3)\frac{N^2 - 1}{2N} = -D_{S,2}.\end{aligned} \tag{6.58}$$

Also, in this case, the doublet does not contribute to the astigmatism since

$$D_{H,4} - D_{H,3} = 0.$$

Again, this system looks to be a sixth-degree system. However, it is possible to verify that it is equivalent to a second-degree system. In fact, we adopt the notations

$$x = \frac{c_1}{c_3} = \frac{R_3}{R_1}, \quad y = \frac{c_2}{c_3} = \frac{R_3}{R_2},$$

so that the system becomes

$$
\begin{aligned}
&(y-1)(x-y)\left(-\frac{1}{8}(3x-2y+1)(N+1)+\right.\\
&\left.\frac{2x-y+1}{4N}+\frac{N^2}{4}(x-y)\right)=-D_{S,1}R_3^3,\\
&(x-y)(y-1)\frac{N^2-1}{2N}=D_{S,2}R_3^2.
\end{aligned}
\tag{6.59}
$$

Substituting the relation

$$
(x-y)(y-1)=\frac{2N}{N^2-1}D'_{S,2}R_3^2 \tag{6.60}
$$

deduced from (6.59)$_2$ into (6.59)$_1$, we obtain the second-degree system

$$
\begin{aligned}
&-\frac{1}{8}(3x-2y+1)+\frac{2x-y+1}{4N}+\\
&\frac{N^2}{4}(x-y)=-\frac{N^2-1}{2N}\frac{D_{S,1}}{D_{S,2}}R_3,\\
&(x-y)(y-1)=\frac{2N}{N^2-1}D_{S,2}R_3^2.
\end{aligned}
\tag{6.61}
$$

Taking (6.6) into account, we finally get

$$
\begin{aligned}
&a_1x+a_2y=d_1,\\
&(x-y)(y-1)=d_2,
\end{aligned}
\tag{6.62}
$$

where

$$
\begin{aligned}
r_3=\frac{R_3}{f},\quad a_1&=\frac{4-3N-3N^2+2N^3}{8N},\\
a_2&=\frac{-1+N+N^2-N^3}{4N},\\
d_1&=-\frac{1}{8}-\frac{1}{4N}+\frac{N}{8}+\frac{(N^2-1)r_3}{8N(2-\delta)},\\
d_2&=\frac{N}{4(N^2-1)}(2-\delta)r_3^2.
\end{aligned}
\tag{6.63}
$$

System (6.62) has the following two solutions:

$$
\begin{aligned}
r_1&=2r_3\frac{a_1(a_1+a_2)}{-a_1(a_2-2d_1)+a_2(-a_2+d_1+\sqrt{\Delta})},\\
r_2&=2r_3\frac{a_1+a_2}{a_1+a_2+d_1-\sqrt{\Delta}},
\end{aligned}
\tag{6.64}
$$

or

$$
\begin{aligned}
r_1 &= -2r_3 \frac{a_1(a_1+a_2)}{a_1(a_2-2d_1)+a_2(a_2-d_1+\sqrt{\Delta})}, \\
r_2 &= 2r_3 \frac{a_1+a_2}{a_1+a_2+d_1+\sqrt{\Delta}},
\end{aligned}
\tag{6.65}
$$

These are real provided that the discriminant

$$
\Delta = (a_1+a_2+d_1)^2 - 4(a_1+a_2)(d_1+a_1d_2) > 0. \tag{6.66}
$$

i.e., that the discriminant is positive.

Substituting (6.63) into (6.66) and (6.65), we can determine all the acceptable values of r_3 for a given δ. Figure 6.8 shows the subset of the plane (r_3, δ) where (6.66) is valid.

Using ***Mathematica***, we can analyze the behavior of the radii r_1 and r_2 upon varying r_3 in the set I_δ of acceptable values for a given δ. Figures 6.9–6.10 plot the variables r_1, r_2 and r_4 versus r_3 for $\delta = 0.8$. More precisely, the first figure refers

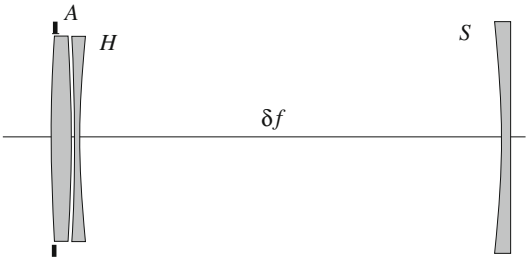

Fig. 6.8 Houghton camera f/2.5

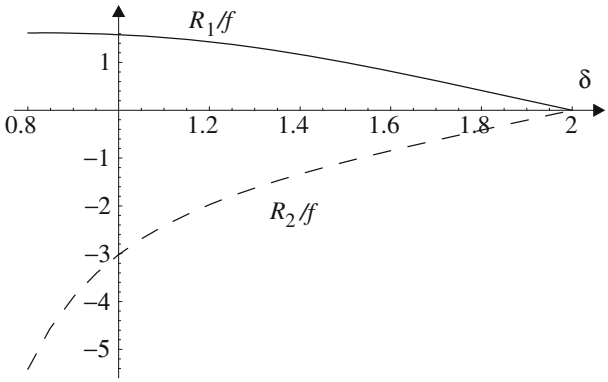

Fig. 6.9 Radii R_1/f and R_2/f versus δ

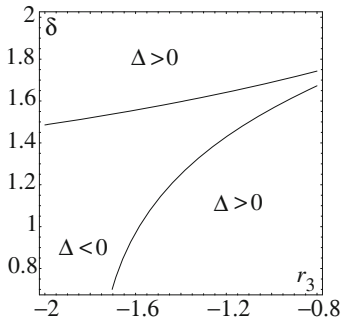

Fig. 6.10 Sign of Δ in the plane (r_2, δ)

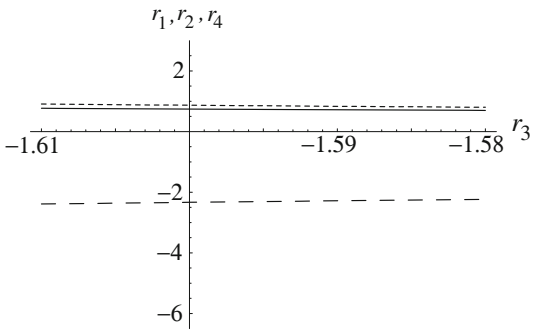

Fig. 6.11 $\delta = 0.8$, solution (6.65)

to solution (6.64) and the second to (6.65). The interval chosen for δ starts from the lower bound of I_δ (see ***Houghton camera***).

In Figures 6.9–6.10 the continuous line refers to r_1, the long-dashed line to r_2 and the short-dotted line to r_4.

Finally, Figures 6.11–6.12 have exactly the same meaning as Figures 6.9–6.10 but correspond to $\delta = 1.1$ instead.

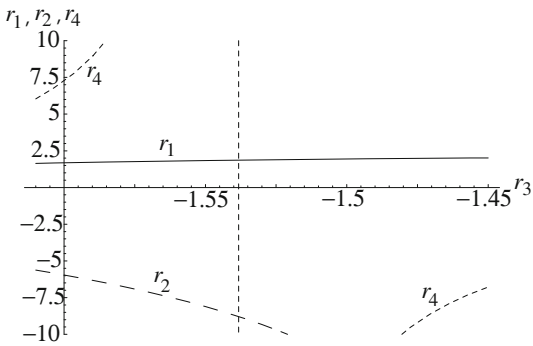

Fig. 6.12 $\delta = 0.8$, solution (6.66)

An analysis of the plots leads us to the following conclusions:

- the highest and thus the most convenient values of r_1, r_2, r_3 and r_4 are obtained for $\delta \in [0.7, 1]$;
- When the assigned δ falls in this interval, solution (6.64) and both r_3, r_4 are greatest at the lower bound of I_δ, whereas solution (6.65) and both r_3, r_4 must be evaluated at $0.8-0.9$ times the lower bound. For instance, if $\delta = 0.8$, from Figure 6.8 we can derive $I_\delta = [-1.65, -0.8]$, so solution (6.64) must be evaluated at $r_3 = -1.65$, whereas (6.65) should be evaluated at $r_3 = -1.5$ (see Figures 6.9 and 6.10, which refer to solutions (6.64), (6.65), respectively);
- In any case, the second solution leads to larger radii.

The notebook ***Hoghton camera*** allows us to design a Houghton's camera with different radii. Good results are obtained for mirrors that are slower than $f/3$ (Figs. 6.13, 6.14, and 6.15).

If we are willing to introduce aspheric surfaces into the system, it then becomes possible to eliminate the astigmatism by adopting a conic mirror S. We have already noted that the corrector does not introduce astigmatism (see notebook ***Houghton camera***), when it is afocal and very thin. Consequently, the total astigmatism of the whole combination corresponds to the astigmatism of the primary mirror. Taking into account the first equation of (6.15), we can then conclude that *it is possible*

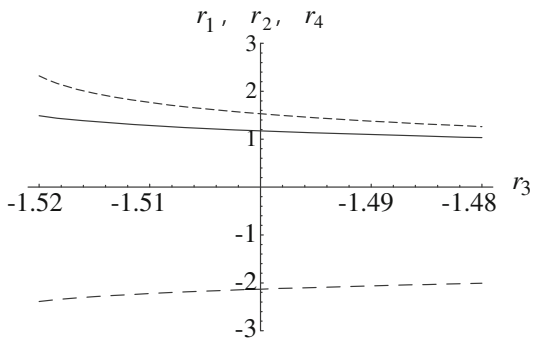

Fig. 6.13 $\delta = 1.1$, solution (6.64)

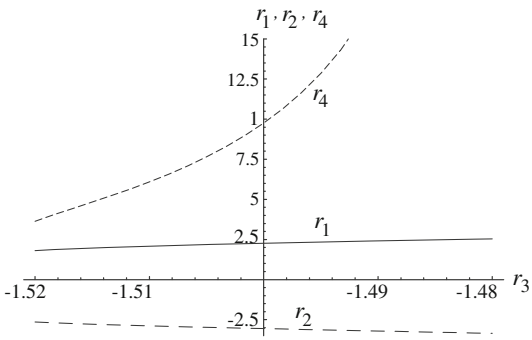

Fig. 6.14 $\delta = 1.1$, solution (6.65)

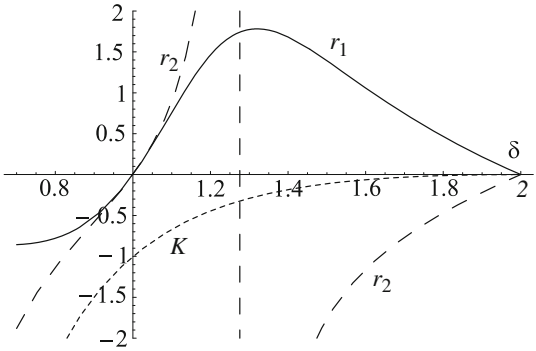

Fig. 6.15 Plots of $r_1 = R_1/f$, $r_2 = R_2/f$ and K versus δ

to eliminate this aberration for any aperture stop position, that is for any $\delta > 0$, provided that the conic constant of S is

$$K = -\frac{(\delta - 2)^2}{\delta^2}. \tag{6.67}$$

When the conic constant of S assumes this value, the spherical aberration and coma coefficients (6.6) become

$$D_{S,1} = \frac{1 - \delta}{8 f^3 \delta^2}, \quad D_{S,2} = \frac{\delta - 2}{4 f^2 \delta}. \tag{6.68}$$

Finally, if these expressions are inserted into (6.55), the following formulae for the radii of a symmetric doublet are derived:

$$\begin{aligned} R_1 &= \frac{4\delta(N^2 - 1)(\delta - 2)(\delta - 1)}{-2(\delta - 1)^2 + N^2\delta(\delta - 2)^3 - N(2 - 12\delta + 14\delta^2 - 6\delta^3 + \delta^4)}, \\ R_2 &= \frac{4\delta(N^2 - 1)(\delta - 2)(\delta - 1)}{2(\delta - 1)^2 + N^2\delta(\delta - 2)^3 - N(2 + 4\delta - 10\delta^2 + 6\delta^3 - \delta^4)}, \end{aligned} \tag{6.69}$$

It is important to note that, when $\delta = 1$ (i.e., the aperture stop is positioned on the focal plane of S), the spherical coefficient of S is equal to zero. Consequently, in order to eliminate the spherical aberration of the whole combination, we must have $D'_{H,1} = 0$, which in turn implies $c_1 = c_2$. On the other hand, for these values of c_1 and c_2, the coma coefficient of corrector vanishes and it is impossible to eliminate coma from the combination. Moreover, the mirror S becomes more and more conic when $\delta \to 0$ (see Figure 6.16).

We can say that

- when $\delta \in [1.4, 2]$, the radii of the corrector surfaces become smaller and consequently higher order aberrations appear. Convenient values of δ belong to the interval [1.2, 1.4].

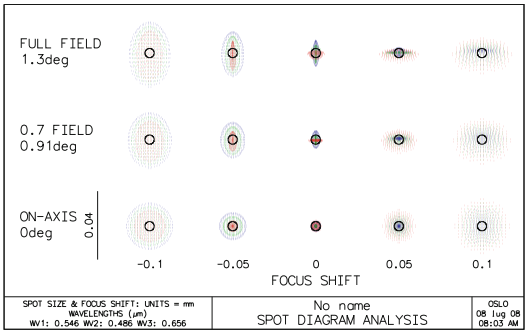

Fig. 6.16 Houghton camera $F/4$

The program ***Houghton camera*** uses all the above formulae to derive the curvature radii of Houghton's corrector and the conic constant of the mirror.

All the results discussed in this section can summarized as it follows:

- if a conic mirror S is used, we can design Houghton's cameras with speed up to $f/2.5$ which are about 40 % shorter than the corresponding Schmidt's cameras;
- using only spherical surfaces, we can design good cameras with speed up to $f/3.5$, if the lens of the corrector have paired radii, or up to $f/3$, if the lens of the corrector have different radii. Moreover, these cameras are about 50 % shorter than Schmidt's cameras.

6.7 Examples

In this section, we show some Houghton cameras realized with the notebook ***Houghton camera*** and their spot diagrams. In all of the examples the corrector has a diameter of 200 mm.

We start with a Houghton camera of the first type with a primary mirror of speed $f/4$. The notebook ***Houghton camera*** then gives

$$R_1 = 1288, \quad R_2 = -5332.4,$$

whereas the distance between corrector and primary mirror is 600 mm. The spot diagram on a sphere of -1000 mm. and for a view angle of 1.3^0, is given in Figure 6.16.

The Figure 6.17 shows the spot diagram for a Houghton's camera $f/3$ of the second type, with a speed $f/3$. The data for this camera, obtained using the program ***Houghton camera*** are

$$R_1 = 2638.5, \quad R_2 = -1608.8, \quad R_3 = -815.23, \quad R_4 = -4423,$$

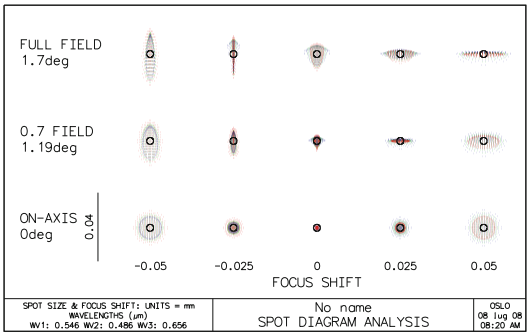

Fig. 6.17 Houghton camera $F/3$

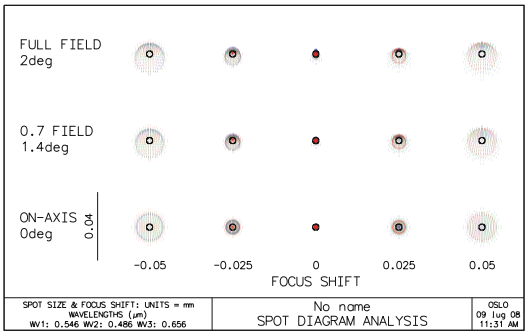

Fig. 6.18 Houghton camera $F/2.7$

with a distance between corrector and primary mirror equal to 750 mm. and a view angle of 1.7^0.

The spot diagram was obtained on a sphere with a radius of -800 mm.

Finally, Figure 6.18 shows the spot diagram for a Houghton's camera with a conic primary mirror of speed $f/2.7$ on a spherical surface of radius -540. The program ***Houghton camera*** gives

$$R_1 = 955.7, \quad R_2 = -8830,$$

with a distance between corrector and primary mirror equal to 700 mm. and a view angle of 2^0.

6.8 Maksutov Camera

In a ***Maksutov camera***, a meniscus C_M is placed in front of a spherical mirror S, so that all the involved surfaces are spherical (see Figure 6.19).

The aperture stop A coincides with the rim of C_M. In his original paper, Maksutov proposed the following empirical formulae to project a photographic camera when

Fig. 6.19 Maksutov camera

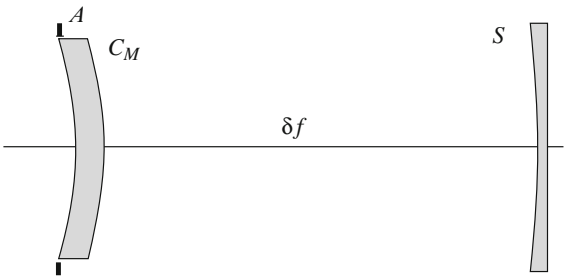

the speed $\mathbb{A}$ of S, the diameter D of C_M are assigned and C_M is made from BK7 glass

$$\begin{aligned} r_1 = -0.612\mathbb{A}^{0.66}D; \quad r_2 = (-0.612\mathbb{A}^{0.66} - 0.0565 - 0.007\mathbb{A})D; \\ \Delta = 0.1D, \quad R = -2.107\mathbb{A}^{0.983}D; \quad h = 1.11\mathbb{A}^{1.14}D, \end{aligned} \tag{6.70}$$

where, r_1, r_2 and Δ denote the radii of curvature for the two surfaces of the corrector and its thickness, respectively. Moreover, R and h are the radius of curvature S and its distance from C_M, respectively. These formulae allow us to determine the radii of the meniscus C_M and primary mirror S, when the speed $\mathbb{A}$ and diameter D of S are given.

However, a camera based on these formulae exhibits consistent third-order spherical aberration. Moreover, due to the strong curvature of the faces of meniscus, there is also residual fifth-order spherical aberration.

The notebook ***Maksutov camera*** is based on the following considerations.[2] First, the corrector C_M has a very long focal length compared with the focal of the primary mirror S. This means (see Section 1) that the aberration coefficients of the whole system are obtained, to a good approximation, by adding the aberration coefficients for the meniscus to those for S and noting that the aperture stop is located at a distance δf in front of S.

According to (6.35) or, equivalently, ***Maksutov camera***, the spherical aberration coefficient of the spherical mirror S, is given by

$$D_{S,1} = -\frac{1}{32f^3}, \tag{6.71}$$

We use the following notations for the meniscus C_M: N is the refractive index, Δ is its thickness, $s = r_1 - r_2$, and D is its diameter. The spherical aberration coefficient of corrector is then (see ***Maksutov camera***)

[2]The analysis provided in this section can be found in [33].

$$D_{M,1} = \frac{N-1}{8N^3 r_1^4 (r_1 - s)^3}[(r_1 + (N-1)(s-\Delta))^2 (N(r_1 - \Delta) + \Delta) \\ (r_1 + (N-1)(s + Ns - N\Delta) - r_1 N (r_1 - s)^3]. \tag{6.72}$$

Finally, the condition that must hold in order to achieve an axially achromatic meniscus is

$$\frac{dz_2'}{dN} = 0. \tag{6.73}$$

Since (see ***Maksutov camera***)

$$z_2' = \frac{-Nr_1^2 + Nsr_1 - \Delta r_1 + N\Delta r_1 + s\Delta - Ns\Delta}{(N-1)(Ns + \Delta - N\Delta)}, \tag{6.74}$$

equation (6.73) becomes

$$\begin{aligned} &(N^2 s + \Delta - N^2\Delta) r_1^2 - \\ &(N^2 s^2 + 2s\Delta - 2Ns\Delta - \Delta^2 + 2N\Delta^2 - N^2\Delta^2) r_1 + \\ &(s^2 - 2Ns^2\Delta + N^2 s^2 \Delta - s\Delta^2 + 2Ns\Delta^2 - N^2 s\Delta^2) = 0. \end{aligned} \tag{6.75}$$

The roots of this equation are

$$s = r_1, \quad s = \frac{(N^2-1)\Delta r_1 - \Delta^2 (N-1)^2}{N^2 r_1 - \Delta (N-1)^2}. \tag{6.76}$$

Only the second root is acceptable, and we write it in the form

$$s = \Delta \frac{(N^2-1)}{\alpha N^2}, \tag{6.77}$$

where

$$\alpha = \frac{1 - \dfrac{\Delta (N-1)^2}{r_1 (N^2-1)}}{1 - \dfrac{\Delta (N-1)^2}{N^2 r_1}}. \tag{6.78}$$

In order to elucidate the behavior of the function in (6.78), we assume that $\Delta = 0.1D$ and that the aperture ratio $\mathbb{A}$ of the primary mirror varies from $1/4$ to $1/3$. Since the ratio f/r_1 lies within the range $(-0.5, -0.3)$ in the applications, the quantity

$$x \equiv \frac{\Delta}{r_1} = \frac{\Delta}{D}\frac{D}{f}\frac{f}{r_1} = 0.1\mathbb{A}\frac{f}{r_1}$$

can be found in the interval (0.007, 0.016). It is straightforward to verify, for the glass BK7 for instance, that the function (6.78) is actually very close to 1.001. Therefore, the condition for axial achromatism is

$$s = \Delta \frac{(N^2 - 1)}{N^2}. \tag{6.79}$$

Although this equation leads to the axial achromatism, it is more convenient to use the following relation instead:

$$s = \Delta \frac{(N^2 - 1)}{\alpha N^2}, \quad \alpha \in (0.95, 1) \tag{6.80}$$

This is because (as demonstrated by the examples in ***Maksutov camera***), for $\alpha = 0.975$, rays of different colors, that intercept C_M at $0.7D$, arrive at the same point of the axis. If $\alpha = 0.95D$, this happens to the marginal rays. From now on, we assume that the thickness $\Delta = 0.1D$ and that the difference $s = r_1 - r_2$ is given by (6.80).

To determine the values of r_1, we now need to impose that the spherical aberration of the whole combination vanishes

$$D_{S,1} + D'_{S,1} = 0. \tag{6.81}$$

Because of (6.71) and (6.73), this is a seventh-degree algebraic equation in the unknown r_1, which can be solved with ***Maksutov camera***, when the *numerical* values of N and Δ are given. It is clear that some of these solutions can be meaningless from a physical point of view. In any case, this equation has two real roots with opposite signs. In practice, the negative root is chosen.

It is evident that this value of r_1 represents a first approximation since it is obtained by calculating the spherical aberration of the mirror S, without taking the presence of the corrector C_M into account. Moreover, no information about the distance δf between C_M and S has been provided so far.

Maksutov camera can supplies the values of r_1 and δ that will reduce the third-order spherical aberration and coma to zero. The input data are D, f, and the field angle θ, and we will assume that C_M is made from BK7 glass. The software also evaluates the value of r_2 as well as the other aberrations in the system.

Note that high-order spherical aberrations are significant when the surfaces of the corrector are highly curved. Therefore, a design based on the third-order theory is not usually acceptable without resorting to some optimization techniques.

Some examples are given in ***Maksutov camera*** where it is shown that good results are obtained for speeds up to $F/4$.

6.9 Examples

The corrector has a diameter of $D = 200$ mm and a thickness $0.1D = 20$ mm.

Figure 6.20 shows the spot diagram for a Maksutov camera with a primary of speed $f/4$. It is clear that this camera will not be satisfactory for photographic purposes due to higher order aberrations.

Figure 6.21 shows the spot diagram of a Maksutov camera with a mirror of speed $f/3.3$ where the camera was designed with the software ***Optisoft*** (see the preface). It is evident that this faster camera will be good enough if intended for photography since the diameter of the circle is 25 μ. The diameter of the image is 36 mm. on a sphere with a radius of −720 mm.

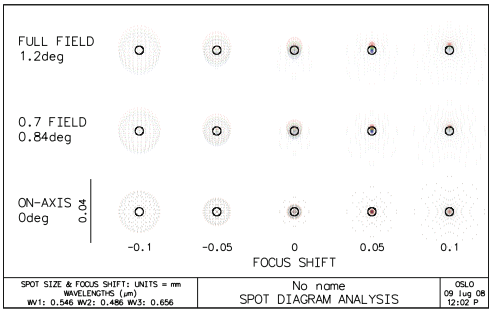

Fig. 6.20 Spot diagram for a Maksutov camera $f/4$

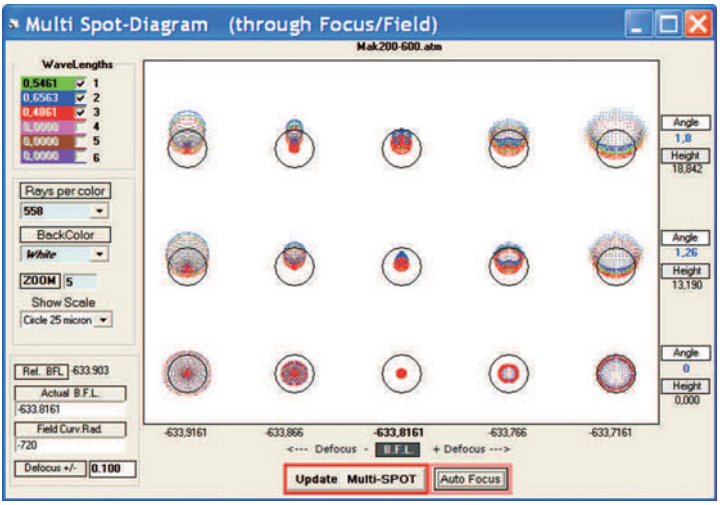

Fig. 6.21 Spot diagram for a Maksutov camera $f/3.3$

The radius of the first surface of the meniscus is −250.48, the radius of the second surface is −261.98 and thickness is 20 mm. The distance between the meniscus and the primary mirror is 762.6 mm and its radius of curvature is equal to −1239. Finally, the meniscus has a diameter of 200 mm. and the total view field is 3.6°.

Chapter 7
Compound Cassegrain Telescopes

7.1 Introduction to Cassegrain Telescopes

Very efficient optical configurations can be obtained for astronomical telescopes by combining one of the correctors described in the previous chapter with the Cassegrain scheme. Depending on the corrector chosen, a Schimdt–Cassegrain, Houghton–Cassegrain, or Maksutov–Cassegrain telescope is obtained (see Figure 7.1).

First, note that it is simpler to eliminate the aberrations in one of the aforesaid configurations than in the corresponding photographic camera for the following two reasons:

- Due to the longer focal length of a telescope compared to a camera, the field angle and the off-axis aberrations are smaller;
- The secondary mirror partially compensates for the aberrations of the primary mirror.

Thus, the corrector must balance out the residual aberrations of a Cassegrain configuration for small field angles. However, it is important to note that much more accurate correction is needed, if we wish to reach the diffraction limit.

This chapter reviews the optical combinations that are obtained by associating a Schmidt corrector C_S, a Houghton corrector C_H, or a Maksutov corrector C_M with the Cassegrain scheme (see Figure 7.1).

The Cassegrain design needs to be developed as shown in Section 4.2: based on the diameter and focal length f_1 of S_1, the total focal length f of the combination, and the distance between S_1 and the focal plane, it is possible to determine the diameter of S_2, its radius of curvature R_2, and the distance $s_{1,2}$ between S_1 and S_2 (back focal) or (equivalently) the nondimensional quantities β and γ.

In the second step, we determine the aberrations of S_1 and S_2 in the absence of the corrector C but the presence of an aperture stop at a distance δf from S_1, proceeding as in the previous chapter. As already noted, this approach is possible

© Springer International Publishing Switzerland 2016

A. Romano and R. Cavaliere, *Geometric Optics*,
Modeling and Simulation in Science, Engineering and Technology,
DOI 10.1007/978-3-319-43732-3_7

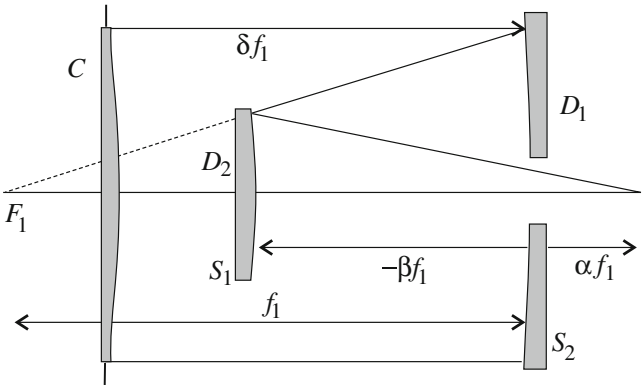

Fig. 7.1 Compound Cassegrain telescope

because the corrector is an almost afocal optical element that does not modify the Gaussian characteristics of the whole system (see Section 5.1).

The calculations involved—although simple—are very tedious so that it is again advantageous to use ***Mathematica*** in order to quickly obtain the final results. By resorting to the notebook ***Schmidt–cassegrain***, the coefficients D_1, D_2 and D_3 of spherical aberration, coma and astigmatism for the whole system comprising S_1 and S_2 with an aperture stop at a distance δf_1 from S_1 are obtained:

$$\begin{aligned} 32 f_1^3\, D_1 &= B_{1,0} - K_1 + B_{1,2} K_2, \\ 8 f_1^2\, D_2 &= B_{2,0} - \delta K_2 + B_{2,2} K_2, \\ 8 f_1\, D_3 &= B_{3,0} - \delta^2 K_2 + B_{3,2} K_2 \end{aligned} \tag{7.1}$$

where

$$\begin{aligned} B_{1,0} &= -1 + \frac{(\alpha+1)(M^2-1)}{M^3}, \quad B_{1,2} = \frac{(M-1)^3(1+\alpha)}{M^3(1+M)}, \\ B_{2,0} &= \frac{M + \alpha - M^3(\delta-1) - \delta(\alpha+1) + M^2(\alpha(\delta-1)+\delta)}{M^3}, \\ D_{2,2} &= \frac{(M-1)^3(M+\alpha(\delta-1)+\delta)}{M^3(1+M)}, \end{aligned} \tag{7.2}$$

$$\begin{aligned} B_{3,0} = \frac{1}{M^3(1+\alpha)} \big(& M^4 + 2M(\alpha(\delta-1)+\delta) - (\alpha(\delta-1)+\delta)^2 + \\ & M^3(1+\alpha)(\delta-1)(1+\alpha(\delta-1)+\delta) - M^3(4-2\delta+\delta^2+\alpha(2-2\delta+\delta^2)) \big), \end{aligned} \tag{7.3}$$

$$B_{3,2} = \frac{(M-1)^2(M+\alpha(\delta-1)+\delta)^2}{M^3(M+1)(\alpha+1)}. \tag{7.4}$$

7.2 Schmidt–Cassegrain Telescopes

We now have the all of the ingredients required to design a ***Schmidt-Cassegrain combination***. In this case, there are three possibilities

- Both primary and secondary mirror are spherical and the corrector must eliminate the spherical aberration of the whole combination. This is realized when

$$B_{1,0} + a_4(N-1) = 0, \tag{7.5}$$

that is, when

$$a_4 = \frac{B_{1,0}}{N-1}. \tag{7.6}$$

The coma and astigmatism are acceptable if the speed of S_1 is less than or equal to $F/4$. In any case, coma can be eliminated if the distance δf_1 between the corrector and the primary mirror is equal to the (positive) root of the equation

$$B_{2,0} = 0. \tag{7.7}$$

It is straightforward to verify that this value is

$$\delta = \frac{M(M^2+1) + \alpha(1-M^2)}{1 + M^3 + \alpha - M^2(1+\alpha)}, \tag{7.8}$$

and that it corresponds to a lengthening of the tube.

- The primary is spherical and the secondary is characterized by a conic constant K_2. In this case, the coefficient a_4 of the corrector and the conic constant K_2 are used to eliminate spherical aberration and coma. This happens when

$$B_{1,0} + B_{1,2}K_2 + a_4(N-1) = 0, \quad B_{2,0} + B_{2,2}K_2 = 0. \tag{7.9}$$

This system is satisfied for

$$a_4 = \frac{B_{1,2}D_{2,0} - B_{1,0}B_{2,2}}{B_{2,2}(N-1)}, \quad K_2 = -\frac{B_{2,0}}{B_{2,2}}. \tag{7.10}$$

- Finally, spherical aberration, coma, and astigmatism can be eliminated by utilizing the three degrees of freedom a_4, K_1 and K_2 and imposing that they satisfy the system

$$\begin{aligned} &B_{1,0} - \frac{1}{32f^3}K_1 + B_{1,2}K_2 + a_4(N-1) = 0, \\ &B_{2,0} - \frac{1}{8f^2}\delta K_1 + B_{2,2}K_2 = 0, \\ &B_{3,0} - \frac{1}{8f}\delta^2 K_1 + B_{3,2}K_2 = 0. \end{aligned} \tag{7.11}$$

The corresponding solution is

$$
\begin{aligned}
a_4 &= \frac{1}{4f_1(N-1)\delta(D_{2,2}f_1\delta - D_{3,2})}\left(-B_{2,0}D_{3,2} - 4B_{1,2}B_{3,0}f_1\delta + \right.\\
&\left. 4B_{1,0}B_{3,2}f_1\delta + 4B_{1,2}B_{2,0}f_1^2\delta^2 + B_{2,2}(B_{3,0} - 4B_{2,0}f_1^2\delta^2)\right),\\
K_1 &= \frac{8(B_{2,2}B_{3,0} - B_{2,0}B_{3,2})f_1^2}{\delta(B_{2,2}f_1\delta - B_{3,2})},\\
K_2 &= \frac{B_{3,0} - B_{2,0}f_1\delta}{B_{2,2}f_1\delta - B_{3,2}}.
\end{aligned}
\tag{7.12}
$$

For the above cases, note that

- First, it is essential to eliminate the spherical aberration. However, one or two conic mirrors are necessary to eliminate coma, or both coma and astigmatism, and this is very difficult to realize in practice.
- If the primary mirror has a speed of more than $F/3.5$, the curvature of the second surface of the corrector becomes appreciable so we must also consider the aberrations introduced by it.
- Due to the high speed of the primary mirror, fifth-order spherical aberration occurs, and the above values of a_4, K_1 and K_2 do not ensure that the corresponding combination performs well.

In order to tackle the second problem, we should evaluate the small variations in a_4, K_1 and K_2 due to the radius of curvature R_c. In regard to the last problem, there are two ways to eliminate the fifth-order spherical aberration

- We could consider a sixth-order profile of the corrector

$$y = a_2y^2 + a_4y^4 + a_6y^6,$$

  and try to work out which value of a_6 eliminates the fifth-order spherical aberration. However, such a corrector is very difficult to produce.
- Alternatively, at least for primary mirrors that are slower than $F/2.5$, we could try to balance the third- and fifth-order spherical aberrations. This approach requires a deeper analysis of the optical combination.

7.3 Examples

In this section, we provide examples of Schmidt-Cassegrain telescopes obtained using the notebook ***Schmidt–cassegrain***. For all of the designs considered here, the diameter of the principal mirror S is 200 mm. In the first three examples, the primary mirror has a speed $f/3$; in the final three examples, the primary mirror has a speed $f/2$.

First, suppose that S has a speed $f/3$ and we are searching for the data on a telescope with a total focal length of 2400 mm, aback focal is 250 mm, and where the corrector and primary mirror are separated by 450 mm. If we denote the radius of the secondary mirror S_s by R_s, the distance between S and S_s by δf, the radius of the second surface of the corrector C at its vertex by R_C, the aspheric constant of C by a_4, the conic constants of S and S_s by K_1 and K_2, respectively, then, for the three cases considered in the previous section, the notebook ***Schmidt–cassegrain*** gives

$$R_s = -453.33, \quad \delta f = -430.$$

- Third-order spherical aberration is absent when:

$$R_c = -715725, \quad a_4 = 1.863 \cdot 10^{-10}.$$

- Third-order spherical aberration and coma are absent when

$$R_c = -590650, \quad a_4 = 2.257 \cdot 10^{-10}, \quad K_2 = -1.18.$$

- Third-order spherical aberration, coma, and astigmatism are absent when

$$R_c = -365946, \quad a_4 = 3.644 \cdot 10^{-10}, \quad K_1 = 0.644, \quad K_2 = 0.005.$$

Figures 7.2, 7.3, and 7.4 show the spot diagrams corresponding to the above data over a focal spherical surfaces of radius -380 mm. We see that in the third case, higher order aberrations reduce the performance of the combination.

In order to shorten the tube containing the optical combination, we now consider a primary mirror S with a speed $f/2$ and diameter of 200 mm. The new input data are: total focal length 2000 mm, back focal 200 mm, distance between corrector and

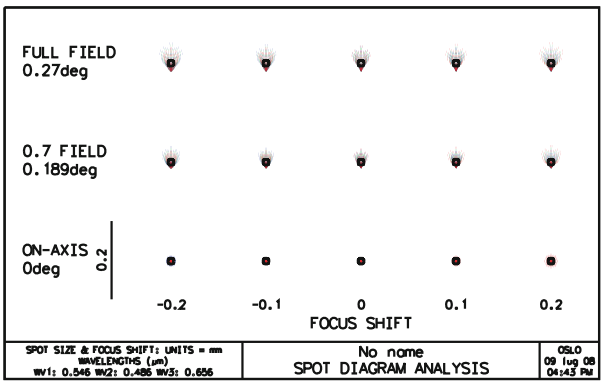

Fig. 7.2 Schmidt–Cassegrain with spherical mirrors

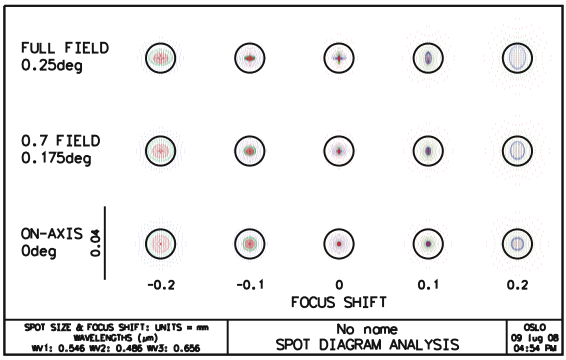

Fig. 7.3 Schmidt–Cassegrain with conic secondary mirror

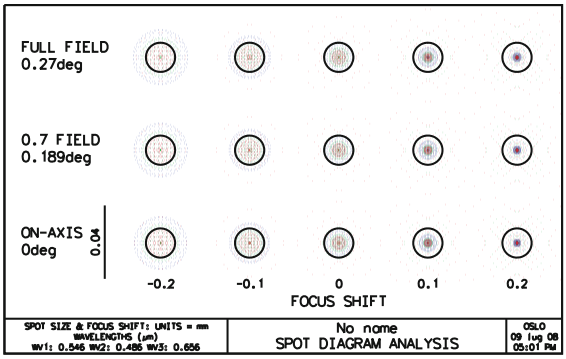

Fig. 7.4 Schmidt–Cassegrain with conic mirrors

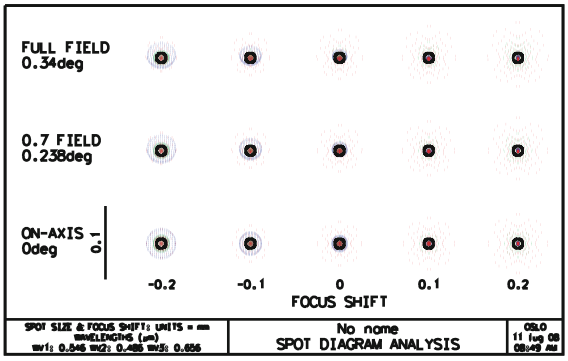

Fig. 7.5 Schmidt–Cassegrain with conic mirrors

primary mirror is 305 mm. Then, the notebook ***Schmidt–cassegrain*** gives

$$R_s = -250, \quad \delta f = -300.$$

Third-order spherical aberration and coma are absent when

$$R_c = -173043, \quad a_4 = 7.705 \cdot 10^{-10}, \quad K_2 = -0.833.$$

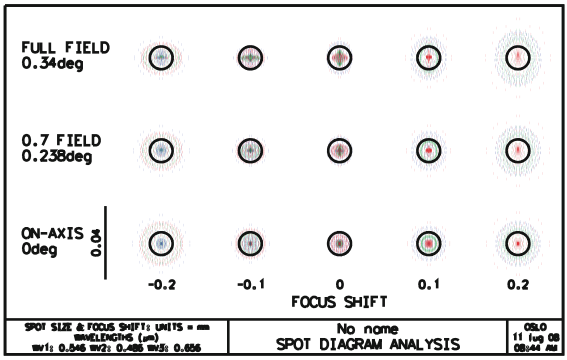

Fig. 7.6 Schmidt–Cassegrain with conic mirrors

The spot diagram on a focal surface with a radius of −200 mm. in Figure 7.5 shows that the third-order correction is not sufficient in this case.

Figure 7.6 shows the spot diagram of the same combination designed with ***Optisoft*** on the focal surface of radius −380 mm.

7.4 Houghton–Cassegrain Telescopes

An aplanatic telescope with **spherical surfaces** is obtained by combining the Cassegrain scheme with Houghton's corrector (see Figure 7.7).

All of the results derived in Chapter 5 for Houghton's cameras can be extended to this case. In particular, for a symmetric doublet we have:

$$
\begin{aligned}
R_1 &= -\frac{2(N^2-1)D_1D_2}{2(N+1)D_1^2+N(N-1)D_2^3},\\
R_2 &= \frac{2(N^2-1)D_1D_2}{2(N+1)D_1^2-N(N-1)D_2^3}.
\end{aligned}
\tag{7.13}
$$

where the aberration coefficients D_1 and D_2 are given by (7.1), (7.2) for $K_1 = K_2 = 0$.

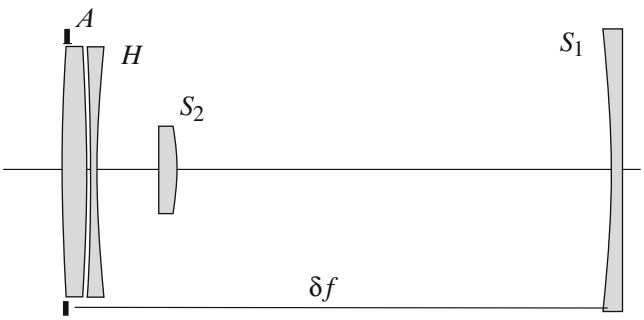

Fig. 7.7 Houghton–Cassegrain telescope

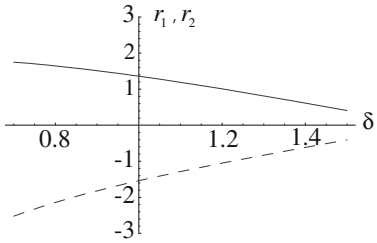

Fig. 7.8 r_1, r_2 versus δ, for $M = 3$

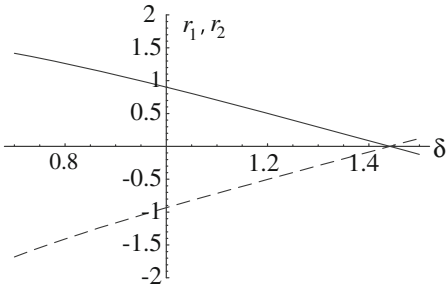

Fig. 7.9 r_1, r_2 versus δ, for $M = 4$

For a fixed pair of mirrors S_1 and S_2 in a Cassegrain combination, the radii R_1 and R_2 depend on the magnification M and the distance factor δ. Figures 7.8 and 7.9 (see the notebook ***HCassegrain***) show the plots of the nondimensional quantities

$$r_1 = \frac{R_1}{f_1}, \quad r_2 = \frac{R_2}{f_1},$$

versus δ for $M = 3$ and $M = 4$, respectively. In both plots, the dotted line refers to r_2. It is evident that the most convenient values of r_1 and r_2 (i.e., the largest absolute values that reduce higher order aberrations) are obtained for $\delta \in [0.7, 1]$. On the other hand, we must increase the magnification M if we wish to reduce the obstruction factor. But the plots in Figure 7.8 show that the radii r_1 and r_2 decrease and higher-order aberrations become more relevant as M increases.

According to the above formulae, very good results are obtained when the principal mirror S is slower than $f/3.5$. When the speed of S is faster than $f/3.5$ and slower or equal to $f/3$, the curvatures supplied by (7.13) are too strong and the higher-order aberrations dominate.

One way to reduce the curvature of the lenses, and consequently the higher-order aberrations, is to use *four* different values of the radii of the lenses comprising the doublet. Again, all the results of Chapter 5 can be applied in this new situation.

First, we have to determine the region in which the discriminant $\Delta > 0$, upon varying δ and r_3 (see Figure 7.10). The Figure 7.10 shows this region for the glass BK7, $\alpha = 0.4$, where α is the ratio between the back distance and the primary focal, and for a magnification factor $M = 4$.

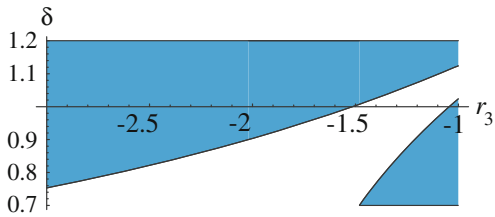

Fig. 7.10 The region in which $\Delta > 0$, for $M = 4$

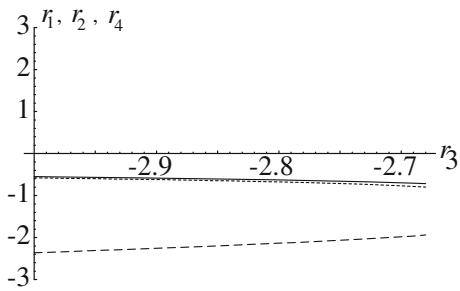

Fig. 7.11 r_1, r_2 and r_3 versus $\delta = 0.8$ and solution (6.55)

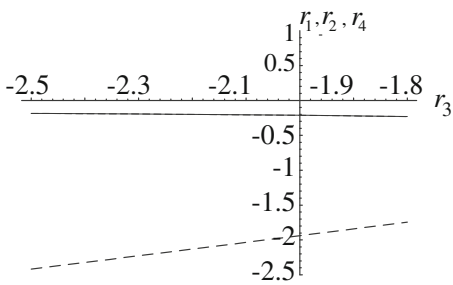

Fig. 7.12 r_1, r_2 and r_3 versus $\delta = 0.8$ and solution (6.63)

Moreover, using ***Mathematica*** it is possible to analyze the behavior of the radii r_1 and r_2 as r_3 is varied in the set I_δ of admissible values corresponding to a given δ (see Chapter 6). Figures 7.11– 7.12 plot the variables r_1, r_2, and r_4 versus r_3, for $\delta = 0.8$. More precisely, the first figure refers to solution (6.55) and the second one to (6.63). The interval chosen for δ starts from the lowest bound of I_δ (see ***HCassegrain***).

In all of the figures shown in this section, the continuous line refers to r_1, the line with longer dashes to r_2 and the line with shorter dashes to r_4.

Finally, Figures 7.13–7.14 are similar to Figures 7.11–7.12 but show the results for $\delta = 1.1$.

Careful analysis of the plots leads us to the following conclusions:

- the highest and thus most convenient values of r_1, r_2, r_3 and r_4 are obtained for $\delta \in [0.7, 1]$;
- For an assigned δ in this interval, solution (6.64) and r_3, r_4 attain their highest values at the lowest bound of I_δ, whereas solution (6.55) and r_3, r_4 must be

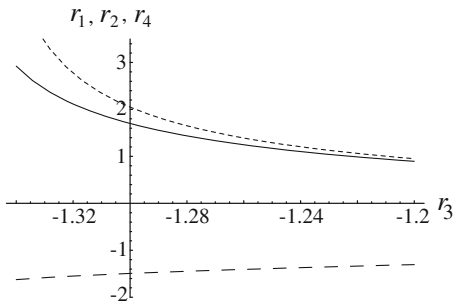

Fig. 7.13 r_1, r_2 and r_3 versus $\delta = 1.1$ and solution (6.55)

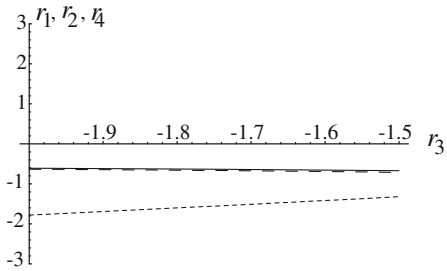

Fig. 7.14 r_1, r_2 and r_3 versus $\delta = 1.1$ and solution (6.55)

evaluated at $0.8 - 0.9$ times the lowest bound. For instance, for $\delta = 0.8$, we derive $I_\delta = [-1.65, -0.8]$ from Figure 7.10, meaning that solution (6.55) must be evaluated at $r_3 = -1.65$, whereas solution (6.63) should be evaluated at $r_3 = -1.5$ (see Figures 7.13 and 7.14, which refer to solutions (6.55), (6.63), respectively);

- In any case, the second solution leads to larger radii.

7.5 Examples

In this section, we provide some examples of Houghton–Cassegrain telescopes. We start with a principal mirror S of diameter $D = 200$ mm. and speed $f/3$. We denote the focal of the primary mirror by f_1, the total focal length of the whole combination by f_t, the thicknesses of the doublet by $spes$, the distance between the corrector and S by δf_1, the back focal by em, the refractive indices of the glasses of the doublet by N_i, $i = 1, 2$, the view angle by θ, the radius of curvature of secondary mirror by R_s, the distance between primary and secondary mirrors by Δ, and the radii of curvature of the surfaces of doublet by R_i, $i = 1, \ldots, 4$. The input data for the program ***Houghton–Cassegrain*** are then

$$
\begin{aligned}
&f_1 = 600,\\
&f_t = 2400,\\
&spes = 15, 5, 5,\\
&em = 200,\\
&D = 200,\\
&\delta = 480/600,\\
&N_i = 1.5187228(\text{BK7 in green light}),\\
&\theta = 0.27.
\end{aligned}
$$

The corresponding output is

$$
\begin{aligned}
&R_s = -426, 667,\\
&\Delta = -440,\\
&R_1 = 53898,\\
&R_2 = -1168,\\
&R_3 = -795.5,\\
&R_4 = -2617.
\end{aligned}
$$

Figure 7.15 shows the spot diagram of this combination, which is diffraction limited (Fig. 7.16).

Now, we will attempt to design a similar combination with a shorter tube and a higher speed. To this end, we start with a faster primary mirror, of speed $S\ f/2.25$, and we consider the following input data

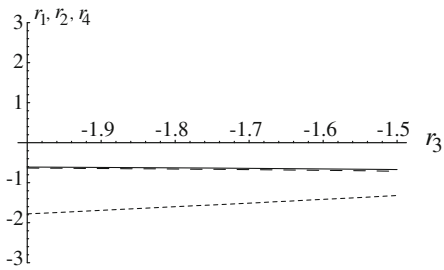

Fig. 7.15 r_1, r_2 and r_3 versus $\delta = 1.1$ and solution (6.63)

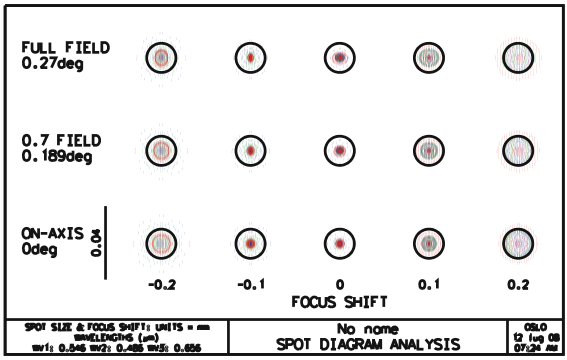

Fig. 7.16 Houghton–Cassegrain; primary speed $f/3$

$$
\begin{aligned}
&f_1 = 450,\\
&f_t = 2000,\\
&spes = 10, 10, 5,\\
&em = 200,\\
&D = 200,\\
&\delta = 340/450,\\
&N_i = 1.5187228(\text{BK7 in green light}),\\
&\theta = 0.3.
\end{aligned}
$$

The corresponding output data, obtained with the notebook ***Houghton–Cassegrain*** are listed below

$$
\begin{aligned}
&R_s = -308.1,\\
&\Delta = -330.6,\\
&R_1 = 84784,\\
&R_2 = -868.1,\\
&R_3 = -593.04,\\
&R_4 = -1914.
\end{aligned}
$$

The spot diagram for this combination (see Figure 7.17), which is produced on a focal surface of radius −200 mm, shows that the third-order correction is not acceptable due to the presence of significant higher-order aberrations introduced by the shorter radius of curvature of the primary. For instance, we must balance out the third-order and fifth-order aberrations, improve the spherochromatism, etc. In other words, increasing the speed of the primary does not improve the third-order design is and so we need to analyze the problem more accurately. For instance, Figure 7.18 shows the spot diagram for a Houghton–Cassegrain combination that was designed using the above data and the software ***Optisoft***. It is clear that this combination is again diffraction limited.

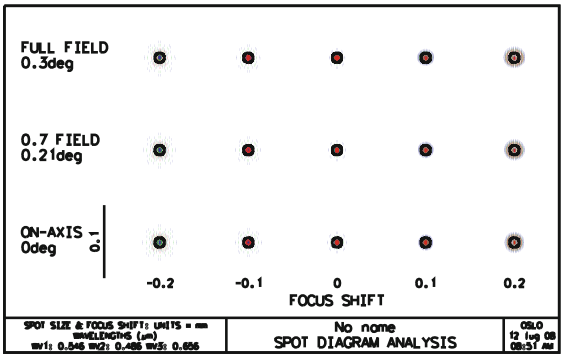

Fig. 7.17 Houghton–Cassegrain; primary speed $f/2.25$

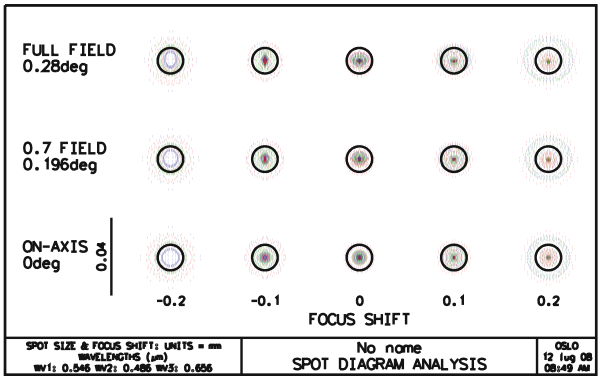

Fig. 7.18 Houghton–Cassegrain (speed of primary: $f/2.25$) designed by ***Optisoft***

7.6 Maksutov–Cassegrain Telescopes

A ***Maksutov–Cassegrain telescope*** is obtained by placing the Maksutov corrector C_M in front of a Cassegrain combination (see Figure 7.19).

Although the number of surfaces of this scheme is less than the corresponding number of surfaces used in the Houghton–Cassegrain telescope, the analysis of this combination is much more difficult for the following reasons:

- the thickness of the meniscus can not be neglected, even in the first approximation, since it has a fundamental role in compensating the aberrations;
- the focal length of the meniscus, although it is still much greater than the focal length of the primary mirror, it modifies the Gaussian behavior of the Cassegrain part. In other words, the principle, which was stated at the beginning of the Chapter 5 and widely used in all the previous designs, in this case leads to designs which can not be acceptable.

Bearing these remarks in mind, we apply the same procedure we have used in the above sections. If f_1 is the focal length of the primary mirror S, γf_1 the focal length of the secondary mirror S_s, *em* the back focal, f_t the total focal length of

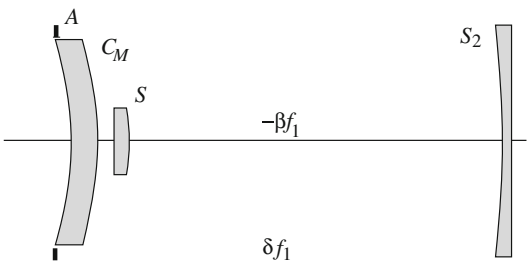

Fig. 7.19 Maksutov–Cassegrain telescope

the Cassegrain combination, δf_1 the distance between the Maksutov corrector M and S, and $-\beta f_1$ the distance between S and S_s, then the coefficient of spherical aberration of the Cassegrain combination with the aperture stop at a distance δf from the primary mirror S is (see Chapter 4 or ***Maksutov–Cassegrain***)

$$D_{S,1} = -\frac{1 + M^3 + \alpha - M^2(1+\alpha)}{32 f_1^3 M^3}. \tag{7.14}$$

where

$$\alpha = \frac{em}{f_1}, \tag{7.15}$$

$$M = \frac{f_t}{f_1}, \tag{7.16}$$

$$\beta = \frac{M - \alpha}{M + 1}, \tag{7.17}$$

$$\gamma = \frac{2M(1+\alpha)}{1 - M^2}. \tag{7.18}$$

Moreover, if R_1 and $R_1 - s$ are the radii of the two surfaces of M, then the coefficient of spherical aberration of M results (see Section 5.8 and ***Maksutov–Cassegrain***):

$$\begin{aligned} D_{M,1} = \frac{N-1}{8N^3 R_1^4 (R_1 - s)^3} & [(R_1 + (N-1)(s-\Delta))^2 (N(R_1 - \Delta) + \Delta) \\ & (R_1 + (N-1)(s + Ns - N\Delta) - R_1 N (R_1 - s)^3], \end{aligned} \tag{7.19}$$

where, in order to have an achromatic corrector, we have to take

$$s = \Delta \frac{N^2 - 1}{0.97 N^2}. \tag{7.20}$$

Finally, we choose $\Delta = 0.1D$, where D is the diameter of M.

An approximate condition to eliminate the spherical aberration, when the Cassegrain combination has been designed, is

$$D_{s,1} + D_{M,1} = 0. \tag{7.21}$$

As it is proved in ***Maksutov–Cassegrain*** and in Chapter 5, (7.21) is a seven degree algebraic equation which admits only three real roots. One of them is too small to be useful, and the remaining two roots are of opposite sign. We choose the negative root.

Owing to the remarks at the beginning of this chapter, (7.21) gives results which can not be accepted, essentially for two reasons

- the strong curvatures of the surfaces of M introduce higher order spherical aberration;
- the high but finite negative focal length of M modifies in a significant way the focal length of the Cassegrain combination.

In the next Section, we give some advices to overcome these problems.

7.7 Examples

The notebook ***Maksutov–Cassegrain*** allows us to design a Maksutov–Cassegrain telescope with a speed $f/11 - f/14$. To have acceptable results, we start with a focal length f_c of the Cassegrain combination less than the desired total focal length f_t. This strategy is due to the effect of the corrector which increases the focal length of the Cassegrain combination. By a few attempts, we can find the right initial value of f_c. Moreover, the radius of the second surface of M, which is obtained by the notebook ***Maksutov–Cassegrain*** must be slightly reduced to introduce a third-order spherical aberration, which can balance the fifth-order one. The following examples show this procedure.

We wish to design a Maksutov–Cassegrain with focal length of 2800 mm, starting with a principal mirror S with a diameter $D = 200$ mm. and speed $f/3.5$. Then, we introduce the following input data

$$\begin{aligned}
&f_1 = 700,\\
&f_t = 2400,\\
&em = 200,\\
&\delta = 520/700,\\
&D = 200,\\
&\theta = 0.25,
\end{aligned}$$

where θ is the field angle. The corresponding output is

$$\begin{aligned}
&R_1 = -300.06,\\
&R_2 = -311.74,\\
&-\beta f_1 = -497.77,\\
&R_s = -573.814,
\end{aligned}$$

Although the third-order spherical aberration of this combination is absent, the spot diagram shows that it is not acceptable. Then, step by step, we reduce the value of R_2 to -311.45 and the corresponding spot diagram is given in Figure 7.20.

Similarly, to design a Maksutov-Cassegrain telescope with a focal length $f_t = 2200$ mm and a principal mirror with a speed $f/3$, we introduce the following input data

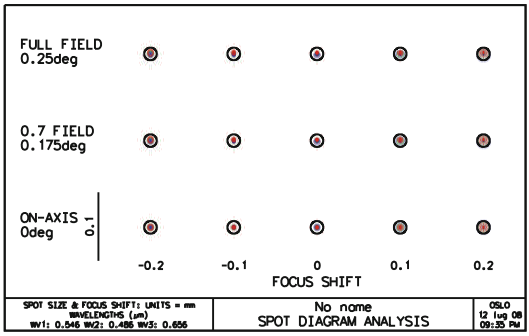

Fig. 7.20 Spot diagram for Maksutov–Cassegrain combination with a primary of speed $f/3.5$

$$
\begin{aligned}
f_1 &= 600,\\
f_t &= 1950,\\
em &= 200,\\
\delta &= 450/600,\\
D &= 200,\\
\theta &= 0.5,
\end{aligned}
$$

The corresponding output is

$$
\begin{aligned}
R_1 &= -269.5,\\
R_2 &= -281.18,\\
-\beta f_1 &= -411.76,\\
R_s &= -543.79,
\end{aligned}
$$

Again the spot diagram is not acceptable and we reduce, step by step, R_2 to the value -280.72. For this value, we obtain ae good result, as it is shown by the spot diagram in Figure 7.21.

This approach does not work for higher aperture ratios. Figure 7.22 shows the spot diagram of a Maksutov–Cassegrain telescope with a focal length 2000 mm. and a primary mirror $f/2.7$ that was designed by ***Optisoft***.

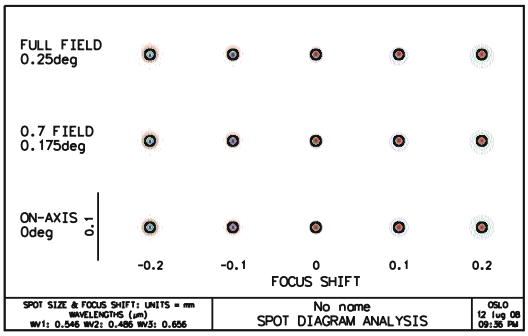

Fig. 7.21 Spot diagram for Maksutov–Cassegrain combination with a primary of speed $f/3$

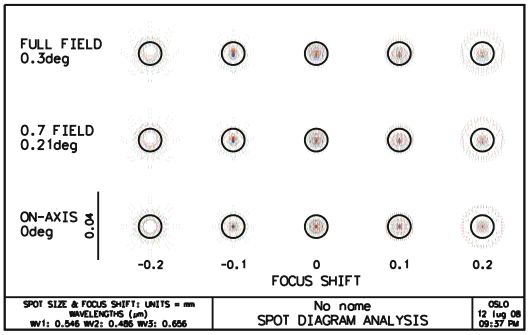

Fig. 7.22 Spot diagram for Maksutov–Cassegrain combination with a primary of speed $f/2.7$ designed using ***Optisoft***

7.8 Final Remarks

In this chapter, and in the previous one, astronomical combinations were presented that are essentially based on mirrors, and more specifically on the Cassegrain combination. The dioptric elements (Schmidt, Houghton, or Maksutov corrector) modify the Gaussian performance of the Cassegrain part as little as possible and are employed in order to balance out some of the third-order aberrations without introducing significant chromatism.

Advantages of these combinations include the following:

- They are very compact;
- For any mirror, there is only one surface to consider;
- The homogeneity and the refractive index of the glass of the mirror are not important;
- Large diameters can be realized at reasonable costs.

These advantages are counterbalanced by the following negative aspects:

- They exhibit sensitive turbulence phenomena (especially the open Cassegrain combination);
- The obstruction caused by the secondary mirror modifies the diffraction pattern, reducing the resolving power of the instrument.

Chapter 8
Doublets and Triplets

8.1 Achromatic Doublets

An achromatic doublet is an optical system S of two lenses L_1, L_2 with different refractive indices and Abbe numbers (see (3.106)), that are separated by a very thin layer of air. In the ***Fraunhofer doublet*** the first lens is positive and the second lens is negative, whereas the opposite is true in the ***Steinheil doublet***. Moreover, the positive lens has a lower refractive index than the negative lens, but its Abbe number is much greater than that of the negative lens. The Steinheil design is used when it offers a better correction than the Fraunhofer or when the positive element exhibits poor resistance to weathering.

More precisely, a doublet is said to be ***achromatic*** if the following conditions are satisfied:

1. The focal f has a given value;
2. The back focal bf_b of blue-light and the back focal of red-light bf_r are equal[1];
3. The third-order spherical aberration in green-light vanishes;
4. The third-order coma in green-light vanishes.

In order to satisfy the above conditions, we manipulate the type of glass used, the thickness of the lenses and their radii of curvature. In particular, the four radii of the lenses can be chosen to satisfy the above four conditions. However, the algebraic system A that is obtained by expressing these four conditions analytically is so complex that it is impossible to solve it, even using a powerful program like ***Mathematica***. Consequently, we instead try to determine approximate values for the roots of A. This is usually done neglecting the thickness of the lenses (i.e., by assuming that the doublet is formed by thin lenses.[2] Assuming this hypothesis, if we

[1]Here and in what follows, green-light corresponds to the line e (546.07 nm), the blue-light to the line F (486.13 nm), and red-light to C line (656.27 nm).
[2]See [34].

© Springer International Publishing Switzerland 2016

A. Romano and R. Cavaliere, *Geometric Optics*,
Modeling and Simulation in Science, Engineering and Technology,
DOI 10.1007/978-3-319-43732-3_8

denote the surfaces of the lenses L_1 and L_2 by S_i, $i = 1, \ldots, 4$ and the curvature of the surface S_i by $c_i = 1/r_i$, and we introduce the ***bendings*** of the two lenses $\xi_1 = c_1 - c_2, \xi_2 = c_3 - c_4$, then the first two conditions are expressed by the system (see the notebook ***Fraunhofer***)

$$(N_1 - 1)\xi_1 + (N_2 - 1)\xi_2 = 1/f, \tag{8.1}$$

$$(N_{1,b} - N_{1,r})\xi_1 + (N_{2,b} - N_{2,r})\xi_2 = 0. \tag{8.2}$$

In the above formulae N_i, $N_{i,b}$, and $N_{i,r}$ denote the refractive indices of the lens L_i in green-light, blue-light, and red-light, respectively. If we refer all of the lengths that appear in (8.2), (8.2) to the focal f and denote the nondimensional quantities with the same symbols, then the above system can be written in the form

$$\alpha_1 V_1 \xi_1 + \alpha_2 V_2 \xi_2 = 1, \tag{8.3}$$

$$\alpha_1 \xi_1 + \alpha_2 \xi_2 = 0. \tag{8.4}$$

where we have introduced the Abbe number

$$V_i = \frac{N_i - 1}{N_{i,b} - N_{i,r}} \tag{8.5}$$

of L_i and the notation

$$\alpha_i = N_{i,b} - N_{i,r}. \tag{8.6}$$

It is straightforward to verify that the solutions of (8.3)–(8.4) are

$$\xi_1 = c_1 - c_2 = -\frac{1}{\alpha_1(V_2 - V1)}, \tag{8.7}$$

$$\xi_2 = c_3 - c_4 = \frac{1}{\alpha_2(V_2 - V1)}. \tag{8.8}$$

provided that the Abbe numbers of the two glasses are not equal. Thus, we need to construct the two lenses from glass with different Abbe numbers in order to find possible values of the bendings ξ_1 and ξ_2 of the two lenses. Since $\alpha_i \in (0.005, 0.02)$ for real glasses, we will obtain small differences in curvatures *if the difference* $V_2 - V_1$ *is as large as possible*. We conclude by noting that, upon imposing the first two conditions that define an achromatic doublet, we can express c_1 in terms of c_2 and c_3 in terms of c_4 by (8.7), (8.8).

8.2 Elimination of Spherical Aberration and Coma

It remains for us to determine the conditions under which the third-order spherical aberration and coma vanish. The calculations are not easy even for thin lenses. However, using the notebook **TotalAberrations** and taking into account (8.7), (8.8), we derive that coma vanishes when

$$\begin{aligned} &N_2(N_1^2-1)(V_2-V_1)\alpha_1\alpha_2^2c_2+N_1(N_2^2-1)(V_1-V_2)\alpha_1^2\alpha_2c_4\\ &+N_1(1-2N_2^2+N_2^3)\alpha_1^2+N_1(N_1-1)(1+N_2-2N_2^2)\alpha_1\alpha_2\\ &+N_2(1-2N_1^2+N_1^3)\alpha_2^2=0. \end{aligned} \tag{8.9}$$

Finally, the spherical aberration vanishes when the following quadratic condition between c_2 and c_4 is satisfied

$$\begin{aligned} &(2-N_1-N_1^2)N_2(V_1-V_2)^2\alpha_1^2\alpha_2^3c_2^2\\ &-(2-N_2-N_2^2)N_1(V_1-V_2)^2\alpha_1^3\alpha_2^2c_4^2\\ &+(4-3N_1-3N_1^2+2N_1^3)N_2(V_1-V_2)\alpha_1\alpha_2^3c_2\\ &[N_1(N_2-1)(V_1-V_2)\alpha_1^2\alpha_2\times\\ &((-4-N_2+2N_2^2)\alpha_1-4(N_1-1)(1+N2)\alpha_2)]c_4\\ &N_1(-2+2N_2+2N_2^2-3N_2^3+N_2^4)\alpha_1^3\\ &-(N_1-1)N_1(4-N_2-6N_2^2+3N_2^3)\alpha_1^2\alpha_2\\ &+(N_1-1)^2N_1(-2-N_2+3N_2^2)\alpha_1\alpha_2^2\\ &-(-2+2N_1+2N_1^2-3N_1^3+N_1^4)N_2\alpha_2^3. \end{aligned} \tag{8.10}$$

It is evident that the two solutions (c_2, c_4) of the system (8.9), (8.10) are obtained from very cumbersome expressions. We therefore assign the types of glass BAK1, FK54 to the system and analyze it. For these types of glass, (8.7), (8.8), (8.9), and (8.10) become

$$c_1-c_2+3.03207=0, \tag{8.11}$$

$$c_3-c_4-6.26055=0, \tag{8.12}$$

$$1.620c_2-2.647c_4-10=0, \tag{8.13}$$

$$-3.5754c_2^2+5.933c_4^2+1.9026c_2+43.33c_4+120.5=0. \tag{8.14}$$

Equations (8.11) and (8.12) which are equivalent to (8.7) and (8.8), respectively, impose the assigned focal and the axial chromatism. The remaining two equations, equivalent to (8.9) and (8.10), ensure that the third-order spherical aberration and coma in green-light are zero. The solutions (in focal units) for the above system are

$$(c_2=-5.2068,\ c_4=-6.9730),\quad (c_2=5.888,\ c_4=-0.18336). \tag{8.15}$$

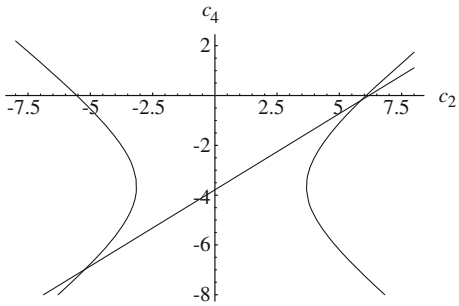

Fig. 8.1 The values of c_2, c_4 which eliminate spherical aberration and coma

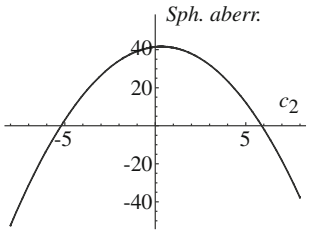

Fig. 8.2 Spherical aberration versus c_2

We can better appreciate these values by plotting the curves that are implicitly defined by the equations (8.13), (8.14) (Figure 8.1). Moreover, if we introduce the value of c_4 obtained from (8.13) into (8.14), we can derive the relationship between the spherical aberration and the curvature c_2 (see Figure 8.2).

The design based on the above values or obtained using the notebook ***Fraunhofer*** is usually not acceptable, especially if the speed of the doublet is greater than $f/11 - f/12$. This is due to the following reasons:

- The thickness of the lenses introduces significant levels of chromatic aberration, coma, spherical aberration, and spherochromatism;
- The fifth-order aberrations can be significant;
- We have no free parameter in the optical system to control the ***secondary spectrum***

$$\Delta = bf_b - bf_g, \tag{8.16}$$

where bf_g is the back focal corresponding to green light.

A doublet is said to be ***achromatic*** if $\Delta/f \simeq 1/2000$, ***semiapochromatic*** if $\Delta/f \simeq 1/6000$, and ***apochromatic*** when $\Delta/f \simeq 1/10000$. Now, it is easy to prove that (see [26], p. 311) we have

$$\frac{\Delta}{f} = \frac{P_1 - P_2}{V_1 - V_2}, \tag{8.17}$$

for a thin doublet, where

$$P_i = \frac{N_{b,i} - N_i}{N_{b,i} - N_{r,i}} \tag{8.18}$$

is the dispersion coefficient of the lens L_i. Equation (8.17) implies that the two glasses must be chosen in such a way that *the difference* $P_1 - P_2$ *is as small as possible and the difference* $V_1 - V_2$ *is as large as possible*.

Assuming that the types of glass are chosen according to this criterion, we must compensate for the aberrations introduced by the thickness of the lenses. We can do this either by resorting to an optimization method included in professional software or by carrying out a deeper analysis of the optical system (see ***Optisoft***).

8.3 Examples

In this section, we consider some examples of doublets of diameter $D = 100$ mm. that were obtained using the notebook ***Fraunhofer***. The input data for this notebook are the set $thick$ of lens thicknesses, the set ind of the refractive indices for green, red and blue light, the diameter D, the field angle θ, and the focal length f. The first of these examples, which is a Fraunhofer objective realized with standard crown-flint glass (BK7-F3), has a speed of $f/15$. The input data are

$$\begin{aligned}
&thick = \{10, 0.5, 7\},\\
&ind = \{\{1, 1.51872218, 1, 1.61685, 1\},\\
&D = 100,\\
&\theta = 0.5,\\
&f = 1500.
\end{aligned}$$

The corresponding output gives the radii of the doublet

$$\{911.428, -511.906, -519.007, -2261.69\}.$$

Figure 8.3 shows the spot diagram for this combination.

The second doublet uses BAK1-F54 glass, and its input data are

$$\begin{aligned}
&thick = \{7, 0.5, 10\},\\
&ind = \{\{1, 1.5725001, 1, 1.43700005, 1\},\\
&\{1, 1.57943481, 1, 1.44033746, 1\},\\
&\{1, 1.56948667, 1, 1.43551944, 1\}\},\\
&D = 100,\\
&\theta = 0.5,\\
&f = 1000.
\end{aligned}$$

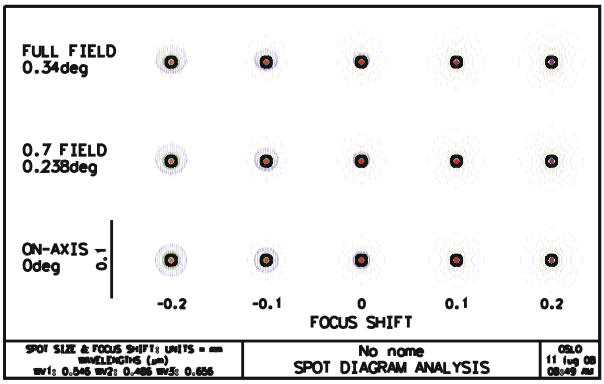

Fig. 8.3 Spot diagram for the BK7-F3 doublet

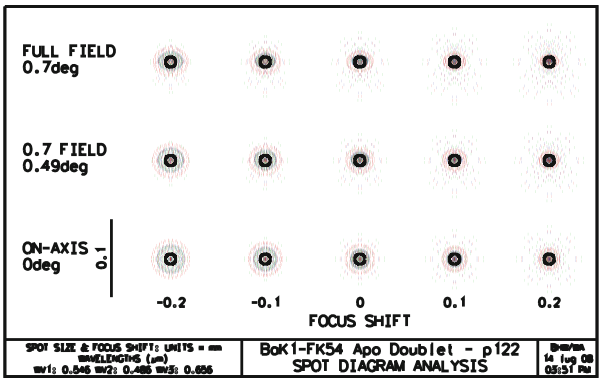

Fig. 8.4 Spot diagram for the BaK1-FK54 doublet

The corresponding output gives the following radii of the doublet

$$\{350.148, 169.837, 164.55, -5453.73\}.$$

The spot diagram shown in Figure 8.4 for this doublet shows that the third-order design is not acceptable, since the higher-order aberrations produce a spot that is larger than the Airy disk.

In the third example, we use Fk51-KZFSN2 glass, and the input data are

$$\begin{aligned}
&thick = \{0, 0, 11\},\\
&ind = \{\{1, 1.56081792, 1, 1.4879367, 1\},\\
&\{1, 1.5655173, 1, 1.49055758, 1\},\\
&\{1, 1.55520714, 1, 1.4847972, 1\}\},\\
&D = 100,\\
&\theta = 0.5,\\
&f = 1000.
\end{aligned}$$

The corresponding output yields the radii of the doublet

$$\{422.856, 179.702, 177.399, -11078.1\}.$$

Again the spot diagram of this combination (Figure 8.4) shows that the third-order design is not acceptable because the higher order aberrations produce a spot that is larger than the Airy disk (Fig. 8.5).

Figures 8.6 and 8.7 show the spot diagrams obtained for the latter two combinations when they were redesigned using the software ***Optisoft***. Both the combinations are now diffraction limited on a image surface of radius −600 mm.

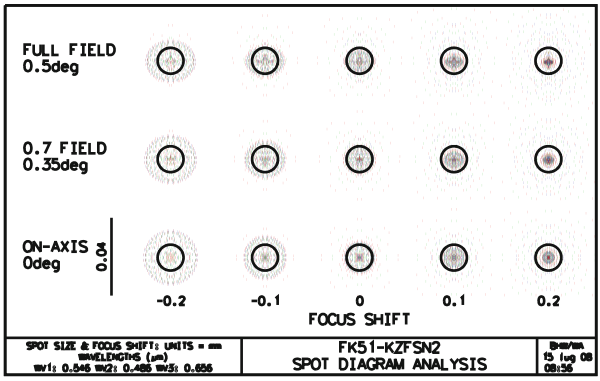

Fig. 8.5 Spot diagram for the Fk51-KZFSN2 doublet

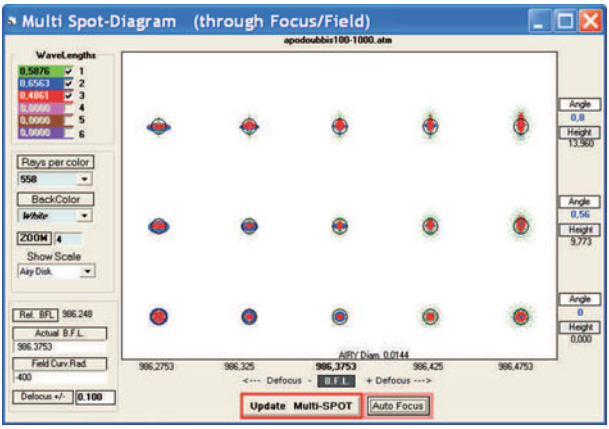

Fig. 8.6 Spot diagram for the Bak1-Fk54 doublet by ***Optisoft***

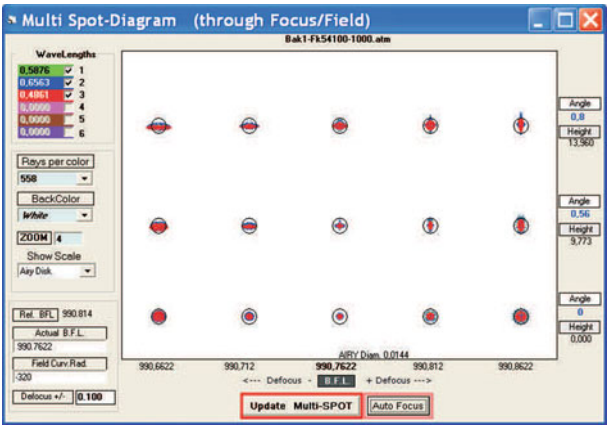

Fig. 8.7 Spot diagram for the Fk51-KZFSN2 doublet by ***Optisoft***

8.4 Triplets

A ***triplet*** is an optical system S that consists of three lenses L_1, L_2, L_3, each made from different glass. One of the main difficulties encountered when designing a triplet is appropriate glass selection. One criterion that can be applied when making this choice is the following: *in the $N_d - V_d$ diagram the area of the triangle formed from the points representing the three glasses should be as large as possible* (see [26]).

When the choice of the glass has been made, we can then consider the thickness of the lenses as well as the radii of curvature of the spherical surfaces of the three lenses. In order to evaluate the approximate values of these quantities, as usual we start with ignoring the thickness of the lenses. Moreover, we analyze a triplet S in which the final two lenses are stuck together. This implies that we only need to determine five radii of curvature R_i, $i = 1, \ldots, 5$. The final design will be acceptable if these radii are large enough to make the higher order aberrations insignificant.

In order to determine the five radii R_i, $i = 1, \ldots, 5$, we impose the following five conditions:

- The focal f of S is given;
- The focal in blue-light and green-light, f_b and f_g, respectively, are equal;
- The focal in red-light and green-light, f_r and f_g, respectively, are equal;
- Third-order coma is absent (in green-light);
- Third-order spherical aberration is absent (in green-light).

We denote the refractive indices of the three lenses L_1, L_2, L_3 of S, corresponding to green-light, blue-light, and red-light, by N_i, $N_{b,i}$, and $N_{r,i}$, $i = 1, 2, 3$, respectively. Moreover, we introduce the curvature $c_i = 1/R_i$ of L_i. It is a tedious but simple exercise to verify that the focal length f in green-light of the system S is given by the formula

$$(N_1 - 1)(c_1 - c_2) + (N_2 - 1)(c_3 - c_4) + (N_2 - 1)(c_4 - c_5)(N_3 - 1) = \frac{1}{f}. \tag{8.19}$$

Alternatively, (8.19) can be obtained using the notebook ***triplet***. Similarly, the conditions $f_b - f_g = 0$ and $f_r - f_g = 0$ can be written as it follows

$$\begin{aligned}(N_{1,b} - N_1)(c_1 - c_2) &+ (N_{2,b} - N_2)(c_3 - c_4) \\ &+ (N_{3,b} - N_3)(c_4 - c_5) = 0, \qquad (8.20)\\ (N_{1,r} - N_1)(c_1 - c_2) &+ (N_{2,r} - N_2)(c_3 - c_4) \\ &+ (N_{3,r} - N_3)(c_4 - c_5) = 0. \qquad (8.21)\end{aligned}$$

Equations (8.19)–(8.21) form a system of three equations in the three unknowns $c_1 - c_2, c_3 - c_4$, and $c_4 - c_5$. If we use f as the length unit and introduce the notations

$$\alpha_i = N_i - 1, \quad \beta_i = N_{i,b} - N_i, \quad \gamma_i = N_{r,i} - N_i, \tag{8.22}$$

$$\xi_1 = c_2 - c_3, \quad \xi_2 = c_3 - c_4, \quad \xi_3 = c_4 - c_5, \tag{8.23}$$

the above system assumes the form

$$\alpha_1\xi_1 + \alpha_2\xi_2 + \alpha_3\xi_3 = 0, \tag{8.24}$$
$$\beta_1\xi_1 + \beta_2\xi_2 + \beta_3\xi_3 = 0, \tag{8.25}$$
$$\gamma_1\xi_1 + \gamma_2\xi_2 + \gamma_3\xi_3 = 0, \tag{8.26}$$

whose solutions are (see ***Triplet***)

$$\xi_i = \frac{(\boldsymbol{\beta} \times \boldsymbol{\gamma})_i}{\boldsymbol{\alpha} \cdot \boldsymbol{\beta} \times \boldsymbol{\gamma}}, \tag{8.27}$$

where $\boldsymbol{\alpha} = (\alpha_i), \boldsymbol{\beta} = (\beta_i), \boldsymbol{\gamma} = (\gamma_i)$. Starting from these values of ξ_1, ξ_2, and ξ_3, we can express c_1, c_3, and c_5 as functions of c_2 and c_4. Substituting these relations into the condition that expresses the elimination of third-order coma, we again obtain a *linear* expression containing c_2 and c_4. Finally, the condition for eliminating the third-order spherical aberration becomes a quadratic relation in c_2. The most convenient solution corresponds to the one with the lowest curvatures c_i. All the above calculations can be carried out by ***Triplet***.

8.5 Examples

In this section, we propose two examples of triplets of diameter $D = 100$ mm and speed $f/10$. The first is constructed from the glasses Bk7-KZFS1-BaF4 and the second from Bk7-KZFS1-BaFN10. Using the notebook ***Triplet*** we obtain, the following radii for the five surfaces of the lenses in each example triplet:

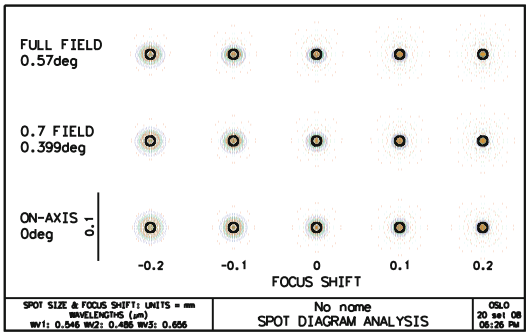

Fig. 8.8 Spot diagram for the Bk7-KZFS1-BaF4 triplet

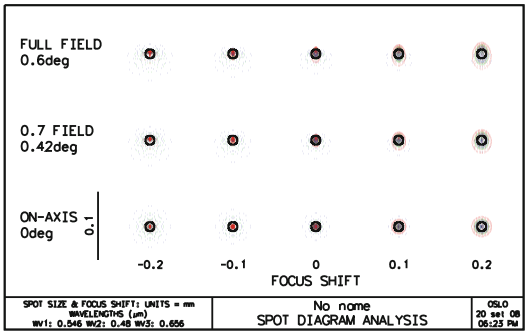

Fig. 8.9 Spot diagram for the Bk7-KZFS1-BaFN10 triplet

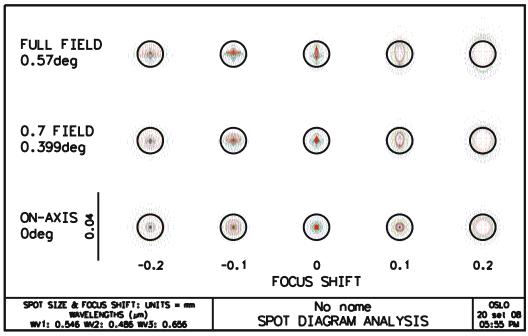

Fig. 8.10 Spot diagram for Bk7-KZFS1-BaF4 triplet obtained using ***Optisoft***

$$R_1 = 589.001, \quad R_2 = -210, \quad R_3 = -217.9,$$
$$R_4 = 211, \quad R_5 = -1185.6.$$

$$R_1 = 3951, \quad R_2 = -228.25, \quad R_3 = -220.3,$$
$$R_4 = 202.211, \quad R_5 = -605.55.$$

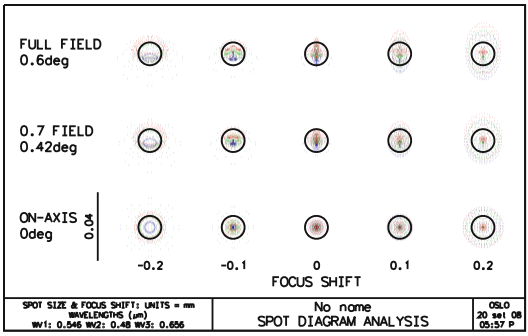

Fig. 8.11 Spot diagram for Bk7-KZFS1-BaFN10 triplet obtained using ***Optisoft***

Figures 8.8 and 8.9 show the spot diagrams of these triplets. It is evident that they are not acceptable considering their higher order aberrations. Figures 8.10 and 8.11 show the spot diagrams of the same triplets designed by ***Optisoft***.

Chapter 9
Other Optical Combinations

9.1 Schmidt–Cassegrain Telescope with Spherical Surfaces

In this section, we show that it is possible to realize an aplanatic Schmidt–Cassegrain telescope using only spherical mirrors. First, we suppose that all the parameters for the Cassegrain combination are derived as shown in Chapter 5. That is, starting from the absolute value of the focal length f_1 of the primary mirror S_1, the required total focal length f_t of the whole combination, and the fixed distance em between S_1 and the focal plane (see Figure 9.1), we determine the focal length $f_2 = \gamma f_1$ of S_2 as well as the distance $-\beta f_1$ between the two mirrors using the relations

$$\alpha = \frac{em}{f_1}, \quad M = \frac{f_t}{f_1}, \tag{9.1}$$

$$\beta = \frac{M - \alpha}{M + 1}, \quad \gamma = \frac{2M(1 + \alpha)}{1 - M^2}. \tag{9.2}$$

Now, we suppose that the aperture stop A with the Schmidt corrector is located at a distance $-\delta f_1$ in front of S_1 instead of being placed at S_1 (see Figure 9.1). The formulae for the spherical aberration and coma coefficients for this configuration can then be derived from the formulae we demonstrated in Chapter 7, provided that we put the conic constants of S_1 and S_2 equal to zero. Alternatively, we can resort to the notebook ***TotalAberrations***. In any case, we obtain the relations

$$D_1 = -\frac{1 + M^3 + \alpha - M^2(1 + \alpha)}{32 f 1^3 M^3}, \tag{9.3}$$

$$D_2 = \frac{M + \alpha - M^3(\delta - 1) - \delta - \alpha\delta + M^2(\alpha(\delta - 1) + \delta)}{8 f 1^2 M^3}. \tag{9.4}$$

© Springer International Publishing Switzerland 2016

A. Romano and R. Cavaliere, *Geometric Optics*,
Modeling and Simulation in Science, Engineering and Technology,
DOI 10.1007/978-3-319-43732-3_9

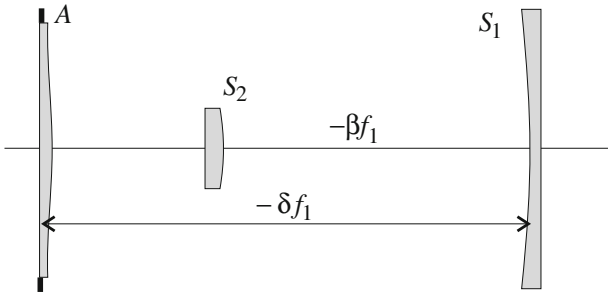

Fig. 9.1 Cassegrain combination with corrector

Fig. 9.2 Plot of δ versus M

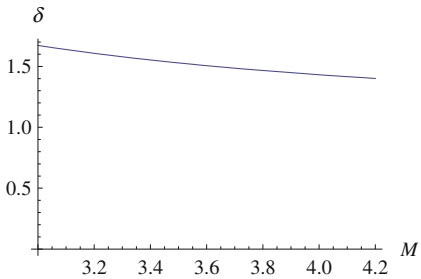

Since the spherical aberration coefficient of the corrector C is $a_4(N-1)$, where a_4 is the aspheric coefficient of the second surface of C and N is the refractive index of C, the third-order spherical aberration is eliminated if we choose

$$a_4 = -\frac{D_1}{N-1}. \tag{9.5}$$

In order to eliminate the third-order coma, in view of (9.4), we can verify whether the root δ of the equation

$$M + \alpha - M^3(\delta - 1) - \delta - \alpha\delta + M^2(\alpha(\delta - 1) + \delta) = 0,$$

in other words, the value

$$\delta = \frac{M + M^3 + \alpha - M^2\alpha}{1 - M^2 + M^3 + \alpha - M^2\alpha} \tag{9.6}$$

is acceptable or not. A plot of (9.6) for the typical value $\alpha = 0.33$ is shown in Figure 9.2.

For instance, for a mirror S_1 with a focal length $f_1 = 600$ mm, diameter 200 mm, $\alpha = 0.33$ and $M = 4$, the third-order coma vanishes when $\delta = 1.4313$. Consequently, we must place the corrector at a distance of 858.78 mm from S_1.

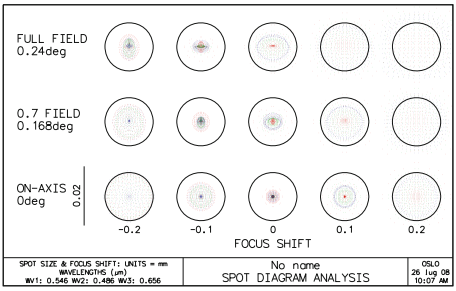

Fig. 9.3 Spot diagram of a Schmidt–Cassegrain combination with primary $f/3$ and spherical mirrors

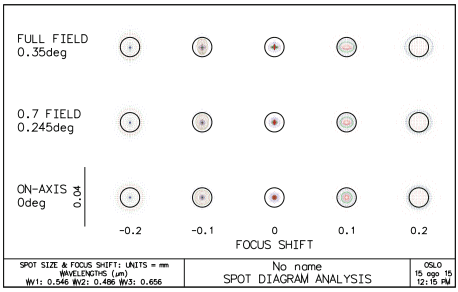

Fig. 9.4 Spot diagram of a Schmidt–Cassegrain with primary $f/2$ and spherical mirrors

Figure 9.3 shows the corresponding spot diagram for this combination on an image surface of radius -600 mm, and we can see that it is diffraction-limited for a view angle of $0.24°$. If we realize this optical combination with a primary mirror with the high speed of $f/2$, we note the presence of unacceptable higher-order aberrations. However, we can obtain an excellent design by using ***Optisoft*** to balance third-order and higher-order aberrations (see Figure 9.4). In this way, we obtain a cheap combination since both the mirrors are spherical. The only disadvantage of this combination over the usual Schmidt–Cassegrain combination is represented by the tube that is longer than the corresponding tube of a Schmidt–Cassegrain of 40 %. Other examples can be found in the notebook ***Schmidt–CassegrainCBeforeSM***.

9.2 The Flat-field Baker–Schmidt Camera

In this section we analyze some ***flat-field Baker-Schmidt cameras***, as devised by Baker, Linfoot, and others (see [35–41]), which are free from spherical aberration, coma, astigmatism, and, in some cases, from field curvature. More precisely, we analyze cameras in which the primary mirror S_1 is spherical and the secondary mirror S_2 is conic.

Using the notation adopted in the above section (see Figure 9.1), we suppose that

- The obstruction coefficient α due to the mirror S_2 is equal to 0.4 and so $\beta = 1 - \alpha = 0.6$. This obstruction is acceptable for photographic purposes.
- The back focal $bf > 0$, so that the focal surface π is located after the primary S_1.

This camera presents the following advantages over a Schmidt camera with the same speed:

- Its focal surface π is planar and external to the tube containing the whole combination.
- It is shorter than the corresponding Schmidt camera.

We begin our analysis by considering the two mirrors along with the aperture stop at a distance $-\delta f_1$ from S_1. Using the notebook ***Baker–SchmidtCameraSM***, we then find that the total focal length f_t and the back focal bf are given by the following formulae when $\beta = 0.6$:

$$f_t = \frac{\gamma}{\gamma - 0.8} f_1, \tag{9.7}$$

$$bf = \frac{0.48 - 0.2\gamma}{\gamma - 0.8} f_1. \tag{9.8}$$

In what follows, we choose a value of γ that lies in the range

$$1 < \gamma < 2.4 \tag{9.9}$$

so that $bf > 0$.

With the help of the notebook ***Baker–SchmidtCameraSM***, we then find that, for $\beta = 0.6$, the coefficient of curvature vanishes when the distance $-\delta f_1$ of the aperture stop from S_1 complies the condition

$$-\delta f_1 = \frac{1.2 + \gamma}{\gamma - 0.8} f_1. \tag{9.10}$$

At this point, the geometry of the whole combination is determined by choosing a value of γ that satisfies condition (9.9). Moreover, the astigmatism coefficient D_3 vanishes for the corresponding value of δ given by (9.10), whereas the coefficients D_1 and D_2 (for spherical aberration and coma, respectively) are given by the formulae

$$\begin{aligned} D_1 = \frac{1}{32 f_1^3 \gamma^3} \big(& 8 + 8K_2(-1+\beta)^4 + 8\beta^4 + 16\beta^3(-2+\gamma) \\ & - 16\gamma + 8\gamma^2 - \gamma^3 + 8\beta^2(6 - 6\gamma + \gamma^2) \\ & - 16\beta(2 - 3\gamma + \gamma^2)\big), \end{aligned} \tag{9.11}$$

$$\begin{aligned} D_2 = \frac{1}{8 f_1^2 \gamma^2 (-2 + 2\beta + \gamma)} \big(& -8 - 8K_2(-1+\beta)^3 + 8\beta^3 + \\ & 8\beta^2(-3+\gamma) + 8\gamma - 4\gamma^2 + \gamma^3 + 2\beta(12 - 8\gamma + \gamma^2)\big). \end{aligned} \tag{9.12}$$

Ignoring the coma introduced by the corrector C and recalling that the coefficient of spherical aberration for C is given by $a_4(N-1)$, where a_4 is the aspheric constant of C and N its refractive index in green-light, the third-order spherical aberration and coma are eliminated for a_4 and K_2 verifying the system

$$D_1 + a_4(N-1) = 0, \tag{9.13}$$

$$D_2 = 0, \tag{9.14}$$

where D_1 and D_2 are given by (9.11) and (9.12). Solving the above system, we obtain

$$\begin{aligned} a_4 = -\frac{1}{32 f_1^3 (N-1)\gamma^3} \big[& 16\beta^4 - 2(-2+\gamma)^3 + \\ & 8\beta^3(-8+3\gamma) + 2\beta^2(48 - 36\gamma + 5\gamma^2) + \\ & \beta(-64 + 72\gamma - 22\gamma^2 + \gamma^3)\big], \end{aligned} \tag{9.15}$$

$$\begin{aligned} K_2 = \frac{1}{8(-1+\beta)^3} \big[& -8 + 8\beta^3 + 8\beta^2(-3+\gamma) + 8\gamma - \\ & 4\gamma^2 + \gamma^3 + 2\beta(12 - 8\gamma + \gamma^2)\big]. \end{aligned} \tag{9.16}$$

Note that all the characteristics of the combination are functions of γ.

However, we cannot accept the design realized on the basis of the above formulae for the following reasons:

- The corrector introduces significant chromatism
- Combining the corrector and the mirrors leads to field curvature and significant astigmatism
- When the speed of the primary is high, higher order aberrations degrade the final image.

We can overcome the first problem by assigning a suitable radius of curvature to the second surface of the corrector, as done in the program ***Baker–SchmidtCameraSM***, whereas the other problems require a deeper analysis.

Figure 9.5 shows the spot diagram obtained using the above formulae. The principal mirror has a diameter $D = 200$ mm and a speed $f/2$. The camera has a total focal of 628 mm. Figure 9.6 shows the spot diagram of the same camera designed by ***Optisoft***.

It is possible to realize a flat-field camera in which both the mirrors are spherical (see [41]). The major disadvantage of this combination, beside the presence of a very

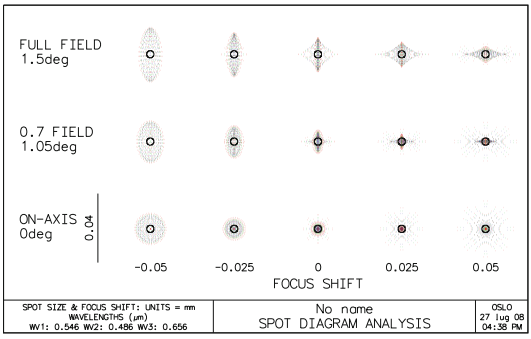

Fig. 9.5 Baker-Schmidt camera $f/2$

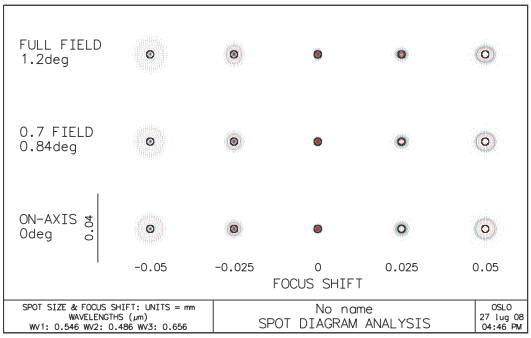

Fig. 9.6 Baker–Schmidt camera $f/2$, by ***Optisoft***

small astigmatism, is the large obstruction factor (about 55 %). This combination is essentially based on the condition that the radii of curvature of the mirrors are equal. A full analysis of this configuration is carried out in the notebook ***Baker–SchmidtCameraCP***, together with some examples that exhibit different obstruction factors.

9.3 Cassegrain Telescope with the Corrector at the Prime Focus

In some of the preceding chapters, we analyzed optical devices in which the aberrations of a Cassegrain combination S were compensated for by introducing a suitable corrector C *before* S. When C is placed in this position, it is said to be a ***full aperture corrector***. It is evident that inserting C *close* to S or between secondary and primary mirror should reduce the size of C. In the rest of this chapter, we analyze two examples in which the corrector is located at or close to the primary mirror of a Cassegrain combination.

In Figure 9.7, a Schmidt corrector C is positioned at the primary mirror.

This combination works only when both mirrors are *conic*. In fact, when one mirror is or both mirrors are spherical, the coma and astigmatism are relevant and the aspheric constant a_4 of C is too high. The aberration formulae for this combination are very complex but *they are linear in the unknowns* a_4, K_1, and K_2, where K_1 and K_2 are the conic constants of S_1 and S_2, respectively. Since the corrector C does not modify the Gaussian behavior of the two mirrors, we analyze this combination starting from a given Cassegrain scheme. The notebook ***Schmidt–CassegrainCAfter*** allows us to determine both the Cassegrain data and the unknowns a_4, K_1, and K_2 starting from the same input data of a Cassegrain combination.

We assume a principal mirror S_1 with a diameter $D = 200$ mm and an aperture ratio $f/2$. If the requested total focal length is 2000 mm and the back focal $em = 200$ mm, then the data of the Cassegrain combination are (see ***Schmidt–CassegrainCAfter***)

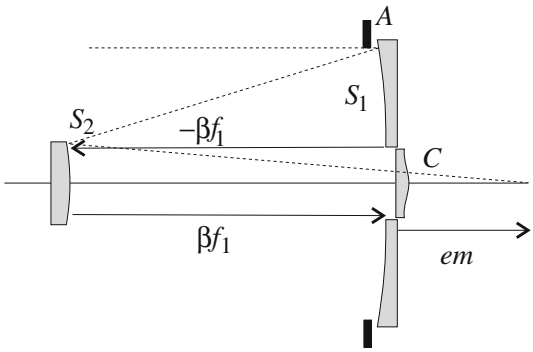

Fig. 9.7 New Schmidt–Cassegrain telescope

$$\text{curvature radius of } S_1 = -800,$$
$$\text{curvature radius of } S_2 = -250,$$
$$\text{distance between } S_1, S_2 = -300.$$

Now, we consider the combination S which is obtained placing the corrector C at a distance 300 mm from S_2. In order to determine the unknowns a_4, K_1, K_2, and the radius R_c of the second surface of C, which makes the corrector achromatic, we must equate the coefficients of spherical aberration D_1, coma D_2, astigmatism D_3, as well as the difference Δ between the back distances, corresponding to blue light and red light, to zero. To this end, we use the notebook ***TotalAberrations*** (in ***Schmidt–CassegrainCAfter***) to verify that the condition $\Delta = 0$ is expressed by the equation

$$311.63R_c + 0.0174R_c^2 = 0, \tag{9.17}$$

which has significant solution of

$$R_c = -17840.6. \tag{9.18}$$

Moreover, equating the corresponding expressions of D_1, D_2 and D_3 to zero, we obtain the linear system

$$D_1 = -3.47 + 485401a_4 - 4.88K_1 + 0.625K_2 = 0, \tag{9.19}$$
$$D_2 = 7.369 + 2.62791 * 10^7 a_4 + 3K_2 = 0, \tag{9.20}$$
$$D_3 = -0.000095 + 119555a_4 + 0.00121K_2 = 0 \tag{9.21}$$

which has the solution

$$a_4 = 2.81537 * 10^{-8}, \quad K_1 = -1.05524, \quad K_2 = -2.70306. \tag{9.22}$$

Figure 9.8 shows the spot diagram of this combination on a focal surface with a radius of −200 mm on which the combination is diffraction limited.

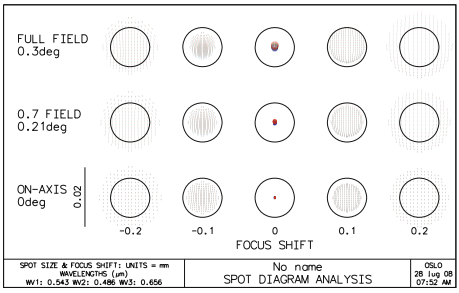

Fig. 9.8 Spot diagram of Schmidt–Cassegrain telescope with the corrector positioned at the primary mirror

9.4 The Klevtsov Telescope

In this section and the next two, we analyze another interesting combination, where the corrector C is placed *close* to the secondary mirror of a Cassegrain combination, which was devised by ***Klevtsov***. The optical scheme for this combination is shown in Figure 9.9.

All of the surfaces are spherical. The secondary mirror S_2 is a Mangin mirror (i.e., the second surface of S_2 is reflecting). The light crosses the meniscus and the secondary mirror S_2 (which we assume is constructed from BK7) twice. The disadvantages of this combination are as follows

- The tube is open;
- It requires a very accurate collimation;

The analysis we develop over the next few sections shows how useful ***Mathematica*** can be for solving the problems we encounter. The formulae of the third-order aberrations of this combination are very complex, in terms of both the large number of surfaces involved and the finite thicknesses of its optical elements. As a consequence, we cannot hope to develop a theoretical analysis of this scheme starting from general formulae. Therefore, we develop the design of a Klevtsov telescope assigning the following parameters:

- The total focal length f_t;
- The primary speed A;
- The primary focal length f_1.

Fig. 9.9 Klevtsov telescope

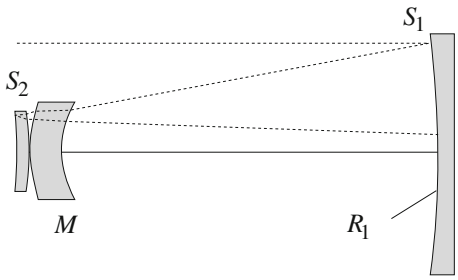

This leaves us with numerical equations where the radii of curvature of the surfaces involved are the unknowns.

To illustrate this approach, suppose that $f_t = 2200$ mm, $A = f/3$, and $f_1 = 600$ mm. Since we intend to use a Newton method to solve our equations, we need approximate values for our unknowns. To this end, we develop our design using a procedure based on a number of steps. Each of these steps yields approximate values for the unknowns that are closer to the final values. The process is encapsulated in the notebook ***Klevtsov Telescope***, which simplifies the design of this combination. However, the final result obtained using this process could require improvement to be accepted.

9.5 A First Analysis of the Meniscus

In the first step of our process, we use the notebook ***Cassegrain*** to evaluate the Cassegrain combination on which the Klevtsov telescope is based. If we introduce the input data (see ***Cassegrain***)

$$f_1 = 600, \quad f_t = 2200, \quad em = 240, \quad D = 200, \quad \theta = 0.26$$

for the primary focal length, the total focal length, back focal, diameter of primary mirror, and field angle, respectively, then we obtain the following output

$$R_2 = -495, \quad \Delta = -420,$$

for the radius R_2 of the secondary mirror S_2 and the distance Δ between S_1 and S_2. It is important to note that the meniscus reduces the back distance of the Cassegrain scheme. Therefore, we have fixed a back focal greater than the usual value of 200 mm for the dimensions we have chosen.[1]

These data represent our starting data for designing the Klevtsov telescope. In the second step of the process, we analyze whether it is possible to eliminate the third-order spherical aberration and coma of the Cassegrain combination by choosing the curvatures c_3 and c_4 of the meniscus M appropriately. To this end, we consider a Klevtsov combination in which

- The primary has the radius $R_1 = 600$
- The Mangin mirror has *both* radii equal to -495 and a thickness of 3 mm.,
- The meniscus M has a thickness $\Delta_M = 30$ mm.

We use the notebook ***TotalAberrations*** to determine the very complex expressions for the third-order spherical aberration and coma of the above optical scheme. We do not try to write it out; instead, we use the built-in function ***ContourPlot*** of ***Mathematica*** to have Figure 9.10, showing the values of c_3 and c_4, for which the spherical aberration and coma vanish.

[1] The notebook ***Klevtsov*** uses a back focal *em* increased of the thickness of the meniscus.

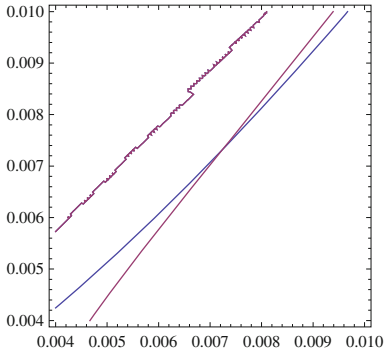

Fig. 9.10 The curves for which the spherical aberration and coma vanish

This figure allows us to determine an approximate value of c_3 and c_4 to use as starting values in the built-in function ***FindRoot*** of ***Mathematica*** (see notebook ***Klevtsov Telescope***). In this way, we obtain

$$c_3 = 0.00723701, \quad c4 = 0.00732246.$$

In the notebook ***Klevtsov Telescope*** it is proved that the spherical aberration and coma are absent but the other data are not acceptable. In particular, we have a total focal length of 1830 mm. In the next section, we show how to solve this problem.

9.6 Analysis of Mangin Mirror

The third step of our design involves varying the first curvature c_2 of the ***Mangin mirror*** as well as the curvatures of the meniscus in such a way that the third-order spherical aberration and are eliminated coma and to have a total focal of 2200 mm. The above values of c_3, c_4, and $c_2 = -1/495$ are taken as starting value in ***FindRoot***. In this way, we obtain

$$c_2 = -0.00163342, \quad c_3 = 0.00681001, \quad c_4 = 0.00683396.$$

Analysis of the corresponding combination using the notebook ***TotalAberrations*** shows that the third-order spherical aberration and coma are absent and that the total focal length is 2200 mm. Further, there is a consistent chromatism. In the fourth step, we introduce as a new unknown the curvature c_1 of the primary mirror. Then, starting from the values of c_2, c_3, c_4 that we have found, we again apply the built-in function ***FindRoot*** to the system obtained by eliminating the spherical aberration, coma, axial chromatism, for the given total focal length. This yields the final design, and the whose spot diagram for it is shown in Figure 9.11. We can see that the design must be optimized still further. Figure 9.12 shows the spot diagram for the same combination designed by ***Optisoft***.

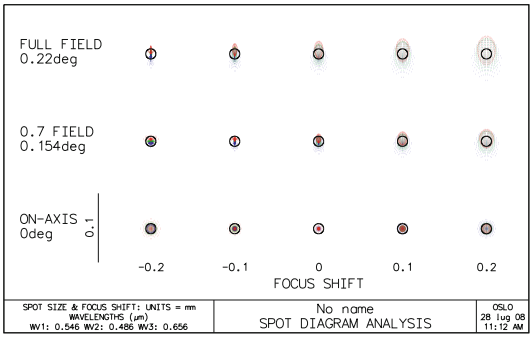

Fig. 9.11 Spot diagram of the Klevtsov telescope designed by the notebook ***Klevtsov***

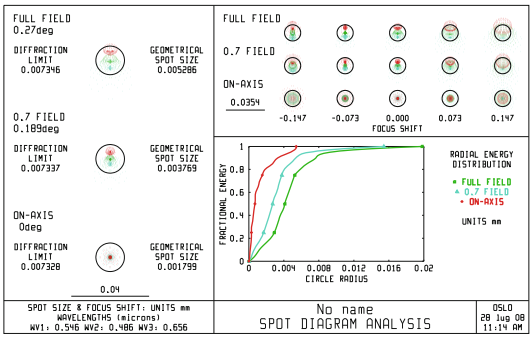

Fig. 9.12 Spot diagram of the Klevtsov telescope designed by ***Optisoft***

In any case, this combination is limited by its strong astigmatism and field curvature. However, by placing an achromatic doublet close to the end of the optical path, it is possible to have a very good performance.

9.7 Buchroeder's Camera

The ***Buchroeder camera*** employs a corrector C consisting of three thin lenses made of the same glass (for instance BK7), which is placed at the center of curvature of the primary mirror S. The radii of curvature of the six surfaces of the three lenses satisfy the condition (Fig. 9.13)

$$R_2 = \infty, \quad R_3 = -R_1, \quad R_4 = R_1, \quad R_5 = \infty, \quad R_6 = -R_1. \tag{9.23}$$

In other words, triplet C has a plane of symmetry (see Figure 9.14) and we assume that the aperture stop A lies in this plane.

It is evident that, just like the Houghton corrector (see Chapter 7), also the Buchroeder corrector is afocal, *for any refractive index value*. Therefore, it does not disturb the Gaussian behavior of the mirror S. The system $C - S$ has only one degree of freedom, i.e., the radius R_1. We can determine the value of R_1 by

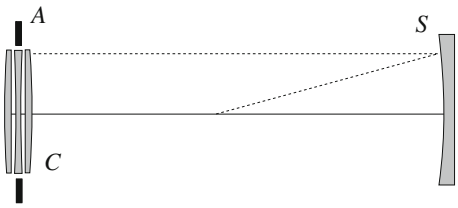

Fig. 9.13 Buchroeder camera

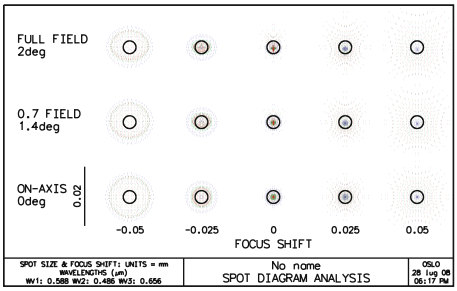

Fig. 9.14 $f/3$ Buchroeder camera

requiring that the spherical aberration vanishes. Using the notebook ***Buchroeder-Camera***, we find that the corrector has no coma and astigmatism, whereas its coefficient of spherical aberration is given by

$$D_1 = \frac{c_1^3(N-1)^2(N+1)}{2N}, \tag{9.24}$$

where $c_1 = 1/R_1$ is the curvature of the surface of the first lens of C, and N is its refractive index.

On the other hand, the mirror S (which has the aperture stop at its center of curvature), has no coma and astigmatism. Since its coefficient of spherical aberration is $-1/(32f^3)$, the absence of spherical aberration requires that

$$\frac{c_1^3(N-1)^2(N+1)}{2N} - 1/(32f^3) = 0, \tag{9.25}$$

The only real solution of the above equation is

$$c_1 = \frac{1}{2}\frac{N^{1/3}}{2^{1/3}f(N-1)^{2/3}(N+1)^{1/3}}. \tag{9.26}$$

A camera based on this value of c_1 should be free of aberrations except for the field curvature, provided that we can neglect the thickness of the lenses of C. The notebook ***Buchroeder Camera*** allows us to design this kind of camera modifying the value (9.26) in order to balance out the effect of the finite thickness of the lenses.

Figure 9.14 shows the spot diagram for a camera with an $f/3$ mirror whereas Figure 9.15 shows a corresponding diagram for a camera with an $f/2$ mirror. Finally,

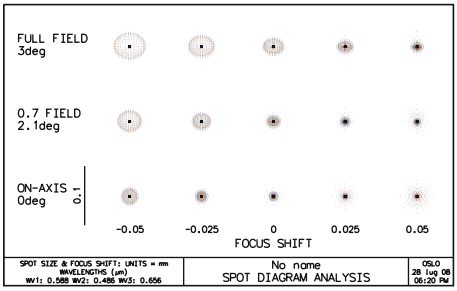

Fig. 9.15 $f/2$ Buchroeder camera

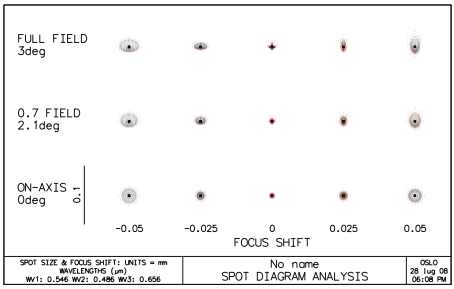

Fig. 9.16 $f/2$ Buchroeder camera designed by ***Optisoft***

Figure 9.16 shows the spot diagram for a camera with an $f/2$ mirror but designed using ***Optisoft***.

9.8 The Baker–Nunn Camera

In this section, we describe a highly sophisticated camera that was designed by Baker and Nunn for the purpose of tracking earth satellites. This important task required a very speed camera and a wide field of view in order to record faint and fast satellites. The original specification of optics was to concentrate the 80 % of light within a 20 μ diameter blur circle over the $5° \times 12°$ field of the film.

Baker and Nunn succeeded in designing a camera with speed $f/1$ that realized the above specifications. Essentially it is a Buchroeder camera in which the corrector is still a symmetric system of three lenses made with the glasses KZFSN2 and SK14. In all over the world only 12 specimens of this camera with a diameter of 50 cm exist since its realization is very expensive. The single spots of the spot diagram of this camera have a diameter of 10 μ for a view field of 8–10°. In conclusion, this camera is very fast and gives perfect images over a very high field.

However, this excellent performance is obtained with a very complex optical system sketched in Figure 9.17. S_1 is a spherical mirror and the corrector is formed by three lenses H placed at the center of curvature of S_1. These lenses are made with expensive glasses (KZFSN2 and SK14) and four of their six surfaces have sixth-order

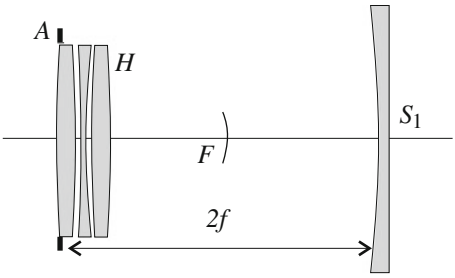

Fig. 9.17 Baker–Nunn camera $f/1$

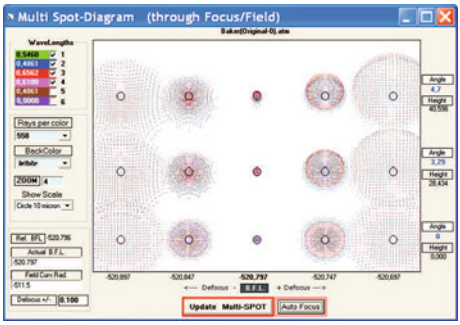

Fig. 9.18 Baker–Nunn camera $f/1$ and diameter 500 mm

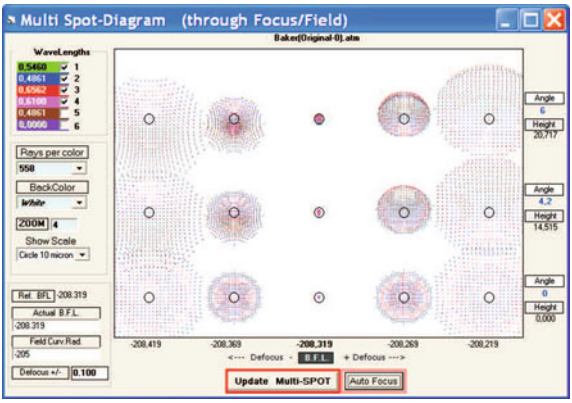

Fig. 9.19 Baker–Nunn camera $f/1$ and diameter 200 mm.

aspheric profiles. The design of this camera is a very difficult task that can only be realized by optimization methods.

Figure 9.18 shows the spot diagram of this camera for a total view field of 9° on a spherical surface of −512 mm. The single spots have a diameter of 10 μ on the whole view field.

Figure 9.19 shows the spot diagram of a Baker–Nunn camera $f/1$ with a diameter 200 mm. The total view angle is 12° and the image is formed on a spherical surface of radius −205 mm. The spots have a diameter of 10 μ (Fig. 9.20).

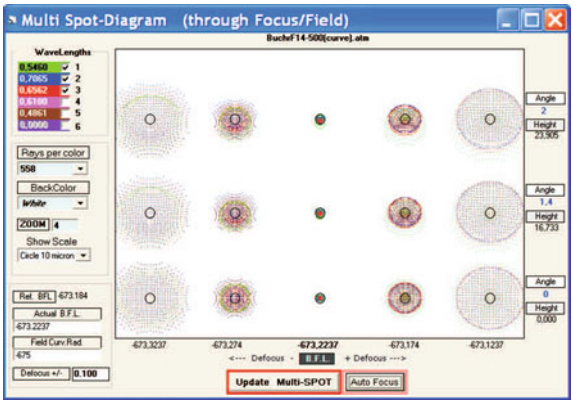

Fig. 9.20 Spot diagram of Buchroeder camera $f/1.4$ and diameter 500 mm

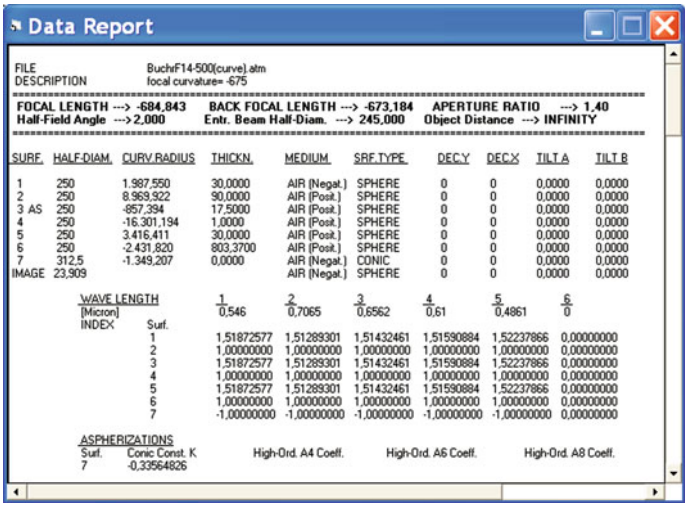

Data Report

FILE BuchrF14-500(curve).atm
DESCRIPTION focal curvature= -675

FOCAL LENGTH ---> -684,843 BACK FOCAL LENGTH ---> -673,184 APERTURE RATIO ---> 1,40
Half-Field Angle ---> 2,000 Entr. Beam Half-Diam. ---> 245,000 Object Distance ---> INFINITY

SURF.	HALF-DIAM.	CURV.RADIUS	THICKN.	MEDIUM	SRF.TYPE	DEC.Y	DEC.X	TILT A	TILT B
1	250	1.987,550	30,0000	AIR (Negat.)	SPHERE	0	0	0,0000	0,0000
2	250	8.969,922	90,0000	AIR (Posit.)	SPHERE	0	0	0,0000	0,0000
3 AS	250	-857,394	17,5000	AIR (Posit.)	SPHERE	0	0	0,0000	0,0000
4	250	-16.301,194	1,0000	AIR (Posit.)	SPHERE	0	0	0,0000	0,0000
5	250	3.416,411	30,0000	AIR (Posit.)	SPHERE	0	0	0,0000	0,0000
6	250	-2.431,820	803,3700	AIR (Posit.)	SPHERE	0	0	0,0000	0,0000
7	312,5	-1.349,207	0,0000	AIR (Negat.)	CONIC	0	0	0,0000	0,0000
IMAGE	23,909			AIR (Negat.)	SPHERE	0	0	0,0000	0,0000

WAVE LENGTH [Micron]	1	2	3	4	5	6
	0,546	0,7065	0,6562	0,61	0,4861	0
INDEX Surf.						
1	1,51872577	1,51289301	1,51432461	1,51590884	1,52237866	0,00000000
2	1,00000000	1,00000000	1,00000000	1,00000000	1,00000000	0,00000000
3	1,51872577	1,51289301	1,51432461	1,51590884	1,52237866	0,00000000
4	1,00000000	1,00000000	1,00000000	1,00000000	1,00000000	0,00000000
5	1,51872577	1,51289301	1,51432461	1,51590884	1,52237866	0,00000000
6	1,00000000	1,00000000	1,00000000	1,00000000	1,00000000	0,00000000
7	-1,00000000	-1,00000000	-1,00000000	-1,00000000	-1,00000000	0,00000000

ASPHERIZATIONS

Surf.	Conic Const. K	High-Ord. A4 Coeff.	High-Ord. A6 Coeff.	High-Ord. A8 Coeff.
7	-0,33564826			

Fig. 9.21 Data of Buchroeder camera $f/1.4$ and diameter 500 mm

It is interesting to note that reducing the speed of the camera, the total view field, and making the corrector with the common glass BK7 and spherical lenses, it is still possible to realize a good camera provided that the principal mirror is conic. For instance, Figure 9.21 shows the spot diagram of a camera whose corrector is made with spherical lenses, has a diameter of 500 mm. and the principal mirror is conic. The total field of view is 4°, the speed is $f/1.4$ and the image has a diameter of 50 mm over a spherical image with a radius of -670 mm. The data of this camera are listed in Figure 9.21. To obtain this camera we first used ***Optisof*** to design a Buchroeder camera with a diameter of 500 mm and focal length 670 mm. We then optimized this camera by ***Atmos***. Note that the final improvement has been obtained by a conic principal mirror and an asymmetric corrector.

9.9 Houghton–Cassegrain Telescope with Sub-Aperture Corrector

In this section, we design a Houghton combination in which the full-aperture corrector of the original Houghton combination is replaced by a sub-aperture corrector which is still made with two lenses of glass BK7 (see Figure 9.22). The performance of this combination is excellent provided that the primary mirror is conic (elliptic) rather than spherical. The advantage of this combination is evident: since the sub-corrector is mounted close to the primary it has a diameter that is a small fraction of the diameter of primary mirror. Further, the combination exhibits a very good chromatic correction and the image is formed over a surface that has a radius of curvature 2–3 times greater than the radius of curvature of the image sphere of Houghton's combination. Finally, all of these results can also be obtained with a primary mirror with a speed $f/2$.

Suppose that we want to design a Houghton telescope with a sub-aperture corrector starting from a primary mirror S_1 with a diameter of D cm. and speed $A = D/f_1$, where f_1 is the focal length of S_1. The design of this combination starts with the design of a Dall–Kirkham telescope (see Section 5.3) which is a Cassegrain telescope with conic primary mirror and spherical secondary mirror. Denote, respectively, by f_t the focal length and e_{em} the back distance for Hougthon's telescope with sub-aperture corrector. We start evaluating the data of a Dall–Kirkham combination with a focal length $f_{DK} = fact\ f_t$ and a back distance $e_{DK} = \sigma e_{em}$, where $fact = 0.8$ and σ assumes values in the interval [0.4, 0.5]. This choice allus the reduction of the obstruction factor of Dall–Kirkham combination. The geometric characteristics of the Dall–Kirkham telescope are obtained by the formulae of Section 5.3:

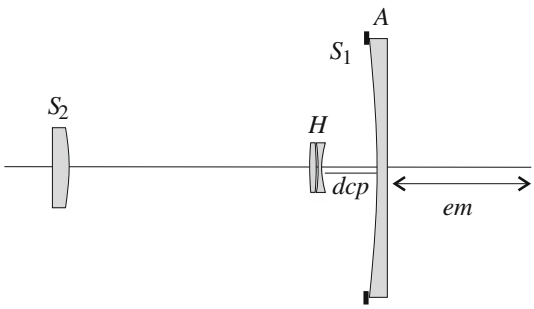

Fig. 9.22 Houghton–Cassegrain with sub-corrector

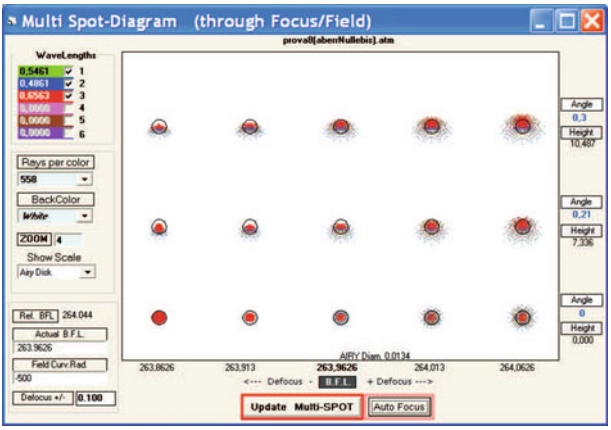

Fig. 9.23 First design of Houghton–Cassegrain with sub-corrector

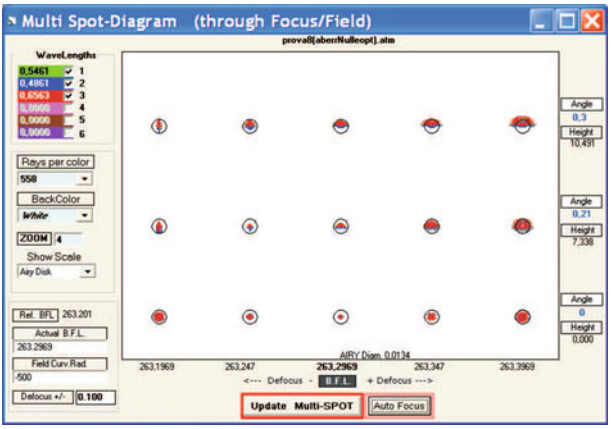

Fig. 9.24 Final design of Houghton–Cassegrain with sub-corrector, principal mirror $f/2$ and diameter 200 mm

$$
\begin{aligned}
\alpha &= \frac{e_{DK}}{f_1}, \quad M = \frac{f_{DK}}{f_1}, \\
\beta &= \frac{M-\alpha}{M+1}, \quad sd = -\beta f 1, \\
\gamma &= \frac{2M(1+\alpha)}{1-M^2}, \quad R_2 = \gamma f_1, \\
K_0 &= -\frac{1+M^3+\alpha-M^2(1+\alpha)}{M^3}.
\end{aligned}
\tag{9.27}
$$

Then, we must to evaluate the four radii of the lenses of corrector. This can be done by resorting to the notebook ***Houghton–CassegrainC*** that evaluates these radii imposing that the total focal is equal to f_t, the back focal is equal to e_{em}, and requiring that the axial chromatism, third-order spherical aberration, coma and astigmatism

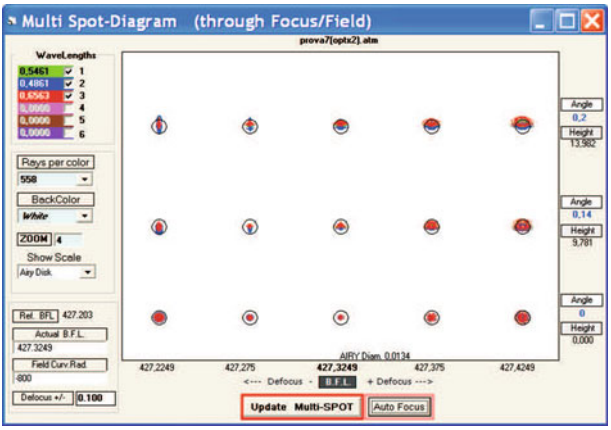

Fig. 9.25 Houghton–Cassegrain with sub-corrector, principal mirror $f/2$ and diameter 400 mm

vanish. The obtained design is not acceptable for the presence of higher order aberrations. However, if we insert this design in a professional software and apply an optimization method, we easily obtain the final result. For instance, if we want to design this Houghton–Cassegrain combination of total focal length $f_t = 1700$ mm using a primary mirror having a diameter of 200 mm and a focal $f_1 = 400$ (speed $f/2$), the notebook ***Houghton–CassegrainC*** gives the following output (in mm):

- Radius of curvature of primary mirror $R_1 = -811.27$
- Radius of curvature of secondary mirror $R_2 = -256$
- Distance between primary and secondary $d_{ps} = -304$
- Distance between the secondary mirror and the first surface of corrector $dcp = 279$
- conic constant of primary mirror $K = -0.774518$
- radii of curvature of the surfaces of corrector

$$r_1 = 134.03,\ r_2 = 79.76,\ r_3 = -108.63,\ r_4 = -63.90.$$

- the two lenses are far apart 3 mm and have a thickness of 4 mm

The spot diagram corresponding to this data is shown in Figure 9.23 over an image surface with a radius of curvature of -500 mm. The combination is close to be diffraction limited. Inserting the above data in a professional software (for instance ***Atmos***) we obtain the final combination whose spot diagram is shown in Figure 9.24. Finally, we remark that this final combination has a speed $f/7$.

Another advantage of this optical combination is that its performance is independent of the size of the mirror. Figure 9.25 shows the spot diagram of an Houghton–Cassegrain telescope with a sub-aperture corrector whose primary mirror has a diameter of 400 mm and speed $f/2$. This instrument, that has been designed by ***Optisoft***, is diffraction limited on a region of about 30 mm located on the image surface that has a radius of curvature of -500 mm.

9.10 Petzval's Objective

Since the invention of the photographic camera in the early nineteenth century a large amount of photographic objectives have been proposed. A good photographic objective must to have the following characteristics:

- High speed to reduce the exposition time
- supply a corrected image over a wide flat region

The first photographic objective designed by the Hungarian mathematician Petzval in 1841 had a speed $f/4$ and a focal length 100 mm. Although the speed of this objective were very high compared with the speed of the photographic objectives existing at that time, it exhibited severe field curvature, astigmatism and distortion. This objective, called ***Petzval portrait objective***, uses four element formula consisting of a front cemented achromatic and a rear air-spaced achromatic (see Figure 9.26). A 150mm focal length Petzval lens was realized by Voigtlnder in 1841. The Voigtlnder–Petzval was the first camera and lens specifically designed to take photographs. Data in Figure 9.27 refers to a Petzval objective of focal length 100 mm and speed $f/4.6$. The spot has a diameter of 25 μ for a view field of 20°. In this section, we show that we can realize an excellent dioptric telescope by slightly modifying the Petzval configuration. In this way, we obtain a telescope that has a speed up to $f/8$, is apochromatic and diffraction limited. The only price to pay is that the instrument is longer than its focal length.

To design this combination, we can resort to ***Optisoft*** that achieves the result in three steps. First, we neglect the thickness of the lenses, suppose that the two doublets are cemented and have the last surfaces flat. We impose that the combination satisfies the following four conditions that allow us to determine the rays of the remaining four surfaces

- The total focal length is given
- The back focal is given
- The axial chromatism is zero
- The magnification chromatism is zero

Then, we take into account the thickness of the lenses and separate the two lenses of the doublets. In this way, we dispose of eight rays of curvature $R_1, \ldots, R_8$. We suppose that the fifth surface is flat ($R_5 = \infty$) and $R_6 = R_7$. Thus, to evaluate the

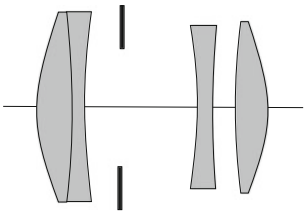

Fig. 9.26 Petzval's objective

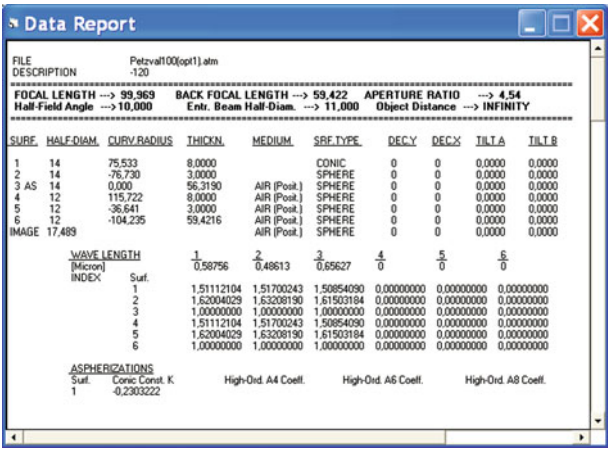

Data Report

FILE Petzval100(opt1).atm
DESCRIPTION -120

FOCAL LENGTH ---> 99,969 BACK FOCAL LENGTH ---> 59,422 APERTURE RATIO ---> 4,54
Half-Field Angle ---> 10,000 Entr. Beam Half-Diam. ---> 11,000 Object Distance ---> INFINITY

SURF.	HALF-DIAM.	CURV.RADIUS	THICKN.	MEDIUM	SRF.TYPE	DEC.Y	DEC.X	TILT A	TILT B
1	14	75,533	8,0000		CONIC	0	0	0,0000	0,0000
2	14	-76,730	3,0000		SPHERE	0	0	0,0000	0,0000
3 AS	14	0,000	56,3190	AIR (Posit.)	SPHERE	0	0	0,0000	0,0000
4	12	115,722	8,0000	AIR (Posit.)	SPHERE	0	0	0,0000	0,0000
5	12	-36,641	3,0000	AIR (Posit.)	SPHERE	0	0	0,0000	0,0000
6	12	-104,235	59,4216	AIR (Posit.)	SPHERE	0	0	0,0000	0,0000
IMAGE	17,489			AIR (Posit.)	SPHERE	0	0	0,0000	0,0000

WAVE LENGTH [Micron]	1	2	3	4	5	6
	0,58756	0,48613	0,65627	0	0	0

INDEX Surf.						
1	1,51112104	1,51700243	1,50854090	0,00000000	0,00000000	0,00000000
2	1,62004029	1,63208190	1,61503184	0,00000000	0,00000000	0,00000000
3	1,00000000	1,00000000	1,00000000	0,00000000	0,00000000	0,00000000
4	1,51112104	1,51700243	1,50854090	0,00000000	0,00000000	0,00000000
5	1,62004029	1,63208190	1,61503184	0,00000000	0,00000000	0,00000000
6	1,00000000	1,00000000	1,00000000	0,00000000	0,00000000	0,00000000

ASPHERIZATIONS

Surf.	Conic Const. K	High-Ord. A4 Coeff.	High-Ord. A6 Coeff.	High-Ord. A8 Coeff.
1	-0,2303222			

Fig. 9.27 Petzval objective data

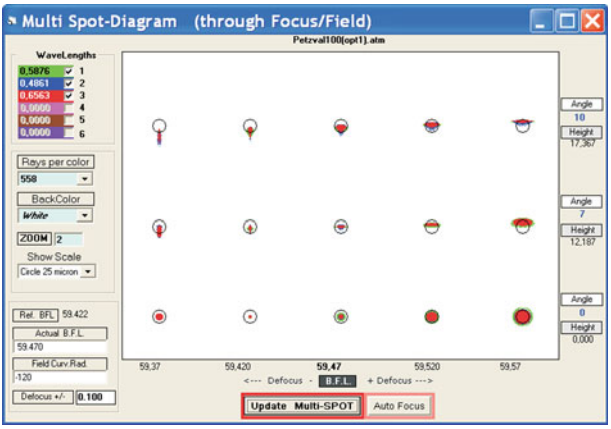

Fig. 9.28 Spot diagram of Petzval objective $f/4.6$, $f = 100$ mm

remaining six radii of curvature R_1, R_2, R_3, R_4, R_7, R_8, we impose the following six conditions:

- The total focal length is given
- The back focal is given
- The axial chromatism is zero
- The magnification chromatism is zero
- The third-order spherical aberration vanishes
- The third-order coma vanishes

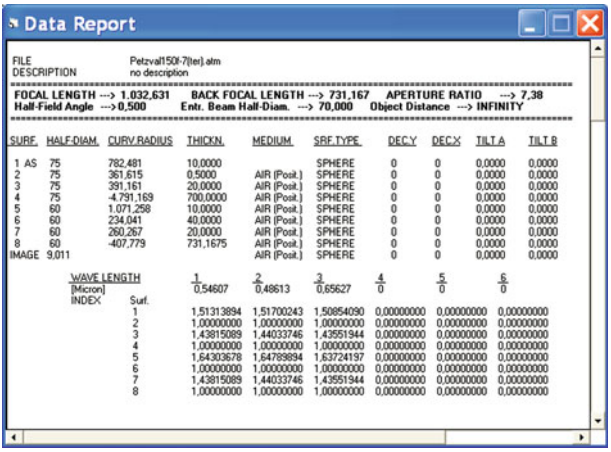

Data Report

FILE Petzval150f-7(ter).atm
DESCRIPTION no description

FOCAL LENGTH ---> 1.032,631 BACK FOCAL LENGTH ---> 731,167 APERTURE RATIO ---> 7,38
Half-Field Angle ---> 0,500 Entr. Beam Half-Diam. ---> 70,000 Object Distance ---> INFINITY

SURF.	HALF-DIAM.	CURV.RADIUS	THICKN.	MEDIUM	SRF.TYPE	DEC.Y	DEC.X	TILT A	TILT B
1 AS	75	782,481	10,0000		SPHERE	0	0	0,0000	0,0000
2	75	361,615	0,5000	AIR (Posit.)	SPHERE	0	0	0,0000	0,0000
3	75	391,161	20,0000	AIR (Posit.)	SPHERE	0	0	0,0000	0,0000
4	75	-4.791,169	700,0000	AIR (Posit.)	SPHERE	0	0	0,0000	0,0000
5	60	1.071,258	10,0000	AIR (Posit.)	SPHERE	0	0	0,0000	0,0000
6	60	234,041	40,0000	AIR (Posit.)	SPHERE	0	0	0,0000	0,0000
7	60	260,267	20,0000	AIR (Posit.)	SPHERE	0	0	0,0000	0,0000
8	60	-407,779	731,1675	AIR (Posit.)	SPHERE	0	0	0,0000	0,0000
IMAGE	9,011			AIR (Posit.)	SPHERE	0	0	0,0000	0,0000

WAVE LENGTH [Micron] INDEX Surf.	1 0,54607	2 0,48613	3 0,65627	4 0	5 0	6 0
1	1,51313894	1,51700243	1,50854090	0,00000000	0,00000000	0,00000000
2	1,00000000	1,00000000	1,00000000	0,00000000	0,00000000	0,00000000
3	1,43815089	1,44033746	1,43551944	0,00000000	0,00000000	0,00000000
4	1,00000000	1,00000000	1,00000000	0,00000000	0,00000000	0,00000000
5	1,64303678	1,64789894	1,63724197	0,00000000	0,00000000	0,00000000
6	1,00000000	1,00000000	1,00000000	0,00000000	0,00000000	0,00000000
7	1,43815089	1,44033746	1,43551944	0,00000000	0,00000000	0,00000000
8	1,00000000	1,00000000	1,00000000	0,00000000	0,00000000	0,00000000

Fig. 9.29 Data of Petzval telescope $f/8$, diameter 140 mm

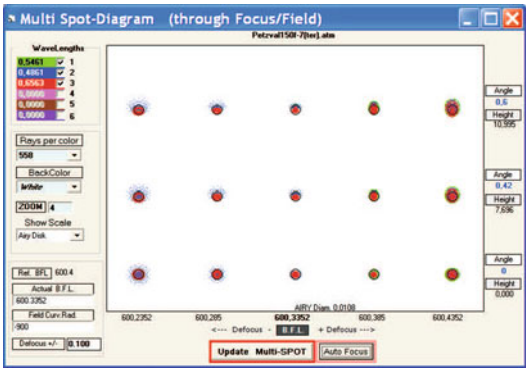

Fig. 9.30 Spot diagram of Petzval telescope $f/8$, diameter 140 mm

In this way, we achieve a configuration that is the starting point of an optimization method. Figures 9.28 and 9.29, respectively, show the data and the spot diagram of a Petzval telescope with a diameter of 140 mm, a total focal length of 1040 mm and a speed $f/8$ that has been designed by ***Optisoft*** (Fig. 9.30).

Chapter 10
Fermat's Principle and Wave Fronts

10.1 Fermat's Principle

In Chapter 1 we introduced Fermat's principle in an elementary way, without any critical analysis of its consequences. In contrast, in this chapter, we analyze Fermat's principle in depth, together with the related Lagrangian formalism and partial differential equations, in view of introducing the Hamiltonian formalism (see [44], [50], [51]).

Let us consider the propagation of a monochromatic light wave in an isotropic inhomogeneous medium Σ. If the wavelength of the light is small compared with the dimensions, of both the region in which the light propagates and the interposed obstacles (stops), then the propagation of the light can be described by ***rays*** (see Section 1.1). The refractive index $N(\mathbf{x})$ of the medium Σ is assumed to be a smooth function of the position vector $\mathbf{x} \in \Sigma$, except for the points belonging to a finite number of surfaces $S_l,\ l = 1, \ldots, k$, across which $N(\mathbf{x})$ exhibits finite discontinuities. We have already defined (see Section 1.1) the ***optical path length*** $OPL(\gamma_0)$ along a curve γ_0 using the following formula

$$OPL(\gamma_0) = \int_{\gamma_0} N(\mathbf{x}) ds. \tag{10.1}$$

In Chapter 1, ***Fermat's Principle*** was formulated in the following way:

The optical path length of a light ray from point $\overline{\mathbf{x}}$ to point $\overline{\mathbf{x}}'$, is the minimum among all potential optical path lengths corresponding to all potential paths between these points.

In this section, we formulate Fermat's principle in a more precise form and provide answers to the questions posed in Section 1.1. It is relevant to note that almost all of the results we prove can be extended to the following general functional

© Springer International Publishing Switzerland 2016

A. Romano and R. Cavaliere, *Geometric Optics*,
Modeling and Simulation in Science, Engineering and Technology,
DOI 10.1007/978-3-319-43732-3_10

$$I(\gamma) = \int_a^b L(\mathbf{x}, \dot{\mathbf{x}}, t)dt, \tag{10.2}$$

where L is an arbitrary regular function of the variables $\mathbf{x}$, $\dot{\mathbf{x}}$, t, and γ is any curve $\mathbf{x}(t)$ such that $\mathbf{x}(a) = \overline{\mathbf{x}}_a$ and $\mathbf{x}(a) = \overline{\mathbf{x}}'_a$.

In order to characterize the minimum among the potential path lengths, we first introduce a Cartesian coordinate frame (x_i), $i = 1, 2, 3$. *Any* path γ between $\overline{\mathbf{x}}$ and $\overline{\mathbf{x}}'$ is thus represented by three parametric equations $x_i = f_i(t)$, $i = 1, 2, 3$, $t \in [a, a']$, which give the coordinates $(f_i(t))$ of the points of γ as the parameter t varies. The points $\overline{\mathbf{x}} = (\overline{x}_i)$ and $\overline{\mathbf{x}}' = (\overline{x}'_i)$ will be the end points of γ provided that

$$f_i(a) = \overline{x}_i, \qquad f_i(a') = \overline{x}'_i. \tag{10.3}$$

In particular, the parametric equations for the *ray* γ_0 between $\overline{\mathbf{x}}$ and $\overline{\mathbf{x}}'$—in other words, for the *effective* light path from $\overline{\mathbf{x}}$ to $\overline{\mathbf{x}}'$—will be denoted by the functions $x_i(t)$, $i = 1, 2, 3$, that satisfy the conditions

$$x_i(a) = \overline{x}_i, \; x_i(a') = \overline{x}'_i. \tag{10.4}$$

The next step is to search for the expression for the optical path length of any path γ, between the points $\overline{\mathbf{x}}$ and $\overline{\mathbf{x}}'$, in order to determine the curve along which γ_0 has a minimum.

Analysis shows that the infinitesimal arc length ds of γ is given by

$$ds = \sqrt{\sum_{i=1}^{3} \dot{f}_i^2} dt, \tag{10.5}$$

where the notation $df_i/dt = \dot{f}_i$ has been used. Instead of (10.1), the following expression is now considered, which supplies the optical path length along any path γ between $\overline{\mathbf{x}}$ and $\overline{\mathbf{x}}'$

$$OPL(\gamma) = \int_\gamma N(\mathbf{x}) \sqrt{\sum_{i=1}^{3} \dot{f}_i^2} dt. \tag{10.6}$$

Recalling known results, we derive the *necessary* conditions for the optical path length (10.4) to be minimized upon varying the curve $f_i(t)$. To this end, we consider the following arbitrary one-parameter family Γ of curves between the points $\overline{\mathbf{x}}$ and $\overline{\mathbf{x}}'$ that contain the effective ray γ_0

$$x_i = f_i(t, \epsilon), \quad \forall t \in [a, a'], \qquad i = 1, 2, 3, \tag{10.7}$$

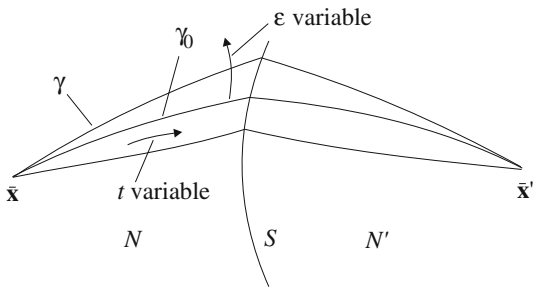

Fig. 10.1 The family Γ of optical paths between $\overline{\mathbf{x}}$ and $\overline{\mathbf{x}}'$

where

$$f_i(a, \epsilon) = \overline{x}_i, \qquad f_i(a', \epsilon) = \overline{x}'_i, \quad \forall \epsilon \in (-\delta, \delta)$$
$$f_i(t, 0) = x_i(t), \tag{10.8}$$

and $(-\delta, \delta)$ denotes the neighborhood of the value $\epsilon = 0$ (see Figure 10.1).

The optical path length of a curve belonging to Γ depends on the curve chosen (i.e., on the value of ϵ) according to the following formula, which is obtained from (10.4):

$$OPL(\epsilon) = \int_a^{a'} N(\mathbf{x}) \sqrt{\sum_{i=1}^{3} \dot{f}_i^2(t, \epsilon)} dt. \tag{10.9}$$

In other words, Fermat's principle can be equivalently stated as follows: *determine the condition under which the function $OPL(\epsilon)$ has a minimum at $\epsilon = 0$ for any member of the family $(f_i(t, \epsilon))$ of curves, verifying* (10.11). A **necessary** condition to achieve this is that

$$OPL'(0) = 0, \tag{10.10}$$

for any choice of Γ.

Consequently, we must

- Evaluate the first derivative of $OPL(\epsilon)$ at $\epsilon = 0$;
- Determine the conditions under which it vanishes for any member of the family Γ;
- Check if this condition characterizes the ray γ_0;
- to check whether $OPL(0)$ is a minimum of $OPL(\epsilon)$.

A general situation is considered here. This will enable other important results to be derived in Chapter 11 without repeating similar calculations. More precisely, we evaluate the derivative at $\epsilon = 0$ of the following function:

$$I(\epsilon) = \int_{t_1(\epsilon)}^{t_2(\epsilon)} N(\mathbf{x}) \sqrt{\sum_{i=1}^{3} \dot{f}_i^2(t, \epsilon)} dt, \tag{10.11}$$

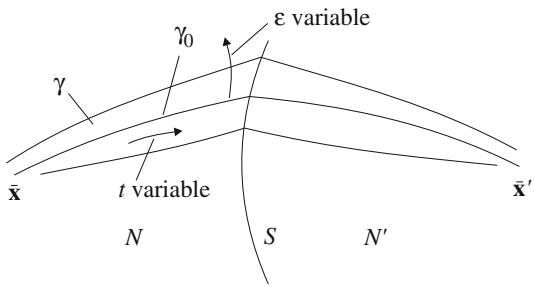

Fig. 10.2 A more general family of optical paths

where the curves $f_i(t, \epsilon)$ of family Δ comply with the following conditions instead of (10.7), (10.8):

$$x_i = f_i(t, \epsilon), \quad \forall t \in [t_1(\epsilon), t_2(\epsilon)], \qquad i = 1, 2, 3, \tag{10.12}$$

$$\begin{gathered} f_i(t_1(0), 0) = \overline{x}_i, \qquad f_i(t_2(0), 0) = \overline{x}_i', \quad \forall \epsilon \in (-\delta, \delta), \\ f_i(t, 0) = x_i(t), \end{gathered} \tag{10.13}$$

where $(-\delta, \delta)$ is the neighborhood of zero (see Figure 10.2).

In other words, the curves of Δ still contain the ray γ_0 for $\epsilon = 0$ but they have different initial and final points as ϵ varies. It is clear that the family Δ reduces to Γ, and so the function $I(\epsilon)$ reduces to $OPL(\epsilon)$, when

$$t_1(\epsilon) = a, \quad t_2(\epsilon) = a', \quad \forall \epsilon \in (-\delta, \delta). \tag{10.14}$$

Before determining the derivative $I'(\epsilon)$ and evaluating it at $\epsilon = 0$, it is important to note that

1. The coordinates of the extreme points of the curves $\gamma \in \Delta$ are

$$f_i(t_1(\epsilon), \epsilon), \quad f_i(t_2(\epsilon), \epsilon), \tag{10.15}$$

so that, in going from the ray γ_0 (which correspond to $\epsilon = 0$ in (10.13)) to the curve γ (corresponding to the value $d\epsilon$) the coordinates of the extreme points vary according to the relations

$$d\overline{x}_i = (\dot{x}_i \frac{dt_1}{d\epsilon} + \frac{\partial f_i}{\partial \epsilon})_{\epsilon=0} d\epsilon, \quad d\overline{x}_i' = (\dot{x}_i \frac{dt_2}{d\epsilon} + \frac{\partial f_i}{\partial \epsilon})_{\epsilon=0} d\epsilon. \tag{10.16}$$

2. The function $N(\mathbf{x})$ exhibits finite discontinuities across some surfaces S_i, $i = 1, \ldots, n$, included in the optical system. For the sake of simplicity, for the remainder of this section, it is assumed that there is a single discontinuity surface S. As a consequence, we hypothesize that the functions $f_i(t, \epsilon)$ may have discontinuous

first derivatives; in other words, the vector of the tangent to any path from Δ could abruptly vary in direction while crossing S.

More precisely, if $F(\mathbf{x}) = 0$ denotes the equation of the surface S, the above discontinuities must be localized at the points of intersection of the curves of Δ with S. In order to determine the locus $\boldsymbol{\varphi}$ of these points, we first verify that the equation

$$F(f_i(t, \epsilon)) = 0, \tag{10.17}$$

implicitly defines a function $t = \psi(\epsilon)$ that gives the value of t corresponding to the point of intersection P between γ and S. In fact, Dini's condition

$$\frac{\partial}{\partial t} F(f_i(t, \epsilon)) \neq 0, \tag{10.18}$$

can be written

$$\frac{\partial F}{\partial x_i} \frac{\partial f_i}{\partial t} \neq 0, \tag{10.19}$$

or, equivalently,

$$\mathbf{n} \cdot \mathbf{t} \neq 0, \tag{10.20}$$

where $\mathbf{n} = \nabla F / |\nabla F|$ is the *internal* normal unit vector to S and $\mathbf{t}$ the tangent unit vector to γ at P. Therefore, if γ is not tangent to S at P, (10.17) implicitly defines a function $t = \psi(\epsilon)$, and the locus $\boldsymbol{\varphi}$ is a curve (see Figure 10.3) with parametric equations that yield

$$\varphi_i(\epsilon) = f_i(\psi(\epsilon), \epsilon), \tag{10.21}$$

where

$$F(\boldsymbol{\varphi}_i(\epsilon)) = F(f_i(\psi(\epsilon), \epsilon)) = 0. \tag{10.22}$$

Due to the continuity of the curves of Δ while crossing S, $\boldsymbol{\varphi}(\epsilon)$ is assumed to be a regular curve.

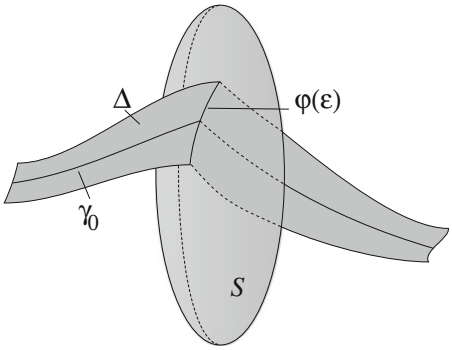

Fig. 10.3 The locus of the intersection points between the optical paths and S

By differentiating (10.22) with respect to ϵ from both sides of S, and taking into account (10.21), the following two conditions are obtained:

$$\begin{aligned} n_i \left(\frac{\partial f_i}{\partial t} \frac{\partial \psi}{\partial \epsilon} + \frac{\partial f_i}{\partial \epsilon} \right)^- &\equiv n_i \xi_i^- = 0, \\ n_i \left(\frac{\partial f_i}{\partial t} \frac{\partial \psi}{\partial \epsilon} + \frac{\partial f_i}{\partial \epsilon} \right)^+ &\equiv n_i \xi_i^+ = 0, \end{aligned} \tag{10.23}$$

where the summation over the index i is intended and $()^+$, $()^-$ denote the limits of the quantities appearing between the parentheses when S is approached from the right-hand side and from the right-hand side, respectively.

Moreover, the regularity of $\boldsymbol{\varphi}(\epsilon)$ implies the equality

$$\varphi_i'(\epsilon) = \left(\frac{\partial f_i}{\partial t} \frac{\partial \psi}{\partial \epsilon} + \frac{\partial f_i}{\partial \epsilon} \right)^- = \left(\frac{\partial f_i}{\partial t} \frac{\partial \psi}{\partial \epsilon} + \frac{\partial f_i}{\partial \epsilon} \right)^+. \tag{10.24}$$

which can be written

$$\xi_i^- = \xi_i^+. \tag{10.25}$$

In what follows, the discontinuity of any quantity a across S will be denoted by

$$[[a]] = a^+ - a^-. \tag{10.26}$$

We are now able to evaluate the derivative $I'(0)$. First, we have

$$\begin{aligned} I(\epsilon) &= \int_{t_1(\epsilon)}^{t_2(\epsilon)} L(f_i(t,\epsilon), \dot{f}(t,\epsilon))dt \\ &= \int_{t_1(\epsilon)}^{\psi(\epsilon)} L(f_i(t,\epsilon), \dot{f}_i(t,\epsilon))dt \\ &+ \int_{\psi(\epsilon)}^{t_2(\epsilon)} L(f_i(t,\epsilon), \dot{f}_i(t,\epsilon))dt, \end{aligned} \tag{10.27}$$

where

$$L = N(\mathbf{x}) \sqrt{\sum_{i=1}^{3} (\dot{f}_i)^2}. \tag{10.28}$$

By applying a well-known derivation formula of an integral, the above derivative becomes

$$\begin{aligned}\frac{dI}{d\epsilon}(0) &= L(\overline{x}_i', \dot{x}_i(a'))t_2'(0) - L(\overline{x}_i, \dot{x}_i(a))t_1'(0)\\ &+ \int_a^{\psi(0)} \left[\frac{\partial L}{\partial x_i}\frac{\partial f_i}{\partial \epsilon} + \frac{\partial L}{\partial \dot{x}_i}\frac{d}{dt}\left(\frac{\partial f_i}{\partial \epsilon}\right)\right] dt\\ &+ \int_{\psi(0)}^{a'} \left[\frac{\partial L}{\partial x_i}\frac{\partial f_i}{\partial \epsilon} + \frac{\partial L}{\partial \dot{x}_i}\frac{d}{dt}\left(\frac{\partial f_i}{\partial \epsilon}\right)\right] dt - [[L]]\psi'(0),\end{aligned}$$

where all of the quantities that appear on the right-hand side are evaluated at $\epsilon = 0$. By integrating the second term in each integral in the above relation by parts, we get

$$\begin{aligned}\frac{dI}{d\epsilon}(0) &= L(\overline{x}_i', \dot{x}_i(a'))t_2'(0) - L(\overline{x}_i, \dot{x}_i(a))t_1'(0)\\ &+ \int_a^{a'} \left[\frac{\partial L}{\partial x_i} - \frac{d}{dt}\frac{\partial L}{\partial \dot{x}_i}\right]\frac{\partial f_i}{\partial \epsilon} dt + \left[\frac{\partial L}{\partial \dot{x}_i}\frac{\partial f_i}{\partial \epsilon}\right]_a^{\psi(0)}\\ &+ \left[\frac{\partial L}{\partial \dot{x}_i}\frac{\partial f_i}{\partial \epsilon}\right]_{\psi(0)}^{a'} - [[L]]\psi'(0),\end{aligned} \tag{10.29}$$

so that

$$\begin{aligned}\frac{dI}{d\epsilon}(0) &= -\left(\frac{\partial L}{\partial \dot{x}_i}\dot{x}_i - L\right)_{a'} t_2'(0) + \left(\frac{\partial L}{\partial \dot{x}_i}\dot{x}_i - L\right)_a t_1'(0)\\ &+ \int_a^{a'} \left(\frac{\partial L}{\partial x_i} - \frac{d}{dt}\frac{\partial L}{\partial \dot{x}_i}\right)\frac{\partial f_i}{\partial \epsilon} dt\\ &+ \left(\frac{\partial L}{\partial \dot{x}_i}\left(\frac{\partial f_i}{\partial \epsilon} + \dot{x}_i t_2'\right)\right)_{a'} - \left(\frac{\partial L}{\partial \dot{x}_i}\left(\frac{\partial f_i}{\partial \epsilon} + \dot{x}_i t_1'\right)\right)_a\\ &- \left[\left[\frac{\partial L}{\partial \dot{x}_i}\frac{\partial f_i}{\partial \epsilon}\right]\right]_{\psi(0)} - [[L]]\psi'(0).\end{aligned} \tag{10.30}$$

Finally, recalling (10.23), (10.24), we get

$$\begin{aligned}\frac{dI}{d\epsilon}(0) &= -\left(\frac{\partial L}{\partial \dot{x}_i}\dot{x}_i - L\right)_{a'} t_2'(0) + \left(\frac{\partial L}{\partial \dot{x}_i}\dot{x}_i - L\right)_a t_1'(0)\\ &+ \int_a^{a'} \left(\frac{\partial L}{\partial x_i} - \frac{d}{dt}\frac{\partial L}{\partial \dot{x}_i}\right)\frac{\partial f_i}{\partial \epsilon} dt\\ &+ \left(\frac{\partial L}{\partial \dot{x}_i}\right)_{a'} \frac{d\overline{x}_i'}{d\epsilon} - \left(\frac{\partial L}{\partial \dot{x}_i}\right)_a \frac{d\overline{x}_i}{d\epsilon}\\ &- \left[\left[\frac{\partial L}{\partial \dot{x}_i}\left(\frac{\partial x_i}{\partial \epsilon} + \dot{x}_i\psi'(0)\right)\right]\right]_{\psi(0)}\\ &- [[L - \frac{\partial L}{\partial \dot{x}_i}\dot{x}_i]]_{\psi(0)}\psi'(0).\end{aligned} \tag{10.31}$$

Since the function L is homogeneous of the first degree in the variables $\dot{x}_i$, it follows that[1]

$$L - \frac{\partial L}{\partial \dot{x}_i}\dot{x}_i = 0, \tag{10.32}$$

and the above formula becomes

$$\begin{aligned}\frac{dI}{d\epsilon}(0) = &\int_a^{a'} \left(\frac{\partial L}{\partial x_i} - \frac{d}{dt}\frac{\partial L}{\partial \dot{x}_i}\right)\frac{\partial f_i}{\partial \epsilon}dt \\ &+ \left(\frac{\partial L}{\partial \dot{x}_i}\right)_{a'} \frac{d\overline{x}_i'}{d\epsilon} - \left(\frac{\partial L}{\partial \dot{x}_i}\right)_{a} \frac{d\overline{x}_i}{d\epsilon} \\ &- \left[\left[\frac{\partial L}{\partial \dot{x}_i}\left(\frac{\partial x_i}{\partial \epsilon} + \dot{x}_i\psi'(0)\right)\right]\right]_{\psi(0)}.\end{aligned} \tag{10.33}$$

In order to apply Fermat's principle to (10.33), *we must assume that all the curves have the same end points*. In this case, (10.33) reduces to the following equation

$$\frac{dI}{d\epsilon}(0) = \int_a^{a'} \left[\frac{\partial L}{\partial x_i} - \frac{d}{dt}\frac{\partial L}{\partial \dot{x}_i}\right]\frac{\partial x_i}{\partial \epsilon}dt + \left[\left[\frac{\partial L}{\partial \dot{x}_i}\right]\right]_{\psi(0)} \xi_i, \tag{10.34}$$

where

$$\xi_i = \left(\frac{\partial x_i}{\partial \epsilon} + \dot{x}_i\psi'(0)\right)_{\psi(0)}$$

and (10.23), (10.24) were used at $\epsilon = 0$.

Fermat's principle requires that the derivative of the optical path vanishes *for any choice of quantities* $(\partial x_i/\partial \epsilon)_{\psi(0)}$ *and* ξ_i such that

$$\xi_i n_i = 0.$$

From the right-hand side of (10.34), it is easy to show that the above condition is equivalent to the following ones

[1]This result can directly be obtained starting from (10.28) or resorting to Euler's theorem about the homogeneous functions. In fact this theorem states that if $f(x_1, \ldots, x_n)$ is a homogeneous function of degree α, that is a function for which

$$f(\mu x_1, \ldots, \mu x_n) = \mu^\alpha f(x_1, \ldots, x_n),$$

then, the following identity holds

$$\alpha f = \frac{\partial f}{\partial x_i}x_i$$

(summation over i). Since L in (10.28) is homogeneous of the first order, we obtain (10.32).

$$\frac{\partial L}{\partial x_i} - \frac{d}{dt}\frac{\partial L}{\partial \dot{x}_i} = 0, \tag{10.35}$$

$$\left[\left[\frac{\partial L}{\partial \dot{x}_i}\right]\right]_{\psi(0)} = \lambda n_i, \quad i = 1, 2, 3, \tag{10.36}$$

where λ is an unknown Lagrangian multiplier.

The equations (10.35) and (10.36) are, respectively, the ***Euler–Lagrange equations*** and the ***Weierstrass–Erdman jump conditions*** for the functional

$$\int_a^{a'} L dt \equiv \int_a^{a'} N \sqrt{\sum_{i=1}^{3} (\dot{x}_i)^2} dt. \tag{10.37}$$

In order to convert (10.35) and (10.36) into a more expressive form, it is convenient to introduce the unit vector tangent to the ray γ_0, which propagates from the point $\overline{\mathbf{x}}$ to $\overline{\mathbf{x}}'$

$$\mathbf{t} = \frac{\dot{x}_i}{\sqrt{\sum_{i=1}^{3} (\dot{x}_i)^2}}, \tag{10.38}$$

and to recall the relation

$$\frac{ds}{dt} = \sqrt{\sum_{i=1}^{3} (\dot{x}_i)^2}. \tag{10.39}$$

It is then straightforward to verify that (10.35) yields

$$\frac{d}{ds}(N\mathbf{t}) = \nabla N. \tag{10.40}$$

In particular, this equation implies that *light propagates in straight line in any medium with a constant refractive index N*.

Using this notation, condition (10.36) can be written as follows[2]

$$N'\mathbf{t}' - N\mathbf{t} = \lambda \mathbf{n}, \tag{10.41}$$

so that the incident ray, the refracted ray, and the unit vector $\mathbf{n}$ that is normal to S and oriented in the direction propagation of the light are *coplanar* at the incidence point. Moreover, vector multiplication of (10.41) with $\mathbf{n}$ leads to the relation

$$N'\mathbf{t}' \times \mathbf{n} = N\mathbf{t} \times \mathbf{n} \tag{10.42}$$

from which it follows

$$N' \sin i' = N \sin i, \tag{10.43}$$

[2]See Exercise 1 at the end of Chapter 1.

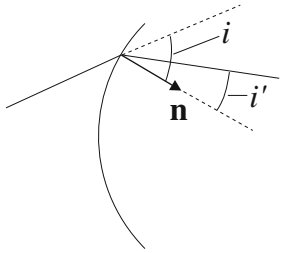

Fig. 10.4 The refraction law

where i and i' are the angles of incidence and refraction, respectively (i.e., the angles that $\mathbf{t}$ and $\mathbf{t}'$ form with $\mathbf{n}$; (see Figure 10.4)). The property that $\mathbf{t}$, $\mathbf{t}'$ and $\mathbf{n}$ are coplanar as well as relation (10.43), represent the ***refraction law*** of geometric optics.

It is now possible to evaluate the Lagrangian multiplier λ. In fact, the scalar product between $\mathbf{n}$ and (10.41) supplies the relation

$$\lambda = N' \cos i' - N \cos i = N' \sqrt{1 - \sin^2 i'} - N \cos i,$$

which, in view of (10.43), yields

$$\lambda = \sqrt{N'^2 - N^2 \sin^2 i} - N \cos i. \tag{10.44}$$

We have now shown that Fermat's principle includes all the properties of light rays. In particular, (10.43) and the fact that $N' = -N$ applies to reflection result in the ***reflection law***: *the incident and reflected rays are coplanar with* $\mathbf{n}$ *and subtend the same angle with* $\mathbf{n}$.

Bearing in mind what we have said so far, Fermat's principle could be more precisely stated as follows:

the light ray γ_0 *between two points* $\mathbf{x}$ *and* $\mathbf{x}'$ *is an* ***extremum*** *of the optical path function* $OPL(\epsilon)$, *although not necessarily a minimum.*

10.2 The Boundary Value Problem

It is worth noting that the determination of the light ray γ_0 between two points $\mathbf{x}$ and $\mathbf{x}'$ by Fermat's principle has now been reduced to a search for that solution $(x_i(t))$, $i = 1, 2, 3$, to the differential equation (10.35) that satisfies the boundary conditions (10.4) as well as the jump condition (10.36); in other words

$$\begin{aligned}
&\frac{\partial L}{\partial x_i} - \frac{d}{dt}\frac{\partial L}{\partial \dot{x}_i} = 0,\\
&x_i(a) = x_a^i, \quad x_i(b) = x_b^i,\\
&\left[\left[\frac{\partial L}{\partial \dot{x}_i}\right]\right]_{\psi(0)} = \lambda n_i, \quad i = 1, 2, 3.
\end{aligned} \tag{10.45}$$

It has already been noted that this problem is very different from Cauchy's initial value problem. There are well-known existence and uniqueness theorems that apply under very general conditions for the latter. However, there is no known general theorem of this kind for the boundary value problem of (10.45).

Using examples, it is possible to verify that the ray γ_0 may be an (absolute or relative) minimum, a maximum, or neither. For instance, during reflection at a plane mirror, the ray $\mathbf{x}\mathbf{x}^*\mathbf{x}'$, where $\mathbf{x}^*$ is the incident point, is a relative minimum, whereas the direct ray from $\mathbf{x}$ to $\mathbf{x}'$ is an absolute minimum of this optical path.

The exercise at the end of Chapter 1 on the conic mirrors show that the boundary value problem (10.45) can have infinite solutions.

In order to gain a deeper insight into this problem, we recall that a curve of $\Re^3$ is defined as a set of three functions $t \in [a, b] \to (x_1(t), x_2(t), x_3(t))$. Consequently, a change of the parameter $t = t(\tau)$ generates a *new* curve. In other words, a curve is a mapping $t \to \Re^3$, not a locus of points of $\Re^3$. On the other hand, (10.4) is independent of any choice of the parameter t since Fermat's principle defines a ray as locus of points. Correspondingly, the boundary value problem (10.45) must define the solution *up to a change in the parameter* so the equations (10.45) cannot be *independent*. In fact, the identity (summation over i)

$$L - \dot{x}_i \frac{\partial L}{\partial \dot{x}_i} = 0,$$

implies that

$$\frac{\partial L}{\partial x_h} = \dot{x}_i \frac{\partial^2 L}{\partial \dot{x}_i \partial x_h}, \quad \frac{\partial L}{\partial \dot{x}_h} = \frac{\partial L}{\partial \dot{x}_h} + \dot{x}_i \frac{\partial^2 L}{\partial \dot{x}_i \partial \dot{x}_h}, \tag{10.46}$$

and so[3]

$$\dot{x}_i \frac{\partial^2 L}{\partial \dot{x}_i \partial \dot{x}_h} = 0. \tag{10.47}$$

Due to (10.46) and (10.47), we can easily verify that

[3]Note that at least one of the $\dot{x}_i$ is different from zero. Consequently, the homogeneous system (10.47) must have solutions different from zero. Then, necessarily

$$\det\left(\frac{\partial^2 L}{\partial \dot{x}_i \partial \dot{x}_h}\right) = 0.$$

In this case the Lagrangian function (10.2) is said to be *degenerate*.

$$\dot{x}_i \left(\frac{\partial L}{\partial x_i} - \frac{d}{dt} \frac{\partial L}{\partial \dot{x}_i} \right) = 0$$

and so one of Lagrange's equations is verified as a consequence of the others.

In conclusion, one of the three Lagrange equations in (10.45) can be eliminated. In fact, since the solutions of these equations are independent of the parameter, we can assume that it is possible to introduce a coordinate frame in which all of the rays of interest can be represented by the following parametric equations:

$$x_\alpha = x_\alpha(x_3), \quad \alpha = 1, 2. \tag{10.48}$$

According to this hypothesis, we have

$$L = N(x_i)\sqrt{1 + \dot{x}_1^2 + \dot{x}_2^2}, \tag{10.49}$$

where the dot denotes *differentiation with respect to* x_3, and the independent equations (10.45) are

$$\begin{aligned} &\frac{\partial L}{\partial x_\alpha} - \frac{d}{dx_3} \frac{\partial L}{\partial \dot{x}_\alpha} = 0, \\ &x_\alpha(a) = x_a^\alpha, \quad x_\alpha(b) = x_b^\alpha, \\ &\left[\left[\frac{\partial L}{\partial \dot{x}_\alpha} \right]\right]_{\psi(0)} = \lambda n_\alpha, \quad \alpha = 1, 2, \end{aligned} \tag{10.50}$$

where λ is given by (10.44).

Let x_3^* be the value of the parameter corresponding to the point of intersection of the ray with the surface S and let $x_\alpha^1(x_3, A_\alpha, B_\alpha)$, $x_\alpha^2(x_3, C_\alpha, D_\alpha)$ be the general integrals of (10.50) in the intervals (a, x_3^*) and (x_3^*, b), respectively. In order to find the solution to the boundary value problem (10.50), the eight constants A_α, B_α, C_α, D_α must be determined. To achieve this, the six equations (10.50) together with the two continuity conditions

$$x_\alpha^1(x_3^*, A_\alpha, B_\alpha) = x_\alpha^2(x_3^*, C_\alpha, D_\alpha), \tag{10.51}$$

are, at least in principle, sufficient.

10.3 Maupertuis' Principle

Let S be a mechanical system with holonomic, fixed, and smooth constraints, upon which conservative forces deriving from the potential energy U act. The system S is assumed to have n degrees of freedom, and we denote its configuration space by V_n. This means that the configurations of S are in a one-to-one correspondence

with the points of V_n. Then, if the Lagrangian coordinates $\mathbf{q} = (q_1, \ldots, q_n)$ are introduced in V_n, the motion of S will be geometrically described by a curve $\mathbf{q}(t) = (q_1(t), \ldots, q_n(t))$ of V_n. These curves are defined by another variational principle. In order to attain its formulation, we introduce the Lagrangian kinetic energy

$$T = \frac{1}{2} a_{hk}(\mathbf{q}) \dot{q}_h \dot{q}_k \tag{10.52}$$

and consider the class of motions that have a prefixed but arbitrary value E of energy. Moreover, we consider the Riemannian manifold obtained by equipping V_n with the metrics

$$d\sigma^2 = 2(E - U(\mathbf{q})) a_{hk}(\mathbf{q}) dq_h dq_k. \tag{10.53}$$

Maupertuis' Principle can be formulated as follows:

Let S be a mechanical system with holonomic, fixed, and smooth constraints, subjected to forces deriving from the potential energy U. The curves of V_n, representing motions of S with energy E, between two configurations $\mathbf{q}_1$ and $\mathbf{q}_2$, are geodesics of the Riemannian metrics (10.53), i.e., extrema of the functional

$$\int_{\mathbf{q}_1}^{\mathbf{q}_2} d\sigma. \tag{10.54}$$

Moreover, the point P (representing S in V_n) moves along these curves according to the following law

$$\frac{d\sigma}{dt} = 2(E - U). \tag{10.55}$$

In particular, if S is a material point P with mass m and orthogonal Cartesian coordinates (x_i) are introduced, we have

$$T = \frac{1}{2} \sum_{i=1}^{3} (\dot{x}_i)^2,$$

and so (10.53), (10.54), respectively, yield

$$d\sigma^2 = 2(E - U) \sum_{i=1}^{3} dx_i^2, \qquad \int_{\mathbf{x}_1}^{\mathbf{x}_2} \sqrt{2(E - U) \sum_{i=1}^{3} dx_i^2}, \tag{10.56}$$

where $\mathbf{x}_1, \mathbf{x}_2$ are the initial and final positions of P.

A comparison between (10.37) and (10.56) shows that, for fixed initial and final configurations, the material point P, when subjected to forces deriving from the potential energy U, follows the same trajectory as a light ray between the same points provided that

$$\sqrt{2(E - U)} = N.$$

It is well known that this perfect correspondence between mechanics and optics is one of the foundation of Quantum Mechanics.

Remark 10.1 Let V_3 be the Riemannian manifold obtained by equipping the Euclidean three-dimensional space E_3 with the metrics

$$d\sigma^2 = N^2(\mathbf{x})ds^2, \tag{10.57}$$

where $\mathbf{x} \in E_3$, and ds is the elementary distance evaluated by the Euclidean metrics of E_3. The manifolds V_3 describes the geometry of E_3 filled with an inhomogeneous medium with refractive index N. In this description, Fermat's principle states that the trajectories of light rays are geodesics of metrics (10.57).

10.4 Fermat's Principle and the Formation of Mirages

Many interesting phenomena are due to variation of refractive index $N(\mathbf{x})$ in the atmosphere (see, for instance, [44]). Introduce a frame $Oxyz$ of Cartesian coordinates with the coordinate plane Oxy on earth ground and the axis Oz vertical and suppose that the refractive index $N(\mathbf{x})$ is a function of z (which represents the height above ground). Consider a path γ in the vertical plane Oxz defined by the equation

$$z = z(x), x_1 \leq x \leq x_2, \tag{10.58}$$

connecting two points $P(x_1, z_1)$ and $Q(x_2, z_2)$. Then the optical path length of γ is

$$OPL(P, Q) = \int_P^Q N(z)\sqrt{1 + z'(x)^2}dx \equiv \int_P^Q L(z, z')dx, \tag{10.59}$$

where $z'(x) = dz/dx$.

Since the integrand $f(z, z') = N(z)\sqrt{1 + z'(x)^2}$ does not depend explicitly on the independent variable x, the Euler–Lagrange equation of functional (10.59) becomes

$$\frac{\partial L}{\partial z} - \frac{\partial^2 L}{\partial z \partial z'}z' - \frac{\partial^2 L}{\partial z' \partial z'}z'' = 0.$$

Multiplying this equation by z', we easily obtain that

$$\frac{d}{dx}\left(L - z'\frac{\partial L}{\partial z'}\right) = 0$$

and then the following first integral holds

$$L - z'\frac{\partial L}{\partial z'} = k, \tag{10.60}$$

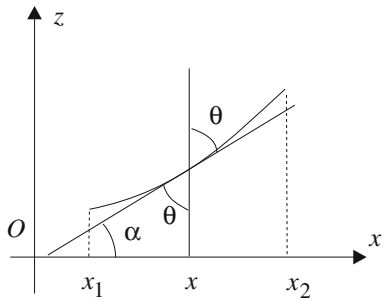

Fig. 10.5 Tangent to the ray at the point x

where k is a constant. In view of (10.59) the preceding equation becomes

$$\frac{N(z)}{\sqrt{1+z'^2}} = k, \tag{10.61}$$

so that k is the value of the refractive index when $z'(x) = 0$. Physically this represents the point where the ray becomes horizontal. Let θ be the angle that the tangent to the ray at the point $(x, z(x))$ forms with the axis Ox. Then, it is (Fig. 10.5)

$$\sin\theta = \cos\alpha = \frac{\cos\alpha}{\sqrt{\sin\alpha^2 + \cos\alpha^2}} = \frac{1}{\sqrt{1+z'^2}},$$

and we can write (10.61) as follows

$$N(z)\sin\theta = k. \tag{10.62}$$

Equation (10.61) can also be written as follows

$$1 + z'^2 = \frac{N^2(z)}{k^2}, \tag{10.63}$$

and differentiating this equation with respect to z, we get

$$2z'z'' = \frac{1}{k^2}\frac{dN^2(z)}{dz}z'$$

or

$$\frac{d^2z}{dx^2} = \frac{N(z)}{k}\frac{dN(z)}{dz}. \tag{10.64}$$

If we assume that $N(z)$ has the form

$$N(z) = N_0 - \alpha z, \tag{10.65}$$

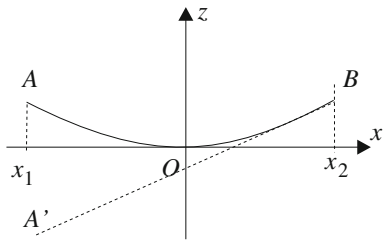

Fig. 10.6 Mirage when $\alpha < 0$

then (10.64) becomes

$$\frac{d^2z}{d^2x} = \lambda^2 z - N_1^2, \tag{10.66}$$

where

$$\lambda^2 = \frac{\alpha^2}{k^2}, \quad N_1^2 = \frac{N_0\alpha}{k^2}. \tag{10.67}$$

The solution of (10.66) is

$$z(x) = c_1 e^{-\lambda x} + c_2 e^{\lambda x} - \frac{N_1^2}{\lambda^2}, \tag{10.68}$$

where c_1 and c_2 are integration constants. We assume the initial values to be $z(0) = 0$ and $z'(0) = 0$. It is easy to verify that from these initial data we obtain

$$c_1 = \frac{N_1^2}{\lambda^2}, \quad c_2 = c_1,$$

and (10.68) becomes

$$z(x) = \frac{N_0}{2\lambda k^2}\left(e^{-\lambda x} + e^{\lambda x} - 2\right). \tag{10.69}$$

The behavior of the function (10.69) when $\alpha > 0$ (i.e., the refraction index decreases with the eight) is shown in Figure 10.6. This figure shows that the object at A is seen by the observer at B in the position A' (mirage). Inversely, if $\alpha < 0$ (i.e., the refraction index increases with the eight), the behavior of (10.69) is shown in Figure 10.7. In this case, the observer at B sees the object A at the position A' (Morgana fairy mirage).

10.5 Rotational Symmetry and Lagrange's invariant

Let $\mathbb{S}$ be an **axially symmetric optical system** (i.e., a system with a rotational symmetry around an axis a), and choose the frame of reference $Ox_1x_2x_3$ in such a way that $x_3 \equiv a$. If polar coordinates (ρ, θ), where

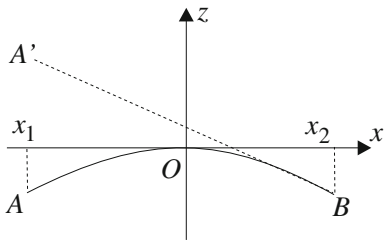

Fig. 10.7 Mirage when $\alpha > 0$

$$\begin{aligned} x_1 &= \rho\cos\theta, \qquad \rho = \sqrt{x_1^2 + x_2^2}, \\ x_2 &= \rho\sin\theta, \qquad \theta = \arctan\frac{x_2}{x_1}, \end{aligned} \tag{10.70}$$

are introduced in the plane Ox_1x_2, then, due to the symmetry, the Lagrangian function (10.49) of $\mathbb{S}$ yields

$$L = N(\rho, x_3)\sqrt{1 + \dot{\rho}^2 + \rho^2\dot{\theta}^2}. \tag{10.71}$$

Since L does not depend on θ, the quantity

$$I \equiv \frac{\partial L}{\partial\dot{\theta}} = N(\rho, x_3)\frac{\rho^2\dot{\theta}}{\sqrt{1 + \dot{\rho}^2 + \rho^2\dot{\theta}^2}}, \tag{10.72}$$

is independent of x_3. Again expressing this quantity in terms of Cartesian coordinates, we obtain

$$I = N(\rho, x_3)\frac{\dot{x}_2x_1 - \dot{x}_1x_2}{\sqrt{1 + \dot{x}_1^2 + \dot{x}_2^2}}, \tag{10.73}$$

which, taking into account (10.38) and introducing the notation

$$p_i = N(\rho, x_3)\frac{\dot{x}_i}{\sqrt{1 + \dot{x}_1^2 + \dot{x}_2^2}}, \tag{10.74}$$

becomes

$$I = p_2x_1 - p_1x_2 = \text{const.} \tag{10.75}$$

In other words, the quantity I is constant along a ray *in any region in which the refractive index is a continuous function of* ρ *and* x_3.

We now verify that I is an *optical invariant*; in other words, that it is constant along any ray, regardless of the reflections and refractions it undergoes. In fact, for any surface S that is discontinuous in the refractive index N, in view of (10.74), the discontinuity condition $(10.50)_3$ can be written as follows

$$[[p_\alpha]] = \lambda n_i. \tag{10.76}$$

Consequently, since $x_i^+ = x_i^-$, when the ray meets S, we have

$$p_2^+ x_1^+ - p_1^+ x_2^+ = p_2^- x_1^- - p_1^- x_2^- + \lambda(x_1^- n_2 - x_2^- n_1), \tag{10.77}$$

because of the continuity of the ray. On the other hand, if S exhibits a rotational symmetry around the axis x_3, we have $x_3 = f(x_1^2 + x_2^2) \equiv f(\rho)$ and so the components n_1 and n_2 of its normal unit vector become

$$\begin{aligned} n_1 &= \frac{f_{,x_1}}{\sqrt{1 + (f_{,x_1})^2 + (f_{,x_2})^2}} = \frac{2f' x_1}{\sqrt{1 + (f_{,x_1})^2 + (f_{,x_2})^2}}, \\ n_2 &= \frac{f_{,x_2}}{\sqrt{1 + (f_{,x_1})^2 + (f_{,x_2})^2}} = \frac{2f' x_2}{\sqrt{1 + (f_{,x_1})^2 + (f_{,x_2})^2}}, \end{aligned} \tag{10.78}$$

where $f_{,x_i} = \partial f / \partial x_i$ and $f' = df/d\rho$. Introducing these expressions into (10.77), we can easily derive

$$I^+ = p_2^+ x_1^+ - p_1^+ x_2^+ = p_2^- x_1^- - p_1^- x_2^- = I^-, \tag{10.79}$$

and so the complete invariance of I along a ray is proven. The quantity I is called ***Lagrange's optical invariant.***

To make clear the geometrical meaning of the invariant (10.75), we consider a ray of light γ and the intersection point A of γ with a plane π orthogonal to the optical axis a (see Figure 10.8). Let $\mathbf{t}$ the unit vector tangent to γ at the point A. The projection $\mathbf{p}$ of the vector $N\mathbf{t}$ on π has components $p_1 = N\dot{x}_1$ and $p_2 = N\dot{x}_2$. Consequently, if $\mathbf{r}$ is the position vector of A with respect to the origin O, then the optical invariant I is equal to the oriented area of the parallelogram with sides $\mathbf{r}$ and $\mathbf{p}$ (see Figure 10.9). In other words, the area of this parallelogram is constant along the ray of light. In the next chapter this invariant will be derived in the Hamiltonian formalism, together with other aspects of symmetric optical systems.

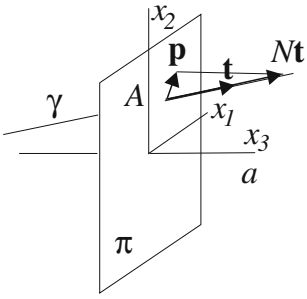

Fig. 10.8 Meaning of vector **p**

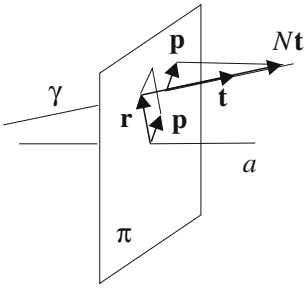

Fig. 10.9 Meaning of the invariant I

10.6 Wave Fronts and Fermat's Principle

Until now we based geometric optics on Fermat's principle and the linked concept of ray of light. In the middle of seventeenth century the Danish astronomer Rømer discovered that light propagates with finite velocity by observing the motion of Jupiter's satellites. At the same time, the Dutch physicist Huygens showed that the reflection and refraction laws of optics could be deduced from the assumption that light propagates with finite velocity $v = c/N$ by waves. About two centuries later, Maxwell formulated the equations of electrodynamics showing that the light waves are electromagnetic waves. It is then evident that geometric optics can be deduced from the electromagnetic theory. In a next chapter, we sketch this derivation but at the present we analyze the consequences of the assumption that light propagates by waves with a velocity $v = c/N$. In particular, in this section we prove that geometric optics only requires the concepts of rays or wavefronts, that are surfaces orthogonal to the rays and moving with normal velocity $v = c/N$. In other words, we prove the equivalence of these two approaches without presenting the physical background of propagation.

First, we note that equations (10.40)

$$\frac{d}{ds}\left(N\frac{dx_i}{ds}\right) = \frac{\partial N}{\partial x_i},$$

are equivalent to the first-order differential system

$$\frac{dx_i}{ds} = \frac{p_i}{N}, \tag{10.80}$$

$$\frac{dp_i}{ds} = \frac{\partial N}{\partial x_i}. \tag{10.81}$$

Let us suppose that the propagation of light is described by wavefronts $\Sigma(t)$, that is, by moving surfaces given by the equation $f(\mathbf{x}, t) = 0$. At a point $\mathbf{x} \in \Sigma(t)$, consider the straight line a of equation $\mathbf{x} + s\mathbf{n}$, where $\mathbf{n}$ is the unit vector normal to $\Sigma(t)$ at $\mathbf{x}$. If $f(\mathbf{x}, t + \tau) = 0$ is the equation of the surface $\Sigma(t + \tau)$, let $\mathbf{y}$ be

the intersection point of a with $\Sigma(t+\tau)$. The distance between $\Sigma(t)$ and $\Sigma(t+\tau)$ measured along the normal $\mathbf{n}$ at $\mathbf{x}$ is given by $s(\tau)$, and we define the ***normal speed*** of $\Sigma(t)$ as the limit

$$v = \lim_{\tau \to 0} \frac{s(\tau)}{\tau} = s'(0). \tag{10.82}$$

The limit (10.80) can also be expressed in terms of the equation $f(\mathbf{x}, t) = 0$ if we note that $s(\tau)$ is implicitly defined by equation

$$f(\mathbf{x} + s\mathbf{n}, t + \tau) \equiv \varphi(s, \tau) = 0, \tag{10.83}$$

so that, from Dini's theorem on implicit functions, it follows that

$$s'(0) = -\left(\frac{\partial\varphi/\partial\tau}{\partial\varphi/\partial s}\right) = -\frac{\partial f/\partial t}{\nabla f \cdot \mathbf{n}}.$$

Since ∇f is parallel to $\mathbf{n}$ and has the same orientation, we finally have

$$-\frac{\partial f}{\partial t}\frac{1}{|\nabla g|} = \frac{c}{N}. \tag{10.84}$$

If the wavefronts are not at rest, then $\partial f/\partial t \neq 0$. Therefore, we can always give the equation $f(\mathbf{x}, t) = 0$ the form $\psi(\mathbf{x}, t) - ct = 0$ and (10.84) can be written as follows

$$|\nabla\psi| = N$$

or equivalently as

$$\sum_{i=1}^{3}\left(\frac{\partial\psi}{\partial x_i}\right)^2 = N^2. \tag{10.85}$$

(10.85) is called ***eikonal equation*** and it is a nonlinear partial differential equation in the unknown $\psi(x_i)$.

We are interested in the following Cauchy problem for (10.85):

determine a solution $\psi(x_i)$ ***of*** (10.85) ***that assumes a constant value*** ψ_0 ***on an assigned surface*** Σ_0

$$x_{0i} = x_{0i}(\xi_\alpha), \quad \alpha = 1, 2,$$

where ξ_α ***are surface parameters.***

The standard way to solve such a problem involves resorting to the ***characteristic system*** of (10.85) (see Appendix A). In fact, the solutions of this system, which are called the ***characteristic curves*** of eikonal equation, allow us to derive the solution of Cauchy's problem.

The characteristic system yields

$$\frac{dx_i}{d\tau} = 2p_i, \tag{10.86}$$

$$\frac{dp_i}{d\tau} = 2N\frac{\partial N}{\partial x_i}, \tag{10.87}$$

$$\frac{d\psi}{d\tau} = 2N^2, \tag{10.88}$$

where

$$p_i = \frac{\partial \psi}{\partial x_i}. \tag{10.89}$$

Before we go any further, we note that an important conclusion can be derived from these preliminary considerations. Let us introduce the parameter s by the relation $ds = 2Nd\tau$. If $(x_i(\tau),\ p_i(\tau))$ is a solution of (10.86), (10.87), the curvilinear abscissa along the curve $(x_i(\tau))$ is given by

$$ds = \sqrt{\sum_{i=1}^{3}\left(\frac{dx_i}{d\tau}\right)^2}\,d\tau = 2\sqrt{\sum_{i=1}^{3} p_i^2}\,d\tau$$

which means that, taking into account (10.89) and (10.85), we have

$$ds = 2Nd\tau.$$

In other words, s coincides with the curvilinear abscissa along the curve $(x_i(\tau))$.

In terms of the parameter s, system (10.86)–(10.88) becomes

$$\frac{dx_i}{ds} = \frac{p_i}{N}, \tag{10.90}$$

$$\frac{dp_i}{ds} = \frac{\partial N}{\partial x_i}, \tag{10.91}$$

$$\frac{d\psi}{ds} = N. \tag{10.92}$$

Equations (10.90)–(10.92) are identical to (10.80)–(10.82). Taking into account (10.89), we can therefore conclude that

- *The curves $x_i(s)$ that solve the characteristic system coincide with the corresponding rays*;
- *The rays are orthogonal to the surfaces $\psi =$* const.;

In order to solve system (10.86)–(10.88), we need initial data. However, the points $x_{0i} = x_{0i}(\xi_\alpha)$ on the given surface Σ_0 supply the initial data for the unknowns x_i, but not for p_i. The initial data $p_{0i} = p_{0i}(\xi_\alpha)$ to use for this other set of unknowns

can be obtained from the following conditions (see Appendix A):

$$\sum_{i=1}^{3}(p_{0i}(\xi_\alpha))^2 = N^2(x_{0i}(\xi_\alpha)), \tag{10.93}$$

$$\sum_{i=1}^{3}\frac{\partial x_{0i}(\xi_\alpha)}{\partial \xi_\alpha}p_{0i}(\xi_\alpha) = 0. \tag{10.94}$$

The first condition, when (10.89) is taken into account, guarantees that the initial values of p_i satisfy the eikonal equation; the second one insures that the vector (p_{0i}) is orthogonal to Σ_0 at any point. The two equations (10.93)–(10.94) can be solved with respect the variables p_{0i} since the Jacobian matrix on Σ_0 is

$$J = \begin{pmatrix} 2p_{0i}(\xi(\alpha)) \\ \dfrac{\partial x_{0i}(\xi_\alpha)}{\partial \xi_\alpha} \end{pmatrix}.$$

However, at any point of Σ_0, the vector (p_{0i}) is orthogonal to the vectors $\frac{\partial x_{0i}(\xi_\alpha)}{\partial \xi_\alpha}$ which are tangent to Σ_0. Therefore, we have

$$J \neq 0$$

and equations (10.93)–(10.94) can be solved with respect to (p_{0i}) (see Figure 10.10).

Let

$$x_i(x_{0i}(\xi_\alpha), s) = \hat{x}_i(\xi_\alpha, s), \tag{10.95}$$

$$p_i(p_{0i}(\xi_\alpha), s) = \hat{p}_i(\xi_\alpha, s), \tag{10.96}$$

denote the solution of (10.93)–(10.94) starting from any point of the surface Σ_0. Substituting this into (10.92), we finally obtain

$$\psi(\xi_\alpha, s) = \psi_0 + \int_0^s N(\hat{x}_i(\xi_\alpha, s))ds. \tag{10.97}$$

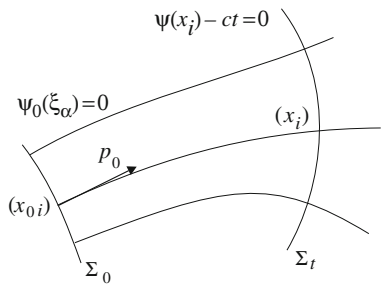

Fig. 10.10 Rays from Σ_0

Upon solving (10.95) with respect to the variables ξ_α, s, relation (10.97) becomes

$$\psi(x_i) = \psi_0 + \int_{x_0}^{x} N(\hat{x}_i(x_i))ds, \tag{10.98}$$

where the integration is performed along a ray. From (10.98) we find that

the difference between the values at two points of a solution to the eikonal equation is equal to the optical path length along the ray between these points.

The eikonal equation shows that the first derivatives of ψ are discontinuous across a surface S that separates an optical medium from another one. This means that S is a singular surface for ψ. Applying Maxwell's theorem, we can write

$$\left[\left[\frac{\partial\psi}{\partial x_i}\right]\right] = \lambda n_i. \tag{10.99}$$

Taking into account (10.89), this condition becomes

$$[[p_i]] = \lambda n_i \tag{10.100}$$

and the refraction law is obtained.

Conversely, if the rays are known, it is sufficient to introduce the function (10.98) in order to obtain a family $\psi(x_i, t) - ct = 0$ of moving surfaces orthogonal to the rays with advancing velocity c/N. Moreover, condition (10.99) can be derived from the refraction law. Finally, as it is shown by (10.98), $\psi(x_i)$ satisfies the eikonal equation.

10.7 Huygens' Principle

Let Σ_0 be a wavefront at the initial time with an equation $\psi(\xi_\alpha) = 0$. In the above section we described how to determine the front wave Σ_t at the instant t as represented by the equation $\psi(x_i) - ct = 0$. It is sufficient to integrate the equations (10.90), (10.91) of the characteristic system by utilizing initial data consisting of the points $x_{0i}(\xi_\alpha)$ of Σ_0 and the vectors $p_{0i}(\xi_\alpha)$, orthogonal to Σ_0 and verifying the condition (10.93). The function $\psi(x_i)$ is obtained by (10.98); the integration is performed along the rays from Σ_0 that have initial directions of $p_{0i}(\xi_\alpha)$ (see Figure 10.11).

In this section, a different way to obtain the wavefront Σ_t is described. To this end, an arbitrary but *fixed* point $(x_{0i}) \in \Sigma_0$ is chosen and the set of *all* vectors (p_{0i}) at (x_{0i}) is considered, with the condition (10.93) verified (see Figure 10.11).

By integrating the equations (10.90), (10.91) of the characteristic system, and utilizing the initial data x_{0i} and p_{0i}, where (p_{0i}) is arbitrary to within the condition (10.93), the set Γ of the rays sorting from (x_{0i}) can be obtained. Let us represent the wavefront Σ_t^* at the instant t, corresponding to the propagation along these rays, by the equation $\psi^*(\xi_\alpha, x_i) - ct = 0$, where $\psi^*(\xi_\alpha, x_i)$ is always given by (10.98), but

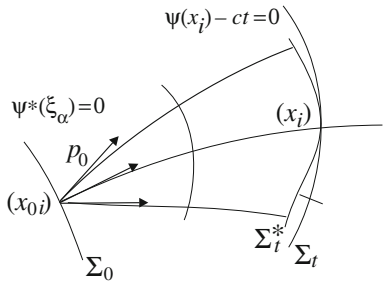

Fig. 10.11 Huygens' Principle

in this case the integration is performed *along the rays of* Γ. As a consequence, ψ^* verifies eikonal equation.

Huygens' Principle states that:

The wave front Σ_t ***is the envelope of all of the surfaces*** Σ_t^*, ***upon varying*** $(x_{0i}) \in \Sigma_0$.

To prove this statement, it is sufficient to recall that the envelope of the wave-fronts $\psi^*(\xi_\alpha, x_i) - ct$ upon varying (x_{0i}) (i.e., the parameters ξ_α) can be obtained by eliminating these parameters in the system

$$\psi^*(\xi_\alpha, x_i) - ct = 0, \tag{10.101}$$

$$\frac{\partial \psi^*}{\partial \xi_\alpha}(\xi_\alpha, x_i) = 0. \tag{10.102}$$

More precisely, if we assume that (10.102) can be solved with respect to the parameters ξ_α,

$$\xi_\alpha = \xi_\alpha(x_i),$$

substitution of these equations into (10.101) yields

$$\psi^*(\xi_\alpha, x_i) - ct \equiv \psi(x_i) - ct = 0. \tag{10.103}$$

To prove that the function $\psi(x_i)$ in (10.103) is a solution to eikonal equation, we note that we can derive the following from (10.102)

$$\frac{\partial \psi}{\partial x_i} = \frac{\partial \psi^*}{\partial \xi_\alpha}\frac{\partial \xi_\alpha}{\partial x_i} + \frac{\partial \psi^*}{\partial x_i} = \frac{\partial \psi^*}{\partial x_i}.$$

This result states that, at the point (x_i), the surface $\psi(x_i) - ct = 0$ has the same tangent plane as the wave $\psi^*(\xi_\alpha, x_i) - ct = 0$, which originates from $x_{0i}(\xi_\alpha)$. However, $\psi*$ satisfies the eikonal equation and that is true for $\psi(x_i)$.

Chapter 11
Hamiltonian Optics

11.1 Hamilton's Equations in Geometric Optics

In Chapter 10, we formulated the fundamental laws of geometrical optics using the Lagrangian formalism. It is well known that any theory expressed in Lagrangian terms could be (equivalently) formulated via the Hamiltonian formalism with significant advantages. This chapter describes this new formalism together with its consequences (see [49, 4, 23–25, 48, 1].).

It is important to remark that, in general, it is impossible to develop a Hamiltonian formalism starting from the Fermat principle (10.4) or, equivalently, from the Lagrange equations (10.35), (10.36). In fact, we must start with a nondegenerate Lagrangian $L(\mathbf{x}, \dot{\mathbf{x}})$, that is, with a Lagrangian for which the following condition is satisfied:

$$\det\left(\frac{\partial^2 L}{\partial \dot{x}_i \partial \dot{x}_j}\right) \neq 0. \tag{11.1}$$

However, (10.47) shows that the Lagrangian function that appears in Fermat's principle (10.4) does not satisfy (11.1), whereas this condition is satisfied by the Lagrangian function (10.49). Consequently, we develop the Hamiltonian formalism starting from (10.49) and the associate Lagrange equations (10.50).

First, we again suppose that it is possible to introduce a coordinate frame in which all of the rays of interest can be represented by the parametric equations (10.48). In this hypothesis, the two independent Lagrangian equations are written in the form (10.50), where the Lagrangian $L(x_\alpha, \dot{x}_\alpha, x_3)$, $\alpha = 1, 2$, is given by (10.49) and ***the dot expresses the derivation with respect to the variable*** x_3.

As usual, the kinetic momenta are defined by the relations

$$p_\alpha = \frac{\partial L}{\partial \dot{x}_\alpha} = N \frac{\dot{x}_\alpha}{\sqrt{1 + \dot{x}_1^2 + \dot{x}_2^2}}. \tag{11.2}$$

© Springer International Publishing Switzerland 2016

A. Romano and R. Cavaliere, *Geometric Optics*,
Modeling and Simulation in Science, Engineering and Technology,
DOI 10.1007/978-3-319-43732-3_11

Before introducing the Hamiltonian function, we must express the quantities $\dot{x}_\alpha$ in terms of p_α. Since

$$p_3^2 = N^2 - p_1^2 - p_2^2 = \frac{N^2}{1 + \dot{x}_1^2 + \dot{x}_2^2},$$

we have

$$\frac{N}{\sqrt{1 + \dot{x}_1^2 + \dot{x}_2^2}} = \sqrt{N^2 - p_1^2 - p_2^2}. \tag{11.3}$$

Therefore, (11.2) lead us to the relations

$$\dot{x}_\alpha = \frac{p_\alpha}{\sqrt{N^2 - p_1^2 - p_2^2}}. \tag{11.4}$$

On the other hand, $L = N\sqrt{1 + \dot{x}_1^2 + \dot{x}_2^2}$ and the Hamiltonian function is

$$H(x_\alpha, p_\alpha, x_3) = \sum_{\alpha=1}^{2} p_\alpha \dot{x}_\alpha - L = -\sqrt{N^2 - p_1^2 - p_2^2}. \tag{11.5}$$

Finally, in the present case, Hamilton's equations

$$\dot{x_\alpha} = \frac{\partial H}{\partial p_\alpha},$$
$$\dot{p_\alpha} = -\frac{\partial H}{\partial x_\alpha},$$

assume the following form

$$\dot{x_\alpha} = \frac{p_\alpha}{\sqrt{N^2 - p_1^2 - p_2^2}}, \tag{11.6}$$

$$\dot{p_\alpha} = \frac{N}{\sqrt{N^2 - p_1^2 - p_2^2}} \frac{\partial N}{\partial x_\alpha}. \tag{11.7}$$

whereas the jump conditions (10.50) in the Hamiltonian formalism become

$$[[p_\alpha]] = \lambda n_\alpha. \tag{11.8}$$

Again we find that, provided that the refractive index is constant, the rays are straight lines.

11.2 Hamilton's Principal Functions

This section is devoted to the ***principal or characteristic functions*** introduced by Hamilton to study an optical system (see [23]). Knowledge of one of these functions allows us to perform a complete analysis of the aberrations in an optical system. Unfortunately, exact knowledge of them is not possible. However, this fact does not mean that these functions have no practical value. Indeed, it is possible to obtain approximate expressions for them. In particular, Gaussian optics is obtained from their first approximation. Moreover, their second approximation leads to the third-order aberration theory; their third-order approximation to fifth-order aberration theory, and so on. However, the calculations needed to attain more accurate approximations of the Hamiltonian principal functions become so complex that only the first two approximations are actually useful.

There are also other advantages of using the principal functions:

- We noted in Chapter 10 that Maupertuis' principle, which describes mechanical systems, is analogous to Fermat's principle in Optics. Consequently, Jacobi proposed that the principal functions could also be applied in Mechanics. This approach led to the famous Hamilton–Jacobi theory of canonical transformations, from which very important results were derived.
- Using the principal functions and Noether's theorem, we can easily recognize the implications of symmetries in an optical system.

We recall that the ***object space*** is a term used to denote the region (containing the object) that the optical system forms the image of. The light originates from this region and by convention it is assumed to be situated on the left-hand side of the optical system. Similarly, the ***image space*** is the region containing the image formed by the optical system. It may coincide with the object space, for example, in the reflecting systems we analyzed in previous chapters.

Practically speaking, it may be convenient to refer the object and image spaces using either the same coordinate system $Ox_1x_2x_3$ or two different frames, $Ox_1x_2x_3$ and $Ox_1'x_2'x_3'$.

In order to introduce the first principal function, we suppose that:

for any pair of points $\mathbf{x}$ ***and*** $\mathbf{x}'$ ***where the former occurs in the object space and the latter in the image space, there is one ray*** γ ***that has these points as end points***.

In other words, we are assuming that there are no pairs of stigmatic points in the above regions. This hypothesis implies that the optical path length $OPL(\gamma_0)$ along a ray depends only on the end points selected, since the ray γ_0 is uniquely determined by these points.

The ***point principal function*** is defined as follows:

$$V(x_i, x_j') = OPL(\gamma_0), \tag{11.9}$$

where (x_i) and (x_j') denote the coordinates of $\mathbf{x}$ and $\mathbf{x}'$, respectively, and *the optical path length is evaluated along the unique ray* γ_0 *that connects them.*

To illustrate the importance of the point principal function V, we need to evaluate its differential with respect to the points (x_i) and (x'_j). To this end, it is sufficient to take into account the one-parameter family Δ of curves with variable end points (see (10.12) and (10.13)), and to calculate the differential of the function $I(\epsilon)$ (see (10.11)) at $\epsilon = 0$; in other words, we need to use (10.33) *for a family of rays*. From (10.33), and taking (10.36) into account, we have:

$$dV = \frac{\partial V}{\partial x_i} dx_i + \frac{\partial V}{\partial x'_i} dx'_i = -\frac{\partial L}{\partial \dot{x}_i} dx_i + \frac{\partial L}{\partial \dot{x}'_i} dx'_i \tag{11.10}$$

In turn, owing to the arbitrary nature of the variations dx_i and dx'_i, this relation implies the equations

$$\frac{\partial V}{\partial x_i} = -\frac{\partial L}{\partial \dot{x}_i}, \quad \frac{\partial V}{\partial x'_i} = \frac{\partial L}{\partial \dot{x}'_i}, \tag{11.11}$$

which, due (10.28) and (10.38), assume the form

$$p_i = -\frac{\partial V}{\partial x_i} = p_i(x_i, x'_i), \tag{11.12}$$

$$p'_i = \frac{\partial V}{\partial x'_i} = p'_i(x_i, x'_i), \tag{11.13}$$

where the usual notation

$$p_i = N t_i.$$

has been used. The system corresponding to (11.12), (11.13) applies to any pair of points where one occurs in the object space and the other in the image space; the direction of the unique ray that connects them is $\mathbf{p}$ or $\mathbf{p}'$, respectively. We remark that (11.12), (11.13) are not independent since the following identities hold

$$\mathbf{p} \cdot \mathbf{p} = N^2, \quad \mathbf{p}' \cdot \mathbf{p}' = N'^2, \tag{11.14}$$

which can also be written as follows due to (11.12), (11.13):

$$\sum_{i=1}^{3} \left(\frac{\partial V}{\partial x_i} \right)^2 = N^2, \quad \sum_{i=1}^{3} \left(\frac{\partial V}{\partial x'_i} \right)^2 = N'^2. \tag{11.15}$$

We conclude that V is a solution of the eikonal equation in both the object and image spaces.

Suppose that the first two equations of (11.12) and the first two equations of (11.13),

$$p_\alpha = -\frac{\partial V}{\partial x_\alpha} = p_\alpha(x_\beta, x'_\beta, x_3, x'_3), \tag{11.16}$$

$$p'_\alpha = \frac{\partial V}{\partial x'_\alpha} = p'_\alpha(x_\beta, x'_\beta, x_3, x'_3), \quad \alpha = 1, 2, \tag{11.17}$$

form a system of 4 independent equations; in other words that the following condition is satisfied:

$$\det\left(\frac{\partial^2 V}{\partial x_\alpha \partial x'_\beta}\right) \neq 0. \tag{11.18}$$

In this hypothesis, the variables x'_β can be obtained from system (11.16). Upon substituting these variables into (11.17), the system corresponding to (11.16), (11.17) assumes the form

$$x'_\alpha = x'_\alpha(x_\beta, p_\beta, x_3, x'_3), \tag{11.19}$$

$$p'_\alpha = p'_\alpha(x_\beta, p_\beta, x_3, x'_3). \tag{11.20}$$

Now let $x_3 = \overline{x}_3$ and $x'_3 = \overline{x}'_3$ be two planes in the object space and in the image space, respectively, which are assumed to have no pairs of stigmatic points. These planes are called the ***anterior base plane*** and the ***posterior base plane***, respectively.

We can say that:

(11.19), (11.20) ***define a correspondence such that any particular point*** (x_α) ***in the anterior base plane*** $x_3 = \overline{x}_3$ ***and any particular ray direction*** p_α ***at this point is associated with only one point*** (x'_α) ***in the posterior base plane*** $x'_3 = \overline{x}'_3$ ***and only one ray direction at*** $(x'_\alpha, \overline{x}'_3)$.

We note that V cannot be used when the planes x_3 and x'_3 contain stigmatic points. If that happens, we can resort to other principal functions.

The ***angular function*** is defined as follows:

$$T = V + \mathbf{p} \cdot \mathbf{x} - \mathbf{p}' \cdot \mathbf{x}'. \tag{11.21}$$

If the media in the object and image spaces are homogeneous, a simple meaning can be attributed to the angular function T. Let r and r' lines that come from O and at O', respectively, and that are also perpendicular to the rays γ and γ' that emerge from A and A', respectively; denote by Q and Q' the intersection points of r and r' with γ and γ', respectively. Noting the meaning of V, we recognize that T coincides with the optical path length along the ray $QAA'Q'$ (see Figure 11.1)

From (11.10) and (11.21), we obtain

$$dT = \mathbf{x} \cdot d\mathbf{p} - \mathbf{x}' \cdot d\mathbf{p}', \tag{11.22}$$

where the variations $d\mathbf{p}$ and $d\mathbf{p}'$ are not arbitrary since (11.14) imply the conditions:

$$\mathbf{p} \cdot d\mathbf{p} = 0, \quad \mathbf{p}' \cdot d\mathbf{p}' = 0. \tag{11.23}$$

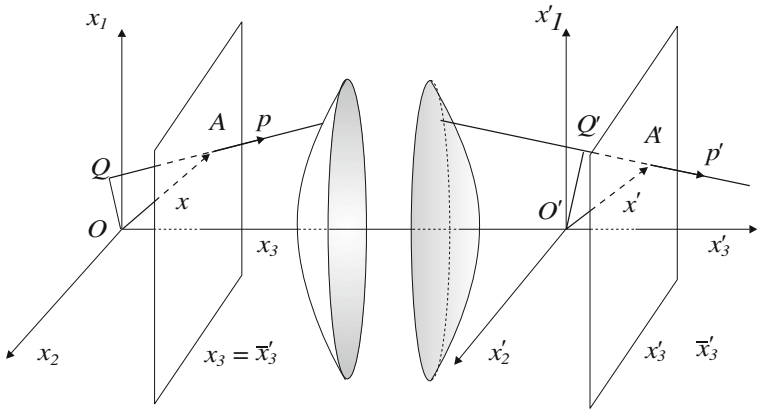

Fig. 11.1 Angular function

Consequently,

$$dp_3 = -\frac{1}{p_3}\sum_{\alpha=1}^{2} p_\alpha dp_\alpha, \quad dp'_3 = -\frac{1}{p'_3}\sum_{\alpha=1}^{2} p'_\alpha dp'_\alpha, \tag{11.24}$$

so that, substituting these expressions into (11.22), the following relation is obtained

$$dT = \sum_{\alpha=1}^{2}\left[\left(x_\alpha - \frac{p_\alpha}{p_3}x_3\right)dp_\alpha - \left(x'_\alpha - \frac{p'_\alpha}{p'_3}x'_3\right)dp'_\alpha\right], \tag{11.25}$$

where the variations dp_α and dp'_α are now arbitrary. Then, one obtains

$$x_\alpha = \frac{p_\alpha}{p_3}x_3 + \frac{\partial T}{\partial p_\alpha}, \tag{11.26}$$

$$x'_\alpha = \frac{p'_\alpha}{p'_3}x'_3 - \frac{\partial T}{\partial p'_\alpha}. \tag{11.27}$$

In conclusion, if the angular function $T(p_\alpha, p_\alpha)$ is known and x_3, x'_3 are fixed, the equations (11.26), (11.27) associate to any pair of directions $\mathbf{p}$, $\mathbf{p}'$ the points $\mathbf{x}$ and $\mathbf{x}'$, at which the considered rays intersect the anterior and posterior base planes.

Similarly, the ***mixed functions*** can be defined in the following way

$$W_1 = V + \mathbf{p}\cdot\mathbf{x}, \quad W_2 = V - \mathbf{p}'\cdot\mathbf{x}', \tag{11.28}$$

where W_1 and W_2 denote the optical paths QA' and AQ' respectively (see Figure 11.1).

From (11.21) and the above relations, we obtain

$$dW_1 = -\mathbf{x} \cdot \mathbf{dp} + \mathbf{p}' \cdot \mathbf{dx}', \tag{11.29}$$

$$dW_2 = -\mathbf{dx} \cdot \mathbf{p} - \mathbf{dp}' \cdot \mathbf{x}'. \tag{11.30}$$

When the constraints (11.24), which the variations $d\mathbf{p}$ and $d\mathbf{p}'$ must satisfy, are taken into account and the posterior base plane is fixed, from (11.29), (11.30) the following relations are derived

$$x_\alpha = \frac{p_\alpha}{p_3} x_3 - \frac{\partial W_1}{\partial p_\alpha}, \tag{11.31}$$

$$p'_\alpha = \frac{\partial W_1}{\partial x'_\alpha}. \tag{11.32}$$

$$x'_\alpha = \frac{p'_\alpha}{p'_3} x'_3 + \frac{\partial W_2}{\partial p'_\alpha}, \tag{11.33}$$

$$p_\alpha = -\frac{\partial W_2}{\partial x_\alpha}. \tag{11.34}$$

About the systems (11.31), (11.32) and (11.33), (11.34) the same considerations relative to the system (11.26), (11.27) can be repeated. Finally, we have to remark that also for the functions T, W_1, and W_2 anomalous situations exist. In fact, if happens that, for fixed $\mathbf{p}$ and $\mathbf{p}'$, infinite pairs of points $\mathbf{x}$ and $\mathbf{x}'$ exist satisfying (11.26), (11.27) (telescopic systems), then the function T can not be used. Similarly, if to a fixed pair $\mathbf{x}$, $\mathbf{p}'$, system (11.31), (11.32) associates infinite pairs $\mathbf{p}$, $\mathbf{x}'$ (focal point in the object plane), the function W_1 can not be used. A similar situation holds for W_2.

11.3 Symmetries and Characteristic Functions

From now on, an optical system $\mathbb{S}$ is considered having a symmetry axis a, which is called the **optical axis** of the system. In this section the restrictions relative to the characteristic functions, which derive from the axial symmetry, are analyzed. Moreover, for such a kind of systems, a further symmetry is considered with respect to a plane which is orthogonal to a (reversible systems).

Let $\mathbf{Q}$ any orthogonal matrix describing a rotation around a and $[\mathbf{Q}]_a$ the set of these matrices. Then, the above symmetry property is equivalent to the condition that any function $F(\mathbf{u}_1, \ldots, \mathbf{u}_n)$ of the vector variables $\mathbf{u}_1, \ldots, \mathbf{u}_n$ verifies the condition

$$F(\mathbf{u}_1, \ldots, \mathbf{u}_n) = F(\mathbf{Q}\mathbf{u}_1, \ldots, \mathbf{Q}\mathbf{u}_n), \quad \forall \mathbf{Q} \in [\mathbf{Q}]_s. \tag{11.35}$$

If $\mathbf{u}_i^{\perp}$ is the component of the vector $\mathbf{u}_i$ orthogonal to a and $\mathbf{u}_i^{\parallel}$ denotes the component parallel to s, in Algebra it is proved that (11.35) is satisfied if and only if

$$F(\mathbf{u}_1, \ldots, \mathbf{u}_n) = F(|\mathbf{u}_i^{\perp}|, \mathbf{u}_i^{\perp} \cdot \mathbf{u}_j^{\perp}, \mathbf{u}_i^{\parallel}). \tag{11.36}$$

For a system with axial symmetry, the axis a is a ray for the optical system $\mathbb{S}$. In the sequel, the axis Ox_3 of the frame of reference $Ox_1x_2x_3$ in the object space will be chosen coinciding with a. In the image space, the same frame of reference will be adopted or, equivalently, another frame Ox_1', x_2', x_3' having the axis Ox_3' coinciding with Ox_3 and the other two axes parallel to the corresponding axes of $Ox_1x_2x_3$ (see Figure 11.1). As a consequence of this choice of the reference axes, the refractive index $N(\mathbf{x})$ must verify the condition

$$N(\mathbf{x}) = N(u, x_3), \quad u = x_1^2 + x_2^2. \tag{11.37}$$

Moreover, if $V(\mathbf{x}, \mathbf{x}')$ is the principal point function of an optical system $\mathbb{S}$ having an axial symmetry around a, in the aforesaid coordinates we have

$$V(x_1, x_2, x_3, x_1', x_2', x_3') = V(u, u', x_3, x_3'), \tag{11.38}$$

where

$$u = x_1^2 + x_2^2, \quad u' = {x_1'}^2 + {x_2'}^2, \quad w = x_1x_1' + x_2x_2'. \tag{11.39}$$

Similar considerations can be repeated for the other principal functions. For instance, for the angular function, it results

$$T(\mathbf{p}, \mathbf{p}') = T(\xi, \xi', \eta), \tag{11.40}$$

where

$$\xi = p_1^2 + p_2^2, \quad \xi' = {p_1'}^2 + {p_2'}^2, \quad \eta = p_1p_1' + p_2p_2'. \tag{11.41}$$

Note that p_3 and p_3' do not explicitly appear on the right hand side of (11.40) since $p_3^2 = N^2 - (p_1^2 + p_2^2) = N^2 - \xi^2$ and a similar relation holds for p_3'.

An optical system $\mathbb{S}$ with axial symmetry is said to be **reversible** if a symmetry plane π, orthogonal to a, exists (see Figure 11.1) (Fig. 11.2).

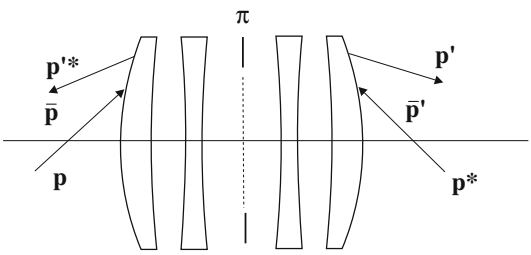

Fig. 11.2 Reversible optical system

Let γ be a ray determined by the pair $\mathbf{p} = (p_1, p_2, p_3)$ and $\mathbf{p}' = (p_1', p_2', p_3')$. Its mirror-like reflection with respect to π is again a ray γ^* determined by $\mathbf{p}^* = (p_1, p_2, -p_3)$ in the image space, now interpreted as object space, and by $\mathbf{p}^{*\prime} = (p_1^{*\prime}, p_2^{*\prime}, -p_3^{*\prime})$ in the object space, now regarded as image space. Owing to the reversibility of rays, γ can be covered in the opposite direction so that the pair $\overline{\mathbf{p}} = -\mathbf{p}^{*\prime} = (-p_1', -p_2', -p_3')$ again characterizes a ray $\overline{\mathbf{p}}' = -\mathbf{p}^* = (-p_1, -p_2, -p_3)$. By applying the reversibility condition to (11.40), one has

$$T(\xi, \xi', \eta) = T(\xi', \xi, \eta), \tag{11.42}$$

i.e., $T(\xi, \xi', \eta)$ is symmetric with respect the exchange of variables ξ and ξ'.

11.4 Lagrange's Optical Invariant for Axially Symmetric Systems

Let $\mathbb{S}$ be an axially symmetric system with optical axis a. Moreover, by

$$\mathbf{x}^* = \phi(\epsilon, \mathbf{x}), \tag{11.43}$$

is denoted the one-parameter group of rotations of $\mathbb{S}$ around a. Here, the parameter is the rotation angle ϵ. If the axes of the frames $Ox_1x_2x_3$ and $O'x_1'x_2'x_3'$ are chosen as in the previous section, i.e., with Ox_3 and $O'x_3'$ coinciding with a and the planes Ox_1x_2 and $O'x_1'x_2'$ orthogonal to a, the transformations (11.43) rotate the components of $\mathbf{x}$ and $\mathbf{x}'$, orthogonal to a, and do not modify the components parallel to a.

Owing to the symmetry, the principal point function $V(\mathbf{x}, \mathbf{x}')$ must verify the condition

$$V(\mathbf{x}^\perp, \mathbf{x}'^\perp, \overline{x}_3, \overline{x}_3') = V(\phi(\epsilon, \mathbf{x}^\perp), \phi(\epsilon, \mathbf{x}'^\perp), \overline{x}_3, \overline{x}_3'), \tag{11.44}$$

for any angle ϵ. Explicitly, the rotation group (11.43) around a is expressed by the following relations

$$x_1^* = x_1 \cos\epsilon + x_2 \sin\epsilon, \tag{11.45}$$

$$x_2^* = -x_1 \sin\epsilon + x_2 \cos\epsilon, \tag{11.46}$$

so that

$$\left(\frac{dx_1^*}{d\epsilon}\right)_{\epsilon=0} = x_2^*, \quad \left(\frac{dx_2^*}{d\epsilon}\right)_{\epsilon=0} = -x_1^*. \tag{11.47}$$

Differentiating (11.44) with respect to ϵ and evaluating the result at $\epsilon = 0$, the following relation is obtained

$$\frac{\partial V}{\partial x_1} x_2 - \frac{\partial V}{\partial x_2} x_1 + \frac{\partial V}{\partial x_1'} x_2' - \frac{\partial V}{\partial x_2'} x_1' = 0. \tag{11.48}$$

Reminding (11.12), (11.13), the above equation becomes

$$I \equiv p_2 x_1 - p_1 x_2 = p_2' x_1' - p_1' x_2'. \tag{11.49}$$

The quantity I is **Lagrange's optical invariant** since its value is constant in crossing the whole optical system (see Section 9.3 to take into account the discontinuities of the refractive index).

It is evident that the obtained result is independent of the used principal function. For example, if the angular function T is used, instead of (11.44), (11.45), (11.46), (11.47) and (11.49), we have the following equations

$$T(\mathbf{p}^{\perp}, \mathbf{p}'^{\perp}) = T(\phi(\epsilon, \mathbf{p}^{\perp}), \phi(\epsilon, \mathbf{p}'^{\perp})), \tag{11.50}$$

$$p_1^* = p_1 \cos\epsilon + p_2 \sin\epsilon, \tag{11.51}$$

$$p_2^* = -p_1 \sin\epsilon + p_2 \cos\epsilon, \tag{11.52}$$

$$\left(\frac{dp_1^*}{d\epsilon}\right)_{\epsilon=0} = p_2^*, \quad \left(\frac{dp_2^*}{d\epsilon}\right)_{\epsilon=0} = -p_1^*. \tag{11.53}$$

$$\frac{\partial T}{\partial p_1} p_2 - \frac{\partial T}{\partial p_2} p_1 + \frac{\partial T}{\partial p_1'} p_2' - \frac{\partial T}{\partial p_2'} p_1' = 0. \tag{11.54}$$

Then, because of (11.26) and (11.27), we again derive (11.49).

11.5 Hamiltonian Equations and Primary Aberrations

In the next chapter the primary aberrations will be analyzed starting from *Hamilton's principal functions*. In this section we present Luneburg's approach to aberrations (see [1]) which is based on *Hamilton's equations*.[1] This approach presents many advantages over the traditional method based on the characteristic functions:

- It is simpler to apply;
- Unlike the method based on the principal functions (see Chapter 12), Hamilton's equations can always be applied;
- It holds also for optical systems having variable refractive indices;
- The additivity of the primary aberrations is a consequence of the additivity of the integral.

This approach is based on the expansion of the Hamilton function H supposing that the refractive index is continuous. This assumption is not verified by the usual optical systems for which the refractive index is constant between two optical surfaces

[1] see also [48], [49].

but changes crossing any surface. However, we show that this case can be obtained as a limit of the continuous case.

Let $\mathbb{S}$ be an optical system with a symmetry of revolution about the axis a. Introduce a Cartesian frame of reference $Ox_1x_2x_3$ with the axis $Ox_3 \equiv a$. Then, the symmetry of revolution of $\mathbb{S}$ about a and the continuity of the refractive index N imply that N is a continuous function of $u = x_1^2 + x_2^2$ and x_3. Consequently, the Hamilton function (11.5) of $\mathbb{S}$ assumes the form

$$H = -\sqrt{N^2(u, x_3) - v}, \tag{11.55}$$

where $v = p_1^2 + p_2^2$. If $N(u, x_3)$ is supposed to be an analytic function of u, we can consider the first terms of Taylor's expansion of H with respect to u and v

$$H = H_0 + H_u u + H_v v + \frac{1}{2} H_{uu} u^2 + H_{uv} uv + \frac{1}{2} H_{vv} v^2, \tag{11.56}$$

where

$$H_0 = -N(0, x_3) \equiv -N(x_3), \quad H_u = -N_u(x_3), \tag{11.57}$$

$$H_v = \frac{1}{2N(x_3)}, \quad H_{uu} = -N_{uu}(x_3), \tag{11.58}$$

$$H_{vv} = \frac{1}{4N^3(x_3)}, \quad H_{uv} = -\frac{N_u(x_3)}{2N^2(x_3)}. \tag{11.59}$$

Introducing the expansion (11.56) into (11.6), (11.7), we obtain the approximate form of Hamilton's equations

$$x_1' = 2H_v p_1 + 2H_{vv} p_1 v^2 + 2H_{uv} p_1 u^2, \tag{11.60}$$

$$x_2' = 2H_v p_2 + 2H_{vv} p_2 v^2 + 2H_{uv} p_2 u^2, \tag{11.61}$$

$$p_1' = -2H_u x_1 - 2H_{uv} x_1 v^2 - 2H_{uu} x_1 u^2, \tag{11.62}$$

$$p_2' = -2H_u x_2 - 2H_{uv} x_2 v^2 - 2H_{uu} x_2 u^2. \tag{11.63}$$

We now suppose that the solutions of Hamilton's equations admit a Taylor expansion

$$x_\alpha(x_3) = \epsilon x_\alpha^{(1)}(x_3) + \epsilon^3 x_\alpha^{(3)}(x_3) + \cdots, \tag{11.64}$$

$$p_\alpha(x_3) = \epsilon p_\alpha^{(1)}(x_3) + \epsilon^3 p_\alpha^{(3)}(x_3) + \cdots, \tag{11.65}$$

where $\alpha = 1, 2$ and the auxiliary parameter ϵ has the only aim to specify the degree of its factors and it will be posed equal to one at the end of the calculations. When (11.64), (11.65) are introduced into (11.60)–(11.63), (11.60)–(11.63) are taken into account, and we match the terms that are multiplied by the same power of ϵ, we obtain the following equations

$$x_1^{(1)'} = 2H_v p_1^{(1)}, \tag{11.66}$$
$$x_2^{(1)'} = 2H_v p_2^{(1)}, \tag{11.67}$$

$$p_1^{(1)'} = -2H_u x_1^{(1)}, \tag{11.68}$$
$$p_2^{(1)'} = -2H_u x_2^{(1)}, \tag{11.69}$$

for the first-order quantities $x_\alpha^{(1)}$, $p_\alpha^{(1)}$ and the equations

$$x_1^{(3)'} = 2H_v p_1^{(3)} + 2H_{vv} p_1^{(1)} v^2 + 2H_{uv} p_1^{(1)} u^2, \tag{11.70}$$
$$x_2^{(3)'} = 2H_v p_2^{(3)} + 2H_{vv} p_2^{(1)} v^2 + 2H_{uv} p_2^{(1)} u^2, \tag{11.71}$$

$$p_1^{(3)'} = -2H_u x_1^{(3)} - 2H_{uv} x_1^{(1)} v^2 - 2H_{uu} x_1^{(1)} u^2, \tag{11.72}$$
$$p_2^{(3)'} = -2H_u x_2^{(3)} - 2H_{uv} x_2^{(1)} v^2 - 2H_{uu} x_2^{(1)} u^2, \tag{11.73}$$

determining the third-order quantities $x_\alpha^{(3)}$, $p_\alpha^{(3)}$.

Equations (11.66)–(11.69) and (11.70)–(11.73) are *linear* ODEs with *variable* coefficients depending on x_3. Further, system (11.66)–(11.69) is homogeneous and its solutions supply the first-order terms $x_\alpha^{(1)}$, $p_\alpha^{(1)}$. System (11.70)–(11.73) is nonhomogeneous but it has the same form of system (11.66)–(11.69) and the nonhomogeneous terms are known functions of x_3 once the first-order solutions are determined.

The general integral of (11.66)–(11.69) depends on x_3 and four arbitrary constants. These constants can be determined by either an initial value problem, in which we assign the initial point and the initial direction of a ray, or by a boundary value problem, in which we give two points belonging to a ray. We must note that the application of this second method requires that the boundary value problem admits one solution and this circumstance could not be verified since the refractive index into (11.66)–(11.69) is not constant but depends on x_3. The same considerations hold for system (11.70)–(11.73). However, for this system we can adopt *homogeneous* initial or boundary conditions if the initial or boundary data of a ray are associated with system (11.66)–(11.69). We now search for two independent solutions of (11.66)–(11.69) that correspond to a marginal ray and a principal ray. We consider a marginal ray starting from the point $(0, 0, z_1)$ of the object plane and intercepting the plane $x_3 = w_e$ of the entrance pupil at the point $(x_1^{(e)}, x_2^{(e)})$. The parametric equations of this ray are

$$x_1^{(1)} = x_1^{(e)} h(x_3), \tag{11.74}$$
$$x_2^{(1)} = x_2^{(e)} h(x_3), \tag{11.75}$$
$$p_1^{(1)} = x_1^{(e)} \vartheta(x_3), \tag{11.76}$$
$$p_2^{(1)} = x_2^{(e)} \vartheta(x_3), \tag{11.77}$$

where the function $h(x_3)$ verifies the boundary conditions

$$h(z_1) = 0, \quad h(w_e) = 1. \tag{11.78}$$

Functions (11.74)–(11.77) are a solution of system (11.66)–(11.69) if

$$h' = 2H_v\vartheta, \tag{11.79}$$
$$\vartheta' = -2H_u h. \tag{11.80}$$

These equations imply that $\vartheta = h'/2H_v$ and h is a solution of the following linear boundary value problem

$$h'' = -4H_u H_v h, \tag{11.81}$$
$$h(z_1) = 0, \quad h(w_e) = 1, \tag{11.82}$$

where the coefficient $-4H_u H_v$ depends on x_3.

We can now consider the principal ray starting from the point $(x_1^{(0)}, x_2^{(0)}, z_1)$ of the object plane and intersecting the entrance pupil at the point $(0, 0, w_e)$. Its parametric equations are

$$X_1^{(1)} = x_1^{(0)} k(x_3), \tag{11.83}$$
$$X_2^{(1)} = x_2^{(0)} k(x_3), \tag{11.84}$$
$$P_1^{(1)} = x_1^{(0)} \theta(x_3), \tag{11.85}$$
$$P_2^{(1)} = x_2^{(0)} \theta(x_3), \tag{11.86}$$

where the function k verifies the boundary conditions

$$k(z_1) = 1, \quad k(w_e) = 0. \tag{11.87}$$

We have again

$$k' = 2H_v\theta, \tag{11.88}$$
$$\theta' = -2H_u k, \tag{11.89}$$

$\theta = k'/2H_v$ and k is a solution of the boundary value problem

$$k'' = -4H_u H_v k, \tag{11.90}$$
$$k(z_1) = 1, \quad k(w_e) = 0. \tag{11.91}$$

Since system (11.66)–(11.69) is linear, the functions

$$x_1^{(1)} = x_1^{(0)} k(x_3) + x_1^{(e)} h(x_3), \tag{11.92}$$
$$x_2^{(1)} = x_2^{(0)} k(x_3) + x_2^{(e)} h(x_3), \tag{11.93}$$
$$p_1^{(1)} = x_1^{(0)} \theta(x_3) + x_1^{(e)} \vartheta(x_3), \tag{11.94}$$
$$p_2^{(1)} = x_1^{(0)} \theta(x_3) + x_2^{(e)} \vartheta(x_3), \tag{11.95}$$

are a solution of (11.66)–(11.69) verifying the boundary data (11.78) and (11.91).

We conclude this section proving a generalization of optical invariant (2.62). Consider Equations (11.66), (11.68) relative to the marginal ray

$$x_1^{(1)\prime} = \frac{1}{N} p_1^{(1)}, \quad p_1^{(1)\prime} = -2N_u x_1^{(1)}, \tag{11.96}$$

and to the axial ray

$$X_1^{(1)\prime} = \frac{1}{N} P_1^{(1)}, \quad P_1^{(1)\prime} = -2N_u X_1^{(1)}, \tag{11.97}$$

We conclude from (11.96), (11.97) that

$$x_1^{(1)} P_1^{(1)\prime} - X_1^{(1)} p_1^{(1)\prime} = 0, \tag{11.98}$$

$$P_1^{(1)} x_1^{(1)\prime} - p_1^{(1)} X_1^{(1)\prime} = 0, \tag{11.99}$$

and hence

$$(X_1^{(1)} p_1^{(1)} - x_1^{(1)} P_1^{(1)})' = 0.$$

It follows that the determinant

$$\hat{\Gamma} = \det \begin{pmatrix} X_1^{(1)} & P_1^{(1)} \\ x_1^{(1)} & p_1^{(1)} \end{pmatrix}, \tag{11.100}$$

relative to the principal and axial rays is constant along the optical axis. Taking into account (11.74)–(11.77) and (11.83)–(11.86), we can write (11.100) as follows

$$x_1^{(e)} y_1 (k\vartheta - h\theta) = x_1^{(e)} y_1 M \vartheta(z_n') \tag{11.101}$$

since on the image plane, i.e., when $x_3 = z_n'$, it is $h(z_n') = 0$ and $k(z_n') = M$, where M is the magnification of the optical system. Finally, introducing the notation $\Gamma = \hat{\Gamma}/(x_1^{(e)} y_1)$, we have that

$$\Gamma = k\vartheta - h\theta = M\vartheta(z_n'). \tag{11.102}$$

11.6 Equations of Primary Aberrations

In this section we search for a solution of equations (11.70)–(11.73) satisfying the homogeneous boundary data:

$$x_1^{(3)}(z_1) = x_1^{(3)}(w_e) = 0, \quad x_2^{(3)}(z_1) = x_2^{(3)}(w_e) = 0. \tag{11.103}$$

We first consider equations (11.70) and (11.79) and take into account (11.58):

$$x_1^{(3)'} - \frac{p_1^{(3)}}{N} = 2(H_{vv}v^2 + H_{uv}u^2)p_1^{(1)}, \tag{11.104}$$

$$h' = \frac{1}{N}\vartheta, \tag{11.105}$$

From these equations it follows that

$$x_1^{(3)'}\vartheta - hp_1^{(3)} = 2f(H_{vv}v^2 + H_{uv}u^2)p_1^{(1)}\vartheta. \tag{11.106}$$

In a similar way, from the equations (11.85) and (11.80)

$$p_1^{(3)'} + N_u x_1^{(3)} = -2(H_{uu}u^2 + H_{uv}v^2)x_1^{(1)}, \tag{11.107}$$

$$\vartheta' = N_u h, \tag{11.108}$$

we conclude that

$$x_1^{(3)}\vartheta' - hp_1^{(3)'} = 2(H_{uu}u + H_{uv}v)x_1^{(1)}h. \tag{11.109}$$

By adding (11.106) and (11.107), we finally obtain

$$\frac{d}{dx_3}(x_1^{(3)}\vartheta - hp_1^{(3)}) = 2(H_{uv}u + H_{vv}v)p_1^{(1)}\vartheta + 2(H_{uu}u + H_{uv}v)x_1^{(1)}h. \tag{11.110}$$

We integrate this equation from z_1 and z_n' and make use of the conditions $x_1^{(3)}(z_1) = h(z_1) = h(z_n') = 0$. In this way, we obtain

$$x_1^{(3)}(z_n')\vartheta(z_n') = 2\int_{z_1}^{z_n'}[(H_{uv}u^2 + H_{vv}v^2)p_1^{(1)}\vartheta + (H_{uu}u^2 + H_{uv}v^2)x_1^{(1)}h]dx_3, \tag{11.111}$$

and

$$x_2^{(3)}(z_n')\vartheta(z_n') = 2\int_{z_1}^{z_n'}[(H_{uv}u^2 + H_{vv}v^2)p_2^{(1)}\vartheta + (H_{uu}u^2 + H_{uv}v^2)x_2^{(1)}h]dx_3. \tag{11.112}$$

In view of (11.102) we can write the last two equations as follows

$$x_1^{(3)}(z_n') = \frac{2M}{\Gamma}\int_{z_1}^{z_n'}[(H_{uv}u^2 + H_{vv}v^2)p_1^{(1)}\vartheta + (H_{uu}u^2 + H_{uv}v^2)x_1^{(1)}h]dx_3, \tag{11.113}$$

$$x_2^{(3)}(z_n') = \frac{2M}{\Gamma}\int_{z_1}^{z_n'}[(H_{uv}u^2 + H_{vv}v^2)p_2^{(1)}\vartheta$$

$$+ (H_{uu}u^2 + H_{uv}v^2)x_2^{(1)}h]dx_3. \tag{11.114}$$

The right hand sides become third order polynomial of $x_1^{(0)}$, $x_2^{(0)}$, $x_1^{(e)}$, $x_2^{(e)}$ if $x_1^{(1)}$, $x_2^{(1)}$, $p_1^{(1)}$, $p_1^{(1)}$ are substituted by (11.92)–(11.95). In fact, it is

$$u = k^2\mathfrak{u} + h^2\mathfrak{v} + kh\mathfrak{w}, \tag{11.115}$$

$$v = \theta^2\mathfrak{u} + \vartheta^2\mathfrak{v} + \theta\vartheta\mathfrak{w}, \tag{11.116}$$

where

$$\mathfrak{u} = x_1^{(0)2} + x_2^{(0)2}, \tag{11.117}$$

$$\mathfrak{v} = x_1^{(e)2} + x_2^{(e)2}, \tag{11.118}$$

$$\mathfrak{w} = 2(x_1^{(0)}x_1^{(e)} + x_2^{(0)}x_2^{(e)}). \tag{11.119}$$

Introducing (11.115)–(11.116) into (11.113)–(11.114), by tedious calculations, it is possible to prove that

$$\frac{x_1^{(3)}}{M} = E\mathfrak{u} + \frac{1}{3}B\mathfrak{v} + \frac{1}{2}(C - D)\mathfrak{w}, \tag{11.120}$$

$$\frac{x_2^{(3)}}{M} = D\mathfrak{u} + A\mathfrak{v} + \frac{1}{3}B\mathfrak{w}, \tag{11.121}$$

where

$$A = \frac{2}{\Gamma}\int_{z_1}^{z_n'}[H_{uu}h^4 + 2H_{uv}h^2\vartheta^2 + H_{vv}\vartheta^4]dx_3, \tag{11.122}$$

$$B = \frac{6}{\Gamma}\int_{z_1}^{z_n'}[H_{uu}h^3k + H_{uv}h\vartheta(k\vartheta + h\theta) + H_{vv}\theta\vartheta^3]dx_3, \tag{11.123}$$

$$C = \frac{6}{\Gamma}\int_{z_1}^{z_n'}[H_{uu}h^2k^2 + 2H_{uv}kh\vartheta\theta + H_{vv}\theta^2\vartheta^2]dx_3, \tag{11.124}$$

$$D = \frac{2}{\Gamma}\int_{z_1}^{z_n'}[H_{uu}h^2k^2 + H_{uv}(k^2\vartheta^2 + h^2\theta^2) + H_{vv}\theta^2\vartheta^2)]dx_3, \tag{11.125}$$

$$E = \frac{2}{\Gamma}\int_{z_1}^{z_n'}[H_{uu}hk^3 + H_{uv}k\theta(k\vartheta + h\theta) + H_{vv}\theta^3\vartheta)]dx_3, \tag{11.126}$$

and H_{uu}, H_{uv}, and H_{vv} are given by (11.58), (11.59).

If we introduce the notations

$$N(0, x_3) = N(x_3),\ \ N_u(0, x_3) = N_1(x_3),\ \ N_{uu}(0, x_3) = N_2(x_3), \tag{11.127}$$

then (11.58), (11.59) assume the form

$$H_{uu} = -N_2(x_3),\ H_{uv} = -\frac{N_1(x_3)}{2N^2},\ H_{vv} = \frac{1}{4N^3}. \tag{11.128}$$

We can now express N_1 and N_2 in terms of the geometric characteristics of the refracting surfaces of the optical system. We first note that on these surfaces it is $N(u, x_3)$ =const. Further, if $Z = g(u)$ is the equation of the refracting surface Σ containing the point x_3 on the optical axis, then the following identity holds

$$N(u, g(u)) = N(0, x_3). \tag{11.129}$$

Differentiating (11.129) with respect to u and letting $u = 0$, we obtain

$$N_1 + \dot{N}g'(0) = 0, \tag{11.130}$$
$$N_2 + 2\dot{N}_1 g'(0) + \ddot{N}(g'(0)^2 + \dot{N}g''(0) = 0. \tag{11.131}$$

On the other hand, we represent the equation $Z = g(u)$ in the neighborhood of $u = 0$ by the power expansion

$$g(u) = x_3 + \frac{u}{2R(x_3)} + \frac{c_4}{2}u^2 + \cdots. \tag{11.132}$$

where $R(x_3)$ is the radius of curvature of Σ at its vertex, and $c_4(x_3) = g''(0)$. We then obtain

$$2N_1 = -\frac{\dot{N}}{R},\ N_2 = \frac{1}{4}\left(\frac{\dot{N}}{R^2}\right)^{\cdot} - \dot{N}c_4, \tag{11.133}$$

and hence

$$H_{uu} = c_4\dot{N} - \frac{1}{4}\left(\frac{\dot{N}}{R^2}\right)^{\cdot},\ H_{uv} = -\frac{1}{4R}\left(\frac{1}{N}\right)^{\cdot},\ H_{vv} = \frac{1}{4N^3}. \tag{11.134}$$

Da (11.122)–(11.125) we obtain the condition

$$3D - C = \frac{6}{\Gamma}\int_{z_1}^{z_n'}(k\vartheta - h\theta)^2 H_{uv}dx_3 - 2\Gamma\int_{z_1}^{z_n'} H_{uv}dx_3. \tag{11.135}$$

Since $k\vartheta - h\theta = \Gamma$ and (11.134) holds we can write that

$$\frac{1}{\Gamma}(C - 3D) = \int_{z_1}^{z_n'}\frac{1}{R}d\left(\frac{1}{N}\right). \tag{11.136}$$

We have again found the Petzval equation that implies that C and D can be zero only if the Petzval sum vanishes

$$\int_{z_1}^{z_n'} \frac{1}{R} d\left(\frac{1}{N}\right) = 0. \tag{11.137}$$

11.7 The Case of Spherical Surfaces

Let us assume that the refracting surfaces are spherical. Then we have (see Chapter 1)

$$Z = g(u) = z + \frac{1}{2R}u + \frac{1}{8R^3}u^2 + \cdots \tag{11.138}$$

so that $c_4 = 1/4R^3$. Then (11.134) become

$$2H_{uu} = \frac{1}{2}\left(\frac{\dot{N}}{R^3} - \left(\frac{\dot{N}}{R^2}\right)^{\cdot}\right), \; 2H_{uv} = -\frac{1}{2}\frac{\dot{N}}{N^2 R}, \; 2H_{vv} = \frac{1}{2N^3}. \tag{11.139}$$

It is possible to simplify the integral formulae for the coefficients A, B, C, E by replacing the radius R by the data of paraxial ray h, ϑ. We have the equation

$$\dot{\vartheta} = -\frac{\dot{N}}{R}h,$$

so that

$$\frac{1}{R} = -\frac{\dot{\vartheta}}{Nh}. \tag{11.140}$$

By introducing this result into (11.139) and into the integral formulae (11.122)–(11.126) we obtain the coefficients A, B, C, E expressed by the two paraxial rays h,ϑ and k, θ and by the refractive index N on the optical axis. Defining the following quantities:

$$S = h\frac{\left[\left(\frac{\vartheta}{N}\right)^{\cdot}\right]^2 \left(\frac{\vartheta}{N^2}\right)^{\cdot}}{\left(\frac{1}{N}\right)^{\cdot}} \tag{11.141}$$

$$P = \frac{1}{R}\left(\frac{1}{N}\right)^{\cdot}, \; \omega = \frac{\left(\frac{\theta}{N}\right)^{\cdot}}{\left(\frac{\vartheta}{N}\right)^{\cdot}}, \tag{11.142}$$

it is possible to write the coefficients A, B, C, E as follows

$$A = -\frac{1}{2\Gamma}\int_{z_1}^{z_n'} S dx_3, \tag{11.143}$$

$$B = -\frac{3}{2\Gamma}\int_{z_1}^{z_n'} S\omega dx_3, \tag{11.144}$$

$$C = -\frac{3}{2\Gamma}\int_{z_1}^{z_n'} S\omega^2 dx_3 - \frac{\Gamma}{2}\int_{z_1}^{z_n'} P dx_3, \tag{11.145}$$

$$E = -\frac{1}{2\Gamma}\int_{z_1}^{z_n'} S\omega^3 dx_3 - \frac{\Gamma}{2}\int_{z_1}^{z_n'} P\omega dx_3, \tag{11.146}$$

It is interesting to evaluate the above coefficients when the refractive index is constant between two surfaces and is discontinuous across any surface of the optical system. For the details of these calculations the reader is invited to consult [1].

11.8 Recalls of Symplectic Mechanics

This section is devoted to a brief introduction to ***symplectic mechanics***. Since this topic is based on advanced tools of differential geometry, the reader is supposed to be aware of this subject.[2]

It is well known that a differentiable $n-$dimensional manifold V_n can be associated to any mechanical system S of material points or rigid bodies subjected to *fixed* and smooth constraints (see also Section 10.3). This manifold has the property that to any point $x \in V_n$ corresponds a configuration of S and viceversa. Local coordinates $(q^1, \ldots, q^n)$ on V_n are called *Lagrangian coordinates* of the mechanical system S and V_n is called the *configuration space* of S. If the Lagrangian coordinates are n, we say that S has *n degrees of freedom*.

For instance, the bar AB of Fig. 11.3 is contained in a vertical plane Oxy, has the point A constrained to move on the straight line Ox, and can rotate about an axis containing A and orthogonal to Oxy. The configuration space is a cylinder $\Re \times S^1$, x and φ are Lagrangian coordinates, and S has two degrees of freedom.

A motion of this system is described by the pair of functions $\varphi(t)$ and $x(t)$ that define a curve γ on the configuration space V_2. More generally, the motion of an arbitrary mechanical system S is described by giving the Lagrangian coordinates as functions of time $q^h(t)$, $h = 1, \ldots, n$. Again these functions are the parametric equations of a curve γ on the configuration space V_n. The components $\dot{q}^h(t)$ of

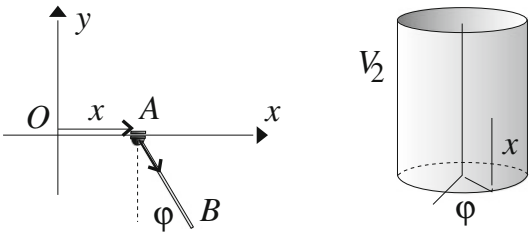

Fig. 11.3 Constrained bar

[2]The reader interested in this topic could refer to [54–60].

the tangent vector to γ (the components of Lagrangian velocity) are evaluated in the holonomic basis $(\partial/\partial q^h)$. If S is acted upon by conservative force, then the parametric equations of γ are solutions of the Lagrange equations

$$\frac{d}{dt}\frac{\partial L}{\partial \dot{q}^h} - \frac{\partial L}{\partial q^h} = 0, \tag{11.147}$$

where

$$L = T(q, \dot{q}) - U(q), \tag{11.148}$$

is the *Lagrangian function*, T the kinetic energy, and $U(q)$ the potential energy. If the auxiliary variables $v^h(t) = \dot{q}^h(t)$ are introduced, then (11.147) can be transformed into a system of $2n$ ordinary differential equations in the unknowns $v^h(t)$ and $q^h(t)$:

$$\dot{q}^h = v^h(t), \tag{11.149}$$

$$\frac{d}{dt}\frac{\partial L}{\partial v^h} - \frac{\partial L}{\partial q^h} = 0. \tag{11.150}$$

A solution $(q^h(t), v^h(t))$ of this system, that is the geometric representation of motion of S, is a curve Γ of the fiber bundle TV_n of V_n that becomes the natural space of the Lagrangian dynamics. Let X_L be the vector field on TV_n tangent to all the curves Γ_L whose parametric equations are solutions of (11.149). These curves and X_L form the *Lagrangian phase portrait* of S.

Denote by T^*V_n the cotangent bundle of V_n, that is the $2n-$dimensional manifold whose elements are the pairs (q, p), where $q \in V_n$ and $p \in T_q^*(V_n)$. This space is named the ***phase space*** of the mechanical system S. The point $q \in V_n$ is determined by the Lagrangian coordinates $(q^1, \ldots, q^n)$ and the components $(p_1, \ldots, p_n)$ of the covector p evaluated in the holonomic basis (dq^h) of $T_q^*(V_n)$.

We denote by $\mathfrak{L}$ the ***Legendre map***

$$\mathfrak{L} : TV_n \to T^*V_n \tag{11.151}$$

that in the local coordinates (q^h, v^h) of TV_n and (q^h, p_h) of T^*V_n is defined by the functions[3]

$$q^h = q^h, \tag{11.152}$$

$$p_h = \frac{\partial L}{\partial v^h}(q, v). \tag{11.153}$$

These functions define locally a diffeomorphism since it is possible to prove that in any mechanical system with fixed smooth constraints the following condition holds

[3]It is easy to verify that under a natural coordinate transformation $q' = q'(q)$ the variables p_h transform with covariance law, so that they are the components of covectors.

$$\det\left(\frac{\partial^2 L}{\partial v^h \partial v^k}\right) \neq 0. \tag{11.154}$$

The diffeomorphism (11.153) transforms the family Γ_L of curves that are solutions of (11.149), (11.150) into a family Γ_H of curves of the phase space T^*V_n. Further, the differential

$$\mathfrak{L}_* : T(TV_n) \to T(T^*V_n), \tag{11.155}$$

is a one-to-one map between the space $T(TV_n)$ of the vector fields over TV_n into the space $T(T^*V_n)$ of the vector fields over T^*V_n. It maps the vector field X_L into a vector field X_H over T^*V_n that is tangent to the curves Γ_H. It is possible to prove that the curves of Γ_H are solutions of the *Hamilton equations*

$$\dot{q}^h = \frac{\partial H}{\partial p_h}(q, p), \tag{11.156}$$

$$\dot{p}_h = -\frac{\partial H}{\partial q_h}(q, p), \tag{11.157}$$

where

$$H(q, p) = \sum_{h=1}^{n} v^h p_h - L(q, v) = T + U, \tag{11.158}$$

is the *Hamiltonian function* of the mechanical system S. In (11.157) v^h is expressed in terms of (q, p) inverting (11.153). In we introduce the skew-symmetric matrix in the natural coordinates adopted on T^*V_n

$$(\Omega_{\alpha\beta}) = \begin{pmatrix} \mathbf{0} & \mathbf{I} \\ -\mathbf{I} & \mathbf{0} \end{pmatrix}, \tag{11.159}$$

where $\mathbf{0}$ is the $n \times n$ zero matrix and $\mathbf{I}$ is the $n \times n$ unit matrix, and the notation $(x_\alpha) = (x_1, \ldots, x_{2n}) = (q, p)$, then the Hamilton equations can be written in the form

$$\dot{x}_\alpha = \Omega_{\alpha\beta} \frac{\partial H}{\partial x_\beta}. \tag{11.160}$$

We can associate a $2-$form $\mathbf{\Omega}$ to the skew-symmetric matrix $(\Omega_{\alpha\beta})$ that in natural coordinates can be written as follows

$$\mathbf{\Omega} = dq^h \wedge dp_h. \tag{11.161}$$

This $2-$form is nondegenerate, since $\det(\Omega_{\alpha\beta}) = 1$, and closed since its differential vanishes: $d\mathbf{\Omega} = \mathbf{0}$. The pair $(T^*V_n, \mathbf{\Omega})$ is called a ***symplectic manifold***. Any system of coordinates on T^*V_n in which the components of $\mathbf{\Omega}$ have the form (11.159) is said to be a *symplectic system* of coordinates. Finally, let $\Phi : T^*V_n \to T^*V_n$ be a

diffeomorfism; then, Φ is a symplectic diffeomorphism if the antiscalar product[4] of two arbitrary vectors $\mathbf{X}_x$ and $\mathbf{Y}_x$ of the tangent space $T(T^*V_n)_x$ at an arbitrary point x of T^*V_n remains constant under the diffeomorphism $\mathbf{\Phi}$:

$$\mathbf{\Omega}(\Phi_*(\mathbf{X}_x), \Phi_*(\mathbf{Y}_x)) = \mathbf{\Omega}(\mathbf{X}_x, \mathbf{Y}_x), \tag{11.162}$$

where $\mathbf{\Phi}_*$ is the differential of $\mathbf{\Phi}$.

Let U be any open region of T^*V_n and denote by $x' = \Phi_t(x)$ the solution of Hamilton's equations that starts from the arbitrary initial datum $x \in U$. If we denote by $V = \Phi_t(U)$ the image of U, then it can be proved that the diffeomorphism $\Phi_t : U \to \Phi_t(U)$ is symplectic for any value of time t. In other words, the Hamiltonian evolution $x' = \Phi_t(x)$ of a dynamical system S in the phase space T^*V_n is described by a one-parameter family of symplectic diffeomorphisms $x' = \Phi_t(x)$.

Let (q, p) and (q', p') be local coordinates in the regions U and $\Phi_t(U)$, respectively. The coordinate representation of the motion results

$$q'^h(t) = q'^h(q(t), p(t)), \tag{11.163}$$

$$p'^h(t) = p'^h(q(t), p(t)). \tag{11.164}$$

Under the diffeomorphisms (11.58), (11.59) the 2−form $\mathbf{\Omega}$ retains the form (11.162). Equivalently, this condition can also be written as follows

$$p'_h dq'^h = p_h dq^h + dV, \tag{11.165}$$

where V is an arbitrary function. If V is supposed to be a function of (q, q') satisfying the condition

$$\det\left(\frac{\partial^2 V}{\partial q^h \partial q'^h}\right) \neq 0, \tag{11.166}$$

then the diffeomorphisms (11.163), (11.164) are symplectic if and only if

$$p_h = -\frac{\partial V}{\partial q^h}(q, q'), \;\; p'_h = \frac{\partial V}{\partial q'^h}(q, q'). \tag{11.167}$$

When the constraints of the mechanical system S or the forces acting on S depend on time, we substitute the configuration space with the ***configuration space-time*** $V_n \times \Re$. Further, the Lagrange function depends explicitly on time. Consequently, the Hamiltonian formalism is based on the ***phase space-time*** $T^*V_n \times \Re$ and the Hamiltonian function depends explicitly on time. Since the dimension $2n + 1$ of $T^*V_n \times \Re$ is odd, a nondegenerate 2-form does not exist and $T^*V_n \times \Re$ cannot be equipped with a symplectic structure. In natural coordinates (q^h, p_h, t) on $T^*V_n \times \Re$, we consider the 1−form

$$\omega_H = p_h dq^h - H dt, \tag{11.168}$$

[4]See Appendix B.

whose exterior differential is

$$\mathbf{\Omega}_H \equiv d\boldsymbol{\omega}_H = dp_h \wedge dq^h - dH \wedge dt. \tag{11.169}$$

This 2−form is closed ($d\mathbf{\Omega}_H = \mathbf{0}$) and the components of the skew-symmetric tensor $\Omega_{H\alpha\beta}$ in natural coordinates are given by the matrix

$$(\Omega_{H\alpha\beta}) = \begin{pmatrix} \mathbf{0} & \mathbf{I} & H_{\mathbf{q}} \\ -\mathbf{I} & \mathbf{0} & H_{\mathbf{p}} \\ -H_{\mathbf{q}} & -H_{\mathbf{p}} & 0 \end{pmatrix}, \tag{11.170}$$

whose rank has maximum value $2n$.

In conclusion, we can equip the phase space-time $T^*V_n \times \Re$ with a closed 2−form with maximum rank $2n$ that in natural coordinates has the form (11.169). The pair $(T^*V_n \times \Re, \mathbf{\Omega}_H)$ is an example of a ***contact manifold***. It is possible to prove that the evolutions of the dynamical system S, starting from an arbitrary point $(q_0, p_0, t_0) \in U \times \{t_0\} \subset T^*V_n \times \Re$ is geometrically described by curves

$$q(t) = q(q_0, p_0, t_0, t), \tag{11.171}$$

$$p(t) = p(q_0, p_0, t_0, t), \tag{11.172}$$

that satisfy the Hamilton equations

$$\dot{q}^h = \frac{\partial H}{\partial p_h}(q, p, t), \tag{11.173}$$

$$\dot{p}_h = -\frac{\partial H}{\partial q_h}(q, p, t). \tag{11.174}$$

Let (q, p, t) be coordinates in a region $U \times \{t\}$ of $T^*V_n \times \Re$. A map

$$q' = q'(q, p, t), \tag{11.175}$$

$$p' = p'(q, p, t), \tag{11.176}$$

$$t' = t + a, \tag{11.177}$$

where a is a constant, between $U \times \{t\}$ and its image by (11.173)–(11.175) is said to be a ***contact or canonical transformation*** if it leaves invariant the 2−form (11.169); in other words, if it is such that

$$dq'^h \wedge dp'_h - dH'(q', p', t') = dq^h \wedge dp_h - dH(q, p, t). \tag{11.178}$$

Also in this case it is possible to prove that a contact map can be obtained by the formulae

$$p_h = -\frac{\partial V}{\partial q^h}(q, q', t, t'), \;\; p'_h = \frac{\partial V}{\partial q'^h}(q, q', t, t'), \tag{11.179}$$

provided that

$$\det\left(\frac{\partial^2 V}{\partial q^h \partial q'^h}\right) \neq 0. \tag{11.180}$$

11.9 Symplectic Optics

Formulae (11.12), (11.13) of Hamiltonian formalism of geometric optics are quite similar to (11.177). This similarity suggests the possibility to give geometric optics a symplectic formulation. First, we must define the phase space of symplectic optics. To determine this space we must list the variables that define a ray. Let π_1 be the image plane and $x_3 = z_1$ his abscissa along the optical axis a of the optical system S. Then, a ray of light γ is determined by the coordinates (x_1, x_2) of its starting point in π_1 and the director numbers (p_1, p_2, p_3) verifying the condition

$$p_1^2 + p_2^2 + p_3^2 = N^2, \tag{11.181}$$

where N is the refractive index at the point $(x_1, x_2) \in \pi_1$. Therefore, the phase space of the all rays starting from the image plane is $(\Re^2 \times S_2)(z_1)$, where S_2 is the open circle contained in the plane π_1 such that (see Figure 11.4)

$$p_1^2 + p_2^2 \leq N^2(x_1, x_2, x_3). \tag{11.182}$$

In a similar way we define the phase space $(\Re^2 \times S_2)(z_i)$ of all the rays starting from the points of the plane π_i orthogonal to a and intersecting a at the point of abscissa z_i. Denote by U_{z_1} a subset of $(\Re^2 \times S_2)(z_1)$ and by $U_{z_i} \subset (\Re^2 \times S_2)(z_i)$ the set of all the rays of U_{z_1} that intersect π_i. In view of (11.12), (11.13), the correspondence

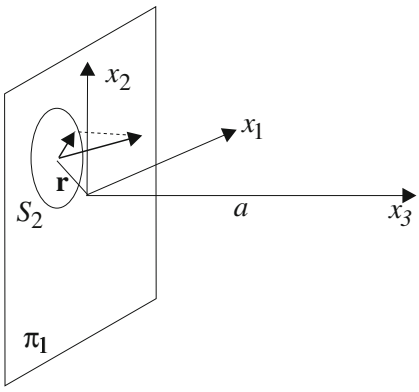

Fig. 11.4 Rays from the image plane

$\mathfrak{F} : U_{z_1} \to U_{z_i}$ is symplectic, that is $\mathfrak{F}$ verifies condition (11.165). In components this condition has the form

$$x_1 p_2 - x_2 p_1 = constant \tag{11.183}$$

that has the following geometric meaning: *throughout the optical system S the area of the parallelogram of sides* (x_1, x_2) and (p_1, p_2) *is constant*.

Finally, the image forming is obtained by composing symplectic maps. The results of this section allow us to apply all the tools of symplectic geometry to an optical system (see [52], [53]).

Chapter 12
Principal Functions and Primary Aberrations

12.1 Introduction to Third-Order Aberrations

In Chapter 2 we presented the paraxial or Gaussian theory. It describes the light propagation across an optical system $\mathbb{S}$ only for rays close to the optical axis a and forming small angles with it. We have shown that, in these conditions, the correspondence between an *assigned pair of object and image planes*, π and π', is given by the linear relations

$$x' = Mx, \tag{12.1}$$
$$y' = My, \tag{12.2}$$

where M is the magnification of $\mathbb{S}$.

Usually the aim of the optical design is to extend, as much as possible, the paraxial correspondence (12.1), (12.2) to points far apart from the optical axis a, and rays forming with a angles greater than the angles considered in the Gaussian approximation.

We recall that a system $\mathbb{S}$ is said to exhibit ***aberrations*** if the effective correspondence

$$x' = x'(x, y, p, q), \tag{12.3}$$
$$y' = y'(x, y, p, q), \tag{12.4}$$

between the object and image planes, π and π', differs from (12.1), (12.2). Therefore, the ***aberration vector*** $\boldsymbol{\epsilon}$ is defined as the vector whose components are expressed by the differences (see Section 1.4)

$$\epsilon_x = x' - Mx, \tag{12.5}$$
$$\epsilon_y = y' - My. \tag{12.6}$$

© Springer International Publishing Switzerland 2016

A. Romano and R. Cavaliere, *Geometric Optics*,
Modeling and Simulation in Science, Engineering and Technology,
DOI 10.1007/978-3-319-43732-3_12

The problem of the aberration theory is to find the analytic expressions of (12.5), (12.6) in terms of the coordinates of the object, the ray, and the characteristics of the optical system $\mathbb{S}$. The aim is to use these expressions both to evaluate the aberrations of a given optical system $\mathbb{S}$ and to design $\mathbb{S}$, in such a way that the components of the aberration vector $\boldsymbol{\epsilon}$ have prefixed values, on varying in a given range, both the coordinates of the object point and the ray.

We have already noted that Taylor's expansion of functions (12.5), (12.6) with respect to the variables x, y, p, q, owing to the symmetry of revolution of $\mathbb{S}$ about the optical axis a, contains odd terms only. The first-order terms define the Gaussian correspondence between π and π', the third-order terms express the ***third-order aberrations***, the fifth-order terms describe the ***fifth-order aberrations***, and so on. Correspondingly, the system $\mathbb{S}$ is said to be free from third-order aberrations, if the third-order terms are absent; corrected up to the fifth order, if the fifth-order aberrations vanish, etc.

In this chapter, formulae expressing the third-order aberrations of an optical system for an assigned pair of object and image planes are explicitly given using the Hamiltonian approach. The corresponding formulae for the fifth-order ones are not given since their complexity makes them not easy to apply (see [3, 4]).

12.2 Third-Order Aberrations via Angular Function

First, we note that, if the refractive index N of the medium before the first surface of the optical system is equal to the refractive index N' after the last surface, then, from (2.113), (2.114), the Gaussian transformations can be written as follows:

$$\begin{aligned} x' &= Mx, \\ y' &= My, \\ p' &= -\frac{N}{f}x + \frac{1}{M}p, \\ q' &= -\frac{N}{f}y + \frac{1}{M}q. \end{aligned} \tag{12.7}$$

On the other hand, in view of (11.40), (11.41), the characteristic angular function $T(p, q, p', q')$, to within sixth-order terms, writes

$$T = T_0 + T_2 + T_4, \tag{12.8}$$

where T_0 is a constant,

$$T_2 = A_\xi \xi + A_{\xi'} \xi' + A_\eta, \tag{12.9}$$

and

$$T_4 = A_{\xi\xi}\xi^2 + A_{\xi'\xi'}\xi'^2 + A_{\eta\eta}\eta^2 + A_{\xi\eta}\xi\eta + A_{\xi\xi'}\xi\xi' + A_{\xi'\eta}\xi'\eta. \tag{12.10}$$

Now, we suppose that the anterior and posterior base planes coincide, respectively with the object plane Oxy and the image plane $O'x'y'$. Consequently, in the formulae (11.26), (11.27), it is $x_3 = x_3' = 0$. Then, the components (12.5), (12.6) of the aberration vector can be written in the following way:

$$\epsilon_x = x' - Mx = -\frac{\partial T}{\partial p'} - M\frac{\partial T}{\partial p}, \tag{12.11}$$

$$\epsilon_y = y' - My = -\frac{\partial T}{\partial q'} - M\frac{\partial T}{\partial q}. \tag{12.12}$$

On the other hand, in the Gaussian approximation, it is $x' - Mx = 0$ and $y' - My = 0$. Consequently, we have that

$$-\frac{\partial T_2}{\partial p'} - M\frac{\partial T_2}{\partial p} = 0, \tag{12.13}$$

$$-\frac{\partial T_2}{\partial q'} - M\frac{\partial T_2}{\partial q} = 0, \tag{12.14}$$

and the relations (12.11), (12.12) assume the following form:

$$\epsilon_x = -\frac{\partial T_4}{\partial p'} - M\frac{\partial T_4}{\partial p}, \tag{12.15}$$

$$\epsilon_y = -\frac{\partial T_4}{\partial q'} - M\frac{\partial T_4}{\partial q}. \tag{12.16}$$

We conclude that the third-order aberrations depend only on T_4.

If (12.10) is taken into account, these equations become

$$\epsilon_x = -\mathbb{A}p - \mathbb{B}p', \tag{12.17}$$

$$\epsilon_y = -\mathbb{A}q - \mathbb{B}q', \tag{12.18}$$

where we have introduced the following notations:

$$\begin{aligned}\mathbb{A} &= 2M(2A_{\xi\xi}\xi + A_{\xi\xi'}\xi' + A_{\xi\eta}\eta)\\ &\quad + (A_{\xi\eta}\xi + A_{\xi'\eta}\xi' + 2A_{\eta\eta}\eta),\end{aligned} \tag{12.19}$$

$$\begin{aligned}\mathbb{B} &= M(A_{\xi\eta}\xi + A_{\xi'\eta}\xi' + 2A_{\eta\eta}\eta)\\ &\quad + 2(A_{\xi\xi'}\xi + 2A_{\xi'\xi'}\xi' + A_{\xi'\eta}\eta).\end{aligned} \tag{12.20}$$

These relations seem not to be useful. In fact, our purpose consists in expressing the aberrations in terms both of the coordinates x, y of the object point and the directional numbers p, q of the emerging ray. On the contrary, in the formulae (12.19), (12.20), together with p, q, appear the directional numbers p', q' of the corresponding ray in the image-space, instead of x, y. Fortunately, this difficulty can easily be overcome.

In fact, since we are interested in relations which are exact to within third-order terms, it is sufficient to resort to the *linear relations* (12.7), which express p' and q' in terms of x, y, p, q. Moreover, a further simplification can be introduced. Owing to the symmetry of the optical system $\mathbb{S}$, it is possible to suppose $x = 0$, without loss of generality. In other words, the following equations can be used:

$$p' = \frac{1}{M} p, \tag{12.21}$$

$$q' = -\frac{N}{f} y + \frac{1}{M} q. \tag{12.22}$$

In what follows, it will be more convenient to describe the emerging ray from the object point $(0, y)$ by the *paraxial* coordinates x_e, y_e of the point in which it crosses the plane of the entrance pupil. Let P_e, P'_e and P' be the points in which a ray γ from an object point P intersects the plane of entrance pupil π_e, of exit pupil π'_e, and the conjugate Gaussian object plane π', respectively. The parametric equations of the ray γ emerging from $(0, y)$ write

$$X = pt, \tag{12.23}$$

$$Y = y + qt, \tag{12.24}$$

$$Z = rt, \tag{12.25}$$

where t is the parameter and (X, Y, Z) the running point on γ. Since we are interested in relations which are linear with respect to the variables p, q, r, y, we have

$$Z \simeq Nt, \tag{12.26}$$

so that the value $\bar{t}$ corresponding to the point P_e is given by

$$\bar{t} = \frac{z_e}{N}, \tag{12.27}$$

where z_e denotes the abscissa of π_e with respect to the object plane. Substituting this value of t in the other two equations (12.24), (12.25), we obtain

$$p = \frac{N}{z_e} x_e, \tag{12.28}$$

$$q = \frac{N}{z_e}(y_e - y). \tag{12.29}$$

Using (12.28), (12.29) into (12.17), (12.18), after tedious algebraic manipulations, we derive the following expressions for the components of the aberration vector:

$$\epsilon_x = \mathbb{D}_1(x_e^2 + y_e^2)x_e + 2\mathbb{D}_2 x_e y_e y + \mathbb{D}_3 x_e y^2, \tag{12.30}$$

$$\begin{aligned}\epsilon_y &= \mathbb{D}_1(x_e^2 + y_e^2)y_e + \mathbb{D}_2 x_e^2 y + 3\mathbb{D}_2 y_e^2 y \\ &\quad + \mathbb{D}_4 y_e y^2 + \mathbb{D}_5 y^3,\end{aligned} \tag{12.31}$$

where the following notations have been introduced:

$$\begin{aligned}\mathbb{D}_1 &= -\frac{4N^3}{z_e^3}A_1, \\ \mathbb{D}_2 &= \frac{N^3}{z_e^3}\left(4A_1 + \frac{z_e}{f}A_2\right), \\ \mathbb{D}_3 &= -\frac{2N^3}{z_e^3}\left(2A_1 + \frac{z_e}{f}A_2 + \frac{z_e^2}{f^2}A_3\right), \\ \mathbb{D}_4 &= -\frac{2N^3}{z_e^3}\left(6A_1 + 3\frac{z_e}{f}A_2 + \frac{z_e^2}{f^2}A_4\right), \\ \mathbb{D}_5 &= \frac{N^3}{z_e^3}\left(4A_1 + 3\frac{z_e}{f}A_2 + 2\frac{z_e^2}{f^2}A_4 + \frac{z_e^3}{f^3}A_5\right),\end{aligned}$$

$$\begin{aligned}A_1 &= MA_{\xi\xi} + \frac{A_{\xi\xi'}}{M} + A_{\xi\eta} + \frac{A_{\xi'\xi'}}{M^3} + \frac{A_{\xi'\eta}}{M^2} + \frac{A_{\eta\eta}}{M}, \\ A_2 &= 2A_{\xi\xi'} + MA_{\xi\eta} + 4\frac{A_{\xi'\xi'}}{M^2} + \frac{3A_{\xi'\eta}}{M} + 2A_{\eta\eta}, \\ A_3 &= MA_{\xi\xi'} + 2\frac{A_{\xi'\xi'}}{M} + A_{\xi'\eta}, \\ A_4 &= MA_{\xi\xi'} + 6\frac{A_{\xi'\xi'}}{M} + 3A_{\xi'\eta} + MA_{\eta\eta}, \\ A_5 &= 4A_{\xi'\xi'} + MA_{\xi'\eta}.\end{aligned}$$

In Chapter 3, we have discussed the meaning of the terms appearing into the above equations.

Up to now, many important properties of the third-order aberrations have been derived using elementary tools. But there are two important questions to answer

- determine, for a *single* optical surface, the fourth-order expansion of the angular function in terms of its optical characteristics;
- evaluate the *total* angular function in order to derive the coefficients $A_1, \ldots, A_5$ appearing in the above formulae.

In a next sections we answer the above questions.

12.3 Reduced Coordinates

In Mechanics, it very frequently happens that a problem in its original formulation cannot be solved. However, a suitable choice of Lagrangian or Hamiltonian coordinates may lead to a new form of the equation of motion, which allows us to derive the

solution or, at least, more information about it. That happens also in studying optical systems. In this section, we introduce the **reduced coordinates** of Seidel, since they allow us to formulate the aberration problem in a more simple form.

Let $\mathbb{S}$ be an axially symmetric optical system, a its axis, and π, π' a pair of Gaussian object and image planes for $\mathbb{S}$. With l and l' two reference lengths are introduced in π and π', respectively, verifying the condition

$$\frac{l'}{l} = M, \tag{12.32}$$

where M is the lateral Gaussian magnification relative to π and π'.

In these planes, the following nondimensional coordinates will be used:

$$X = C\frac{x}{l}, \qquad Y = C\frac{y}{l}, \tag{12.33}$$

$$X' = C\frac{x'}{l'}, \qquad Y' = C\frac{y'}{l'}, \tag{12.34}$$

where C is a constant which will be fixed later.

Similarly, we introduce other two reference lengths l_e and l'_e in the conjugate planes of entrance and exit pupils such that

$$\frac{l'_e}{l_e} = M_e, \tag{12.35}$$

being M_e the magnification relative to these two planes.

Correspondingly, these planes are referred to the nondimensional coordinates

$$X_e = \frac{x_e}{l_e}, \qquad Y_e = \frac{y_e}{l_e}, \tag{12.36}$$

$$X'_e = \frac{x'_e}{l'_e}, \qquad Y'_e = \frac{y'_e}{l'_e}. \tag{12.37}$$

If z_e and z'_e denote, respectively, the distances of entrance and exit pupils from π and π', in the Gaussian approximation (see (12.28), (12.29)) it results

$$\frac{x_e - x}{z_e} = \frac{p}{N}, \qquad \frac{y_e - y}{z_e} = \frac{q}{N} \tag{12.38}$$

$$\frac{x'_e - x'}{z'_e} = \frac{p'}{N'}, \qquad \frac{y'_e - y'}{z'_e} = \frac{q'}{N'}, \tag{12.39}$$

and the relations (12.36), (12.37) can also be written

$$X_e = \frac{x}{l_e} + \frac{z_e p}{l_e N}, \qquad Y_e = \frac{y}{l_e} + \frac{z_e q}{l_e N}, \tag{12.40}$$

$$X'_e = \frac{x'}{l'_e} + \frac{z'_e p'}{l'_e N'}, \qquad Y'_e = \frac{y'}{l'_e} + \frac{z'_e q'}{l'_e N'}. \tag{12.41}$$

It is important to remark that in the Gaussian approximation it is

$$X' = X, \qquad Y' = Y, , \tag{12.42}$$

$$X'_e = X_e, \qquad Y'_e = Y_e. \tag{12.43}$$

Consequently, the differences $X' - X$, $Y' - Y$, $X'_e - X_e$, and $Y'_e - Y_e$ express the presence of aberrations in the optical system $\mathbb{S}$.

In the sequel, to simplify the calculations, it is suitable to choose the constant C in the following way:

$$C = \frac{Nll_e}{z_e} = \frac{N'l'l'_e}{z'_e}. \tag{12.44}$$

This choice is possible since the ratios appearing into (12.44) coincide with Herschel's invariant (2.59).

The quantities defined by (12.33), (12.34), (12.40), and (12.41) are called the **Seidel variables**. We conclude writing the inverse relations of (12.33), (12.34) and (12.40), (12.41) corresponding to the choice (12.44):

$$x = \frac{z_e}{Nl_e} X, \qquad y = \frac{z_e}{Nl_e} Y, \tag{12.45}$$

$$x' = \frac{z'_e}{N'l'_e} X', \qquad y' = \frac{z'_e}{N'l'_e} Y', \tag{12.46}$$

$$p = \frac{Nl_e}{z_e} X_e - \frac{1}{l_e} X, \qquad q = \frac{Nl_e}{z_e} Y_e - \frac{1}{l_e} Y, \tag{12.47}$$

$$p' = \frac{N'l'_e}{z'_e} X'_e - \frac{1}{l'_e} X', \qquad q' = \frac{N'l'_e}{z'_e} Y'_e - \frac{1}{l'_e} Y'. \tag{12.48}$$

12.4 Schwarzschild's eikonal

We start noting that relation (11.25), in the coordinates here adopted, writes

$$dT = xdp + ydq - x'dp' - y'dq'. \tag{12.49}$$

Introducing the Seidel variables (12.45)–(12.48), we obtain

$$\begin{aligned} dT = {} & x\left(\frac{Nl_e}{z_e} dX_e - \frac{1}{l_e} dX\right) + y\left(\frac{Nl_e}{z_e} dY_e - \frac{1}{l_e} dY\right) \\ & - x'\left(\frac{N'l'_e}{z'_e} dX'_e - \frac{1}{l'_e} dX'\right) - y'\left(\frac{N'l'_e}{z'_e} dY'_e - \frac{1}{l'_e} dY'\right) \end{aligned}$$

i.e.,

$$dT = -\frac{z_e}{Nl_e^2}(XdX + YdY) + \frac{z_e'}{N'l_e'^2}\left(X'dX' + Y'dY'\right) + XdX_e + YdY_e - X'dX_e' - Y'dY_e'.$$

It is easy to verify that the above expression is equivalent to the following one:

$$\begin{aligned} dT = &-\frac{z_e}{Nl_e^2}(XdX + YdY) + \frac{z_e'}{N'l_e'^2}\left(X'dX' + Y'dY'\right) \\ &- (X_e' - X_e)dX - (Y_e' - Y_e)dY - X(dX_e' - dX_e) - Y(dY_e' - dY_e) \\ &+ (X_e' - X_e)dX + (Y_e' - Y_e)dY - (X' - X)dX_e' - (Y' - Y)dY_e'. \end{aligned}$$

By introducing the function

$$\begin{aligned} \psi = &\frac{z_e}{2Nl_e^2}(X^2 + Y^2) - \frac{z_e'}{2N'l_e'^2}(X'^2 + Y'^2) \\ &+ (X_e' - X_e)X + (Y_e' - Y_e)Y, \end{aligned} \tag{12.50}$$

the above relation becomes

$$d(T + \psi) = (X_e' - X_e)dX + (Y_e' - Y_e)dY - (X' - X)dX_e' - (Y' - Y)dY_e'. \tag{12.51}$$

In other words, $d(T + \psi)$ is the differential of the function

$$S = T + \psi, \tag{12.52}$$

which is called the **Schwarzschild eikonal**.

In view of (12.51)–(12.52), it can be said that Schwarschild's eikonal, when it is regarded as a function of Seidel's variables X, Y, X_e', Y_e', verifies the following important relations:

$$X_e' - X_e = \frac{\partial S}{\partial X}, \qquad Y_e' - Y_e = \frac{\partial S}{\partial Y}, \tag{12.53}$$

$$X' - X = -\frac{\partial S}{\partial X_e'}, \qquad Y' - Y = -\frac{\partial S}{\partial Y_e'}. \tag{12.54}$$

Remark 12.1 *We have already been noted that, in the Gaussian approximation, it is*

$$X' = X, \quad Y' = Y, \quad X_e' = X_e, \quad Y_e' = Y_e. \tag{12.55}$$

These relations and (12.53), (12.54) imply that Taylor's power expansion of S ***does not contain second-order terms****; i.e., it has the form*

$$S = S^{(0)} + S^{(4)} + S^{(6)} + \cdots , \tag{12.56}$$

where $S^{(2k)}$ is an homogeneous polynomial of degree $2k$ in Seidel's variables.

Remark 12.2 *From (12.53) one obtains*

$$X' = X + O(3), \quad Y' = Y + O(3), \tag{12.57}$$
$$X'_e = X_e + O(3), \quad Y'_e = Y_e + O(3). \tag{12.58}$$

Moreover, owing to the axial symmetry of the optical system $\mathbb{S}$, the Schwarzschild function S depends on the variables X, Y, X'_e, Y'_e by the following three combinations:

$$\mathcal{R}^2 = X^2 + Y^2, \quad \mathcal{R}'_e = X'_e + Y'_e, \quad k = XX'_e + YY'_e. \tag{12.59}$$

In particular the fourth-order term in (12.56) writes

$$S^{(4)} = -\frac{1}{4}A\mathcal{R}^4 - \frac{1}{4}B\mathcal{R}'^4_e - Ck^4 - \frac{1}{2}D\mathcal{R}^2\mathcal{R}^2_e + E\mathcal{R}^2k^2 + F\mathcal{R}^2_e k^2. \tag{12.60}$$

In order to evaluate from $S^{(4)}$ the third-order aberrations, we start noting that, resorting to (12.33), (12.34) and (12.44), we have the relations

$$X' - X = \frac{N'l'_e}{z'_e}(x' - Mx), \qquad Y' - Y = \frac{N'l'_e}{z'_e}(y' - My), \tag{12.61}$$

which, in view of (12.5), (12.6) can also be written as it follows:

$$X' - X = \frac{N'l'_e}{z'_e}\epsilon_x \equiv \alpha\epsilon_x, \qquad Y' - Y = \frac{N'l'_e}{z'_e}\epsilon_y \equiv \alpha\epsilon_y. \tag{12.62}$$

Finally, (12.53) and (12.54) lead us to the following relations:

$$\alpha\epsilon_x = (2Ck^2 - E\mathcal{R}^2 - F\mathcal{R}'^2_e)X + (B\mathcal{R}'^2_e + D\mathcal{R}^2 - 2Fk^2)X'_e,$$
$$\alpha\epsilon_y = (2Ck^2 - E\mathcal{R}^2 - F\mathcal{R}'^2_e)Y + (B\mathcal{R}'^2_e + D\mathcal{R}^2 - 2Fk^2)Y'_e.$$

If, owing to the axial symmetry of the optical system $\mathbb{S}$, we assume $X = 0$ and introduce polar coordinates

$$X'_e = \mathcal{R}'_e \cos\varphi, \qquad Y'_e = \mathcal{R}'_e \sin\varphi,$$

in the exit pupil, the above relations become

$$\alpha\epsilon_x = B\mathcal{R}'^3_e \cos\varphi - FY\mathcal{R}'^2_e \sin 2\varphi + DY^2\mathcal{R}'_e \cos\varphi, \tag{12.63}$$
$$\alpha\epsilon_y = B\mathcal{R}'^3_e \sin\varphi - FY\mathcal{R}'^2(2 - \cos 2\varphi) + (2C + D)Y^2\mathcal{R}'_e \sin\varphi - EY^3. \tag{12.64}$$

Starting from these equations, which have the same form of (12.30), (12.31) we can develop the same analysis of aberrations of Section 3.6.

We conclude this section noting that, since ψ is a second-order function of Seidel's variables and (12.52) hold, it results

$$S^{(4)} = T^{(4)}, \tag{12.65}$$

where $T^{(4)}$ is the fourth-order term of Taylor's expansion of angular function.

12.5 Addition Theorem for Third-Order Aberrations

In this section, the great advantage offered by Seidel's variables in evaluating the third-order aberrations of a compound system is proved.

Consider an optical system $\mathbb{S}$ with axial symmetry consisting of two surfaces of revolution S_1 and S_2 (see Figure 12.1).

Let O_1 be the axial object point for the whole system, O_1' the Gaussian image formed by S_1, $O_2 \equiv O_1'$ the object of S_2 and O_2' the image formed by S_2. If

$$T_1 = T_1(p_1, q_1, p_1', q_1'), \qquad T_2 = T_2(p_2, q_2, p_2', q_2'),$$

denote the angular functions relative to S_1 and S_2 respectively, the angular function of the whole system results

$$T = T_1 + T_2.$$

In this expression the variables $p_1' = p_2$ and $q_1' = q_2$ must be eliminated. According to (12.50) and (12.52), Schwarzschild's eikonals of S_1 and S_2 write

$$\begin{aligned} S_1 &= T_1 + \frac{z_{e1}}{2N_1 l_{e1}^2}(X_1^2 + Y_1^2) - \frac{z_{e1}'}{N_1' l_{e1}'^2}(X_1'^2 + Y_1'^2) \\ &\quad + (X_{e1}' - X_{e1})X_1 + (Y_{e1}' - Y_{e1})Y_1, \end{aligned} \tag{12.66}$$

$$\begin{aligned} S_2 &= T_2 + \frac{z_{e2}}{2N_2 l_{e2}^2}(X_2^2 + Y_2^2) - \frac{z_{e2}'}{N_2' l_{e2}'^2}(X_2'^2 + Y_2'^2) \\ &\quad + (X_{e2}' - X_{e2})X_2 + (Y_{e2}' - Y_{e2})Y_2, \end{aligned} \tag{12.67}$$

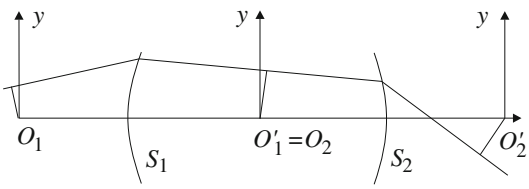

Fig. 12.1 Angular function

whereas the Schwarzschild's eikonal of the whole system is

$$\begin{aligned} S = T + \frac{z_{e1}}{2N_1 l_{e1}^2}(X_1^2 + Y_1^2) - \frac{z'_{e2}}{N'_2 l'^2_{e2}}(X'^2_2 + Y'^2_2) \\ +(X'_{e2} - X_{e1})X_1 + (Y'_{e2} - Y_{e1})Y_1. \end{aligned} \tag{12.68}$$

Since $T = T_1 + T_2$, when we remind that $z'_{e1} = z_{e2}, l'_{e1} = l_{e2}$, we easily obtain that

$$S = S_1 + S_2 + (X_1 - X'_1)(X'_{e2} - X_{e2}) + (Y_1 - Y'_1)(Y'_{e2} - Y_{e2}). \tag{12.69}$$

Using (12.53), (12.54), we finally have

$$S = S_1 + S_2 + \frac{\partial S_1}{\partial X'_{e1}}\frac{\partial S_2}{\partial X_2} + \frac{\partial S_1}{\partial Y'_{e1}}\frac{\partial S_2}{\partial Y_2}, \tag{12.70}$$

where, as usual, S_i is a function of X_i, Y_i and X'_{ei}, Y'_{ei}.

If in (12.70) the power expansion for S_1 and S_2 are introduced, for the absence of second-order terms in these expansion and taking into account (12.53), (12.54), then it follows that

$$S = S_1^{(0)} + S_2^{(0)} + S_1^{(4)} + S_2^{(4)} + \cdots . \tag{12.71}$$

According to (12.60), $S_1^{(4)}$ and $S_2^{(4)}$ can be written as it follows:

$$\begin{aligned} S_1 = &-\frac{1}{4}A_1\mathcal{R}_1^4 - \frac{1}{4}B_1\mathcal{R}'^4_{e1} - C_1 k_1^4 \\ &- \frac{1}{2}D_1\mathcal{R}_1^2\mathcal{R}_{e1}^2 + E_1\mathcal{R}_1^2 k_1^2 + F_1\mathcal{R}_{e1}^2 k_1^2, \end{aligned} \tag{12.72}$$

$$\begin{aligned} S_2 = &-\frac{1}{4}A_2\mathcal{R}_2^4 - \frac{1}{4}B_2\mathcal{R}'^4_{e2} - C_2 k_2^4 \\ &- \frac{1}{2}D_2\mathcal{R}_2^2\mathcal{R}_{e2}^2 + E_2\mathcal{R}_2^2 k_2^2 + F_2\mathcal{R}_{e2}^2 k_2^2, \end{aligned} \tag{12.73}$$

where

$$\begin{aligned} \mathcal{R}_1^2 &= X_1^2 + Y_1^2, \quad \mathcal{R}'^2_{e1} = X'^2_{e1} + Y'^2_{e1}, \\ \mathcal{R}_2^2 &= X_2^2 + Y_2^2, \quad \mathcal{R}'^2_{e2} = X'^2_{e2} + Y'^2_{e2}, \\ k_1 &= X_1 X'_{e1} + Y_1 Y'_{e1}, \quad k_2 = X_2 X'_{e2} + Y_2 Y'_{e2}. \end{aligned}$$

From (12.54) it is plain to derive

$$\begin{aligned} S = &-\tfrac{1}{4}(A_1 + A_2)\mathcal{R}_1^4 - \tfrac{1}{4}(B_1 + B_2)\mathcal{R}'^4_{e2} - (C_1 + C_2)k_{12}^4 \\ &-\frac{1}{2}(D_1 + D_2)\mathcal{R}_1^2\mathcal{R}_{e2}^2 + (E_1 + E_2)\mathcal{R}_1^2 k_{12}^2 + (F_1 + F_2)\mathcal{R}_{e1}^2 k_{12}^2, \end{aligned} \tag{12.74}$$

where

$$k_{12} = X_1 X'_{e2} + Y_1 Y'_{e2}.$$

A similar result holds for a centered system consisting of any number of surfaces. In concluding, the following theorem has been proved:

Each third-order aberration coefficient of a centered system is the sum of the corresponding coefficients of the single surfaces of the system.

12.6 Fourth-Order Expansion of Angular Function

In this section, the angular characteristic function T of a single refractive or reflecting revolving surface S will be determined up to fourth-order terms in ξ, ξ', η.

We remind the general expression (11.21) of angular characteristic function (see also Figure 11.1)

$$T = (p - p')x + (q - q')y + (r - r')z + r'a' - ra, \tag{12.75}$$

where $P = (x, y, z)$ is the intersection point between S and the ray $\mathbf{p}$. As a consequence, its coordinates must minimize the optical path length, i.e., the function

$$T(x, y, z) + \lambda F(x, y, z), \tag{12.76}$$

where λ is a Lagrangian multiplier and $F(x, y, z) = z - z(x, y) = 0$ is the equation of S. The necessary conditions for a minimum write

$$\frac{\partial T}{\partial x} + \lambda \frac{\partial F}{\partial x} = 0, \quad \frac{\partial T}{\partial y} + \lambda \frac{\partial F}{\partial y} = 0, \quad \frac{\partial T}{\partial z} + \lambda \frac{\partial F}{\partial z} = 0,$$

or equivalently,

$$p - p' = \lambda \frac{\partial z}{\partial x}, \quad q - q' = \lambda \frac{\partial z}{\partial y}, \quad r - r' = -\lambda. \tag{12.77}$$

Substituting the value of λ derived by the third of these equations into the other ones, one has

$$\frac{p - p'}{r - r'} = -\frac{\partial z}{\partial x}, \quad \frac{q - q'}{r - r'} = -\frac{\partial z}{\partial y}. \tag{12.78}$$

We also remind (see (1.29)) the equation of the surface S which, up to fourth-order terms, is

$$z = \frac{(x^2 + y^2)}{2R} + \frac{(1 + K)}{8R^3}(x^2 + y^2)^2. \tag{12.79}$$

Consequently, relations (12.78) become

$$\frac{p-p'}{r-r'} = -\frac{x}{R} + \Delta x, \quad \frac{q-q'}{r-r'} = -\frac{y}{R} + \Delta y. \tag{12.80}$$

where Δx and Δy are third-order quantities.

Moreover,

$$r = N - \frac{1}{2N}(p^2+q^2) + O(4), \quad r' = -\frac{1}{2N'}(p'^2+q'^2) + O(4), \tag{12.81}$$

and

$$\begin{aligned}\frac{1}{r'-r} = \frac{1}{N'-N}\Bigg[1 - \frac{1}{2N(N'-N)}(p^2+q^2) \\ + \frac{1}{2N(N'-N)}(p'^2+q'^2)\Bigg].\end{aligned} \tag{12.82}$$

Inserting (12.80) into (12.79), one obtains

$$\begin{aligned}z = \frac{R}{2(r-r')}\left[(p-p')^2+(q-q')^2\right] - \frac{1}{r-r'}\left[(p-p')\Delta x + (q-q')\Delta y\right] \\ + R\frac{1+K}{(r-r')^4}[(p-p')^2+(q-q')^2]^2.\end{aligned} \tag{12.83}$$

Taking into account this relation, (12.75) writes

$$\begin{aligned}T = &-\frac{R}{r-r'}\left[(p-p')^2+(q-q')^2\right. \\ &+ \left.(p-p')\Delta x + (q-q')\Delta y\right] \\ &+ (r-r')\frac{R}{2(r-r')^2}\left[(p-p')^2+(q-q')^2\right] \\ &+ \frac{r-r'}{r-r'}(p-p')\Delta x + (q-q')\Delta y \\ &+ R\frac{(r-r')(1+K)}{8(r-r')^4}\left[(p-p')^2+(q-q')^2\right]^2 \\ &- \frac{R}{r-r'}\left[(p-p')^2+(q-q')^2\right] \\ &+ R\frac{((1+K)}{8(r-r')^3}\left[(p-p')^2+(q-q')^2\right]^2,\end{aligned} \tag{12.84}$$

and the third-order terms Δx and Δy disappear.

Then, the final expression of T results

$$T = T_0 + T_2 + T_4, \tag{12.85}$$

where

$$T_0 = N'a' - Na, \tag{12.86}$$

$$\begin{aligned} T_2 = {} & \frac{R}{2(N'-N)}\left[(p-p')^2 + (q-q')^2\right] \\ & + \frac{a}{2N}(p^2+q^2) - \frac{a'}{2N'}(p'^2+q'^2), \end{aligned} \tag{12.87}$$

$$\begin{aligned} T_4 = {} & -\frac{R}{4(N'-N)^2}\left[(p-p')^2 + (q-q')^2\right]\left[\frac{p^2+q^2}{N^2} - \frac{p'^2+q'^2}{N'}\right] \\ & - \frac{R(1+K)}{8(N'-N)^3}\left[(p-p')^2 + (q-q')^2\right]^2 \\ & + \frac{N}{8N^3}(p^2+q^2)^2 - \frac{N'}{8N'^3}(p'^2+q'^2)^2. \end{aligned} \tag{12.88}$$

Now, the axial points $z = a$ and $z = a'$ will be identified with the axial object point and its Gaussian image, respectively, and the following notations will be adopted:

$$z = a, \quad z' = a', \quad w_e = a + z_e, \quad w'_e = a' + z'_e, \tag{12.89}$$

and

$$\begin{aligned} Q &\equiv N\left(\frac{1}{R} - \frac{1}{z}\right) = N'\left(\frac{1}{R} - \frac{1}{z'}\right), \\ L &\equiv N\left(\frac{1}{R} - \frac{1}{w_e}\right) = N'\left(\frac{1}{R} - \frac{1}{w'_e}\right), \end{aligned} \tag{12.90}$$

where Q and L denote Abbe's invariants of the surface S relative to the object-image planes and entrance-exit pupils (see (2.7)).

Before expressing T_4 in terms of Seidel's variables, it is convenient to rewrite T_4 in (12.88) in a more suitable form. Introducing the notations (12.89) into (12.88), we have

$$\begin{aligned} & -\frac{R(1+K)}{8(N'-N)^3}\left[(p-p')^2 + (q-q')^2\right]^2 \\ & = -\frac{R^2(1+K)}{8(N'-N)^4}\left[\frac{N'}{z'} - \frac{N}{z}\right]\left[(p-p')^2 + (q-q')^2\right]^2, \end{aligned}$$

and (12.88) assumes the following form:

$$
\begin{aligned}
T_4 = {} & \frac{1}{8Nz}\left[\frac{NR}{(N'-N)^2}\left[(p-p')^2+(q-q')^2\right]-\frac{z}{N}(p^2+q^2)\right] \\
& -\frac{1}{8N'z'}\left[\frac{N'R}{(N'-N)^2}\left[(p-p')^2+(q-q')^2\right]-\frac{z'}{N'}(p'^2+q'^2)\right] \\
& -\frac{KR}{8(N'-N)^3}\left[(p-p')^2+(q-q')^2\right]. \qquad (12.91)
\end{aligned}
$$

12.7 Aberrations of Axially Symmetric Systems

In order to find the third-order aberrations of an axially symmetric system, we have to

1. express T_4 in terms of Seidel's variables;
2. apply the theorem of addition of primary aberrations.

As concerns the first point, we start noting that (12.54) allow us to use the Gaussian relations (12.61) in (12.91). Moreover, since Seidel's variables are invariant in the Gaussian approximation, (12.45)–(12.45) can also be written

$$
p = \frac{Nl_e}{z_e}X'_e - \frac{1}{l_e}X, \qquad q = \frac{Nl_e}{z_e}Y'_e - \frac{1}{l_e}Y, \qquad (12.92)
$$

$$
p' = \frac{N'l'_e}{z'_e}X'_e - \frac{1}{l'_e}X', \qquad q' = \frac{N'l'_e}{z'_e}Y'_e - \frac{1}{l'_e}Y'. \qquad (12.93)
$$

Further modifications are necessary. If M and M_e are the lateral magnifications relative to object-image planes and entrance-exit pupil, respectively, we easily verify that

$$
\frac{l'}{l} = \frac{R-z'}{R-z}, \quad \frac{l'_e}{l_e} = \frac{R-z'_e}{R-z_e}.
$$

Taking into account (12.90), these relations can be written

$$
\frac{l'}{l} = \frac{Nz'}{N'z}, \quad \frac{l'_e}{l_e} = \frac{Nz'_e}{N'z_e}. \qquad (12.94)
$$

Introducing the notations

$$
h = \frac{l_e s}{a} = \frac{l'_e z'}{a'}, \quad h_e = \frac{w_e}{Nl_e} = \frac{w'_e}{l'_e}, \qquad (12.95)
$$

and using (12.94) and (12.44), equations (12.92), (12.93) can be transformed as follows:

$$p = N\left(\frac{h}{z}X'_e - \frac{h_e}{w_e}X\right), \qquad q = N\left(\frac{h}{z}Y'_e - \frac{h_e}{w_e}Y\right),$$
$$p' = N'\left(\frac{h}{z'}X'_e - \frac{h_e}{w'_e}X\right), \qquad q = N\left(\frac{h}{z'}Y'_e - \frac{h_e}{w'_e}Y\right). \tag{12.96}$$

Resorting to the above results and notations, with simple but tedious calculations, we can prove that

$$(p-p')^2 + (q-q')^2 = \left(\frac{N'-N}{\mathcal{R}}\right)^2 (h_e^2\mathcal{R}^2 + h^2\mathcal{R}_e'^2 - 2hh_ek^2), \tag{12.97}$$

$$\begin{aligned}&\frac{N}{(N'-N)^2}[(p-p')^2 + (q-q')^2] - \frac{z}{N}(p^2+q^2)\\ &= h_e^2\mathcal{R}^2\left[L - (K-L)\frac{z}{w_e}\right] + h^2\mathcal{R}_e'^2K - 2hh_ek^2L,\end{aligned} \tag{12.98}$$

$$\begin{aligned}&\frac{N'}{(N'-N)^2}[(p-p')^2 + (q-q')^2] - \frac{z'}{N'}(p'^2+q'^2)\\ &= h_e^2\mathcal{R}^2\left[L - (K-L)\frac{z'}{w'_e}\right] + h^2\mathcal{R}_e'^2K - 2hh_ek^2L,\end{aligned} \tag{12.99}$$

where $\mathcal{R}$, $\mathcal{R}'_e$ and k are defined in (12.56).

Introducing these expressions into (12.91) and taking into account (12.65), we finally obtain the fourth-order terms of Schwarzschild's eikonal. Moreover, by applying the addition theorem of Seidel's coefficients (see Section 11.5), we can write

$$S^{(4)} = -\frac{1}{4}A\mathcal{R}^4 - \frac{1}{4}B\mathcal{R}_e'^4 - Ck^4 - \frac{1}{2}D\mathcal{R}^2\mathcal{R}_e^2 + E\mathcal{R}^2k^2 + F\mathcal{R}_e^2k^2, \tag{12.100}$$

where

$$\begin{aligned}A = \frac{1}{2}\sum_i h_{ei}^4\Bigg[&(N_i - N_{i-1})\frac{K_i}{R_i^3} + L_i^2\left(\frac{1}{N_iz'_i} - \frac{1}{N_{i-1}z_i}\right)\\ &-2L_i(Q_i - L_i)\left(\frac{1}{N_iw'_{ei}} - \frac{1}{N_{i-1}w_{ei}}\right)\\ &+(Q_i - L_i)^2\left(\frac{z'_i}{N_iw'^2_{ei}} - \frac{z_i}{N_{i-1}w_{ei}}\right)\Bigg],\end{aligned} \tag{12.101}$$

$$B = \frac{1}{2}\sum_i h_i^4\left[(N_i - N_{i-1})\frac{K_i}{R_i^3} + Q_i^2\left(\frac{1}{N_iz'_i} - \frac{1}{N_{i-1}z_i}\right)\right], \tag{12.102}$$

$$C = \frac{1}{2}\sum_i h_i^2 h_{ei}^2 \left[(N_i - N_{i-1})\frac{K_i}{R_i^3} + L_i^2 \left(\frac{1}{N_i z_i'} - \frac{1}{N_{i-1} z_i} \right) \right], \tag{12.103}$$

$$\begin{aligned} D = \frac{1}{2}\sum_i h_i^2 h_{ei}^2 \Bigg[& (N_i - N_{i-1})\frac{K_i}{R_i^3} + Q_i L_i \left(\frac{1}{N_i z_i'} - \frac{1}{N_{i-1} z_i} \right) \\ & - Q_i (Q_i - L_i) \left(\frac{1}{N_i w_{ei}'} - \frac{1}{N_{i-1} w_{ei}} \right) \Bigg], \end{aligned} \tag{12.104}$$

$$\begin{aligned} E = \frac{1}{2}\sum_i h_i h_{ei}^3 \Bigg[& (N_i - N_{i-1})\frac{K_i}{R_i^3} + L_i^2 \left(\frac{1}{N_i z_i'} - \frac{1}{N_{i-1} z_i} \right) \\ & - L_i (Q_i - L_i) \left(\frac{1}{N_i w_{ei}'} - \frac{1}{N_{i-1} w_{ei}} \right) \Bigg], \end{aligned} \tag{12.105}$$

$$F = \frac{1}{2}\sum_i h_i^3 h_{ei} \left[(N_i - N_{i-1})\frac{K_i}{R_i^3} + Q_i L_i \left(\frac{1}{N_i z_i'} - \frac{1}{N_{i-1} z_i} \right) \right]. \tag{12.106}$$

It remains to apply formulae (12.54) to evaluate the primary aberrations of an axially symmetric system. To this end, it is sufficient to rewrite (12.100)–(12.106) in terms of the ordinary coordinate y of the object point belonging to meridional plane and the coordinates x_e, y_e in the entrance pupil.

Chapter 13
Introduction to Optics in Anisotropic Media

13.1 Maxwell's Equations in Anisotropic Media

Until now we have considered optical media that have a refractive index constant or depending on the point; in other words, we have only considered isotropic homogeneous or nonhomogeneous media. In this section we take into account a dielectric medium S that is homogeneous but anisotropic. If $\mathbf{x}(t)$ is the parametric equation of a ray, then the refractive index N of S depends on the vector $\dot{\mathbf{x}}$ tangent to $\mathbf{x}(t)$. Can we say that the extremals of the following functional

$$\int_{t_1}^{t_2} N(\dot{\mathbf{x}})ds = \int_{t_1}^{t_2} N(\dot{\mathbf{x}}) \sum_{i=1}^{3} \sqrt{\dot{x}_i^2}dt, \tag{13.1}$$

identify the rays in an anisotropic medium S? In other words, Fermat's principle in S is expressed by the condition to minimize (13.1)? If this formulation of Fermat's principle holds, how can we assign the function $N(\dot{\mathbf{x}})$?

We start searching for an answer to the latter question. Since light waves are electromagnetic waves, their propagation in a dielectric is described by Maxwell's equations

$$\nabla \times \mathbf{E} = -\frac{\partial \mathbf{B}}{\partial t}, \quad \nabla \cdot \mathbf{D} = 0, \tag{13.2}$$

$$\nabla \times \mathbf{H} = \frac{\partial \mathbf{D}}{\partial t}, \quad \nabla \cdot \mathbf{B} = 0, \tag{13.3}$$

where $\mathbf{E}$ is the electric field, $\mathbf{H}$ is the magnetic field, $\mathbf{D}$ the electric induction, and $\mathbf{B}$ the magnetic induction. In a linear, homogeneous anisotropic and nonmagnetic dielectric S the following constitutive equations hold

$$\mathbf{D} = \epsilon \cdot \mathbf{E}, \quad \mathbf{B} = \mu \mathbf{H}. \tag{13.4}$$

© Springer International Publishing Switzerland 2016

A. Romano and R. Cavaliere, *Geometric Optics*,
Modeling and Simulation in Science, Engineering and Technology,
DOI 10.1007/978-3-319-43732-3_13

In (13.4) $\boldsymbol{\epsilon}$ and μ are the dielectric tensor and the magnetic permeability, respectively. It is possible to prove that the 2−tensor $\boldsymbol{\epsilon}$ is symmetric and positive definite, i.e.,

$$\epsilon_{ij} = \epsilon_{ji}, \quad \epsilon_{ij} u_i u_j > 0, \tag{13.5}$$

for any vector $\mathbf{u}$.[1] Due to (13.5) we can state that the eigenvalue equation

$$\boldsymbol{\epsilon} \cdot \mathbf{u} = \lambda \mathbf{u}, \tag{13.6}$$

admits three real and positive eigenvalues and at least an orthogonal basis of eigenvectors. The multiplicity of the eigenvalues depends on the crystal class of S. Conditions (13.5) imply that the points (x_i) satisfying the equation

$$(\epsilon_r)_{ij} x_i x_j = 1$$

belong to the surface of an ellipsoid that is named *Fresnel's ellipsoid*.

The speed of propagation of electromagnetic waves in a dielectric S can be determined in many ways. Here, we analyze the propagation of plane waves in a dielectric S since we are assuming that S is homogeneous and both the constitutive equations (13.4) and Maxwell's equations (13.2), (13.3) are linear.

A plane electromagnetic wave is represented by the equations

$$\mathbf{E} = \mathbf{e} e^{i \frac{2\pi}{\lambda} (\mathbf{n} \cdot \mathbf{x} - vt)}, \quad \mathbf{H} = \mathbf{h} e^{i \frac{2\pi}{\lambda} (\mathbf{n} \cdot \mathbf{x} - vt)}, \tag{13.7}$$

where $\mathbf{e}$ is the vector amplitude of electric field, $\mathbf{h}$ the vector amplitude of magnetic field, $\mathbf{n}$ the unit vector that defines the direction of propagation, λ the wavelength, and v the speed of propagation. Introducing (13.7) into (13.2), (13.3) we obtain

$$\mathbf{n} \times \mathbf{e} = \mu v \mathbf{h}, \tag{13.8}$$

$$\mathbf{n} \cdot \boldsymbol{\epsilon} \cdot \mathbf{e} = 0, \tag{13.9}$$

$$\mathbf{n} \times \mathbf{h} = -v \boldsymbol{\epsilon} \cdot \mathbf{e}, \tag{13.10}$$

$$\mathbf{n} \cdot \mathbf{h} = 0. \tag{13.11}$$

In view of (13.11) and (13.9), the vector amplitude of magnetic field $\mathbf{h}$ and the vector amplitude of the electric induction $\mathbf{d} \equiv \boldsymbol{\epsilon} \cdot \mathbf{e}$ are orthogonal to $\mathbf{n}$ so that $\mathbf{h}$, $\mathbf{d}$, and $\mathbf{n}$ form a triad of mutually orthogonal vectors. Finally, from (13.8) follows that $\mathbf{e}$ is contained in the plane formed by $\mathbf{n}$ and $\mathbf{d}$; in particular, $\mathbf{e}$ is orthogonal to $\mathbf{h}$. Therefore, the unit vector $\mathbf{t}$ is parallel to Poynting's vector $\mathbf{e} \times \mathbf{h}$ (see Figure 13.1).

When (13.9) is taken into account, the cross product of (13.8) by $\mathbf{n}$ leads us to the result

$$\mathbf{n} \times (\mathbf{n} \times \mathbf{e}) = \mu v \mathbf{n} \times \mathbf{h} = -v^2 \mu \boldsymbol{\epsilon} \cdot \mathbf{e}. \tag{13.12}$$

[1] Here and in the sequel we adopt the convention of summation over repeated indices.

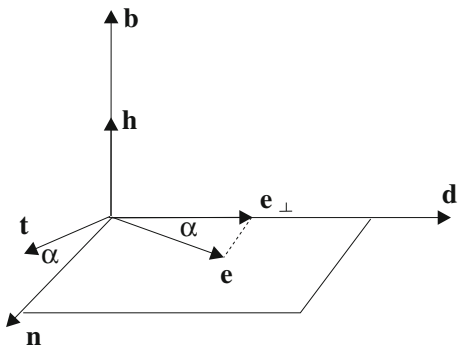

Fig. 13.1 Orientation of electromagnetic fields

On the other hand, the following vector identity holds

$$\mathbf{n} \times (\mathbf{n} \times \mathbf{e}) = (\mathbf{n} \cdot \mathbf{e})\mathbf{n} - (\mathbf{n} \cdot \mathbf{n})\mathbf{e}, \tag{13.13}$$

and noting that $\mathbf{n} \cdot \mathbf{n} = 1$, we can give (13.12) the form

$$(\mathbf{n} \cdot \mathbf{e})\mathbf{n} - \mathbf{e} = -v^2 \mu \boldsymbol{\epsilon} \cdot \mathbf{e}. \tag{13.14}$$

Multiplying (13.14) by $\boldsymbol{\epsilon}^{-1}$, we finally obtain

$$\mathbf{Q}(\mathbf{n}) \cdot \mathbf{e} = v^2 \mathbf{e}, \tag{13.15}$$

where the 2−tensor

$$\mathbf{Q}(\mathbf{n}) = \frac{1}{\mu}(\mathbf{I} - \mathbf{n} \otimes \mathbf{n}) \cdot \boldsymbol{\epsilon}^{-1}, \tag{13.16}$$

is named the ***acoustic tensor***. Equation (13.15) shows that the speeds of propagation of the electromagnetic waves along the direction $\mathbf{n}$ are eigenvalues of the acoustic tensor $\mathbf{Q}$ while their vector amplitudes are eigenvectors of $\mathbf{Q}$.

13.2 Refractive Index in Anisotropic Media

If we adopt a Cartesian frame of orthogonal coordinates $Ox_1x_2x_3$ whose axes are eigenvectors of the tensor $\boldsymbol{\epsilon}$, the components of this tensor are given by the matrix

$$(\mu\epsilon_{ij}) = \mu \begin{pmatrix} \epsilon_1 & 0 & 0 \\ 0 & \epsilon_2 & 0 \\ 0 & 0 & \epsilon_3 \end{pmatrix}, \tag{13.17}$$

where ϵ_1, ϵ_2, and ϵ_3 are the eigenvalues of $\boldsymbol{\epsilon}$.

Further, recalling that $\boldsymbol{\epsilon}$ and $\boldsymbol{\epsilon}^{-1}$ have the same eigenvectors and that the eigenvalues of $\boldsymbol{\epsilon}^{-1}$ are the reciprocal of the eigenvalues of $\boldsymbol{\epsilon}$, the components of $\frac{1}{\mu}\boldsymbol{\epsilon}^{-1}$ in the frame $Ox_1x_2x_3$ are given by the matrix

$$\left(\frac{1}{\mu}\epsilon_{ij}^{-1}\right) = \frac{1}{\mu}\begin{pmatrix} 1/\epsilon_1 & 0 & 0 \\ 0 & 1/\epsilon_2 & 0 \\ 0 & 0 & 1/\epsilon_3 \end{pmatrix}. \tag{13.18}$$

Before analyzing the eigenvalue equation (13.16), we consider the particular case in which the electromagnetic wave propagates along one of the eigenvectors of $\boldsymbol{\epsilon}$, that is, along one of the coordinate axes of the frame $Ox_1x_2x_3$, for instance, along Ox_3. In this case $\mathbf{n} = \mathbf{k} = (0, 0, 1)$, where $\mathbf{k}$ is the unit vector along Ox_3, and the equation (13.16) becomes

$$\mu^{-1}\begin{pmatrix} \epsilon_1^{-1} & 0 & 0 \\ 0 & \epsilon_2^{-1} & 0 \\ 0 & 0 & 0 \end{pmatrix}\begin{pmatrix} e_1 \\ e_2 \\ e_3 \end{pmatrix} = v^2\begin{pmatrix} e_1 \\ e_2 \\ e_3 \end{pmatrix}. \tag{13.19}$$

Then, the acoustic tensor $\mathbf{Q}(\mathbf{k})$ admits the following eigenvalues

$$v_1 = \frac{1}{\sqrt{\mu\epsilon_1}}, \quad v_2 = \frac{1}{\sqrt{\mu\epsilon_2}}, \tag{13.20}$$

and the eigenvectors belonging to these eigenvalues are

$$\mathbf{e}_1 = (1, 0, 0), \quad \mathbf{e}_2 = (0, 1, 0), \tag{13.21}$$

respectively. In other words, two waves can propagate along the principal axis Ox_3 with velocity of propagation given by (13.20). Further, the wave with a velocity of propagation v_1 is polarized since the electric field is directed along the principal axis Ox_1 and the second wave is polarized with the electric field directed along Ox_2. If we consider the propagation along the principal axis Ox_2, we obtain that the two waves propagate with velocities $v_1 = 1/\sqrt{\mu\epsilon_1}$ and $v_3 = 1/\sqrt{\mu v_3}$. The velocities

$$v_1 = \frac{1}{\sqrt{\mu\epsilon_1}}, \; v_2 = \frac{1}{\sqrt{\mu\epsilon_2}}, \; v_3 = \frac{1}{\sqrt{\mu\epsilon_3}}, \tag{13.22}$$

are called the three *principal velocities of propagation*.

Now, we analyze equation (13.15) for any direction $\mathbf{n}$ different from the principal axes. From equation (13.14), that is equivalent to (13.14), we obtain

$$v^2\mu\epsilon_k e_k = (e_k - n_k(\mathbf{n}\cdot\mathbf{e})), \quad k = 1, 2, 3. \tag{13.23}$$

Solving this equation with respect to e_k we obtain

$$e_k = \frac{v_k^2 n_k}{v_k^2 - v^2}(\mathbf{n} \cdot \mathbf{e}). \tag{13.24}$$

Multiplying (13.24) by n_k and summing over k, we have

$$1 = \sum_{k=1}^{3} \frac{v_k^2 n_k}{v_k^2 - v^2}.$$

Since $n_1^2 + n_2^2 + n_3^2 = 1$, the above equation can also be written as

$$\sum_{k=1}^{3} n_k^2 = \sum_{k=1}^{3} \frac{v_k^2 n_k}{v_k^2 - v^2},$$

or, equivalently, as *Fresnel's equation of wave normals*.

$$\frac{n_1^2}{v_1^2 - v^2} + \frac{n_2^2}{v_2^2 - v^2} + \frac{n_3^2}{v_3^2 - v^2} = 0. \tag{13.25}$$

This equation can be written in different equivalent forms. In fact, when we recall that the refractive index is given by

$$N = \frac{c}{v}, \tag{13.26}$$

it is easy to verify that each of the following two equations is equivalent to (13.25):

$$\frac{n_1^2}{\dfrac{c^2}{N^2} - \dfrac{1}{\mu\epsilon_1}} + \frac{n_2^2}{\dfrac{c^2}{N^2} - \dfrac{1}{\mu\epsilon_2}} + \frac{n_3^2}{\dfrac{c^2}{N^2} - \dfrac{1}{\mu\epsilon_3}} = 0, \tag{13.27}$$

$$\frac{n_1^2}{N^2 - c^2\mu\epsilon_1} + \frac{n_2^2}{N^2 - c^2\mu\epsilon_2} + \frac{n_3^2}{N^2 - c^2\mu\epsilon_3} = \frac{1}{N^2}. \tag{13.28}$$

It is important to note that in the above formulae the propagation unit vector $\mathbf{n}$ must be different from one of the principal axes of $\boldsymbol{\epsilon}$. In fact, if $\mathbf{n} = (1, 0, 0)$, then (13.25) seems to lead to an absurd result. However, when $\mathbf{n} = (1, 0, 0)$ the denominators of the second and third terms on the left-hand side of (13.25) go to zero as the corresponding numerators.

In conclusion, *in an anisotropic homogeneous medium two monochromatic plane waves with two different linear polarizations and two different velocities of propagation can propagate along any given direction. Consequently, in any direction the medium exhibits two different diffractive indices. The values of these indices can be obtained solving one of the equations* (13.25)–(13.28).

13.3 Fermat's Principle in Anisotropic Media

The considerations of the above sections show that the light traversing an anisotropic medium consists of two distinct waves that propagate independently of each other. We distinguish the two kinds of waves and the quantities associated with them by the subscripts a and b. In particular we have two kinds of rays $\mathfrak{R}_a$ and $\mathfrak{R}_b$ with the property that the tangent to $\mathfrak{R}_a$ at a point P gives the direction along which the radiant energy is transported at P; we can attribute an analogous meaning to the tangent vector to $\mathfrak{R}_b$.

Now, we state that *each kind of ray is governed by Fermat's principle*, granted that the optical medium is supposed to be defined by two distinct refractive indices $N_a(P)$ and $N_b(P)$. For instance, the ray $\mathfrak{R}_a$ joining two points A and A' is that curve for which the functional

$$F_a = \int_A^{A'} N_a(P)ds \tag{13.29}$$

is stationary. A similar statement holds for the ray $\mathfrak{R}_b$. As a consequence, there are two optical distances $V_a(A, A')$ and $V_b(A, A')$ between the points A and B and then two point characteristics $V_a(x', y', z', x, y, z)$ and $V_b(x', y', z', x, y, z)$, one for each kind of ray.

If we denote by (t_1, t_2, t_3) the director cosines of a ray, the refractive index in an isotropic medium can be written as follows:

$$N = N_i\sqrt{t_1^2 + t_2^2 + t_3^2} = N_i. \tag{13.30}$$

The simplest formal anisotropic generalization of (13.30) is

$$N = \sqrt{\sum_{h,k} a_{hk}t_h t_k}, \tag{13.31}$$

where $a_{hk} = a_{kh}$ are six constants such that $N^2 > 0$ for all the values of t_k. By the adjective formal we mean that we are not necessarily able to find a physical material satisfying (13.31). However, we know that it is not a quite arbitrary choice since a *uniaxial crystal* has the refractive indices

$$N_a = \sqrt{b}\sqrt{t_1^2 + t_2^2 + t_3^2} = \sqrt{b}, \tag{13.32}$$

$$N_b = \sqrt{bt_1^2 + a(t_2^2 + t_3^2)}, \tag{13.33}$$

where a and b are positive constants and the axes have been appropriately chosen. Note that the crystal behaves as an isotropic medium for a-rays. Further, N_b is invariant under rotations about the x-axis.

We now analyze Fermat's principle when the refractive index is given by (13.31). That means that we are analyzing the behavior of one of the two possible rays. The results of our analysis will describe a real situation provided that (13.31) corresponds to a real medium.

Fermat's principle we analyze consists of searching for the extremals of the functional

$$\mathfrak{F} = \int_A^B N(\mathbf{x}, \dot{\mathbf{x}})ds = \int_A^B \sqrt{a_{hk}\dot{x}_h\dot{x}_k}ds, \tag{13.34}$$

where $\mathbf{x}(s)$ is a curve between two points A and B, $\dot{\mathbf{x}} = d\mathbf{x}/ds$, and s is the curvilinear abscissa along this curve. We note that integral (13.34) does not depend on parametrization of the curves.

It is well known that the extremals of functional (13.34) are solutions of the Lagrange equations of (13.34)

$$\frac{\partial N}{\partial x_h} - \frac{d}{ds}\left(\frac{a_{hk}\dot{x}_k}{N}\right) = 0, \;\; h = 1, 2, 3. \tag{13.35}$$

If we introduce the notation

$$p_h = \frac{a_{hk}\dot{x}_k}{N}, \tag{13.36}$$

we have also

$$\dot{x}_h = N(a^{-1})_{hk}p_k, \tag{13.37}$$

and Lagrange equations are equivalent to the system

$$\dot{x}_h = N(a^{-1})_{hk}p_k, \tag{13.38}$$

$$\dot{p}_h = \frac{\partial N}{\partial x_h}. \tag{13.39}$$

In particular, when the medium is homogeneous N does not depend on $\mathbf{x}$ and the previous system becomes

$$\dot{x}_h = N(a^{-1})_{hk}p_k s, \tag{13.40}$$

$$\dot{p}_h = 0. \tag{13.41}$$

We conclude this section noting that

$$d\sigma^2 = a_{hk}dx_h dx_k = N^2 ds^2 \tag{13.42}$$

is a Riemannian metric of $\Re^3$ so that the extremals of functional (13.34) are geodesics of (13.42).

Appendix A
First-Order PDE

A.1 Monge's Cone

In this appendix we give a sketch of the method proposed by Monge, Ampere, and Cauchy to reduce the integration of a first-order PDE to the integration of a system of ordinary equations.

Let $F(\mathbf{x}, u, \mathbf{p})$ be a function of class $C^2(\Re^{2n+1})$ verifying the following conditions:

1. the set $\mathfrak{F} = \left\{(\mathbf{x}, u, \mathbf{p}) \in \Re^{2n+1},\ F(\mathbf{x}, u, \mathbf{p}) = 0\right\}$ is not empty;
2. $\sum_{i=1}^{n} F_{p_i}^2 \neq 0,\ \forall(\mathbf{x}, u, \mathbf{p}) \in \mathfrak{F}$.

Under these hypotheses, we consider the following general first-order PDE:

$$F(\mathbf{x}, u, \nabla u) = 0, \tag{A.1}$$

in the unknown $u = u(\mathbf{x}) \in C^2(D)$, with $D \subset \Re^n$, will be considered.

First, we note that, any solution $u = u(\mathbf{x})$ of (A.1) defines a surface Σ which is called an ***integral surface*** of the equation (A.1). Moreover, the vector $\mathbf{N} \equiv (\nabla u, -1) \equiv (\mathbf{p}, -1)$ of $\Re^{n+1}$ is normal to the integral surface Σ. Consequently, the equation (A.1) expresses the relation existing between the normal vectors to all the integral surfaces at any point $(\mathbf{x}, u)$.

To understand the geometrical meaning of this relation, we start noting that the quantities $(\mathbf{x}_0, u_0, \mathbf{p}_0)$ completely define a plane containing the point $(\mathbf{x}_0, u_0)$ and having a normal vector with components $(\mathbf{p}_0, -1)$. Then, for a fixed point $(\mathbf{x}_0, u_0)$, the equation

$$F(\mathbf{x}_0, u_0, \mathbf{p}_0) = 0, \tag{A.2}$$

defines a set Π_0 of planes containing $(\mathbf{x}_0, u_0)$ and tangent to the integral surfaces of (A.1) to which $(\mathbf{x}_0, u_0)$ belongs. Owing to the conditions 1 and 2, Π_0 is not empty and we can suppose that $F_{p_n}(\mathbf{x}_0, u_0, \mathbf{p}_0) \neq 0$. In turn, this result implies that the equation (A.2), at least locally, can be written in the form:

© Springer International Publishing Switzerland 2016

A. Romano and R. Cavaliere, *Geometric Optics*,
Modeling and Simulation in Science, Engineering and Technology,
DOI 10.1007/978-3-319-43732-3

$$p_n = p_n(\mathbf{x}_0, u_0, p_1, \ldots, p_{n-1}).$$

Consequently, the set Π_0 is formed by a family of planes depending on the parameters $(p_1, \ldots, p_{n-1})$. Any plane $\pi \in \Pi_0$, contains the point $(\mathbf{x}_0, u_0)$ and has $(p_1, \ldots, p_{n-1}, p_n(p_1, \ldots, p_{n-1}), -1)$ as normal vector, i.e., it is represented by the following equation

$$f(\mathbf{X}, U, p_1, \ldots, p_{n-1}) \equiv \sum_{\alpha=1}^{n-1} p_\alpha (X_\alpha - x_{0\alpha}) + p_n(p_\alpha)(U - u_0) = 0, \tag{A.3}$$

where $(\mathbf{X}, U)$ are the coordinates of any point of π.

The envelope of all these planes is defined by the system formed by the equation (A.3) and the following other equation

$$(X_\alpha - x_{0\alpha}) + \frac{\partial p_n}{\partial p_\alpha}(X_n - x_{0n}) = 0, \quad \alpha = 1, \ldots, n-1, \tag{A.4}$$

which is obtained differentiating (A.3) with respect to p_α, $\alpha = 1, \ldots, n-1$. By Dini's theorem $\partial p_n / \partial p_\alpha = -F_{p_\alpha}/F_{p_n}$ and (A.4) becomes

$$F_{p_n}(X_\alpha - x_{0\alpha}) - F_{p_\alpha}(X_n - x_{0n}) = 0, \quad \alpha = 1, \ldots, n-1. \tag{A.5}$$

The equations (A.3) and (A.5) constitute a linear system of n equations in the unknowns $((X_\alpha - x_{0\alpha}), (X_n - x_{0n}))$. The determinant of the matrix of the coefficients of this system is

$$\Delta = \begin{pmatrix} p_1 & p_2 & \ldots & p_{n-1} & p_n \\ F_{p_n} & 0 & \ldots & 0 & -F_{p_1} \\ 0 & F_{p_n} & \ldots & 0 & -F_{p_2} \\ \ldots & \ldots & \ldots & \ldots & \ldots \\ 0 & 0 & \ldots & F_{p_n} & -F_{p_{n-1}} \end{pmatrix} = (-1)^{n-1} F_{p_n}^{n-2} (\mathbf{p} \cdot \mathbf{F_p}) \neq 0.$$

Consequently, the parametric equations of the envelope of Π_0 become

$$X_i - x_{0i} = \frac{F_{p_i}}{\mathbf{p} \cdot \mathbf{F_p}}(U - u_0), \quad i = 1, \ldots, n. \tag{A.6}$$

These equations define a cone C_0 since, if the vector $\mathbf{V} = (\mathbf{X} - \mathbf{x}_0, U - u_0)$ is a solution of (A.6), then also the vector $\lambda \mathbf{V}$, where $\lambda \in \Re$, is a solution. This cone C_0 is called ***Monge's cone*** at $(\mathbf{x}_0, u_0)$.

A.2 Characteristic Strips

The above considerations allow us to state that, if $u = u(\mathbf{x})$ is an integral surface Σ of (A.1), then the tangent plane to Σ at the point $(\mathbf{x}_0, u_0)$ belongs to Π_0, i.e., it is tangent to Monge's cone at that point (see Figure A.1). Moreover, the characteristic directions of Monge's cone, which are tangent to Σ, define a field of tangent vectors on Σ whose integral curves are called ***characteristic curves***.

We can associate with any point of this curves $(\mathbf{x}(s), u(s))$ a tangent plane to Σ having director cosines $(\mathbf{p}, -1) \equiv (\nabla u(\mathbf{x}(s)), -1)$. The 1-parameter family of these planes along a characteristic curve is said to be a ***characteristic strip*** (see Figure A.2).

Now, we write the system of ordinary differential equations in the unknowns $(\mathbf{x}(s), u(s), \mathbf{p}(s))$ that define a characteristic strip on the integral surface Σ. Since the tangent to a characteristic curve at a point belongs to Monge's cone at that point, from (A.6) we have that

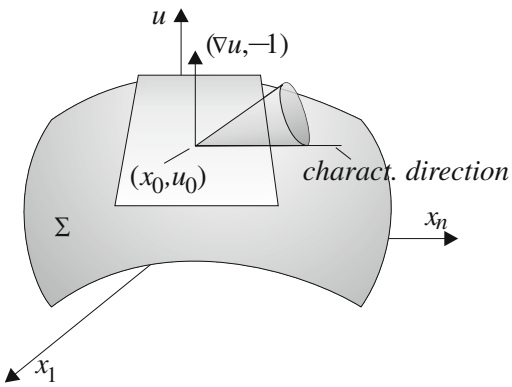

Fig. A.1 Monge's cone

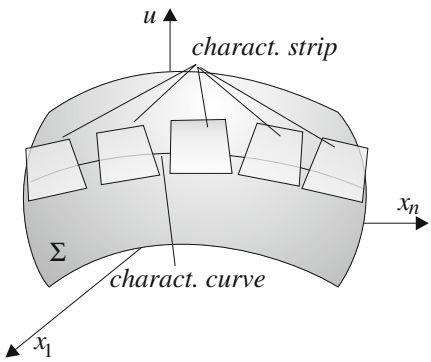

Fig. A.2 Characteristic curve and strip

$$\frac{d\mathbf{x}}{ds} = F_{\mathbf{p}}, \tag{A.7}$$

$$\frac{du}{ds} = \mathbf{p} \cdot F_{\mathbf{p}}. \tag{A.8}$$

Moreover, along a characteristic curve $(\mathbf{x}(s), u(s))$ it is $\mathbf{p}(s) = \nabla u(\mathbf{x}(s))$ and then we have that

$$\frac{dp_i}{ds} = u_{x_i x_j} F_{p_j}.$$

On the other hand, the differentiation of (A.1) with respect to x_i gives

$$F_{x_i} + u_{x_i} F_u + u_{x_i x_j} F_{p_j} = 0.$$

Comparing the two last relations, we obtain the following system of $2n+1$ equations

$$\frac{d\mathbf{x}}{ds} = F_{\mathbf{p}}, \tag{A.9}$$

$$\frac{d\mathbf{p}}{ds} = -(F_{\mathbf{x}} + F_u \mathbf{p}), \tag{A.10}$$

$$\frac{du}{ds} = \mathbf{p} \cdot F_{\mathbf{p}}, \tag{A.11}$$

in the $2n+1$ unknowns $(\mathbf{x}(s), u(s), \mathbf{p}(s))$, which is called the ***characteristic system*** of the equation (A.1).

We have proved that, if $u(\mathbf{x})$ is an integral surface of (A.1), then its characteristic strips satisfy system (A.9)–(A.11). Moreover, any solution of (A.9)–(A.11) is a characteristic strip of an integral surface of (A.1), as it is proved by the following

Theorem A.1 *Let $(\mathbf{x}_0, u_0, \mathbf{p}_0 = \nabla u(\mathbf{x}_0))$ be the tangent plane to an integral surface Σ at the point $\mathbf{x}_0, u_0)$. Then, the solution of (A.9)–(A.11) corresponding to the initial datum $(\mathbf{x}_0, u_0, \mathbf{p}_0)$ is a characteristic strip of Σ.*

Proof It is sufficient to recall what we have already proved and to remark that the characteristic strip determined by the initial datum $(\mathbf{x}_0, u_0, \mathbf{p}_0)$ is unique for the uniqueness theorem. □

Taking into account the function $F(\mathbf{x}(s), u(s), \mathbf{p}(s))$ and recalling (A.9)–(A.11), we verify that

Theorem A.2

$$F(\mathbf{x}(s), u(s), \mathbf{p}(s)) = const. \tag{A.12}$$

Remark A.1 If the equation (A.1) is quasi-linear

$$F(\mathbf{x}, u, \nabla u) = \mathbf{a}(\mathbf{x}, u) \cdot \nabla u - b(\mathbf{x}, u) = 0, \tag{A.13}$$

then the system (A.9), (A.11) becomes

$$\frac{d\mathbf{x}}{ds} = \mathbf{a}(\mathbf{x}, u), \tag{A.14}$$

$$\frac{du}{ds} = b(\mathbf{x}, u). \tag{A.15}$$

This is a system of $n+1$ equations in the unknowns $(\mathbf{x}(s), u(s))$ which can be solved without the help of (A.10). More particularly, if (A.13) is linear, then $\mathbf{a}$ and $\mathbf{b}$ depend only on $\mathbf{x}$. Therefore, the equations (A.14) supply the projection of the characteristic curves in $\Re^n$ and (A.15) gives the remaining unknown $u(s)$.

Remark A.2 Let us suppose that (A.1) has the form:

$$F(\mathbf{x}, \nabla u) = 0. \tag{A.16}$$

Denoting by t the variable x_n, p the derivative F_{u_t}, $\mathbf{x}$ the vector $(x_1, \ldots, x_{n-1})$, and $\mathbf{p}$ the vector $(p_1, \ldots, p_{n-1})$, the above equation becomes

$$F(\mathbf{x}, t, \mathbf{p}, p) = 0, \tag{A.17}$$

If $F_p \neq 0$, then (A.17) can be written as Hamilton–Jacobi equation

$$p + H(\mathbf{x}, t, \mathbf{p}) = 0, \tag{A.18}$$

whose characteristic system is

$$\frac{d\mathbf{x}}{ds} = H_{\mathbf{p}}, \tag{A.19}$$

$$\frac{d\mathbf{p}}{ds} = -H_{\mathbf{x}}, \tag{A.20}$$

$$\frac{du}{ds} = \mathbf{p} \cdot H_{\mathbf{p}} + p, \tag{A.21}$$

$$\frac{dt}{ds} = 1, \tag{A.22}$$

$$\frac{dp}{ds} = -H_t. \tag{A.23}$$

Owing to (A.22), we can identify s with t and the above system becomes

$$\frac{d\mathbf{x}}{dt} = H_{\mathbf{p}}, \tag{A.24}$$

$$\frac{d\mathbf{p}}{dt} = -H_{\mathbf{x}}, \tag{A.25}$$

$$\frac{du}{dt} = \mathbf{p} \cdot H_{\mathbf{p}} - H, \tag{A.26}$$

$$\frac{dp}{ds} = -H_t. \tag{A.27}$$

We note that (A.24), (A.25) are Hamiltonian equations which can be solved independently of the remaining ones.

A.3 Cauchy's Problem

The Cauchy problem relative to (A.1) can be formulated as it follows:

Let Γ be a $(n-1)-$ dimensional manifold, contained in a region D of $\Re^n$, and let $u_0(\mathbf{x}) \in C^2(\Gamma)$ be an assigned function on Γ. Determine a solution $u(\mathbf{x})$ of (A.1) whose restriction to Γ coincides with $u_0(\mathbf{x})$.

In other words, if

$$\mathbf{x}_0 = \mathbf{x}_0(v_\alpha), \quad (v_\alpha) \in V \subset \Re^{n-1}, \tag{A.28}$$

is a parametric representation of Γ, Cauchy's problem consists in finding a solution $u(\mathbf{x})$ of (A.1) such that

$$u(\mathbf{x}_0(v_\alpha)) = u_0(\mathbf{x}_0(v_\alpha)). \tag{A.29}$$

Geometrically, we can say that we want to determine a $n-$dimensional manifold $u(\mathbf{x})$ satisfying (A.1) and containing the initial $(n-1)-$dimensional manifold Γ.

We prove that the requested solution can be obtained as the envelope of a suitable family of characteristic strips. To this regard, we first note that the points of Γ, given by the initial datum (A.29), supply the initial data for the unknowns $\mathbf{x}(s)$, $u(s)$ of the equations (A.9), (A.11). However, up to now, we have no initial data for the unknown $\mathbf{p}(s)$. We show that these data can also be obtained by (A.29). In fact, we recall that the variable $\mathbf{p}$, together with -1, defines the normal vector to the tangent plane to the integral surface Σ at the point $(\mathbf{x}, u(\mathbf{x})) \in \Sigma$. Moreover, Σ must be tangent to the Monge cone along a characteristic direction at any point and, in particular, at any point of Γ (see Figure A.3).

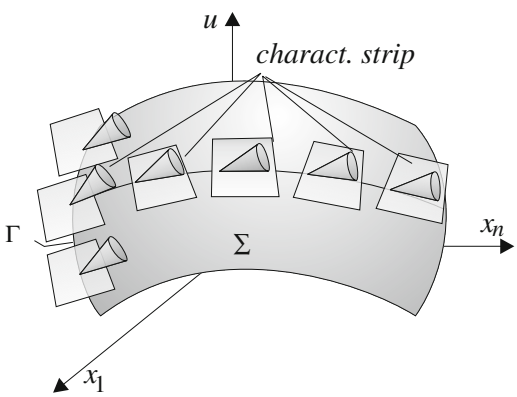

Fig. A.3 Cauchy data for (A.9)–(A.11)

Consequently, we take $\mathbf{p}_0$ in such a way that, at any point of Γ, $(\mathbf{p}_0, -1)$ is orthogonal to the vector $(\partial\mathbf{x}/\partial v_\alpha, \partial u/\partial v_\alpha)$, which is tangent to Γ. In formulae, we have that

$$\frac{\partial \mathbf{x}_0}{\partial v_\alpha} \cdot \mathbf{p}_0 - \frac{\partial u_0}{\partial v_\alpha} = 0, \tag{A.30}$$

$$F(\mathbf{x}_0(v_\alpha), u_0(v_\alpha), \mathbf{p}_0(v_\alpha)) = 0, \tag{A.31}$$

$\alpha = 1, \ldots, n-1$.

If $(\overline{\mathbf{x}}_0(\overline{v}_\alpha), \overline{u}(\overline{v}_\alpha), \overline{\mathbf{p}}_0(\overline{v}_\alpha)) \in \Gamma$ verifies the above system and the following condition is satisfied at this point

$$J = \det\left(\tfrac{\partial \mathbf{x}_0}{\partial v_\alpha}\ F_{\mathbf{p}}\right) \neq 0, \tag{A.32}$$

the system (A.30), (A.31) can be solved with respect to $\mathbf{p}_0(v_\alpha)$ in a neighborhood of the point $(\overline{\mathbf{x}}_0(\overline{v}_\alpha), \overline{u}(\overline{v}_\alpha), \overline{\mathbf{p}}_0(\overline{v}_\alpha))$. In this way we obtain the initial data for (A.9)–(A.11).

In any book on the PDEs, the proof of the following theorem can be found:

Theorem A.3 *If it is possible to complete the initial datum (A.29) by solving with respect to* $\mathbf{p}_0(v_\alpha)$ *the system (A.30), (A.31), then one and only one solution exists of the Cauchy problem.*

Appendix B
Symplectic Vector Spaces

B.1 Definition

Definition B.1 A ***symplectic vector space*** is a pair $(E_{2n}, \mathbf{\Omega})$, where E_{2n} is a vector space with even dimension and $\mathbf{\Omega}$ a skew-symmetric non-degenerate $(0, 2)$-tensor.

Remark B.1 It is fundamental to require that the dimension of the vector space is odd. In fact, owing to theorem 4.2, in a vector space with even dimension, any skew-symmetric $(0, 2)$-tensor is always degenerate.

Definition B.2 In the symplectic vector space $(E_{2n}, \mathbf{\Omega})$, the ***anti-scalar product*** is the map $(\mathbf{x}, \mathbf{y}) \in E_{2n} \times E_{2n} \to [\mathbf{x}, \mathbf{y}] \in \Re$ such that

$$[\mathbf{x}, \mathbf{y}] = \mathbf{\Omega}(\mathbf{x}, \mathbf{y}). \tag{B.1}$$

The anti-scalar product has the following properties:

$$[\mathbf{x}, \mathbf{y}] = -[\mathbf{y}, \mathbf{x}], \tag{B.2}$$

$$\left[\mathbf{x}, \mathbf{y} + \mathbf{z}\right] = \left[\mathbf{x}, \mathbf{y}\right] + \mathbf{x}, \mathbf{z}, \tag{B.3}$$

$$a\left[\mathbf{x}, \mathbf{y}\right] = \left[a\mathbf{x}, \mathbf{y}\right], \tag{B.4}$$

$$\left[\mathbf{x}, \mathbf{y}\right] = 0, \forall \mathbf{y} \in E_{2n} \Rightarrow \mathbf{x} = \mathbf{0}. \tag{B.5}$$

In fact, the first property follows from the skew-symmetry of $\mathbf{\Omega}$. The second and third properties follow from the bilinearity of $\mathbf{\Omega}$. Finally, the fourth property is due to the fact that $\mathbf{\Omega}$ is non-degenerate.

We say that the vectors $\mathbf{x}$ and $\mathbf{y}$ are anti-orthogonal if

$$\left[\mathbf{x}, \mathbf{y}\right] = 0. \tag{B.6}$$

© Springer International Publishing Switzerland 2016

A. Romano and R. Cavaliere, *Geometric Optics*,
Modeling and Simulation in Science, Engineering and Technology,
DOI 10.1007/978-3-319-43732-3

In view of (B.5), we can state that the only vector which is anti-orthogonal to any other vector is $\mathbf{0}$. Further, any vector is anti-orthogonal to itself. In any basis $(\mathbf{e}_i)$ of E_{2n}, the representative matrix of $\boldsymbol{\Omega}$ is skew-symmetric and the anti-scalar product can be written as follows:

$$\left[\mathbf{x}, \mathbf{y}\right] = \Omega_{ij} x^i y^j, \tag{B.7}$$

where x^i, y^i are, respectively, the components of $\mathbf{x}$ and $\mathbf{x}$ relative to $(\mathbf{e}_i)$. In a canonical basis $(\mathbf{u}_i)$ (see Section 4.1), which is also called ***symplectic basis***, $\boldsymbol{\Omega}$ is given by the matrix

$$\Omega = \begin{pmatrix} \mathbb{O} & \mathbb{I} \\ -\mathbb{I} & \mathbb{O} \end{pmatrix}, \tag{B.8}$$

where $\mathbb{O}$ is the zero $n \times n$-matrix and $\mathbf{I}$ is the unit $n \times n$-matrix. Moreover, in a symplectic basis, in view of (B.7) and (B.8), we obtain

$$\left[\mathbf{u}_i, \mathbf{u}_j\right] = \left[\mathbf{u}_{n+i}, \mathbf{u}_{n+j}\right], \tag{B.9}$$

$$\left[\mathbf{u}_i, \mathbf{u}_{n+j}\right] = \delta_{ij}, \tag{B.10}$$

$$\left[\mathbf{x}, \mathbf{y}\right] = \sum_{i=1}^{n} (\overline{x}^i \overline{y}^{n+i} - \overline{x}^{n+i} \overline{y}^i). \tag{B.11}$$

B.2 Symplectic Automorphisms

An automorphism $\mathbf{S} : E_{2n} \to E_{2n}$ of a symplectic vector space E_{2n} is a ***symplectic transformation*** if does not change the anti-scalar product, that is,

$$\left[\mathbf{S}(\mathbf{x}, \mathbf{y})\right] = \left[\mathbf{x}, \mathbf{y}\right], \ \forall \mathbf{x}, \mathbf{y} \in E_{2n}. \tag{B.12}$$

The symplectic transformations correspond to the orthogonal transformations of a Euclidean space. Denoting by $\mathbb{S} = (S_k^h)$ the matrix representative of $\mathbf{S}$ in any basis $(\mathbf{e}_i)$, the condition (B.12) assumes the following form:

$$\Omega_{hk} S_i^h S_j^k = \Omega_{ij}. \tag{B.13}$$

In matrix form this condition can be written as follows

$$\mathbb{S}^T \Omega \mathbb{S} = \Omega. \tag{B.14}$$

In a *symplectic* basis, when we adopt the notation

$$\mathbb{S} = \begin{pmatrix} \mathbb{A} & \mathbb{B} \\ \mathbb{C} & \mathbb{D} \end{pmatrix}, \tag{B.15}$$

the condition (B.14) can explicitly be written

$$\begin{pmatrix} \mathbb{A}^T & \mathbb{B}^T \\ \mathbb{C}^T & \mathbb{D}^T \end{pmatrix} \begin{pmatrix} \mathbb{O} & \mathbb{I} \\ -\mathbb{I} & \mathbb{O} \end{pmatrix} \begin{pmatrix} \mathbb{A} & \mathbb{B} \\ \mathbb{C} & \mathbb{D} \end{pmatrix} = \begin{pmatrix} \mathbb{O} & \mathbb{I} \\ -\mathbb{I} & \mathbb{O} \end{pmatrix}.$$

In conclusion, a transformation $\mathbf{S}$ is symplectic if and only if

$$\mathbb{A}^T\mathbb{B} - \mathbb{C}^T\mathbb{A} = \mathbb{O}, \tag{B.16}$$

$$\mathbb{A}^T\mathbb{D} - \mathbb{C}^T\mathbb{C} = \mathbb{I}, \tag{B.17}$$

$$\mathbb{B}^T\mathbb{B} - \mathbb{D}^T\mathbb{A} = \mathbb{O}, \tag{B.18}$$

$$\mathbb{B}^T\mathbb{D} - \mathbb{D}^T\mathbb{C} = -\mathbb{I}. \tag{B.19}$$

The set $Sp(E_{2n}), \mathbf{\Omega})$ of the symplectic transformations of E_{2n} is called the ***symplectic transformation group*** of E_{2n}. To verify that $Sp(E_{2n}, \mathbf{\Omega})$ is a group, we start noting that, $\forall \mathbf{S}_1, \mathbf{S}_2 \in Sp(E_{2n}, \mathbf{\Omega})$,

$$\big[\mathbf{S}_1(\mathbf{S}_2(\mathbf{x})), \mathbf{S}_1(\mathbf{S}_2(\mathbf{y}))\big] = \big[\mathbf{S}_2(\mathbf{x}), \mathbf{S}_2(\mathbf{y})\big] = \big[\mathbf{x}, \mathbf{y}\big]$$

and $\mathbf{S}_1\mathbf{S}_2 \in Sp(E_{2n})$. Further, from (B.14), since $\det \mathbf{\Omega} = 1$, it follows

$$(\det \mathbf{S})^2 = 1$$

and there is the inverse automorphism $\mathbf{S}^{-1}$. Finally,

$$\big[\mathbf{x}, \mathbf{y}\big] = \big[\mathbf{S}^{-1}(\mathbf{S}(\mathbf{x})), \mathbf{S}^{-1}(\mathbf{S}(\mathbf{y}))\big] = \big[\mathbf{S}^{-1}(\mathbf{x}), \mathbf{S}^{-1}(\mathbf{y})\big]$$

and $\mathbf{S}^{-1} \in Sp(E_{2n})$.

References

1. R.K. Luneburg, *Mathematical Theory of Optics* (University of California Press, Berkeley, 1964)
2. M. Herzberger, *Modern Geometrical Optics* (Interscience Publisher Inc., London, 1958)
3. H.A. Buchdahl, *Optical Aberration Coefficients* (Dover Publications Inc, New York, 1968)
4. H.A. Buchdahl, *An Introduction to Hamiltonian Optics* (Cambridge University Press, 1970)
5. W. Welford, *Aberrations of the Symmetric Optical Systems* (Accademic Press, New York, 1974)
6. H. Cretien, *Calcul des Combinaisons Optique* (Masson, Paris, 1980)
7. M. Born, E. Wolf, *Principles of Optics* (Pergamon, Oxford, 1980)
8. M. Katz, *Introduction to Geometrical Optics* (World Scientific, 2002)
9. P.D. Lin, *New Computation Methods for Geometrical Optics*, Springer Series in Optical Sciences (2014)
10. W.T. Welford, *Aberrations of Optical Systems* (Adam Hilger, Bristol, 1986)
11. V. Mahajan, *Fundamentals of Geometrical Optics* (SPIE Press, 2014)
12. V. Mahajan, *Optical Imaging and Aberrations* (SPIE Press, 2011)
13. O.N. Stavroudis, *Modular Optical Design* (Springer, Berlin, 1982)
14. H.H. Hopkins, *Wave Theory of Aberrations* (Oxford University Press, New York, 1950)
15. A.E. Conrady, *Applied Optics and Optical Design Part I* (Dover Publications Inc, New York, 1957)
16. A.E. Conrady, *Applied Optics and Optical Design Part II* (Dover Publications Inc, New York, 1960)
17. R. Kingslake, *Lens Design Fundamentals* (Academic Press, New York, 1978)
18. W.J. Smith, *Moder Optical Engineering* (McGraw-Hill, New York, 1966)
19. R.R. Shannon, *The Art and Science of Optical Design* (Cambridge University Press, 1997)
20. M.J. Kidger, *Intermediate Optical Design* (Spie Press, 2004)
21. V. Sacek, *Amator Telescope Optics* (2006). www.telescope-optics.net
22. D.J. Schroeder, *Astronomical Optics* (Academic Press Inc, New York, 1987)
23. W.R. Hamilton, The mathematical papers of Sir Willams Rowan Hamilton, *in Geometrical Optics*, vol. I (Cambridge University Press, Cambridge, 1931)
24. L. Seidel, Z. Dioptric, *Ü*ber die Entwiecklung der Glieder 3ter Ordnung, etc. Astron. Navhr. **43** (1856)
25. K. Schwarzschild, Untersuchungen zur geometrischen Optik. Abhandl. Ges. Wiss. G*ö*ttingen, N. F. 4 (1905)

© Springer International Publishing Switzerland 2016

A. Romano and R. Cavaliere, *Geometric Optics*,
Modeling and Simulation in Science, Engineering and Technology,
DOI 10.1007/978-3-319-43732-3

26. H. Rutten, M. van Venrooij, *Telescope Optics: A Comprehensive Manual for Amateur Astronomers* (Willmann-Bell, Inc., 1999)
27. M. Gaj, Fifth-order field aberration coefficients for an optical surface of rotational symmetry. Appl. Opt. **10**(7) (1971)
28. B. Tatian, Aberration balancing in rotationally symmetric lenses. J. Opt. Soc. Am. **64**(8) (1974)
29. G. Hopkins, Proximate ray tracing and optical aberration coefficients. J. Opt. Soc. Am. **66**(5) (1976)
30. A. Walter, Eikonal theory and computer algebra. J. Opt. Soc. Am. A **13**(3) (1996)
31. A. Marasco, A. Romano, Third-order aberrations via Fermat's principle. Nuovo Cimento **121**B(1) (2006)
32. A. Marasco, A. Romano, Houghton's camera and telescope. Int. J. Eng. Sci. (2006)
33. A. Marasco, A. Romano, Maksutov's cameras and telescopes. Int. J. Eng. Sci. (2007)
34. A. Marasco, A. Romano, Achromatic and apochromatic doublets. Int. J. Eng. Sci. (2008)
35. D. Hawkins, E.H. Linfoot, An improved type of Schmidt camera. Monthly Notices of the R.A.S. **105** (1945)
36. E.H. Linfoot, The Schmidt-Cassegrain systems and their applications to astronomical photography. Monthly Notices of the R.A.S. **104** (1944)
37. A.S. DeVany, A Schmidt-Cassegrain optical design with a flat field. Sky Telescope, May, 1965
38. R.D. Sigler, Family of compact Schmidt Cassegrain telescope designs. Appl. Opt. **13** (1974)
39. R.D. Sigler, Compound Schmidt Cassegrain telescope designs with nonzero Petzval curvatures. Appl. Opt. **14** (1975)
40. R. Gelles, A new family of flat-field cameras. Appl. Opt. **2** (1963)
41. R.D. Sigler, A new wide-field all spherical telescope. Telescope Making **30** (1987)
42. V. Mahajan, J. Opt. Soc. Am. **71** (1981)
43. V. Mahajan, J. Opt. Soc. Am. **72** (1982)
44. V. Lakshminarayanan, A. Ghatak, K. Thyagaraian, *Lagrangian Optics* (Springer, 2002)
45. H.G. Zimmer, *Geometrical Optics* (Springer, New York, 1970)
46. G. Giusfredi, *Manuale di Ottica* (Springer, Italia, 2015)
47. M.J. Kidger, Fundamental optical design, in *SPIE–The International Society for Optical Engineering* (2001)
48. F. Corrente, *Hamiltonian Optics*, Thesis (2011). arXiv:1110.2331
49. F. Corrente, P.Onorato, Generalized Luneburg third order aberrations formulae. Opt. Soc. Am. OCIS codes: 000.3860, 080.0080, 220.3630, 2011
50. V. Lakshminarayanan, A.K. Ghatak, K. Thyagarajan, *Lagrangian Optics* (Springer Science+Business Media, LLC, 2002)
51. D.D Holm, *Fermat's Principle and the Geometric Mechanics of Ray Optics* (Imperial College London, 2012). d.holm@ic.ac.uk, http://www.ma.ic.ac.uk/~dholm/
52. V. Guillemin, S. Sternberg, *Symplectic Techniques in Physic* (Cambdrige University Press, 1993)
53. F. Carinena, J. Nasarre, On the symplectic structures arising in geometric optics (Wiley, 2006). doi:10.1002/prop.2190440302
54. H. Flanders, *Differential Forms with Applications to the Physical Sciences* (Academic Press, New York, 1963)
55. R.L. Bishop, S.I. Goldberg, *Tensor Analysis on Manifolds* (The Mac Millan Company, 1968)
56. M. Crampin, F. Pirani, *Applicable Differential Geometry* (Cambridgr University Press, Cambridge, 1968)
57. Y. Choquet-Bruhat, *Gèometrie Diffèrentielle et Systèmes Extèrieurs* (Dunod, 1968)
58. W.M. Boothby, *An introduction to Differential Manifolds and Riemannian Geometry* (Academic Press, 1975)
59. M.P. de Carmo, *Differential Geometry of Curves and Surfaces* (Prentice-Hall, 1976)
60. C. von Westenholz, *Differential Forms in Mathematical Physics* (North-Holland Publishing Company, New York, 1981)

Index

A
Abbe's condition, 91
Abbe's invariant, 25
AberrationCoefficients, 54
Aberration-free system, 7
Aberration function, 53, 55
Aberration vector, 56, 247
Aberrations, 247
Achromatic, 9
Achromatic doublet, 163, 166
Acoustic tensor, 267
Afocal, 34
Airy ring, 104
Airy's disk, 9, 103
Angular function, 225
Anterior base plane, 225
Anterior focal length, 33
Anterior principal planes, 33
Anti-scalar product, 281
Aperture, 109, 120
Aperture stop, 34
Aplanatic, 95
Apochromatic, 9
Apochromatic doublet, 166
Astigmatism, 76
Astigmatism and curvature of field, 74
Auxiliary optical path, 53
Axial chromatic aberration, 9, 81

B
Back focal, 33
Baker-Nunn camera, 187
BakerSchmidt, 178
Bending, 164
Buchroeder, 186
Buchroeder's camera, 185

C
Camera, 120
Cassegrain, 115, 117
Cassegrain combination, 116
Cassegrain telescope, 113
Characteristic curves, 216
Characteristic functions, 53
Characteristic strip, 275
Characteristic system, 216
Chracteristic curves, 275
Chromatic magnification or lateral color aberration, 81
Coma, 72
Configuration space, 239
Configuration space-time, 242
Conic, 12
Conic parameter, 13
Conjugate planes, 7, 25
Contact manifold, 243
Contact or canonical transformation, 243
Curvature of field, 78

D
Dall-Kirkam combination, 115
Degrees of freedom, 239
Diffraction limited, 9

© Springer International Publishing Switzerland 2016

A. Romano and R. Cavaliere, *Geometric Optics*,
Modeling and Simulation in Science, Engineering and Technology,
DOI 10.1007/978-3-319-43732-3

Directrix, 12
Distortion, 76
Distortion, pin-cushion and barrel, 76
Doublet, 164

E
Eccentricity, 13
Eikonal equation, 216
Elliptic coma, 102
Encircled energy fraction, 104
Entrance pupil, 7, 34
Euler–Lagrange equation, 205
Exit pupil, 7, 34

F
Fermat principle, 2, 197
Fermat's principle, 1
Fifth-order aberrations, 248
Fifth-order linear coma, 101
Fifth-order spherical aberration, 100
Flat-field camera, 177
Focal surfaces, 76
Focus, 12
Fraunhofer doublet, 163
Fresnel's ellipsoid, 266
Fresnel's equation of wave normals, 269
Frontal focal, 33
Full aperture corrector, 180

G
Gaussian approximation, 9, 24
Gaussian data, 23, 42
Gaussian image plane, 8
Geometric Optics, 1

H
HCamera, 129, 132, 135, 136, 138
HCassegrain, 152
Helmotz-Lagrange invariant, 37
Houghton's combination, 129
Houghton–Cassegrain, 151
Huygens principle, 1, 220

I
Ideal, 8
Ideal system, 7
Image plane, 7
Image space, 7

K
Klevtsov, 183
Klevtsov telescope, 182

L
Lagrange's optical invariant, 214, 230
Lagrangian coordinates, 239
Lagrangian phase portrait, 240
Legendre map, 240

M
Magnification, 8
Magnification factor, 25
Maksutov camera, 139
Maksutov–Cassegrain telescope, 157
Mangin mirror, 184
Maupertuis' principle, 209
MCamera, 140
MCassegrain, 158
Meridional plane, 7
Meridional ray, 7
Mixed functions, 226
Monge's cone, 274
Monochromatic aberration functions, 11

N
NewCass, 180
NewHCassegrain, 191
Nodal points, 33
Normal speed, 216

O
Object plane, 5
Object space, 7, 223
Optical axis, 5, 227
Optical path length, 2, 197
Overcorrected, 9

P
Parabola, 14
Paraxial approximation, 9, 24
Perfect system, 9
Petzval portrait objective, 193
Petzval's curvature, 78
Petzval's theorem, 78
Phase space, 240
Phase space-time, 242
Point principal function, 223
Point spread function, 102
Posterior base plane, 225

Posterior focal length, 27, 33
Posterior principal planes, 33
Power, 26
Pressman-Camichel combination, 116
Primary aberrations, 58
Primary axial color, 9
Primary lateral color, 9
Principal functions, 223
Principal ray, 34
Principal velocities of propagation, 268

R
Ray, 1
Ray-intercept curve, 11
Ray tracing, 5, 11
Reduced coordinates, 252
Reflection law, 5, 206
Refraction invariant, 46
Refraction law, 4, 206
Reversible system, 228
Ritchey–Cretien combination, 116

S
Sagittal plane, 7
Sagittal ray, 7
SCamera, 125
SCassegrain, 146, 148
Schmidt-Cassegrain combination, 147
Schmidt's camera, 121
Schwarzschild eikonal, 254
Schwarzschild's eikonal, 53
Secondary spectrum, 9, 166
Seidel variables, 253
Semiapochromatic doublet, 166
Sine condition, 91
Skew ray, 7
Speed, 109, 120
Spherical aberration, 72
Spherical aberration curve, 12
Spot diagram, 12
Steinheil doublet, 163
Stigmatic path, 58
Stigmatic points, 5, 7
Surface of revolution, 12
Symplectic basis, 282
Symplectic manifold, 241
Symplectic mechanics, 239
Symplectic transformation, 282
Symplectic transformation group, 283
Symplectic vector space, 281

T
Tangential plane, 7
Tangential ray, 7
Telescopic, 34
Thin lens, 44
Third-order aberrations, 58, 248
TotalAberrations, 86, 107, 112, 165, 175
Triplet, 170, 171

U
Undercorrected, 9

V
Vignetting, 35

W
Wave front, 1
WCamera, 128
Weierstrass–Erdman conditions, 205
Wright's camera, 127